The Use of Hydroamination in the Attempted Synthesis of Ant Alkaloid 223H (xenovenine)

Dissertation Submitted to the
University of KwaZulu-Natal
for the Degree of
Master of Science
(In Chemistry)

By

Allan M. Prior

School of Chemistry
University of KwaZulu-Natal
July 2008

Thesis Declaration

The experimental work described in this thesis was carried out in the School of Chemistry, University of KwaZulu-Natal, Pietermaritzburg, under the supervision of Dr. Ross S. Robinson.

These studies represent original work by the author and have not otherwise been submitted in candidature for any other degree.

Signed:…….A. M. Prior (Candidate)

Signed:…….Dr. R. S. Robinson (Supervisor)

School of Chemistry
University of KwaZulu-Natal
Pietermaritzburg
South Africa

Publication Declaration

My research publication titled "An assessment of late transition metals as hydroamination catalysts in the cyclization of *C*-propargyl vinylogous amides into pyrroles" has been included in the text of this thesis as per faculty guidelines and is found on page 49. The full literature reference for the publication is as follows.

Prior, A. M.; Robinson, R. S. *Tetrahedron Letters* **2008**, *49*, 411-414.

The experimental work discussed in the publication as well as the writing of the publication was performed by me and was carried out within the School of Chemistry, University of KwaZulu-Natal, Pietermaritzburg, under the supervision of Dr. Ross S. Robinson. I was the primary author for the publication and minor grammatical changes were performed at a later stage by me under the suggestion of my research supervisor.

These studies represent original work by the author and have not otherwise been submitted in candidature for any other degree.

Signed:…….A. M. Prior (Candidate)

Signed:…….Dr. R. S. Robinson (Supervisor)

School of Chemistry
University of KwaZulu-Natal
Pietermaritzburg
South Africa

Abstract

The ability to construct C-N bonds is of great importance to organic chemists as exemplified by the vast number of natural products, pharmaceutical agents and fine chemicals that contain such linkages. An atom efficient C-N bond forming reaction namely hydroamination has attracted much interest to date due to its ability in forming amine, imine and enamine functionality. The scope of this project involved the attempted synthesis of a biologically active and nitrogen containing pyrrolizidine alkaloid isolated from cryptic thief ants and poison dart frogs namely **223H** (xenovenine). The method of hydroamination was utilized as the pivotal ring forming step and was established as being a valuable synthetic tool towards the construction of **223H** (xenovenine). The stereoselective synthesis resulted in the successful formation of ethyl (3*R*)-5-heptyl-3-methyl-2,3-dihydro-1*H*-pyrrolizine-7-carboxylate **74**, a novel, and structurally analogous precursor to **223H** (xenovenine) over 10 synthetic steps from (*S*)-pyroglutamic acid. The following research also resulted in the synthesis of two other novel compounds namely ethyl 3-[(2*R*)-2-methyl-5-thioxotetrahydro-1*H*-pyrrol-1-yl]propanoate **86** and ethyl 3-{(5*R*)-2-[(*E*)-2-ethoxy-2-oxoethylidene]-5-methyltetrahydro-1*H*-pyrrol-1-yl}propanoate **87**.

A catalytic hydroamination study on the conversion of *C*-propargyl vinylogous amides into pyrroles demonstrated that transition metal salts of groups 11 and 12 serve as effective hydroamination catalysts. The oxide, acetate, chloride and nitrate derivatives of group 11 and 12 metals namely Cu(II), Ag(I), Zn(II), Cd(II) and Hg(II) were employed as potential hydroamination catalysts in the oxidation states provided. The Zn(II) catalyst series with the exception ZnO provided the greatest hydroamination yields under mild reaction conditions owing to their high Lewis acidities however the Ag(I) and Hg(II) catalyst series also provided excellent yields of product under more forcing reaction conditions.

Acknowledgments

I would firstly like to thank my research supervisor Dr. Ross S. Robinson, without whom this research would not have been possible. I thank him for the interesting research topic, valuable discussions and guidance, financial support and friendship. I also thank the National Research Foundation for the generous funding provided for the duration of this project.

I would like to thank Mr. Craig Grimmer for acquiring NMR data and Dr. Fatima Khan for obtaining HRMS data. Many thanks go out to Mr. Raj Somaru and Mr. Fayzil Shaik for their assistance throughout the time I spent in the Frank Warren organic research laboratory at the School of Chemistry, University of KwaZulu-Natal.

I would also thank my family and friends for their endless encouragement, support and patience.

Contents

1 Introduction

1.1 Hydroamination

The ability to construct C–N bonds is of fundamental importance in organic synthesis as exemplified by the vast number of natural products, pharmacological agents and fine chemicals that contain such linkages.[1-3] The intra- or intermolecular addition of secondary amines, primary amines or ammonia to alkenes and alkynes, namely hydroamination, has attracted a great deal of attention due to its ability and versatility in constructing such bonds.[4] This hydroamination reaction is an atom efficient process[5] which proceeds smoothly without the formation of undesirable side products, providing a convenient synthetic route towards amine, enamine or imine functionalities (Scheme 1).[6]

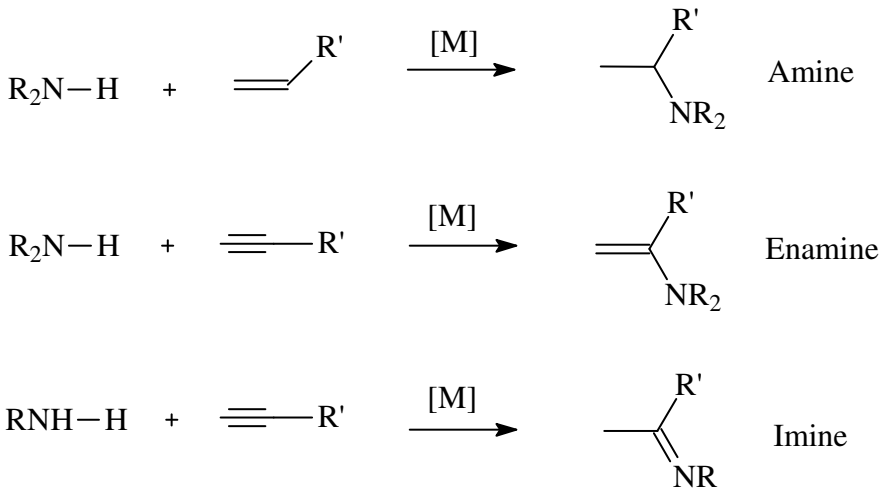

Scheme 1: Intermolecular Hydroamination

The change in enthalpy (ΔH) associated with the addition of an amine to an alkene is approximately –53 kJ.mol^{-1}, whereas the addition of an amine to an alkyne is calculated to be more favorable ($\Delta H_{calcd.}$ *ca.* –71 kJ.mol^{-1}).[7,8] Although the hydroamination reaction is thermodynamically feasible, it is kinetically too slow to be synthetically useful without the aid of a catalyst. It has been suggested that when the nitrogen lone pair from the

amine approaches the π-bond from the electron rich alkene or alkyne in the absence of any catalyst, the electrostatic repulsions that result tend to form high activation energies, leading to particularly low reaction rates.[8] These high activation energies cannot be over come at elevated temperatures due the negative reaction entropy, resulting in the tendency to favor starting materials at high temperatures.[8] The utilization of a catalyst is thus axiomatic in overcoming this energy barrier, and allowing for successful hydroamination to take place.

Howk *et al*.[9] in 1954, showed that primary amines and ammonia could be added to alkenes in the presence of an alkali metal or its hydride, however, high pressures, high temperatures and long reaction times were required in order to bring about such reactions, and in only moderate yields as depicted in Table 1.[9]

Table 1: Hydroamination Reactions Catalyzed by Group I Metals[9]

Cat. (g.)	Amine (g.)	Alkene	Pressure (atm.)	Temp. (^oC)	Time (hr.)	Product(s)	Yield (%)
Na (5)	NH_3 (51)	C_2H_4	205	199-201	10.5	$EtNH_2$	7.6
Li (5)	NH_3 (50)	C_2H_4	820-980	247-252	14.5	$EtNH_2$	5.0
						Et_2NH	15.5
						Et_3N	32.0
Na (8)	*n*-$BuNH_2$ (75)	C_2H_4	800-1000	200	…	Et_2NBu	74.8
Na (5)	NH_3 (53)	C_3H_6	850-975	250-252	18.2	Isopropylamine	82.0
						Diisopropylamine	8.2

More recently, milder and higher yielding reaction conditions employing catalysts based on early transition metals, groups 3–5,[10,11] late transition metals, groups 9–12[12] as well as early lanthanides[13] and actinides[14] have been reported.

Hydroamination may follow one of three generally accepted catalytic amination mechanisms namely,

i. base catalyzed amine activation,
ii. metal catalyzed amine activation (oxidative addition), and
iii. metal catalyzed alkene / alkyne activation.

1.1.1 Base Catalyzed Amine Activation

The base catalyzed hydroamination mechanism is initiated *via* initial amino proton extraction, to form an amide salt with ionic character.[15] It is this metal salt of the activated amide species that can undergo addition to the double bond. This affords the highly polar, β-aminoalkyl metal complex as an intermediate, presumably *via* initial coordination from the alkene to the metal centre as depicted in Scheme 2.

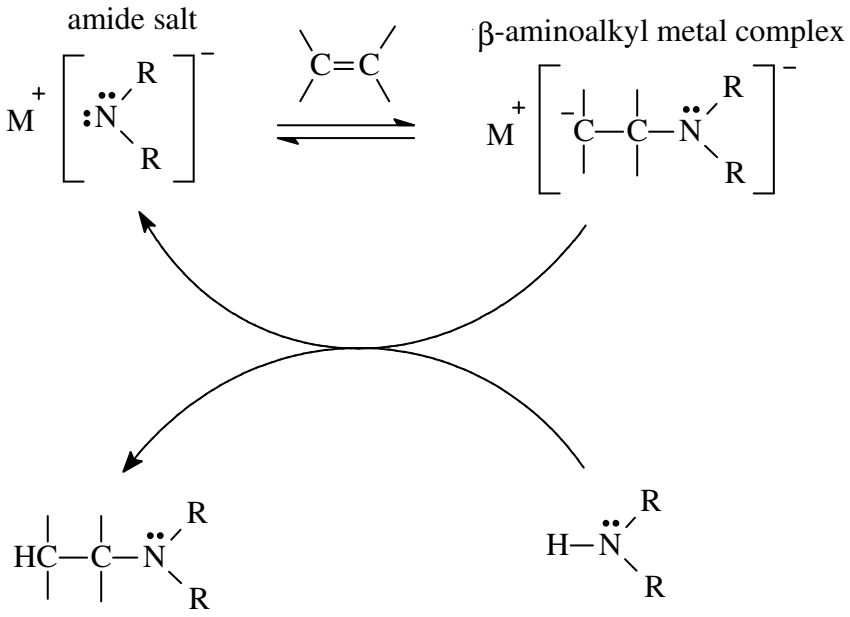

Scheme 2: Base Catalyzed Hydroamination[15]

Bases of strongly electropositive metals such as alkali or alkali-earth metals are required in order to form sufficiently activated amides, which in turn are capable of reacting with C–C double bonds. Protolysis of the β-aminoalkyl metal intermediate by reaction with

another amine substrate generates the alkylamine hydroamination product, as well reforms the metal amide activated species as depicted the catalytic cycle.

An example of a base catalyzed reaction is the hydroamination of phenylacetylene with substituted anilines in the presence of cesium hydroxide ($CeOH.H_2O$) to afford functionalized enamines in high yields (Scheme 3).[16]

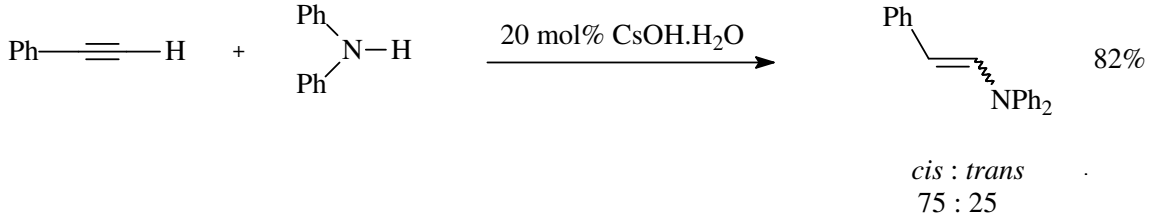

Scheme 3

The reaction takes place in the presence of 20 mol% $CeOH.H_2O$ in *N*-methylpyrrolidone, whilst stirring at 90-100 ^oC for 12-24 hours. Although the yields are high, the product is obtained with poor stereo-selectivity.

Alternatively, *N*-heterocycles are added to phenylacetylene under the same reaction conditions giving rise to 100% *cis*-selectivity and resulting in the formation of heterocyclic functionalized enamines in good yield (Scheme 4).[16]

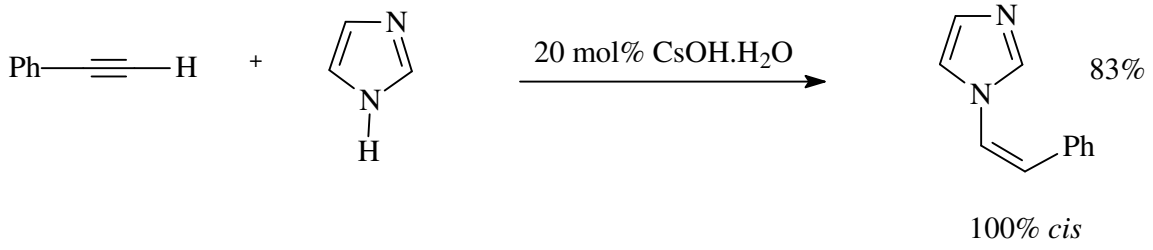

Scheme 4

A problem that is occasionally associated with base catalyzed hydroamination is the oligomerization of the enamine or imine hydroamination products due to the harsh, basic reaction conditions.[17,16]

1.1.2 Metal Catalyzed Amine Activation (Oxidative Addition)

A cycle depicting a metal catalyzed amine activation mechanistic route *via* oxidative addition[15] is presented in Scheme 5. The amine activation step involves insertion of a coordinatively unsaturated, low oxidation state metal such as Ru(0), Cr(I) or La(I)[18,19] into the N–H bond of the amine. This process takes place *via* an oxidative addition process, to form an amido hydrido complex. The metal centre of the resulting complex coordinates with an alkene, followed by insertion of this alkene into the metal-amine bond. Finally, reductive elimination liberates the amine hydroamination product, as well as regenerates the low oxidation state metal catalyst.

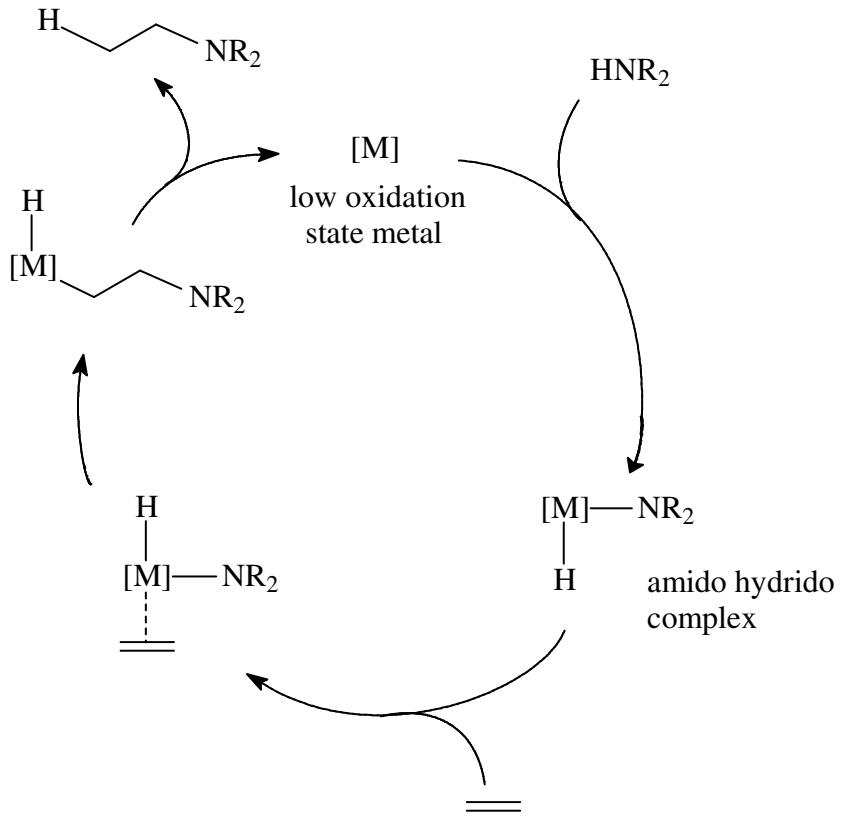

Scheme 5: Metal Catalyzed Hydroamination *via* Amine Activation (Oxidative Addition)[15]

Although the above catalytic scheme is reasonably simple, very few examples of its use exist in practice as the oxidative addition of a metal into an N–H bond is not normally a favorable process.[18,20-22] An example that illustrates this mechanism involves the cyclization of 5-aminopent-1-ene to 2-methylpyrolidine catalyzed by $(cp^*_2LaH)_2$ (Scheme 6), however no yield was reported(!).[23]

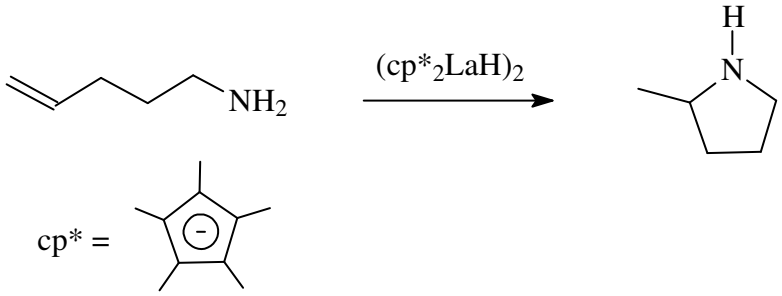

Scheme 6

The limiting step based on kinetic and mechanistic evidence involved the intramolecular insertion of the alkene into the lanthanide-nitrogen bond, followed by subsequent protonolysis of the lanthanide-carbon bond.[23,24]

The mechanism based on amine activation cannot explain Zn(II) and Cu(I) catalyzed hydroamination reactions, as these metals have no oxidation states available for the donation of two more electrons.[25,26] This draws attention to the more generally accepted hydroamination mechanism based on alkene activation.

1.1.3 Metal Catalyzed Alkene / Alkyne Activation

The mechanism illustrated below in Scheme 7, along with a few variants, appears to be the most accepted and relies upon the Lewis acidity of the catalyst's metal centre, and its ability to activate C–C multiple bonds through π-coordination to the unsaturated moiety.[15] Once the metal-alkene complex has been formed, an amine can attack the umpulong double bond forming a new C–N bond. The metal subsequently dissociates from this complex, combing with a free amine to furnish a metal-amine complex, as well as the amine hydroamination product. This metal-amine complex is an apparent resting

state for the catalyst,[25] and represents a potential reaction energy minima. Reaction of the metal-amine complex with another alkene liberates the free amine whilst reforming the metal-alkene activated complex. This may undergo a subsequent hydroamination cycle by reaction with a nucleophilic free amine.

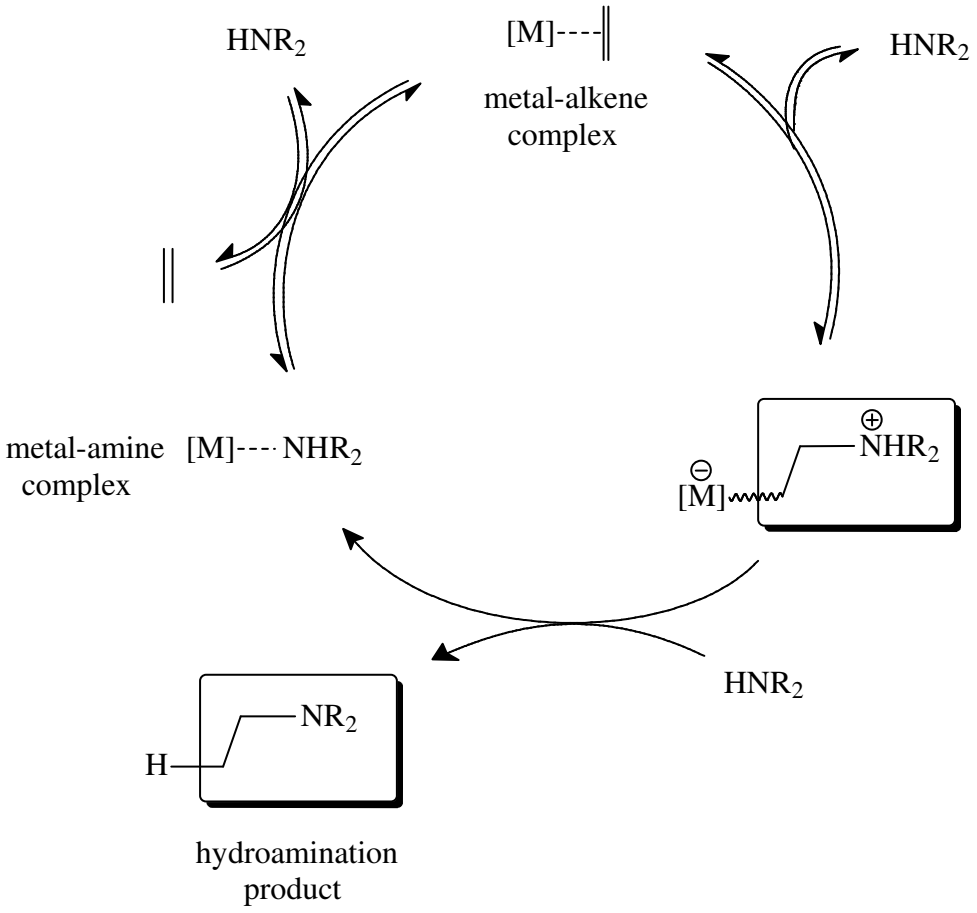

Scheme 7: Metal Catalyzed Hydroamination *via* Alkene Activation[15]

The hydroamination of alkynes may be performed regioselectively, whereas alkenes may be hydroaminated both regioselectively and enantioselectively. The chemistry associated with both of these transition types is discussed below in the subsequent two sections.

1.1.4 Regioselectivity in Hydroamination

Regioselective hydroamination reactions have been achieved yielding Markovnikov,[27] or *anti*-Markovnikov[28,29] amination products *via* inter- or intramolecular reaction pathways (Figure 1).

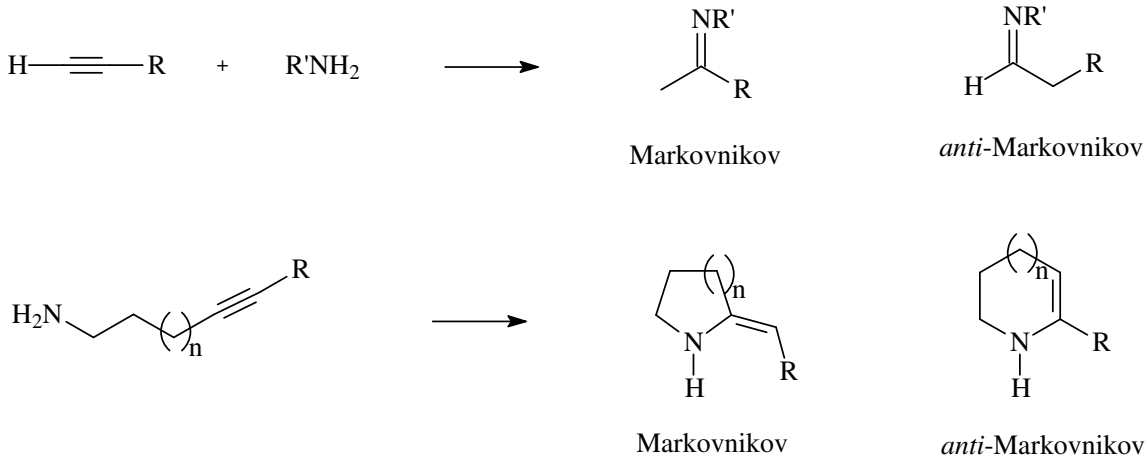

Figure 1: Possible Regioselective Outcomes from Inter- or Intramolecular Hydroamination Reactions

Aliphatic and most aromatic alkenes tend to yield the more commonly encountered Markovnikov amination product, however methods are currently known so as to deliberately obtain *anti*-Markovnikov addition type products if so desired. Some of these methods to achieve the latter include reactions employing electrophilic nitrogen radicals,[30] or the use of pre-catalysts with bulky ligands such as bis(amidate)titanium[29] or aryloxotitanium[31] complexes.

Tillack *et al.*[31] recently reported the use of aryloxotitanium complexes in the regioselective amination of 1-octyne and *sec*-butyl amine (Scheme 8), as well as the effect of minor changes in the ligand group and its effect on the obtained regioselectivity.

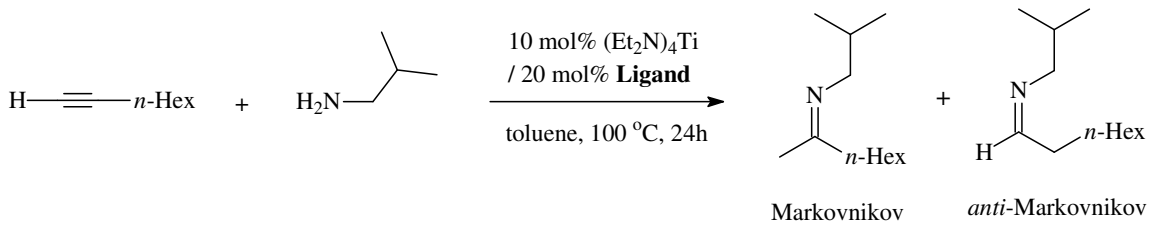

Scheme 8

The four ligand types employed in this study had differing substituents on the aryl ring (Ligands **1-4**, Figure 2).

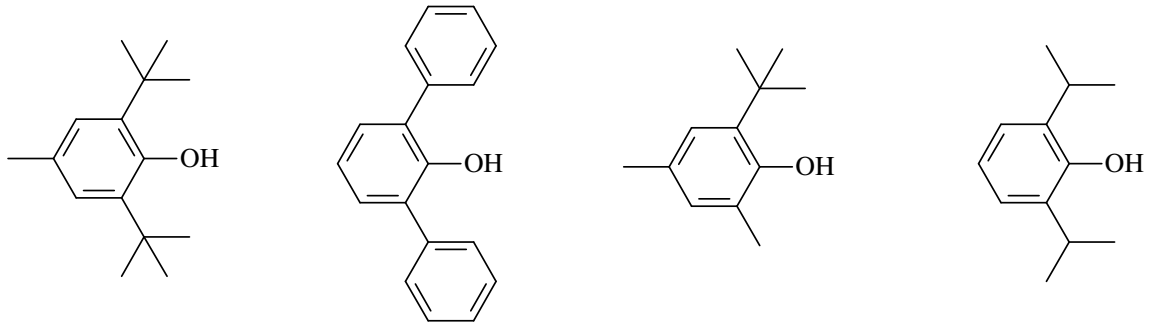

ligand 1 **ligand 2** **ligand 3** **ligand 4**

Figure 2: Ligands Utilized in Regioselective Hydroamination Study[31]

The pre-catalysts were formed *in situ* using a 1:2 ratio of $(Et_2N)_4Ti$ with the relevant ligand group. These specific catalyst systems, when combined with starting materials, all gave rise to high yielding hydroamination reactions and showed remarkably different regioselectivity in the resulting imine products. Hydroamination using the $(Et_2N)_4Ti$ / ligand **1** catalyst system favored Markovnikov addition, whist the $(Et_2N)_4Ti$ / ligand **4** catalyst system encouraged anti-Markovnikov addition (Table 2). Reaction mixtures comprising significant amounts of both isomers were obtained by ligand groups **2** and **3** as determined by gas chromatography. The authors reported that at this early stage, the underlying reasons for the observed regioselective preferences by the above mentioned ligands remain unclear; however steric factors are presumed to play a role.

Table 2: Yield and Regioselectivity Obtained in the Enamine Product[31]

Ligand	Conversion (%)	Yield (%)	Markovnikov : *anti*-Markovnikov ratio
1	100	98	90 : 10
2	100	97	51 : 49
3	100	88	28 : 72
4	100	97	6 : 94

The regioselectivity obtained in hydroamination reactions may also be affected by stereoelectronic factors rather than simple steric factors, as demonstrated by Ryu *et al*.[32] Ryu showed that electron rich and electron neutral vinylarenes exclusively produced *anti*-Markovnikov amination products in excellent yields, while electron deficient vinylarenes exhibited slightly decreased regioselectivity (96:4 *anti*-Markovnikov product:Markovnikov product) when combined with the amine and a Lewis acidic lanthanum catalyst. Figure 3 denotes a catalytic cycle for the hydroamination of vinylarenes facilitated by a cyclopentadienyl lanthanum catalyst, which proceeded *via* an amine activation type mechanism. Insertion of the alkene into the La–N bond may take place *via* a 2,1-addition (**T1**, Figure 3) or a 1,2-addition (**T2**, Figure 3). According to Ryu, 2,1-addition is greatly favored in this instance due to weak coordination between the arene π-system and the Lewis acidic lanthanide centre. This interaction-stabilization resulted in the regiochemical preference to direct *anti*-Markovnikov amination as the lanthanide centre gets delivered to the benzylic position whilst the nitrogen gets delivered to the terminal position.

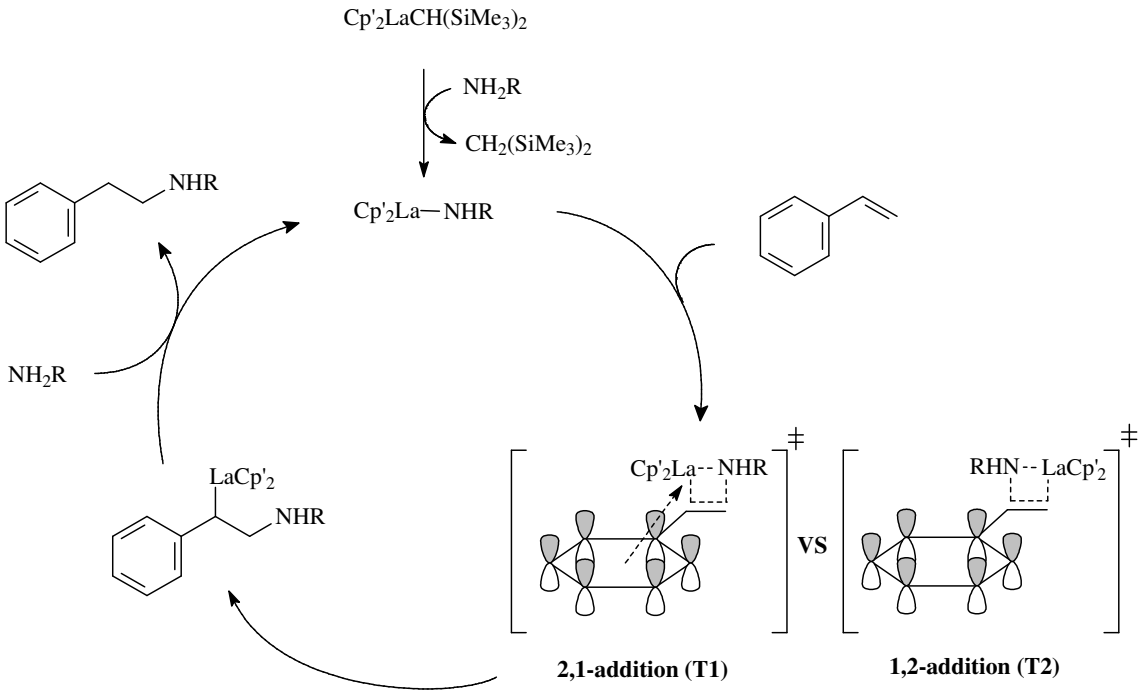

Figure 3: Regioselective Hydroamination[32]

Addition of amines to activated alkenes, i.e. alkenes with an activating electron withdrawing sulfoxide, nitro, nitrile, keto or ester group *alpha* to the double bond, usually gives rise to *anti*-Markovnikov hydroamination naturally, without the need of specialized catalytic systems.[33]

1.1.5 Stereoselectivity in Hydroamination

Hetero-chiral molecules are of great importance due to their varied biological activity, as well as their use in organic synthetic chemistry.[34] Enantioselective additions of amines to alkenes furnishing hetero-chiral compounds have been achieved utilizing bulky, chiral hydroamination catalysts.[35-38] The first reported enantioselective hydroamination reaction was achieved in 1994 by Giardello *et al.*,[39] and was performed utilizing an *ansa*-lanthanocene precatalyst **A** and included a chiral group on one of the cyclopentadienyl rings (Figure 4).

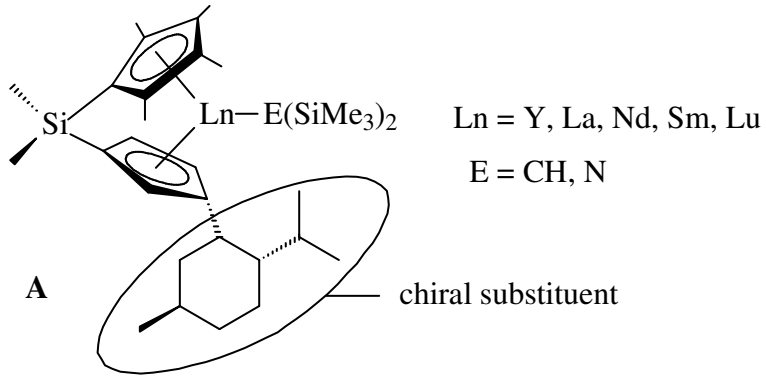

Figure 4

The C_1-symmetric precatalyst **A** was employed in the enantioselective cyclization of the aminopentene substrate to afford the corresponding pyrrolidine (Scheme 9).

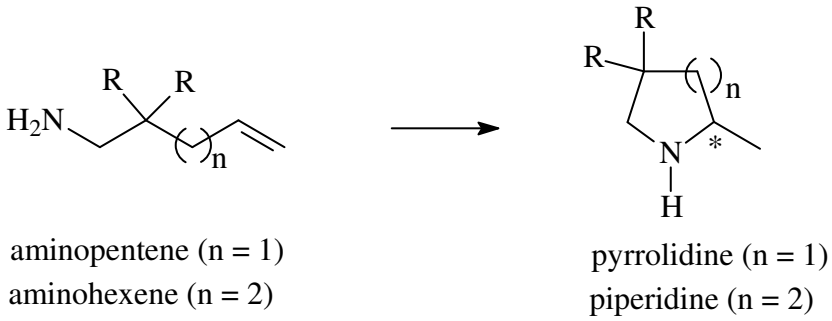

Scheme 9

The reactions proceeded smoothly and efficiently at room temperature, achieving up to 69% enantiomeric excess in the pyrrolidine product (n = 1, R = H) when aminopentene (n = 1, R = H) and precatalyst **A** (Ln = Y) were reacted. A modest enantiomeric excess of 53% in the pyrrolidine was obtained when aminopentene (n = 1, R = CH_3) and precatalyst **A** (Ln = Sm) was utilized, nevertheless this was increased to 74% when the reaction was performed at –30°C. It was reported that catalyst turnover numbers increased with increasing atomic radii, and that enantiomeric excess in the product increased from La to Sm, however the enantiomeric excess obtained from Lu did not follow this trend. Interestingly, the enantiomeric purity of the precatalyst had no effect on the extent of enantiomeric excess in the pyrrolidine product. Instead, it was the nature of the chiral substituent on the cyclopentadienyl ring which imparted enantioselectivity.[40] The opposite pyrrolidine enantiomer was achieved by employing (+)-neomenthyl in place of (–)-menthyl as the chiral substituent on the cyclopentadienyl ring. Although the

enantiomeric excess obtainable in the pyrrolidine product was good, this catalyst system exhibited poor enantioselectivity (17% ee) when an aminohexene substrate (n = 2, R = CH_3) was converted into the corresponding piperidine.

The same research group subsequently developed another C_1-symmetric hydroamination precatalyst (**B,** Figure 5) which was similarly based on the precatalyst **A**.[41] In this catalyst series, one of the cyclopentadienyl rings was replaced with a sterically demanding octahydrofluorenyl (OHF) group and implemented in a number of stereoselective hydroamination reactions.

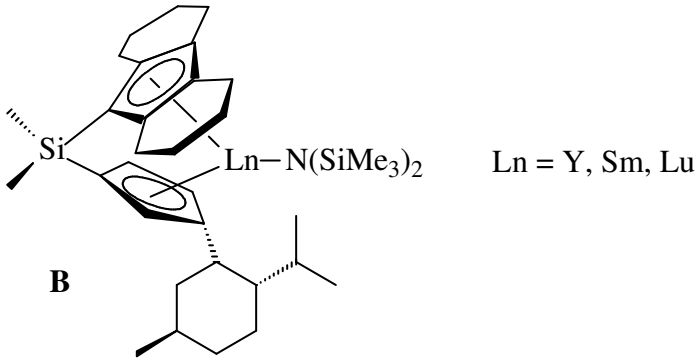

Figure 5

The latter catalyst series proved to be superior in achieving enantiomeric excess in the piperidine (n = 2, R = CH_3) derivatives, as upon cyclization of the aminohexene (n = 2, R = CH_3) substrate, an enantiomeric excess in the piperidine product of up to 67% (Ln = Y) and 41% (Ln = Sm) was achieved. The enantiomeric excess obtained in the pyrrolidine systems unfortunately decreased to 46% when implementing catalyst series **B** as compared to those achieved from the former catalyst series **A**.

Following these developments, alternative catalytic systems efficacious in performing enantioselective hydroamination was reported by Livinghouse and co-workers[13] and made use of simple lanthanide trisamides of the type $\{Ln[N(SiMe_3)_2]_3\}$.[13] O'Shaughnessy *et al.*[42-44] later reported a novel chiral lanthanide aminobis(phenoxide) catalyst (**C**, Figure 6), which at a catalytic loading of 1 mol%, efficiently cyclized

aminopentene (n = 1, R = CH_3) into the corresponding pyrrolidine at 70 ^oC and with 61% enantiomeric excess.[42-44]

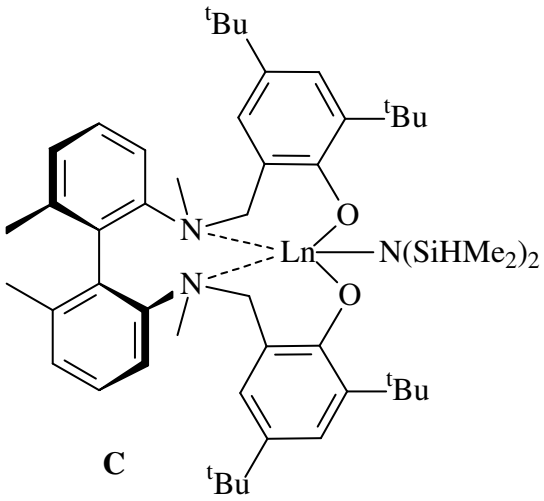

C

Figure 6

Consequential to these discoveries, the area of catalytic enantioselective hydroamination became a "hot topic", and attracted a great deal attention from many research groups internationally.[40] Their goals were, and still are, focused on the development of novel, stereoselective hydroamination catalysts which are capable of producing enantio-enriched compounds from various achiral starting materials *via* an inter- or intra-molecular fashion.

Although the catalytic systems discussed above afforded the pyrrolidine and piperidine products in excellent yields, only mediocre to good enantiomeric excess's had been achieved. In 2006, Hultzsch *et al*.[45] attained a promising 95% enantiomeric excess in the pyrrolidine (n = 1, R = Ph) when implementing a 3,3-bis[tris(aryl)silyl]-substituted binaphthol complex (**D**, Ln = Sc, Figure 7) as the hydroamination catalyst. Soon after, Schafer *et al*.[46,47] similarly obtained a desirable enantiomeric excess (93%) in the pyrrolidine (n = 1, R = CH_3) when applying a chiral zirconium amidate complex (**E**, Figure 7), and with only a few hours reaction time.

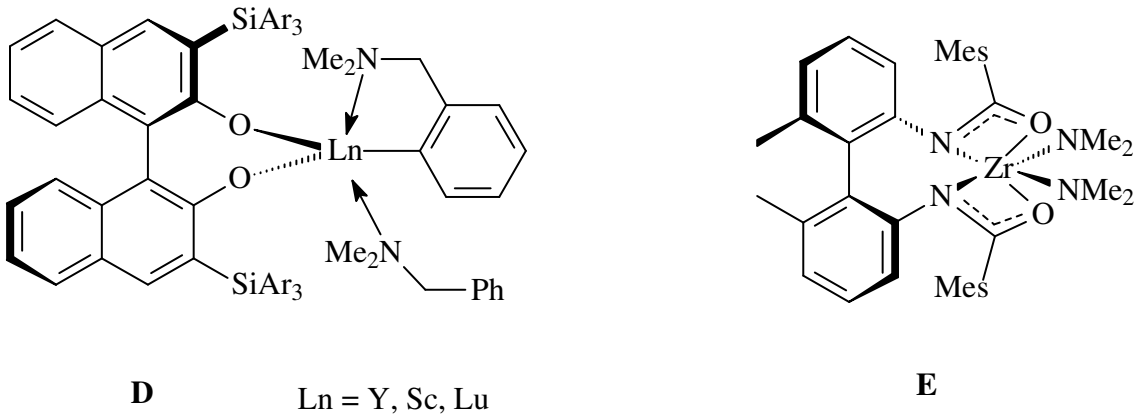

D Ln = Y, Sc, Lu **E**

Figure 7

The enantioselectivity obtained in these hydroamination reactions can be explained by referring to a model based on molecular modeling studies, and adapted from Hultzsch (Figure 8).[8]

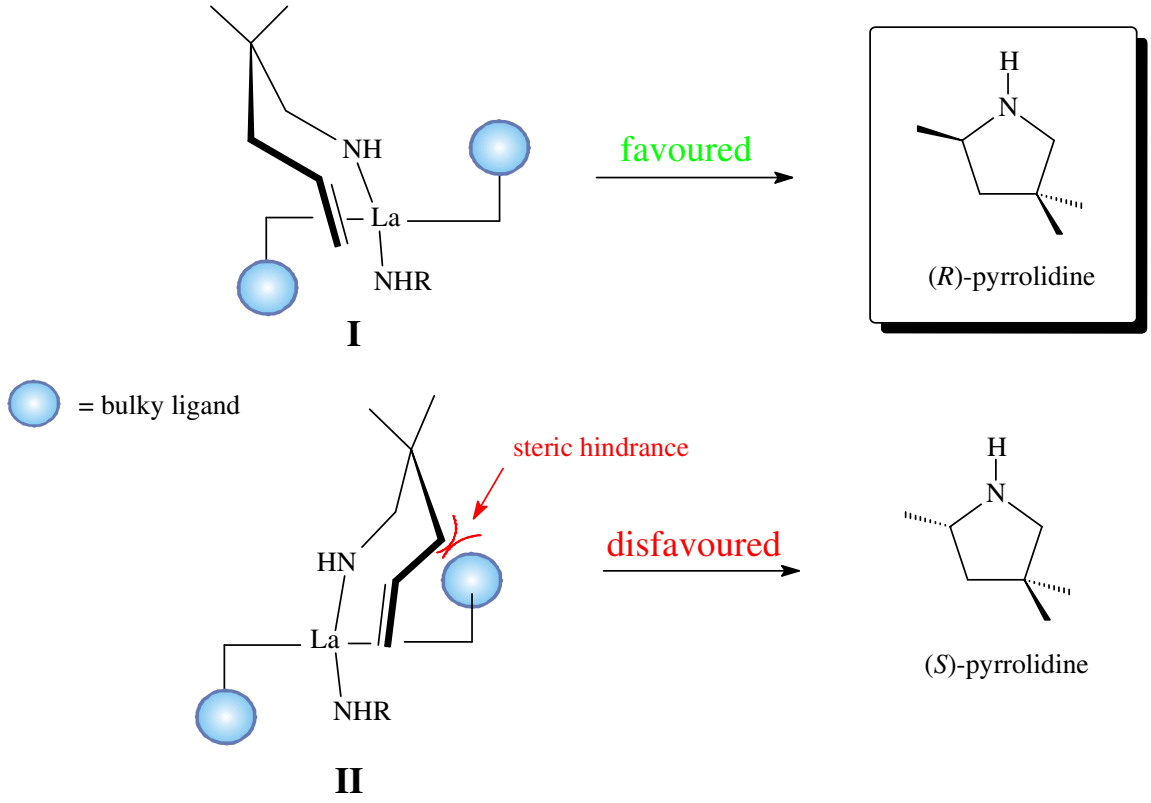

Figure 8: Stereoselective Hydroamination[8]

The model depicted in Figure 8 shows two identical catalyst-substrate complexes in different conformations (**I** and **II**) immediately prior to nitrogen-carbon bond formation. It can be seen that bulky ligand groups attached to the catalytically active metal centre strongly influence the catalyst-substrate conformation resulting from steric interaction between these modular entities. The steric interaction apparent in conformation **II** gives rise to a conformation higher in energy, providing an unfavorable transition state. Conformation **I** thus represents the lower energy alternative, resulting in the nearly exclusive formation of (*R*)-pyrrolidine.

Enantioselective hydroamination is not limited to intramolecular reaction pathways. Excellent enantioselective excess (91%) has been achieved from the intermolecular reaction of cyclohexadiene and aniline in the presence of $[Pd(\pi\text{-allyl})Cl]_2$ and a bulky naphthalene containing ligand (*R*, *R*)-**F** (Scheme 10).[40] The structure of ligand (*R*, *R*)-**F** is denoted in Figure 9.

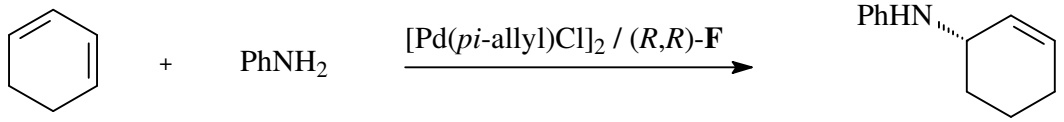

61% yield, 91% ee (*S*)

Scheme 10

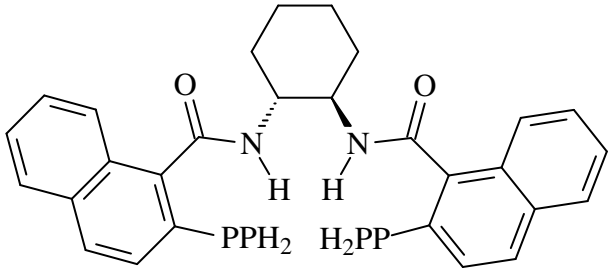

F

Figure 9

1.2 Hydroamination in Natural Product Synthesis

The pharmaceutical industry relies greatly on a chemist's ability to synthesize natural products and related derivatives in the laboratory, as many pharmaceutically active compounds have originated from such studies. This is normally the result of modification of an original "lead compound" so as to obtain enhanced and more defined biological activity.

This hydroamination methodology, amongst others, provides an attractive route towards the synthesis of many naturally occurring organic molecules containing nitrogen, and *N*-bridgehead functionality. It thus provides a convenient synthetic route to access natural products which contain pyrrolidine, piperidine, pyrrolizidine, indolizidine, quinolizidine and lehmizidine base scaffolds (Figure 10).

An example of a pharmaceutically active drug containing an *N*-bridgehead scaffold is the indolizidine alkaloid **(–)-209D**, isolated from the skin secretions of certain neotropical frogs (Figure 11).

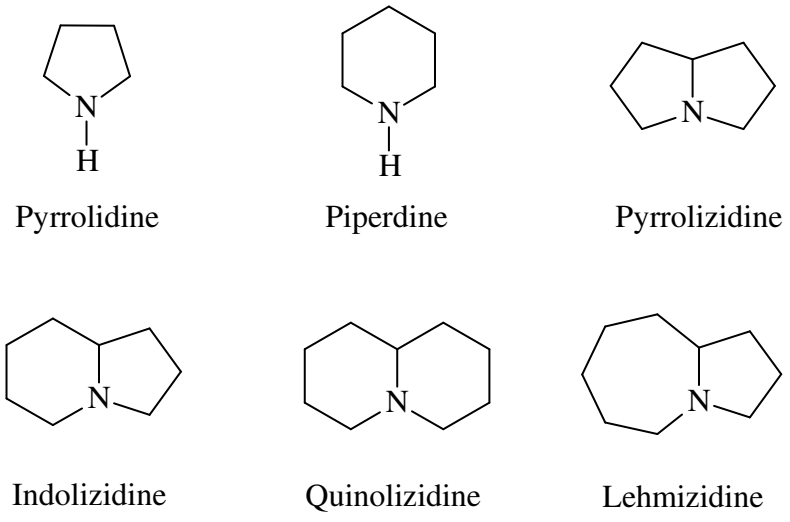

Figure 10: Various Alkaloid Base Scaffolds

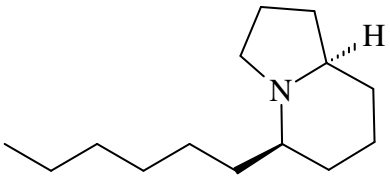

(-)-209D

Figure 11: Indolizidine Alkaloid (–)-209D

Reports have shown this molecule to be pharmaceutically active in the realms of neuromuscular transmission as it functions as a noncompetitive blocker.[48]

Patil *et al*.,[48] recently demonstrated the usefulness of hydroamination in the total synthesis of the above mentioned indolizidine alkaloid **(–)-209D** (Scheme 11). The indolizidine scaffold was obtained by treating the chiral, ε-amino alkyne precursor with 5 mol% $Pd(PPh_3)_4$ and 10 mol % benzoic acid, in 1,4-dioxan at 100 ^oC for 12 hours. This gave rise to the bicyclic indolizidine hydroamination product. Subsequent hydrogenation of the exocyclic double bond in methanol furnished **(–)-209D** in a 63% overall yield from the ε-amino alkyne precursor.

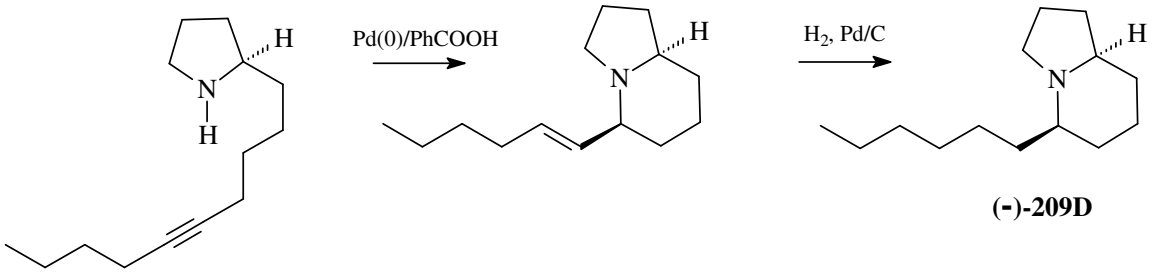

Scheme 11

Although the value for the obtained diastereomeric excess in the indolizidine product **(–)-209D** was not mentioned, the authors claim this synthesis to be highly stereoselective, and provided a plausible explanation for the observed diastereoselectivity. Their reasoning was formulated on the basis of differing 1,3-diaxial interactions that result from an equatorial, or axially arranged π-allyl palladium complex transition state (Figure 12).[48] The palladium catalyst in the π-allyl palladium complex transition state was shown

to coordinate in a η^3 fashion, allowing for the attack of the amino nitrogen at the δ-carbon of the alkyl chain thus forming a 6 membered ring.

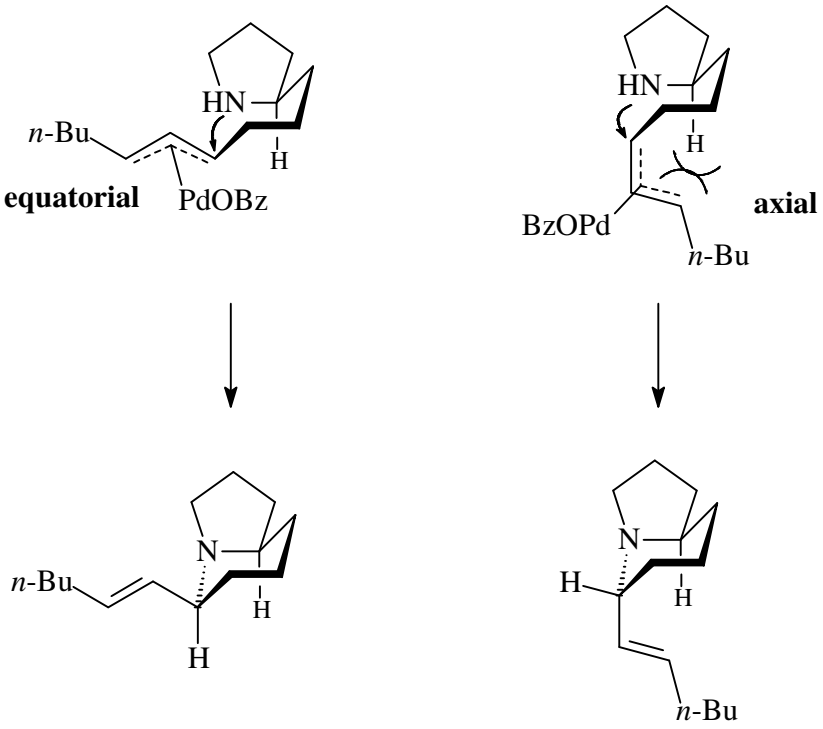

Figure 12: Stereoselective Hydroamination[48]

The authors theorized that the severe 1,3-diaxial interactions resulting from an axially orientated π-allyl palladium complex presented significant steric repulsion, which discouraged the formation of this axially orientated transition state. Alternatively, the π-allyl palladium complex prefers to adopt an equatorial orientation, in which the phenomenon of 1,3-diaxial interactions are not present, explaining the preference to exclusively form one diastereomer over the other in this reaction.

Arredondo *et al*. in 1999, described an organolanthanide catalyzed cyclohydroamination reaction accessing pyrrolizidine scaffolds (Scheme 12).[49] Upon reaction with a samarium based hydroamination catalyst, the aminoallene-alkane precursor was converted into the bicyclic pyrrolizidine intermediate *via* a tandem, bicyclization procedure. Reduction of the double bond using hydrogen (1 atm) and $Pd(OH)_2/C$ afforded (+)-xenovenine in a 78% overall yield from the aminoallene-alkane precursor.

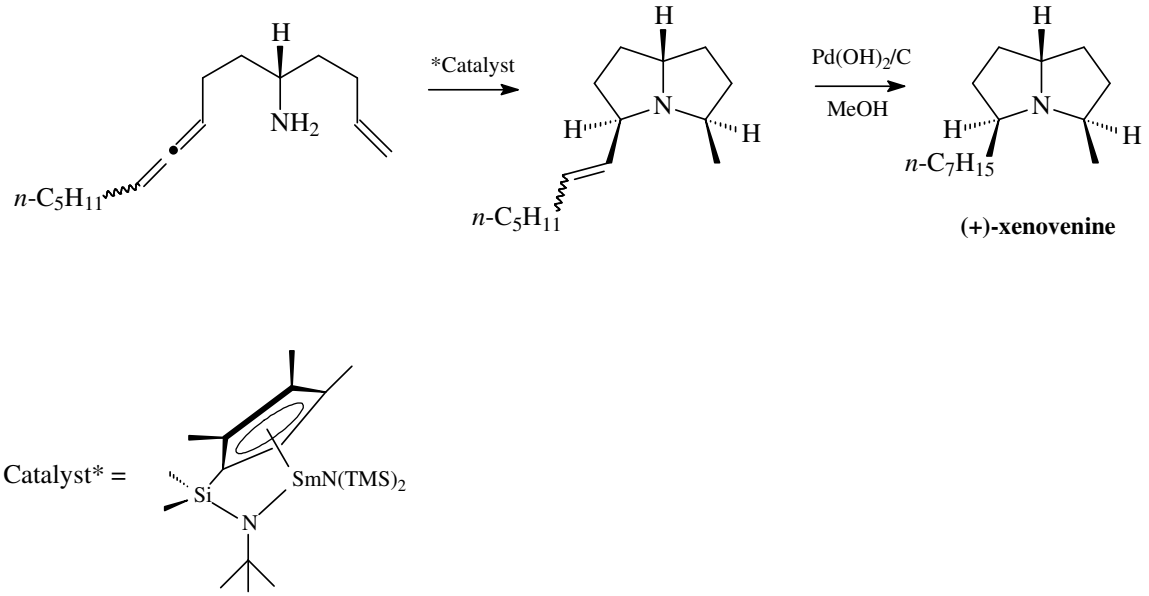

Scheme 12

The above two examples illustrate viable synthetic strategies to indolizidine and pyrrolizidine functionalities, however, by changing the number of carbon atoms in the starting materials, alternative bicyclic ring systems could conceivably be obtained.

Daly[50] reported some examples of naturally occurring organic compounds that contain such scaffolds, a few of which are presented below in figure 13.

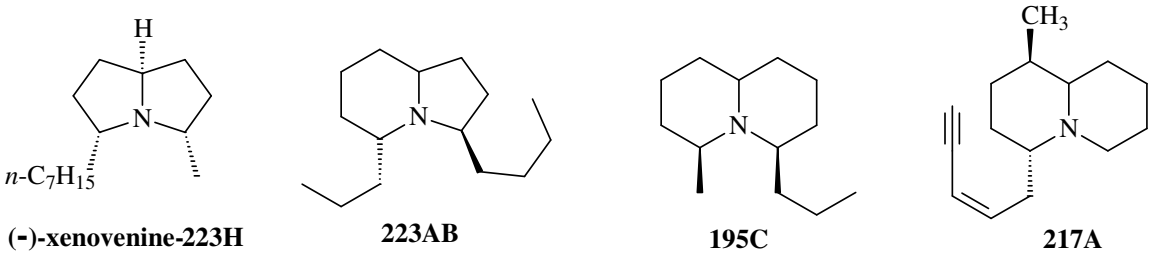

Figure 13

The amount of naturally occurring alkaloids containing such scaffolds is truly vast. For the purpose of this study, attention was focused on the pyrrolizidine alkaloid class. More specifically, we were interested in the application of this hydroamination methodology in the total synthesis of **223H** (xenovenine), a 3,5-disubstituted pyrrolizidine alkaloid.

1.3 Pyrrolizidine Alkaloids

Pyrrolizidine alkaloids constitute an important class of compounds due to their wide spread occurrence within nature, and their toxicity expressed in many biological systems. Derivatives of certain pyrrolizidine alkaloids are found in a wide variety of plant species (*Senecio*, *Crotolaria*, *Heliotropium*, and other genera), some of which have been responsible for numerous livestock poisoning throughout the world.[51] Pyrrolizidine alkaloids have also been found in many species of moths, butterflies, ants, grasshoppers and frogs.[52] Some of these derivatives constitute vital components of certain species' survival mechanisms. For example, many species of moths and butterflies utilize plant derived pyrrolizidine alkaloids as precursors to sex pheromones, a necessity for attracting a mate.[53] The pyrrolizidine alkaloids present in certain ants (*Solenopsis xenovenenum*) and Madagascan frogs (*Mantella*) constitute an array of defensive allomones, providing protection from predators.[54]

Pyrrolizidine alkaloids may be identified by their azabicyclo[3,3,0]octane structural core (Figure 14). The bicyclic ring system is formally numbered as shown, with the bridgehead carbon referred to as position 7a.

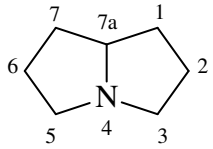

Figure 14

The bridgehead proton (7a-*H*) of the bicyclic scaffold can exist in a *cis*- or *trans*-orientation relative to the nitrogen lone pair. The *trans*-isomer leads to a highly strained and puckered ring system, whereas the *cis*-isomer is much less strained (Figure 15). The *cis*-fused ring system consequently produces more stable compounds,[55] which may support the phenomenon why *cis*-fused ring systems are more predominantly found in nature as opposed to the *trans*-fused isomers.[56] Systematic names are seldom used when

naming pyrrolizidine alkaloids. The alkaloids are rather referred to by their trivial names which are derived from their plant or animal sources. As an example, the alkaloid (–)-xenovenine is isolated from the venom of the thief ant *Solenopsis xenovenenum* (Figure 13, page 20). Pyrrolizidine alkaloids are also referred to by using a code system which employs a boldface number in conjunction with a letter(s). The number represents the nominal mass of the alkaloid, whereas the letters(s) help to distinguish between different alkaloids of the same mass.

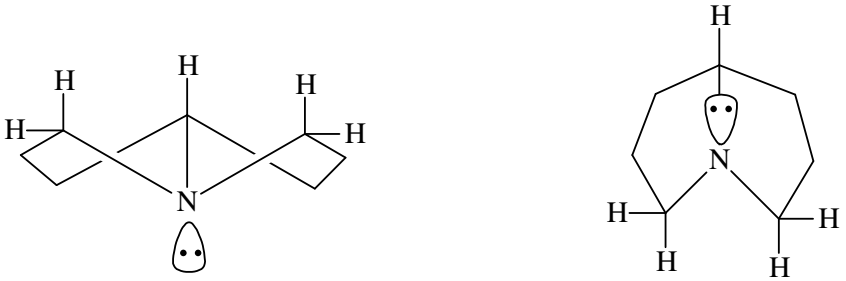

trans-fused *cis*-fused

Figure 15: Trans and Cis-Fused Pyrrolizidine Scaffolds

Pyrrolizidine alkaloids were some of the first natural products to ever be considered carcinogenic.[57] Today, a wealth of literature exists describing the results of *in vivo* pharmacological testing of pyrrolizidine alkaloids on laboratory animals. These experiments show pyrrolizidine alkaloids to be highly hepatotoxic in nature, resulting in a high incidence of tumor formation, and chronic liver damage.[52] Researchers have shown that pyrrolizidine alkaloids themselves are not intrinsically toxic, but rather the toxic 'pyrrolic' metabolites, which are formed as a result of microsomal enzymatic dehydrogenation of pyrrolizidine alkaloids in the liver. It is these 'pyrrolic' metabolites that are responsible for the apparent hepatotoxicity, resulting from their strong alkylating ability, and thus strong affinity for tissue constituents.[52]

The functionality attributed to the toxicity of these compounds has been described by Mattocks,[52] and include:

i. high lipophilicity;
ii. 1,2-unsaturation in the ring;

iii. an esterified hydroxyl group at position 9 and

iv. a bulky, highly branched chain off the ester group.

Although a second hydroxyl group at position 7 is not absolutely necessary for toxicity, results show that if present, and more importantly if it is esterified, a further elevation in pyrrolizidine alkaloid toxicity may result. A few examples of alkaloids containing such functionality required for toxicity are depicted in Figure 16.[52]

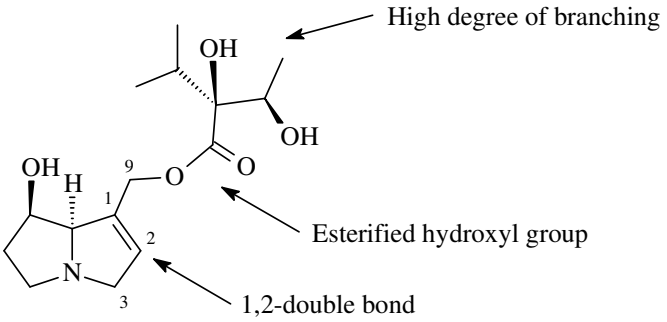

Indicine

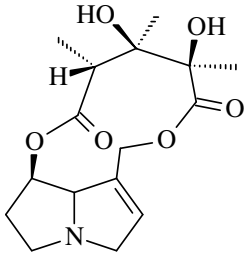

Monocrotaline

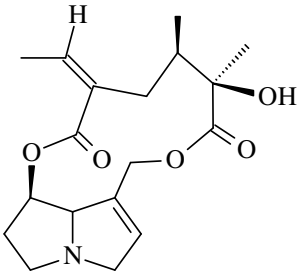

Senecionine

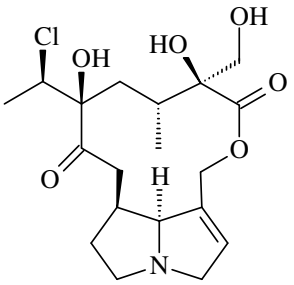

18-Hydroxyjaconine

Figure 16: The Functionality Required for Alkaloid Toxicity[52]

The major detoxification pathways in the liver involve *N*-oxidation and ester hydrolysis, both resulting in the formation of polar, and highly hydrophilic alkaloid derivatives.[52] The presence of highly branched and bulky ester groups obstructs the incidence of ester hydrolysis, rendering these derivatives more toxic than the non-branched, more easily hydrolyzed ester derivatives. Although the *N*-oxide species is a highly soluble detoxification by-product, certain alkaloids can also exist naturally in this non-toxic form.

Despite this, toxicity may still prevail if the pyrrolizidine alkaloid becomes ingested, as the *N*-oxide may translate back into the basic alkaloid in the gastrointestinal tract, and in some cases in the liver.[52] A scheme adapted from Mattocks,[52] showing possible metabolic routes important to pyrrolizidine alkaloid activation and detoxification after ingestion is presented below in Figure 17.

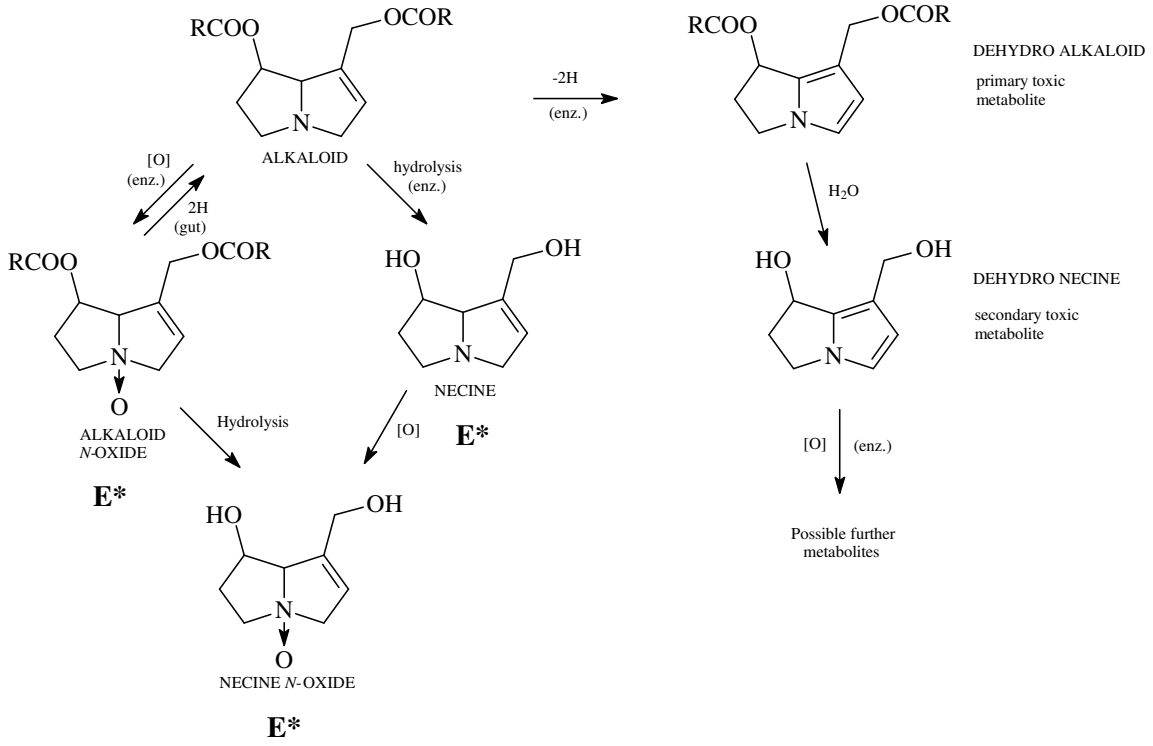

Note: **E*** denotes excretable detoxification byproducts.

Figure 17: Possible Metabolic Routes Important to Pyrrolizidine Alkaloid Activation and Detoxification in the Body[52]

1.3.1 3,5-Disubstituted Pyrrolizidines

The isolation of 3,5-disubstituted pyrrolizidine alkaloids from anuran skin secretions, as well as from certain species of ants, millipedes and beetles has been well documented,[54,58-60] and serve primarily as defensive toxins.[54] In 1980, **223H** (xenovenine) became the first isolated 3,5-disubstituted pyrrolizidine alkaloid, and was extracted from the cryptic thief ant (*Solenopis sp.*).[61] The isolation of 3,5-disubstituted pyrrolizidine

alkaloids from anuran skin was later reported in 1993 from bufonid (*Melanophryniscus*) toads.[58] Subsequently, other species including poison dart frogs (*Mantella*), as well as neotropical ants of the subfamily Myrmicinae, were revealed to contain such alkaloids.[54] One of the poison dart frog alkaloids, *cis*-(5*Z*,7a*E*)-**223H** (xenovenine), was found to be identical to that isolated from the thief ant. Studies have shown that most poison dart frogs can not synthesize their own defense alkaloids, but rather sequester and accumulate them unchanged from dietary sources. Frogs raised in captivity do not hold these toxins, however, will readily accumulate them if added to their diet.[54] Interestingly, a study involving the qualitative analysis of the stomach contents of 15 *Mantella* frogs of four different species showed that ants comprise roughly 74% of their dietary intake.[54] Presently there are about 26 alkaloids, including stereoisomers, that constitute the 3,5-disubstituted pyrrolizidine class, a few of which are illustrated below in Figure 18.

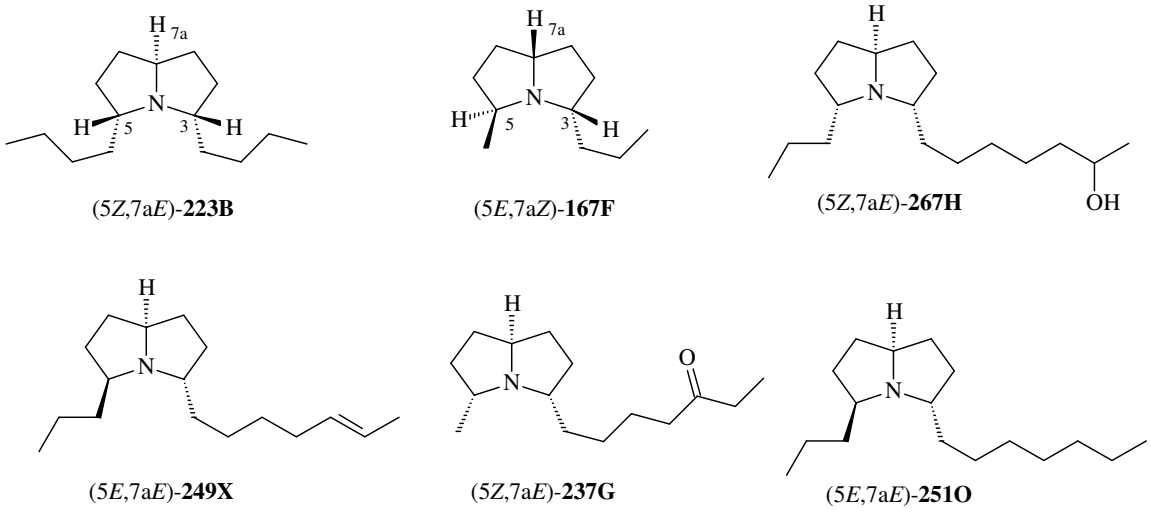

Figure 18

The alkaloids are further differentiated using *zuzammen* (*Z*) and *entgegen* (*E*) terminology, which refer to the orientation of the 5-*H* and 7a-*H* protons relative to the proton at 3-*H*. The pyrrolizidine alkaloid isomer (5*Z*,7a*E*)-**223B** (Figure 8), thus has the proton 5-*H cis*, and proton 7a-*H trans* relative the proton 3-*H*. One must be careful not to confuse this nomenclature with *cis*- and *trans*-fused rings, which refer to the orientation of proton (7a-*H*) relative to the nitrogen lone pair (see Figure 15, page 22).

NMR spectroscopy is a useful tool in distinguishing between the *cis*- or *trans*-fused ring isomers. In the case of *trans*-fused ring isomers, no signals appear further downfield than 2.72 ppm in the entire ^{1}H NMR spectrum. Conversely, *cis*-fused rings contain signals that resonate at *ca*. 3.59-3.66 ppm, which correspond to the bridgehead proton 7a-*H*.[56,62] In the ^{13}C spectra, *trans*-fused isomers contain signals at around 70 ppm, which corresponds to the bridgehead carbon 7a-*C*, whereas the *cis*-fused isomers have 7a-*C* signals that resonate at around 60-66 ppm.[56,61]

Mass Spectrometry of the 3,5-disubstituted pyrrolizidine alkaloid class repeatedly show fragmentation patterns resulting from the loss of α-substituents to the nitrogen, with the higher alkyl substituents being lost more favorably than methyl substituents.[58] Infrared spectroscopy is also used to help identify between stereoisomers, as many of these pyrrolizidine alkaloid isomers show moderate, weak or no Bohlman bands in their absorption spectrum in the region of *ca*. 2800 cm^{-1}.[58]

1.3.2 Routes to 3,5-Disubstituted Pyrrolizidines

The following section describes a variety of synthetic routes accessing 3,5-disubstituted pyrrolizidine alkaloids. Reductive cyclization is a popular ring closure technique. The versatility of this method has been demonstrated using four different approaches which incorporate either:

i. cross-metathesis;[63]
ii. ketopyrrolidines;[59]
iii. triketones;[61] or
iv. nitrodiketones.[64]

In contrast to reductive cyclization, alternative ring closing techniques to be discussed include:

v. double nucleophilic substitution;[56,65] and
vi. reverse Cope elimination.[66]

Finally, an enantioselective synthesis[67] to access a 3,5-disubstituted pyrrolizidine alkaloid **223H** (xenovenine), which employs asymmetric epoxidation as the pivotal step will be discussed. A scheme outlining all that is to be discussed is presented below in Scheme 13.

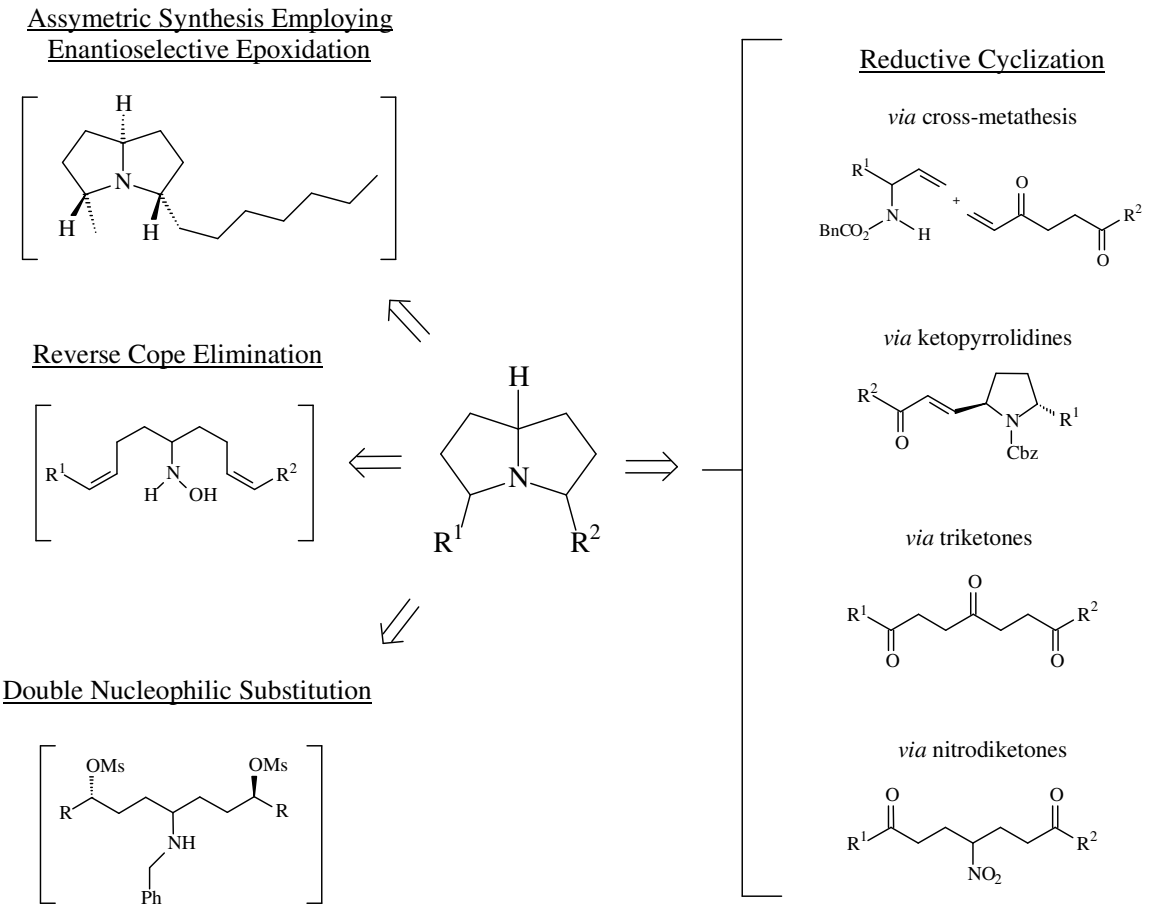

Scheme 13: Various Routes to 3,5-Disubstituted Pyrrolizidines

1.3.2.1 Reductive Cyclization Utilizing Cross-Metathesis

Gebauer *et al*. recently demonstrated the applicability of utilizing cross-metathesis (CM) in conjunction with a reductive cyclization reaction to furnish 3,5-disubstituted pyrrolizidines.[63] The route involved the cross-coupling of *N*-protected allylic amines with α,β-unsaturated ketones, followed by reductive cyclization of the resulting aminoenones (Scheme 14). The *N*-protected allylic amines of the type (R^1=Ph) **1** were

coupled with α,β-unsaturated ketones of the type (R^2 = CH_3) **2** employing 2.5-10% ruthenium catalyst **3** (IHMes = 1,3-bis(2,4,6-trimethylphenyl)-4,5-dihydroimidazol-2-ylidene) in refluxing dichloromethane. The starting materials reacted in a 1:1 ratio to furnish the aminoenone **4** in a 62% yield, and in a *trans*-configured geometry (*E*/*Z* > 20:1).

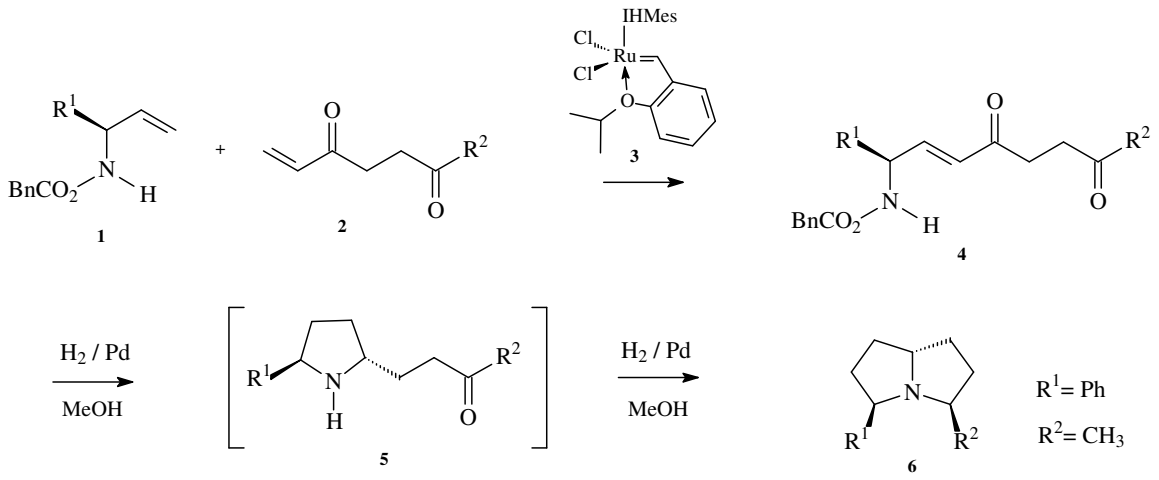

Scheme 14

The aminoenone **4** in methanol, was subject to 1 atm of hydrogen in the presence of 5 mol % Pd(0) to yield the monocyclic pyrrolidine **5**, which underwent a secondary cyclization under the same conditions to afford the 3,5-disubstituted pyrrolizidine **6** in a 68 % yield. This provided the pyrrolizidine alkaloid **6** in a 42% overall yield from the *N*-protected allylic amine **1**, surprisingly however no indication of the diastereomeric excess (de) in the product **6** was mentioned within the article.

1.3.2.2 Reductive Cyclization Utilizing Ketopyrrolidines

The use of ketopyrrolidines as precursors to 3,5-disubstituted pyrrolizidines has been demonstrated by Takahata *et al*. in the synthesis of **223H** (xenovenine), as well as other pyrrolizidine alkaloids (Scheme 15).[59] Sharpless asymmetric dihydroxylation on the diene **7** using a 2,5-diphenyl-4,6-bis(9-*0*-dihydroquinidyl)pyrimidine [mono$(DHQD)_2$-PYR] ligand catalyst yielded the dihydroxyalkene **8** in a 64% yield and with 80% ee.

The dihydroxyalkene **8**, in a two step process, was converted into the alcohol **9** in a 53% yield *via* epoxidation, followed by the regioselective cleavage of the epoxide ring by reaction with 6-hexenylmagnesium bromide and cuprous iodide. The alcohol functionality of **9** was subsequently transformed into an *N*-benzyloxycarbonyl group *via* mesylation (MsCl/pyridine), azidation (NaN_3), reduction ($LiAiH_4$) and carbonation ($CbzCl/K_2CO_3$) to yield the unsaturated carbamate **10**. Upon reaction with mercuric acetate in THF followed by aqueous sodium bromide, the unsaturated carbonate **10** cyclized to give an organomercurial compound, which was demercuralized oxidatively in the presence of $NaBH_4$ and O_2 in DMF to attain the *trans*-diastereomer **11** in a 63% yield.

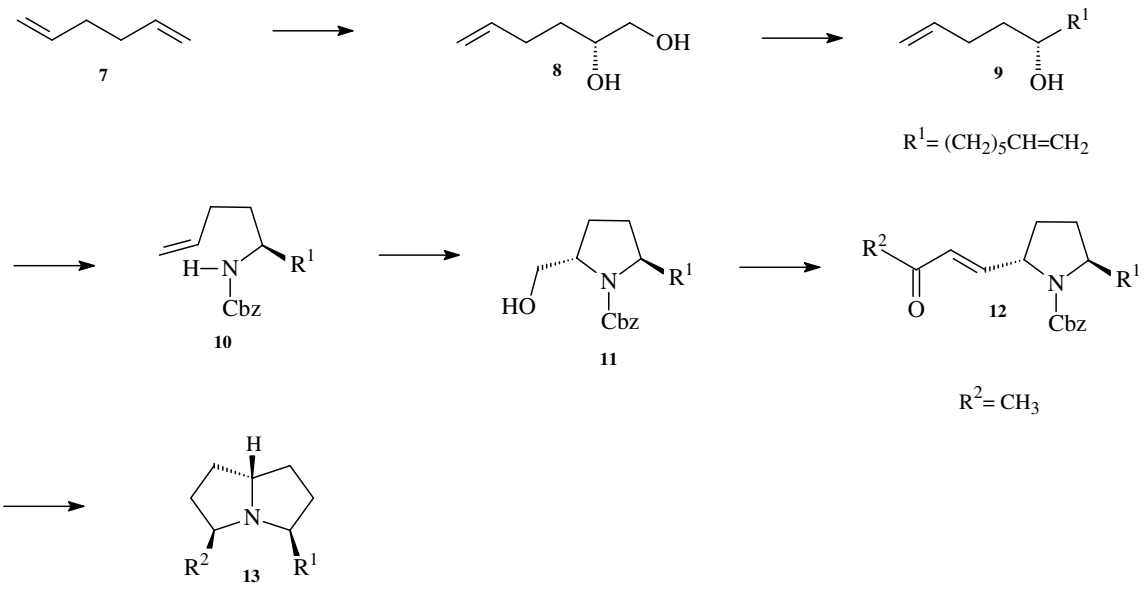

Scheme 15

Elaboration of the hydroxymethyl group of **11** utilizing Swern oxidation conditions using [$(COCl)_2$ / DMSO / Et_3N)], followed by a Horner-Emmons reaction using ($CH_3COCH_2PO(OCH_3)_2$ / $i Pr_2EtN$ / LiCl) furnished the ketopyrrolidine **12** in a 70% yield. Treatment of **12** with H_2 (g), and a catalytic amount of $Pd(OH)_2$ in methanol yielded the 3,5-disubstituted pyrrolizidine **13** in a 59% yield *via* a reductive cyclization process. Although the authors depicted stereoselectivity in the schematics, the degree to

which diastereomeric excess (de) was obtained in the product **13** was not however mentioned.[59]

1.3.2.3 Reductive Cyclization Utilizing Triketones

Jones *et al*., in 1980, demonstrated the use of reductive cyclization of triketones in the first synthesis of **223H** (xenovenine) (Scheme 16).[61] Octanal **14** (R = *n*-C_7H_{15}) was treated with acrolein diethyl acetal and azobisisobutyronitrile (AIBN) followed by hydrolysis to yield 4-oxoundecanal **15**. Compound **15** was subsequently condensed with methyl vinyl ketone in the presence of 5-(2-hydroxyethyl)-4-methyl-3-benzylthiazolium chloride and Et_3N to give the 2,5,8-pentadecatrione **16**, the synthetic precursor to **223H** (xenovenine). **223H** (xenovenine) **17** was ultimately obtained by reaction of **16** with sodium cyanoborohydride and ammonium acetate in a reductive amination fashion.

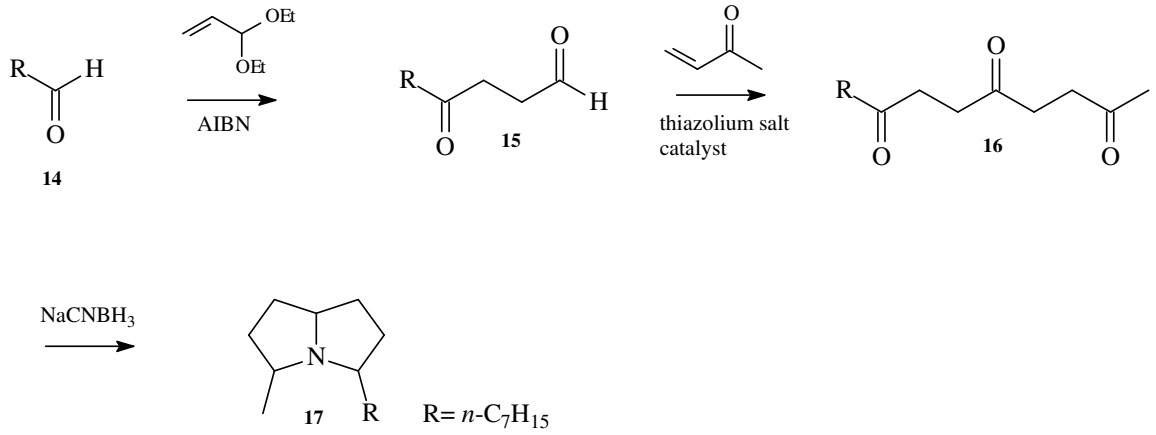

Scheme 16

Despite being a relatively short synthesis, this method showed poor stereo-selectivity, and as a result, four synthetic isomeric products **17a-d** were obtained (Figure 19). NMR and Infrared spectroscopy identified one isomer to exhibit *trans*-fused ring geometry **17a**, whilst the remaining isomers inherited the *cis*-fused ring geometries **17b-c**. Jones reported these isomers to form in a 2:14:2:1 ratio as determined by gas chromatography

and that the major synthetic isomer **17b** had exactly the same retention time as the naturally occurring pyrrolizidine alkaloid.[61]

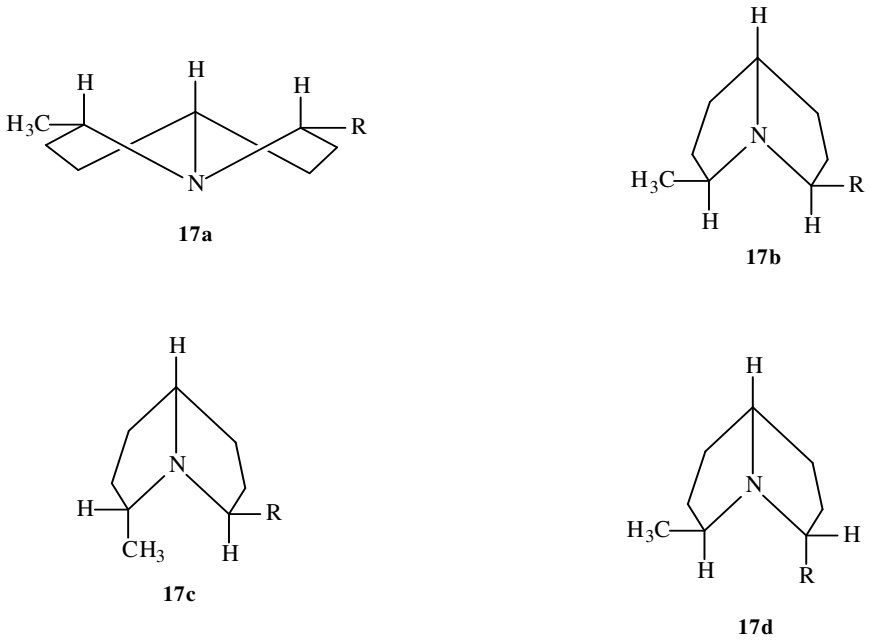

Figure 19: Four Synthetic Isomers for 223H (xenovenine)[61]

1.3.2.4 Reductive Cyclization Utilizing Nitrodiketones

Janowitz *et al*., in 1991, showed that nitrodiketones can be used as precursors to access (5*Z*,7a*E*)-3,5-disubstituted pyrrolizidines, as demonstrated by using **223H** (xenovenine) as the target molecule of choice (Scheme 17).[64] A nitroketone of the type ($R^1 = CH_3$) **18** was condensed in a Michael type reaction with an enone **19** ($R^2 = n\text{-}C_7H_{15}$) in the presence of tributylphosphine, to afford the nitrodiketone **20**. The nitrodiketone was reductively cyclized in the presence of 8-12 atm of hydrogen gas over Pd/C to yield the pyrrolizidine alkaloids **21** and **22** in a 1:12 ratio. The *trans*-fused isomer **22** was converted to a salt by reaction with HCl followed by $Hg(OAc)_2$ oxidation to give an iminium salt. This was immediately reduced using $NaCNBH_3$ and $NaBH_4$ to afford the *cis*-fused pyrrolizidine alkaloid **21**.

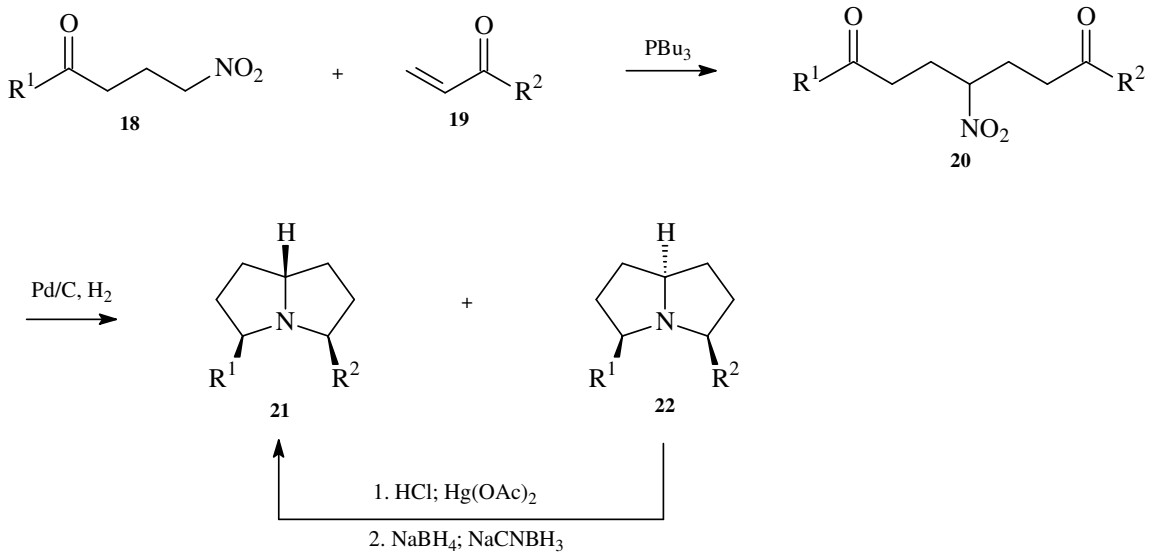

Scheme 17

1.3.2.5 Double Nucleophilic Substitution

The synthesis of (5*E*,7a*E*)-3,5-disubstituted pyrrolizidines using a double nucleophilic substitution reaction was demonstrated by Scarpi *et al*. and is depicted in Scheme 18.[56,65] The nitroketone **23** (R = Ph) was converted into the nitrodiketone **24**, followed by asymmetric reduction into the nitrodiol **25** using either (+)- or (–)-diisopinocampheylchloroborane (DIP-Cl) as the reducing agent. The nitro group was reduced by hydrogenation over Raney Nickel in methanol at 1 atm to give the more nucleophilic aminodiol **26** in an 80% yield. The alcohol moieties were converted into the corresponding mesylates by the reaction of **26** with mesyl chloride and triethylamine to yield the pyrrolizidine alkaloid **28** in a poor yield (20%) *via* the double cyclization of the dimesylate intermediate **27**. Low yields were a result of the undesired mesylation of the nitrogen atom in the aminodiol, and thus an alternative synthetic route was employed. Instead, the amino group of the aminodiol **26** was protected by conversion into the *N*-(*p*-acetyloxy)benzyl derivative **29** in an 84% yield by reaction with *p*-acetyloxybenzaldehyde and $NaBH_3CN$ in methanol at pH 6.

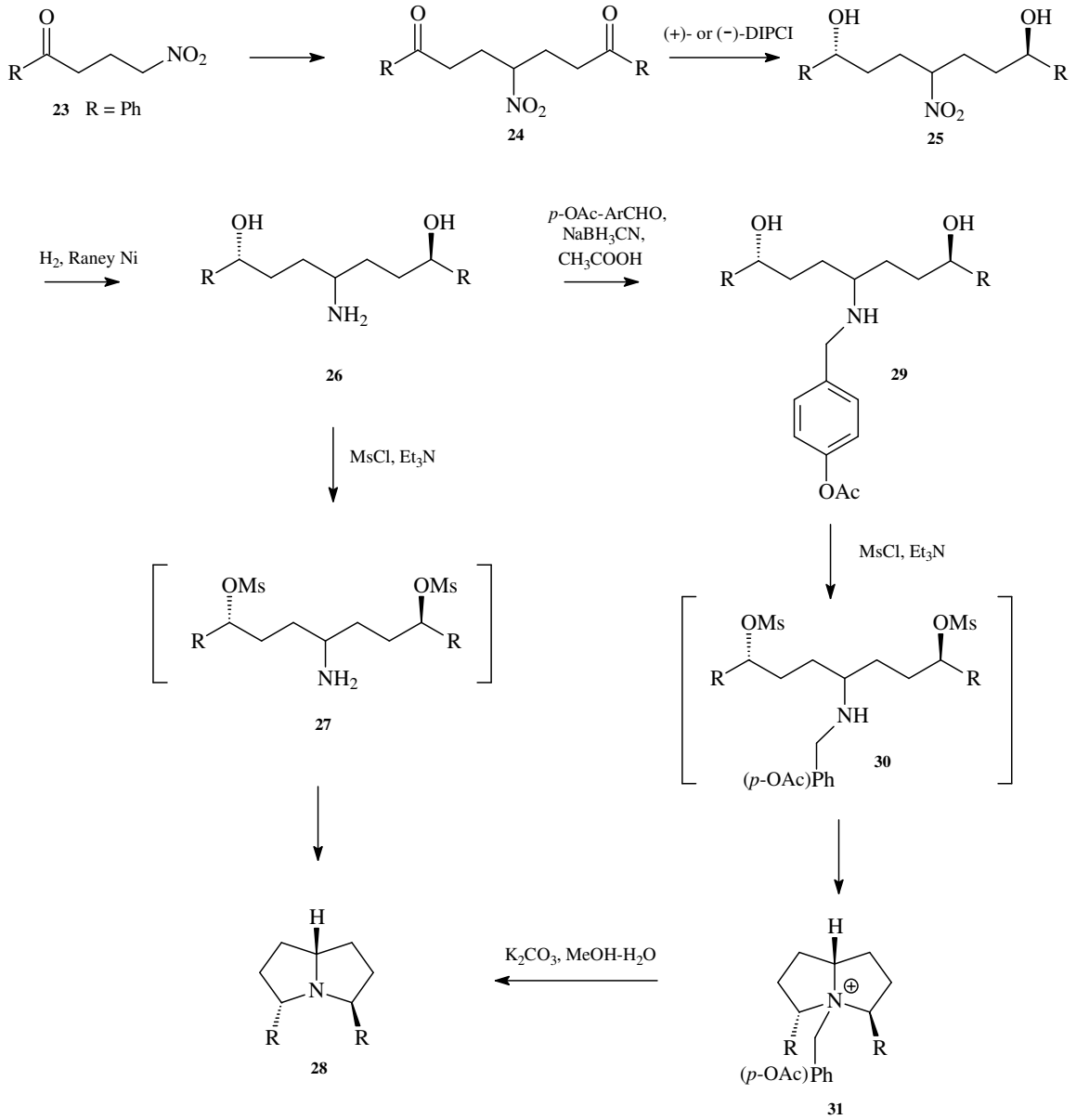

Scheme 18

The *N*-acetyloxybenzyl derivative **29** was treated with mesyl chloride and triethylamine to afford the dimesylate intermediate **30** which underwent subsequent intramolecular nucleophilic substitution to furnish the pyrrolizidine alkaloid salt **31** in a 78% yield. Conversion of **31** into the 3,5-disubstituted pyrrolizidine alkaloid **28** was achieved in a 72% yield by hydrolysis using K_2CO_3 in MeOH/H_2O.

1.3.2.6 Reverse Cope Elimination

A double reverse Cope elimination strategy accessing 3,5-disubstituted pyrrolizidine alkaloids has been demonstrated by Ciganek, and involves the intramolecular addition of an *N*-substituted hydroxylamine across two proximal, unactivated alkenes (Scheme 19).[66]

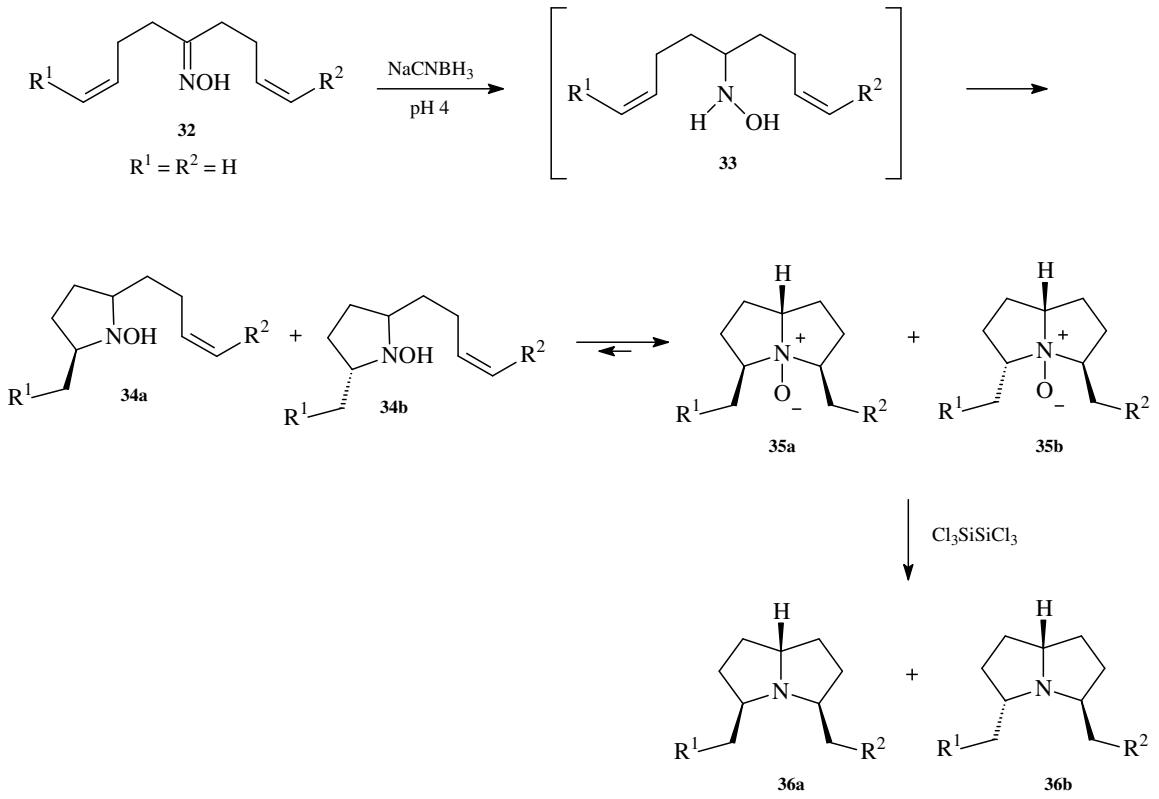

Scheme 19

The oxime **32** ($R^1 = R^2 = H$) was reduced using $NaCNBH_3$ at pH 4 to give the acyclic hydroxylamine intermediate **33**, which underwent a reverse Cope elimination to yield two epimeric monocyclic hydroxylamines **34a** and **34b**. A second reverse Cope elimination partially took place *in situ* forming *N*-oxides **35a** and **35b,** and formed an equilibrium still containing *ca*. 30% of the monocyclic hydroxylamines **34a** and **34b**. It was reported that the equilibrium shifted in favor of the bicyclic analogues **35a** and **35b** by allowing the equilibrium components to stand in a solution of chloroform for two days at room

temperature. This furnished an equilibrium mixture containing only 10% **34a** and **34b**. The *N*-oxides were reduced using hexachlorodisilane to yield a 55:45 mixture of pyrrolizidine alkaloids **36a** and **36b** respectively, and in a 41% overall yield. Although the pyrrolizidine alkaloids were formed in two steps, the synthesis lacks stereocontrol, and forms both the (5*Z*,7a*E*)- and the (5*E*,7a*E*)-3,5-disubstituted pyrrolizidine alkaloids, which were inseparable by distillation.

1.3.2.7 Asymmetric Synthesis Employing Enantioselective Epoxidation

In 1983, Takano *et al*.[67] reported the first enantioselective synthesis of [3S-(3β, 5β, 8α)]-3-heptyl-5-methylpyrrolizidine, the preparation of which is shown in Scheme 20. Triethyl phosphonoacetate was added to 3-(5-methyl-2-furyl)propionaldehyde **37** in a Horner-Emmons reaction, to afford the unsaturated diester **38** in a 96% yield. Reduction of **38** using di-isobutylaluminium hydride afforded the allylic alcohol **39** in a 90% yield, which was subsequently oxidized using *t*-butyl hydroperoxide in the presence of (+)-diethyl-L-tartrate and titanium isopropoxide to furnish the chiral epoxide **40**, in a 92% yield. The resulting epoxide moiety was cleaved regioselectively by reaction with bis-(2-methoxyethoxy)aluminium hydride to yield the 1,3-diol **41** in a 93% yield. One molar equivalent of benzyl chloride was added to **41** to produce the primary benzoate **42** in a 65% yield. The secondary hydroxyl group of **42** was subject to Mitsunobu's conditions which facilitated the substitution of the hydroxyl group for phthalimide and afforded **43** in an 82% yield with an inversion of configuration. Debenzylation of **43** followed by reaction with hydrazine hydrate formed the amino alcohol **45** in a 72% overall yield from **43** *via* the alcohol **44**. Pyrrolidine **46** was formed by reaction of **45** with a slight excess of perchloric acid. Sodium cyanoborohydride was added to the crude pyrrolinium perchlorate of **46** at pH 4 to furnish a (1:1) mixture of the pyrrolizidines **49** and **50** in a stereoselective manor and with an overall yield of 57% from **45**. The stereoselectivity observed in this transformation is due to the participation of the hydroxyl group of **46** which directs the delivery of the hydride (or cyanide) ion to the *si*-face of the imino group

as shown by intermediates **47** and **48**. The nitrile **50** was quantitatively converted back into the pyrrolizidine **49** by reaction with sodium borohydride in ethanol.

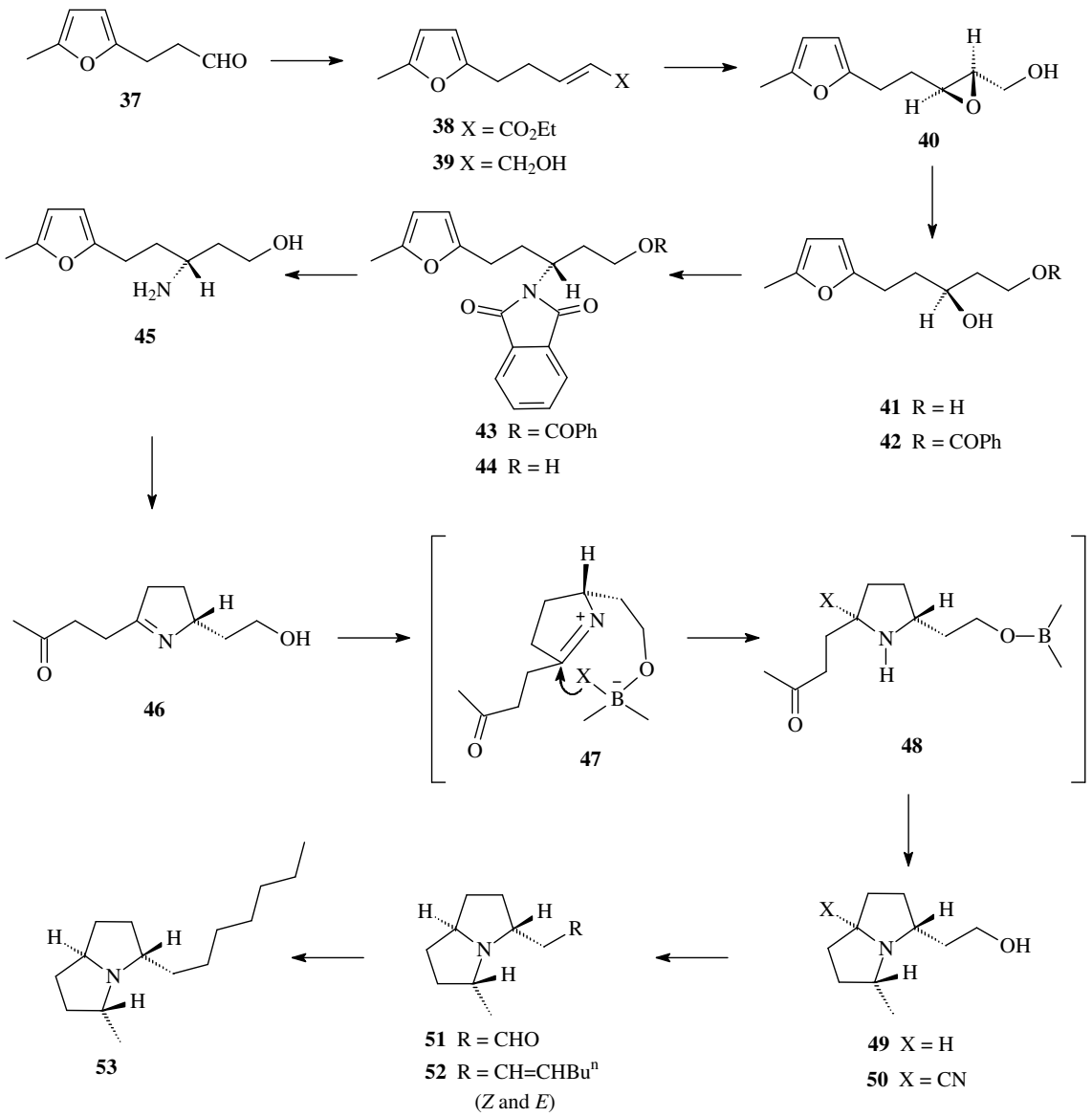

Scheme 20

The alcohol functionality of **49** was oxidized using Moffatt-Swern conditions to yield an unstable amino aldehyde **51**, which was immediately reacted with *n*-pentylidenetriphenylphosphorane in a Wittig type condensation reaction to afford an (*E/Z*) mixture of the olefin **52**. The olefin mixture **52** was subject to catalytic

hydrogenation over platinum giving rise the desired 3,5-disubstituted pyrrolizidine alkaloid **53**, $[\alpha]_D$ – 6.25° (*c* 0.16, $CHCl_3$) in a 28% overall yield from **49**.

The ^{1}H-NMR, Infrared and Mass spectra obtained for this synthetic alkaloid **53** were shown to be identical when compared with the spectroscopic data obtained for the naturally occurring *cis*-fused derivative reported by Jones.[61,67]

1.4 Previous Work by the Group

Previous research within our group resulted in the development of a novel synthetic route that can access pyrrole, and *N*-bridgehead pyrrole functionality.[68] The former were obtained *via* a one pot reaction containing vinylogous amides **54** and propargyl bromide in the presence of $AgNO_3$ in acetonitrile, to afford pyrrole derivatives of the type **55**, albeit in low yields, *ca*. 25% (Scheme 21).[6]

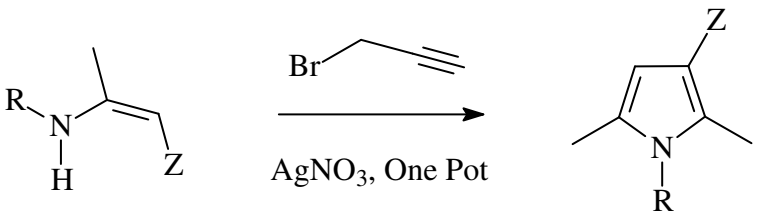

54 **55**

Z = COMe
R = Me, Bu, Cy, Bn, Ph

Scheme 21

These yields were improved upon by Dovey,[6] by implementing an initial base mediated *C*-propargylation on the vinylogous amides **54** followed, by $AgNO_3$ catalyzed hydroamination of the *C*-propargyl vinylogous amides **56** to furnish the pyrrole derivatives **55** (Scheme 22). It is expected that the *C*-propargyl vinylogous amide **56** must initially undergo isomerization (presumably *via* metal catalyzed isomerization in the presence of the hydroamination catalyst)[69] to bring the anime nitrogen in close proximity

to the alkyne, facilitating hydroamination. This generates the exocyclic intermediate **57**, which presumably, *via* a 1,3-hydride shift, furnishes the aromatic pyrrole **55**.

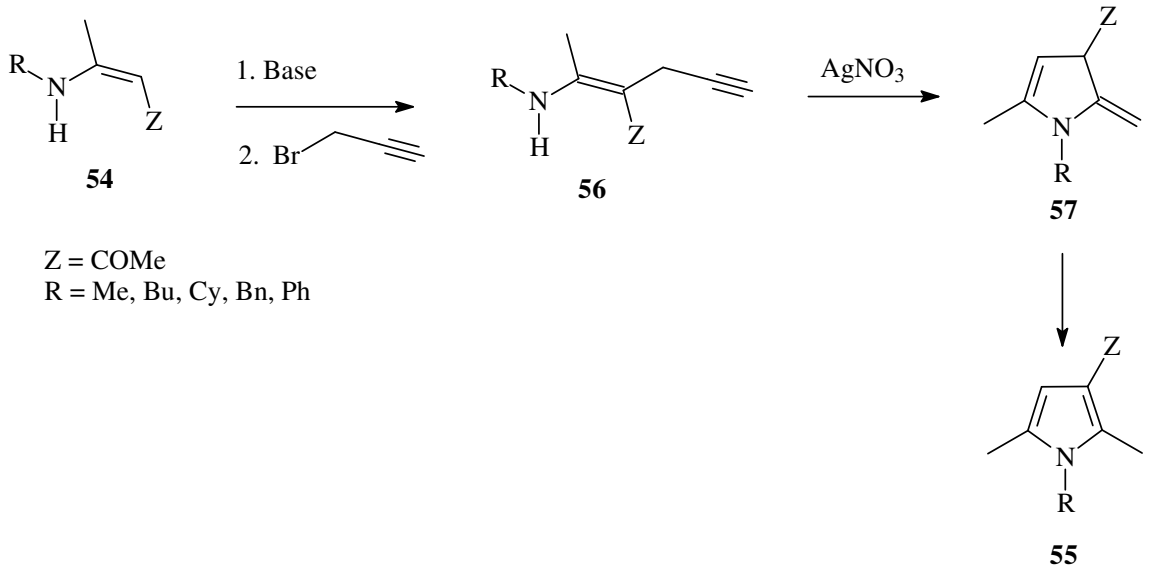

Scheme 22

This methodology afforded excellent yields of *C*-propargyl vinylogous amides **56** and pyrroles **55**, and thus resulted in an overall improvement in the yields of the pyrrole derivatives **55**, as depicted in Table 3.[6]

Table 3

R	Yield 54 (%)	Base	Yield 56 (%)	Yield 55 (%)
Me	80	*n*-BuLi	55	93
Me	80	NaH	46	93
n-Bu	76	*n*-BuLi	51	95
Cy	88	*n*-BuLi	52	87
t-Bu	6	-	-	-
Ph	94	*n*-BuLi	21	75
Bn	95	*n*-BuLi	-	43

This methodology was further extended upon so as to allow for the preparation of bicyclic *N*-bridgehead pyrroles **61** (n = 1,2,3, Scheme 23).[70] The *C*-propargyl secondary enaminones **59** were obtained in a 66% (n = 1), 13% (n = 2) and 24% (n = 3) respectively. The $AgNO_3$ mediated hydroamination of these *C*-propargyl compounds

were much more profitable and afforded the bicyclic *N*-bridgehead pyrrole derivatives in a 75% (n = 1), 75% (n = 2) and 71% (n = 3) yield respectively under microwave conditions. It is expected that **59** will undergo isomerization prior to hydroamination as shown earlier with the acyclic derivatives in Scheme 22.

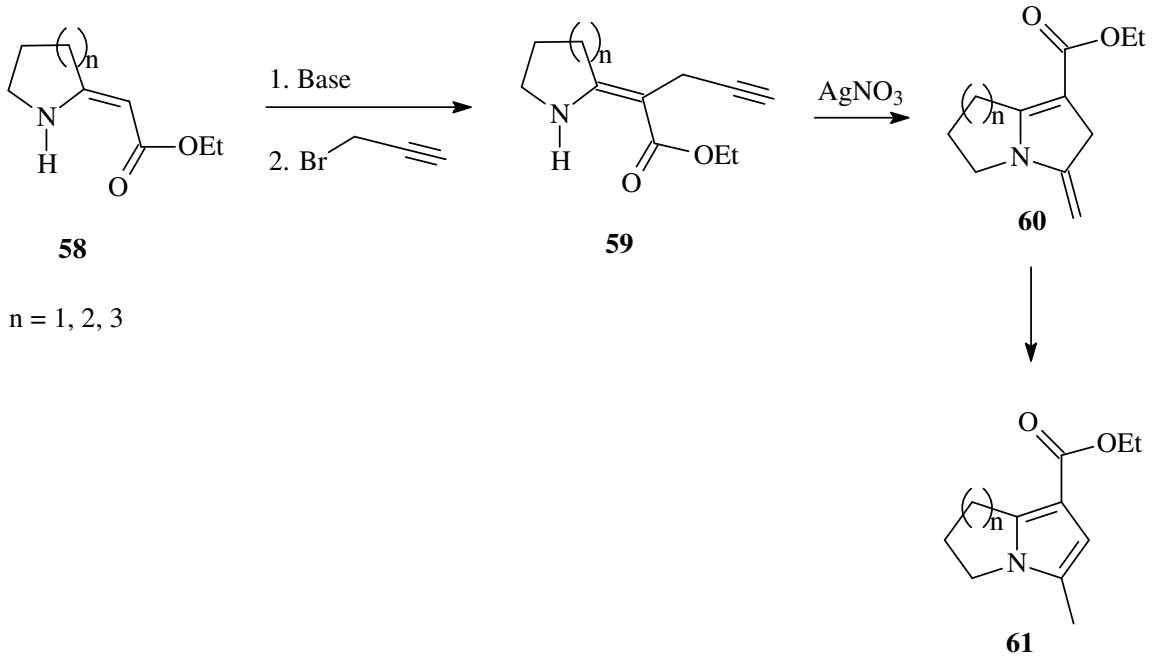

Scheme 23

1.5 Objectives of this Work

Stemming from previous research done within this group, the initial focus of our research was directed towards a better understanding of the role of the catalyst during the pivotal hydroamination step, which is the key step towards the bicyclic *N*-bridgehead pyrroles. We were also interested in the effect that changing the metal salt's counterion had on the hydroamination process. The primary objective of this work was to exploit this resourceful hydroamination methodology into the total synthesis of a natural product. The natural product of choice was **223H** (xenovenine), a biologically active 3,5-disubstituted pyrrolizidine alkaloid isolated from the venom of the cryptic thief ant,[61] and the skin secretions of poisonous Madagascan *Mantella* frogs.[54]

2 Discussion

2.1 Preface

In order to gain a better understanding of the role that the catalyst plays in the key hydroamination reaction, our initial aim for this project was focused on performing a catalytic hydroamination study in which a number of transition metal salts were employed as potential hydroamination catalysts. We were also interested in the effect that changing the metal salt's counterion had on the hydroamination reaction. Our primary objective however was to exploit this resourceful hydroamination methodology as the pivotal step in the total synthesis of a pyrrolizidine ant alkaloid **223H** (xenovenine) (**62**, Figure 20).

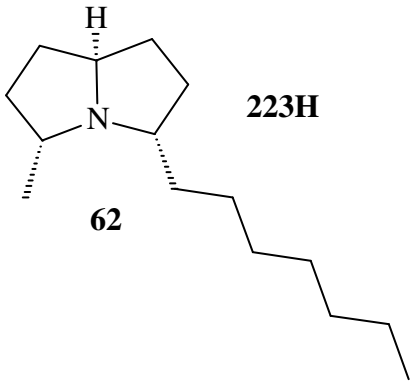

Figure 20

2.2 Catalytic Hydroamination Study

In order to perform the following catalytic hydroamination study, we were in need of a short, simple and high yielding synthesis that could provide sufficient amounts of starting material for the study at hand. A model reaction was thus chosen and exclusively used throughout the duration of the catalytic study which involved the cyclization of a *C*-

propargyl vinylogous amide **66** into a pyrrole **67** (Scheme 24). The following scheme also outlines the proposed synthesis for the *C*-propargyl vinylogous amide hydroamination precursor **66** starting from the coupling of *n*-butylamine **63** and ethyl acetoacetate **64**.

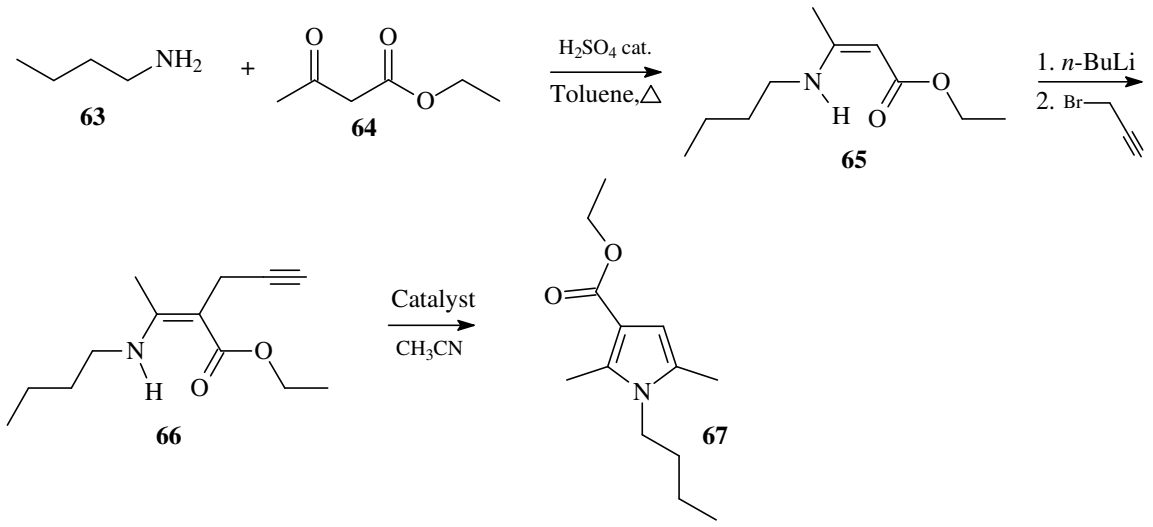

Scheme 24

2.2.1 Preparation of ethyl (*Z*)-3-(butylamino)-2-butenoate [65]

The vinylogous amide **65** was prepared in an excellent isolated yield (96%) by the reaction of *n*-butylamine **63** and ethyl acetoacetate **64** in toluene using a Dean and Stark apparatus (Scheme 25).

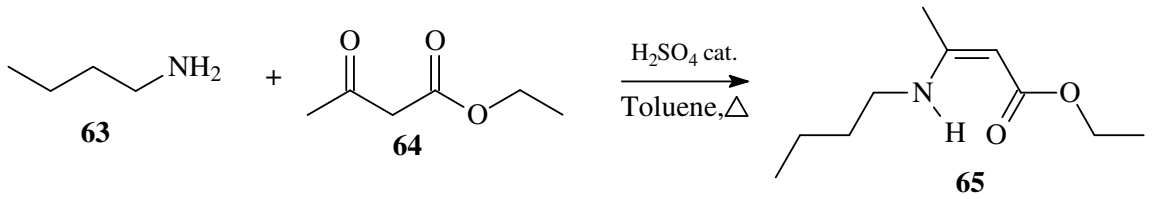

Scheme 25

The reaction mixture was concentrated *in vacuo* to yield the product **65** as a yellow oil. Its structure was confirmed using one and two dimensional NMR spectroscopy. By

analysis of the 2D NOESY spectrum (Figure 21) obtained for the vinylogous amide product, it was noticed that the reaction was regioselective furnishing a product with a *Z*-configuration about the double bond, which is not surprising since it allows for the incidence of hydrogen bonding between the amino proton and the carbonyl oxygen. Absence of coupling between the proton 2-*H* and the amino proton along with the presence of coupling between the proton 2-*H* and the methyl protons 4-*H* provided evidence for a *Z*-configuration about the double bond.

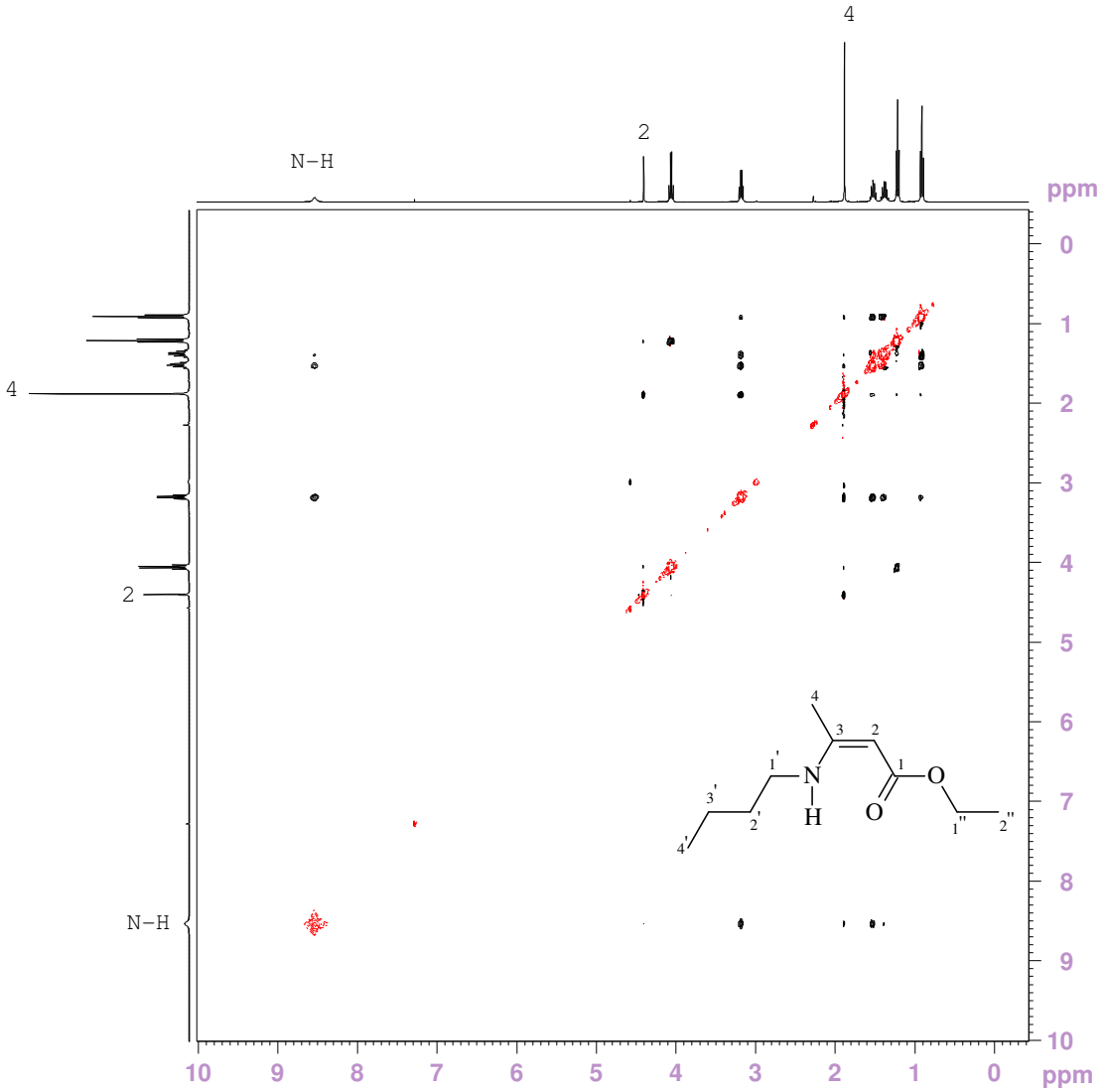

Figure 21: 2D NOESY Spectrum for ethyl (*Z*)-3-(butylamino)-2-butenoate

This configuration was consistent to the observed geometries reported by Dovey[71] and Rechsteiner.[72] High Resolution Mass Spectrometry was performed on the product which

provided a mass of 186.1499 g.mol^{-1} and compared favorably to the calculated (M+H) mass of 186.1494 g.mol^{-1} for $C_{10}H_{20}N0_2$. The ^{1}H NMR spectrum (Figure 22) showed the oil to be sufficiently pure and free from unreacted starting materials.

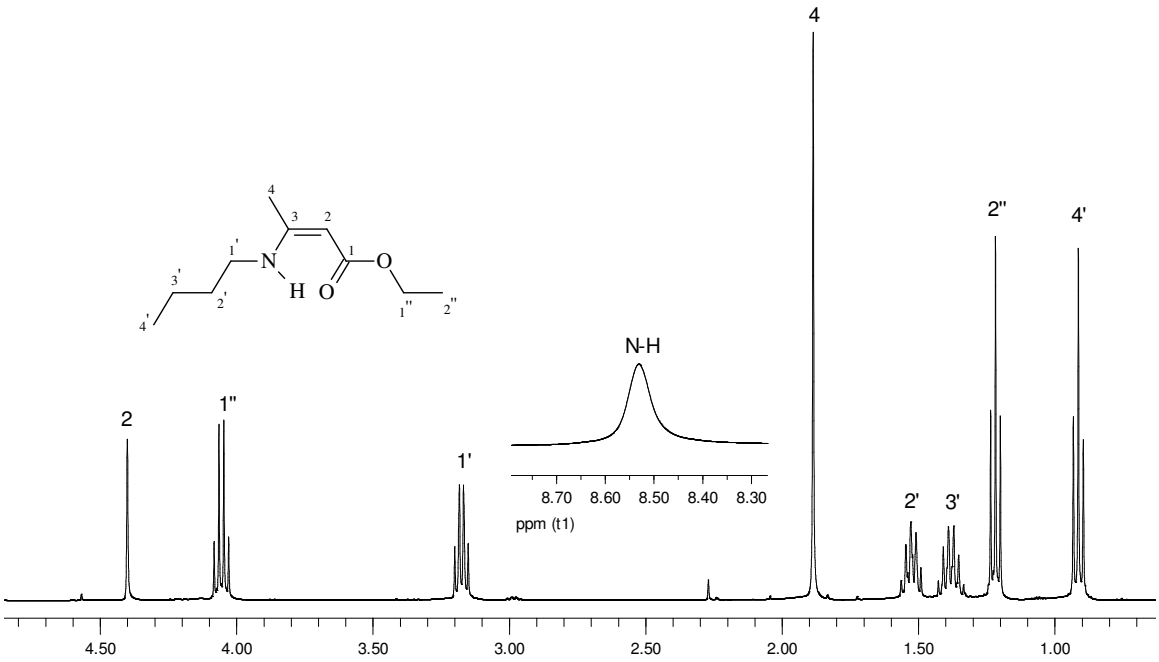

Figure 22: ^{1}H NMR Spectrum for ethyl (*Z*)-3-(butylamino)-2-butenoate

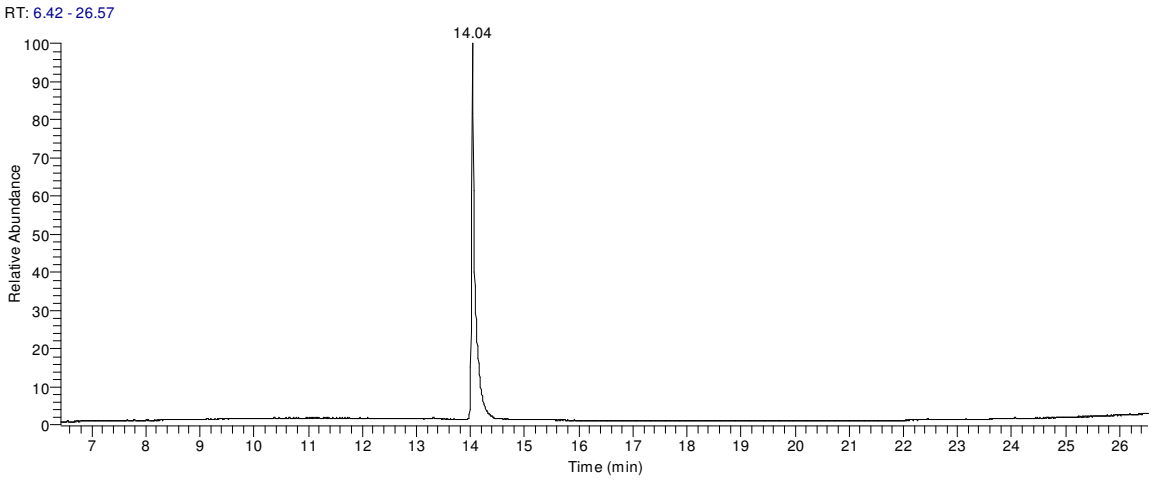

Figure 23

The oil was placed under high vacuum for 3 hours and sent for GC-MS analysis The above chromatograph (Figure 23) showed the presence of one compound with a retention

time of 14.04 min and thus the pure oil was carried onto the next step without further purification.

2.2.2 Preparation of ethyl 2-[(*Z*)-1-(butylamino)ethylidene]-4-pentynoate [66]

The preparation of ethyl 2-[(*Z*)-1-(butylamino)ethylidene]-4-pentynoate **66** was successfully achieved by reaction of the vinylogous amide **65** with *n*-butyllithium and propargyl bromide in a 78% yield as determined by ^{1}H NMR spectroscopy (Scheme 26). The yield was determined by integration and comparison of the N-H proton singlet peaks at 8.51 ppm and 9.37 ppm in the ^{1}H NMR spectrum which correspond to each amino proton on the starting material **65** and product **66** respectively.

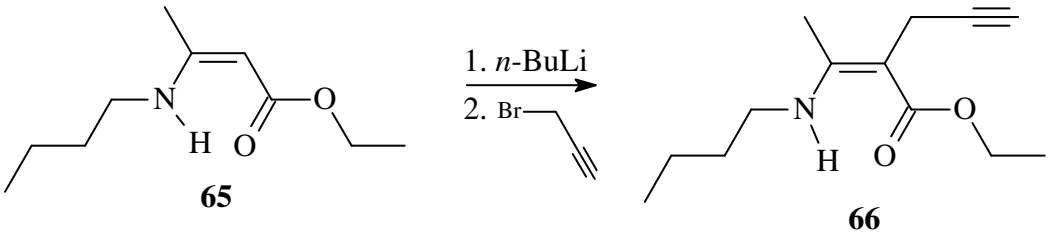

Scheme 26

The chemistry associated with these enamine derivatives is worth mentioning as they behave as ambident nucleophiles,[73] i.e. they possess two nucleophilic sites. Upon abstraction of the amino proton of **65** with a base, two resonance forms (**A** + **B**) can exist due to the ability of a lone pair on the nitrogen to migrate forming an imine and a nucleophilic carbanion *alpha* to the carbonyl (Figure 24).

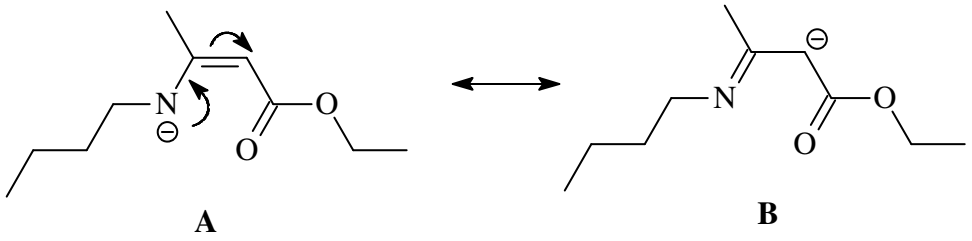

Figure 24

The structure of the product was confirmed using ^{1}H and ^{13}C NMR spectroscopy and GC-MS. Interestingly, the sole product from this reaction was the *C*-propargylated product resulting from the nucleophilic resonance hybrid **B** undergoing an S_N2 type nucleophilic substitution with propargyl bromide. The preference for these enamine derivatives to undergo *C*-propargylation over *N*-propargylation can be rationalized using Hard Soft Acid Base (HSAB) theory.[73] According to this theory, hard bases will react with hard acids and soft bases will react with soft acids. As a result, it is preferable for the 'soft' electrophilic centre of the propargyl bromide to react with the softer nucleophilic site of hybrid **B** as opposed to the harder nucleophilic site of hybrid **A** of the ambident nucleophile.[73]

Careful analysis of the ^{1}H NMR spectrum (Figure 25) of the reaction mixture shows that new peaks have appeared resulting from the newly added propargyl group, and certain signals from the starting material have shifted further downfield in the product spectrum due to their new electronic environment.

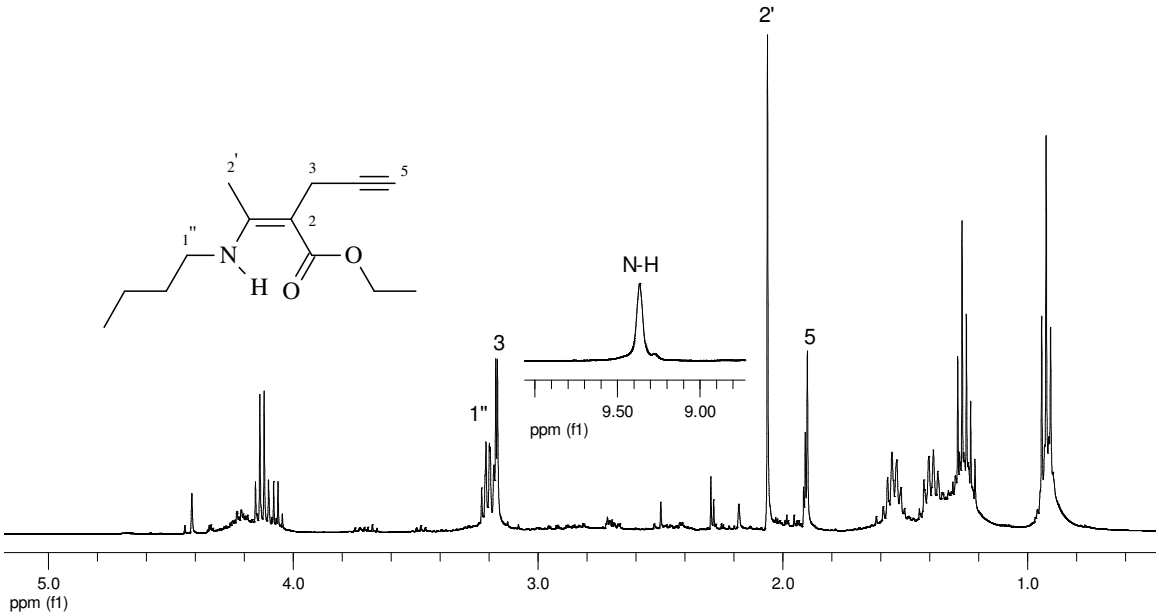

Figure 25: Crude ^{1}H NMR Spectrum for ethyl 2-[(*Z*)-1-(butylamino)ethylidene]-4-pentynoate

The N-*H* singlet is still present, but has shifted further downfield from 8.5 ppm in the starting material **65** (Figure 22) to 9.4 ppm in the product **66** (Figure 25). The methyl

singlet has also shifted downfield from 1.9 ppm in the starting material **65** (Figure 22) to 2.1 ppm in the product **66** (Figure 25). Additionally, a new peak has appeared at 3.2 ppm which corresponds to the CH_2 protons at position 3, which exist as a doublet due to long range coupling through to the acetylenic proton at position 5. The acetylenic proton 5 resonates at 1.9 ppm and exists as a singlet. The ^{13}C NMR data was also analyzed and was consistent with expectations. It was accepted that the *Z*-configuration about the double bond was conserved in the *C*-propargylation reaction due to the downfield position of the N-*H* singlet (9.37 ppm) in the *C*-progargylated product **66**. The same geometric isomer was reported by Dovey,[6] whose assignment was made based on the analogous downfield shift of the N-*H* proton singlet as well as from NOE experiments. The ^1H NMR spectrum showed the exclusive production of the desired product **66** without the formation of undesirable side products, however small amounts of starting material remained. The mixture was deemed sufficiently pure to be carried on to the next step without further purification.

2.2.3 Preparation of ethyl 1-butyl-2,5-dimethyl-1*H* pyrrole-3-carboxylate [67]

With the *C*-propargyl vinylogous amide **66** in hand, a catalytic hydroamination study was conducted on the following hydroamination reaction (Scheme 27).

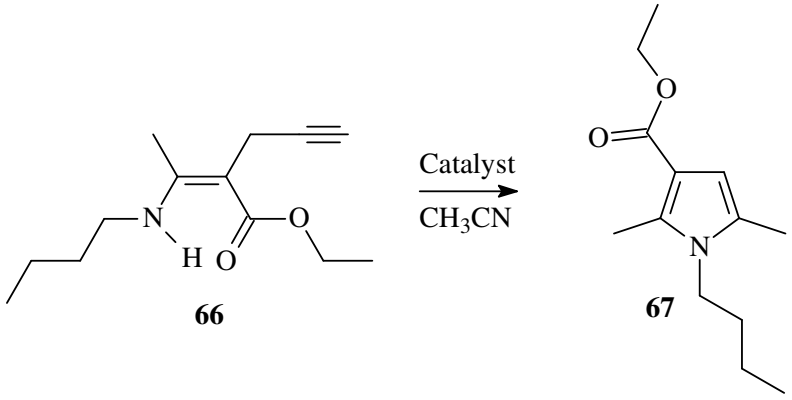

66 **67**

Scheme 27

The *C*-propargyl vinylogous amide **66** was to be converted into the corresponding pyrrole **67** under predetermined reaction conditions.

Due to the previous success employing $AgNO_3$ as a hydroamination catalyst, focus for this study was placed on metals of groups 11 and 12 and their counter ions. The derivatives that were utilized included the oxide, acetate, nitrate and chloride derivatives of the group 11 and 12 transition metals namely Cu(II), Ag(I), Zn(II), Cd(II) and Hg(II) in the oxidation states provided. A trial hydroamination reaction was initially attempted employing 200 mg of the *C*-propargyl vinylogous amide, which was subjected to 100 watts of microwave irradiation for 1 minute in acetonitrile, and using $AgNO_3$ (0.2 equiv.) as the hydroamination catalyst. To our delight, the ^{1}H NMR spectrum (Figure 26) showed a 92% conversion of starting material **66** to product **67**. The compound was fully characterized using both one and two dimensional NMR spectroscopy, and the assignments are depicted in Figure 26.

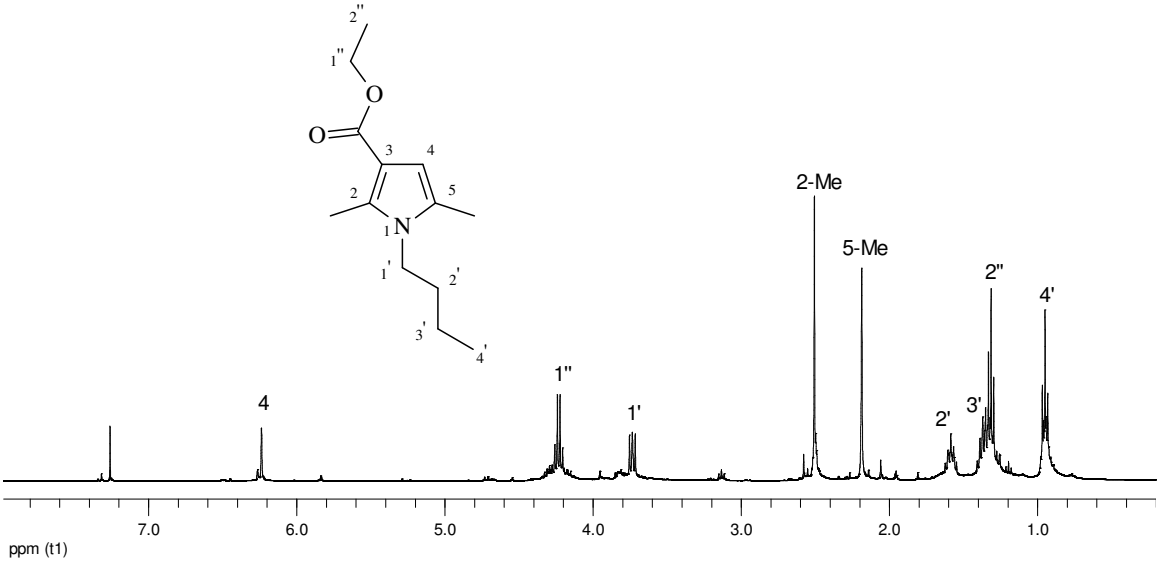

Figure 26: ^{1}H NMR Spectrum for ethyl 1-butyl-2,5-dimethyl-1*H*-pyrrole-3-carboxylate

Our immediate efforts became focused on determining a milder hydroamination reaction condition that did not encourage reaction completion so that the catalytic activities for the various transition metal catalysts could be evaluated. It was subsequently determined that a suitable reaction condition would involve subjecting 200 mg of the *C*-propargyl

vinylogous amide to 40 watts of microwave irradiation for 20 seconds in the presence of a catalyst (0.04 equiv.) in acetonitrile employing concomitant cooling within the microwave cavity. This milder reaction condition furnished pyrrole **67** in a 14% yield and was thus implemented in the following catalytic hydroamination study. The results from this study were accepted by Tetrahedron Letters for publication,[69] and a copy of the paper follows.*

* Copy of paper included in the body of text as per faculty guidelines.

Available online at www.sciencedirect.com
ScienceDirect
Tetrahedron Letters 49 (2008) 411–414
Tetrahedron Letters

An assessment of late transition metals as hydroamination catalysts in the cyclization of *C*-propargyl vinylogous amides into pyrroles

Allan M. Prior, Ross S. Robinson *

Warren Research Laboratory, School of Chemistry, University of KwaZulu-Natal, Corner of Golf and Ridge Roads, Private Bag X01, Scottsville, Pietermaritzburg 3209, South Africa

Received 21 August 2007; revised 12 November 2007; accepted 21 November 2007
Available online 24 November 2007

Abstract

It has been shown that common and inexpensive salts of the late transition metals serve as effective hydroamination catalysts in the conversion of *C*-propargyl vinylogous amides into pyrroles. The oxide, acetate, nitrate and chloride derivatives of Cu(II), Ag(I), Zn(II), Cd(II) and Hg(II) were utilized as hydroamination catalysts in the oxidation states shown. Although the Zn(II) catalysts with the exception of ZnO afforded the highest yields of product under mild conditions, all of the group 12 metal catalysts provided excellent yields of product under more forcing conditions. The nature of the counterion plays an important role in the efficiency of hydroamination reactions, as well as the Lewis acidity of the metal centre.
© 2007 Elsevier Ltd. All rights reserved.

The construction of C–N bonds is an important and often challenging synthetic step, which validates the continued research into alternative catalytic approaches towards their formation.[1] The inter- or intramolecular addition of secondary amines, primary amines or ammonia to double and triple bonds, namely, hydroamination, has attracted a great deal of attention in organic synthesis due to its ability and versatility in forming such bonds.[2] Howk et al. in 1954 showed that primary amines and ammonia could be added to alkenes in the presence of an alkali metal or its hydride, however, high temperatures and pressures were required to bring about such reactions.[3] More recently, milder reaction conditions employing catalysts based on early transition metals, groups 3–5,[4–6] late transition metals, groups 9–12[7] as well as early lanthanides[8] and actinides[9] have been reported.

Dovey et al. recently published a novel synthetic approach towards the preparation of functionalized pyrroles **4a** (Z = COMe) via the C-propargylation of vinylogous amides **1a** followed by intramolecular hydroamination of the *C*-propargyl vinylogous amides **2a** (Scheme 1).[10] The hydroamination reaction proceeds via

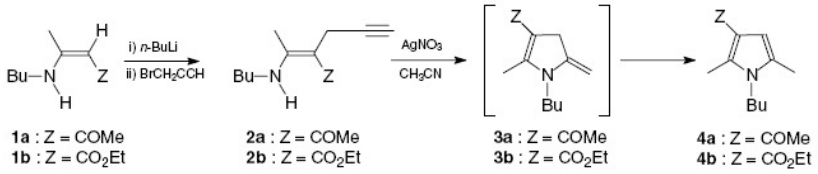

1a : Z = COMe
1b : Z = CO_2Et
2a : Z = COMe
2b : Z = CO_2Et
3a : Z = COMe
3b : Z = CO_2Et
4a : Z = COMe
4b : Z = CO_2Et

Scheme 1.

* Corresponding author. Tel.: +27 33 260 6272; fax: +27 33 260 5009.
E-mail address: robinsonr@ukzn.ac.za (R.S. Robinson).

0040-4039/$ - see front matter © 2007 Elsevier Ltd. All rights reserved.
doi:10.1016/j.tetlet.2007.11.116

the cyclic enamine intermediate **3a** in the presence of a catalytic amount (0.2 equiv) of silver nitrate in acetonitrile at room temperature to afford product **4a** in 95% yield typically after 16–20 h.[10]

Reported herein is a catalytic study assessing the efficacy of late transition metals in facilitating the cyclization of **2b** ($Z = CO_2Et$) into the corresponding pyrrole **4b** under microwave conditions, and in addition, an investigation of the influence of various counterions. It is advantageous to employ the ester functionality due to its ability and versatility in being subsequently transformed into a wide array of functional groups.[11] The ester functionality may alternatively be converted into a carboxylic acid and subsequently removed via decarboxylation.[12] The oxide, acetate, nitrate and chloride, derivatives of group 11 and 12 metals, namely, Cu(II), Ag(I), Zn(II), Cd(II) and Hg(II) were chosen as potential hydroamination catalysts in the oxidation states provided. To perform the study we were in need of a synthetic route to access *C*-propargyl vinylogous amides of the type ($Z = CO_2Et$) **2b**.

In our hands we were able to facilitate this reaction via the direct C-propargylation of the vinylogous amide **1b** ($Z = CO_2Et$) to afford product **2b** in 80% yield as determined by ^1H NMR spectroscopy.[13] This result is in contrast to the report by Dovey et al.,[10] in which the *C*-propargyl vinylogous amides of type **2b** were not successfully synthesized. The *cis*-configuration about the double bond was preserved during the C-propargylation reaction due to hydrogen bonding between the amine N–H and the carbonyl oxygen. This was evident from the downfield shift of the N–H signals in the ^1H NMR spectra, and by NOE experiments.[10]

With the *C*-propargyl vinylogous amides in hand we set about carrying out the microwave assisted hydroamination study utilizing each transition metal at a catalytic loading of 0.04 equiv in acetonitrile (Table 1).[14] Interestingly, all transformations were completely regioselective, yielding exclusively Markovnikov addition type products. These products resulted from the *C*-propargyl vinylogous amides undergoing 5-*exo*-dig cyclizations affording aromatic, 5-membered pyrroles, as opposed to 6-*endo*-dig cyclizations, to form non-aromatic, 6-membered heterocycles.[15]

Due to the C–C triple bond being *trans* relative to the amine in the starting material **2b**, isomerization about the enamine double bond must initially take place, allowing for the amine to approach the activated C–C triple bond, thus initiating hydroamination. In the absence of a metal catalyst, no geometrical isomerization was evident. It is known that geometrical isomerization about double bonds may be facilitated by the presence of a metal catalyst,[17] which could account for the geometrical isomerization observed in our reactions. This isomerization can be attributed to the fact that a metal–olefin complex may exist in equilibrium with a polarized form allowing for rotation about the temporarily polarized double bond (Scheme 2).[18]

It is apparent from entry a that the absence of a catalyst greatly hinders the hydroamination of **2b** into the cyclized product **4b**. It has been suggested that when the nitrogen lone pair from the amine approaches the π-bond of the electron-rich olefin in the absence of any catalyst, the electrostatic repulsions that result tend to cause high activation energies leading to particularly low reaction rates.[19] When a metal catalyst was introduced, a significant increase in reaction rate was noticed with the exception of ZnO, which afforded a 3% yield of pyrrole **4b**. The poor catalytic activity of ZnO as a hydroamination catalyst remains consistent with the literature and is a result of its low Lewis acidity.[20,21]

Whilst assessing the group 11 metals as hydroamination catalysts, it was noticed that the Cu^{2+} catalysts, that is, CuO, $CuAc_2$, $Cu(NO_3)_2$ and $CuCl_2$ were generally superior in contrast to the corresponding Ag^+ catalysts in facilitating hydroamination. Group 12 metals showed similar trends in catalytic activity, with a general decrease in catalytic activity down the periodic group from Zn^{2+} to Hg^{2+}. It was also noted that the nature of the counterion had a marked effect on the catalytic activity of a metal in performing hydroamination. The observed catalytic activity

Table 1
Hydroamination of vinylogous amide **2b** to pyrrole **4b**, implementing numerous transition metal catalysts[a]

Entry	Catalyst	Yield **4b** (%)
a	None	3
b	CuO	13
c	$CuAc_2$	33
d	$Cu(NO_3)_2$	53
e	$CuCl_2$	65
f	Ag_2O	6
g	AgAc	7
h	$Ag(NO_3)$	14
i	AgCl	9
j	ZnO	3
k	$ZnAc_2$	96
l	$Zn(NO_3)_2$	99
m	$ZnCl_2$	93
n	CdO	39
o	$CdAc_2$	30
p	$Cd(NO_3)_2$	85
q	$CdCl_2$	72
r	HgO	24
s	$HgAc_2$	68
t	$Hg(NO_3)_2$	57
u	$HgCl_2$	36
v	ZnI_2	14
w	HgI_2	94

[a] Under more forcing reaction conditions, the catalysts in entries k–u yielded pyrrole **4b** in a ⩾96% yield.[16]

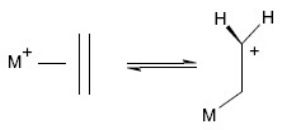

Scheme 2.

of a particular metal within a series generally increased in the order of oxide < acetate < chloride < nitrate.

Burling et al. similarly showed that the nature of the counterion can indeed play a role in the rate of hydroamination reactions.[22] Burling observed that bulkier and less coordinating anions tended to increase the rate of reactions, however, if too non-coordinating, a paradoxical drop off in reaction rate can result due to instability of the catalyst in solution.

As mentioned earlier, the activities of the catalysts employed generally decreased down the periodic groups, from Zn^{2+} to Hg^{2+}, and from Cu^{2+} to Ag^{+}, respectively. In an attempt to account for the observed trends in activity, the stability of metal complexes based upon hard soft acid base theory (HSAB) was considered. It is well known that the stability of Hg^{2+} (soft metal Lewis acid) halide complexes decrease in the order I > Br > Cl > F but with harder, more electropositive metal Lewis acids, the reverse order applies.[23] Looking at the chloride catalysts of group 12 as an example, the yield decreased from 93% ($ZnCl_2$ entry m), to 72% ($CdCl_2$ entry q), and finally to 36% ($HgCl_2$ entry u). To assess whether increasing catalyst instability was a potential cause for the reduced activity from $ZnCl_2$ to $HgCl_2$, a softer counterion was employed in the hope of reversing catalyst stabilities. ZnI_2 and HgI_2 were subsequently employed as potential hydroamination catalysts (entries v and w) with the expectation that the soft–soft interactions in HgI_2 would result in a more stable complex in solution, as opposed to the harder–soft interactions in ZnI_2. As expected, the yield of **4b** decreased from 93% ($ZnCl_2$ entry m) to 14% (ZnI_2 entry v), and increased from 36% ($HgCl_2$ entry u) to 94% (HgI_2 entry w) suggesting that reduced activities may be attributed to the counterions being too non-coordinating, as described by Burling.

Furthermore, the observed trend in catalytic activities down a periodic group may be attributed to the progressive decrease in Lewis acidity of the cationic metal centres, resulting from decreasing charge to radius ratios in moving down a group.[24] The Lewis acidity of a catalyst plays an important role in hydroamination for the reason that if the Lewis acidity of the metal cation is too weak, poor activation of the triple bond may result, leading to lower reaction rates.[21]

A generally accepted catalytic cycle adapted from Muller et al. is depicted in Scheme 3.[25] Despite the number of catalytic hydroamination mechanisms known, such as amine activation[26] or oxidative addition,[27] the following mechanism may be used to rationalize a Lewis acid catalyzed hydroamination process. The C–C triple bond initially becomes activated through π-coordination to the metal centre of the catalyst, followed by nucleophilic attack of the nitrogen lone pair on the activated triple bond.[25]

This is in contrast to the mechanism based on oxidative addition of an amine to the metal centre, which cannot explain Zn(II) and Cu(I) catalyzed hydroamination reactions, as these metals have no oxidation states available for the donation of two more electrons.[25] It is unlikely that

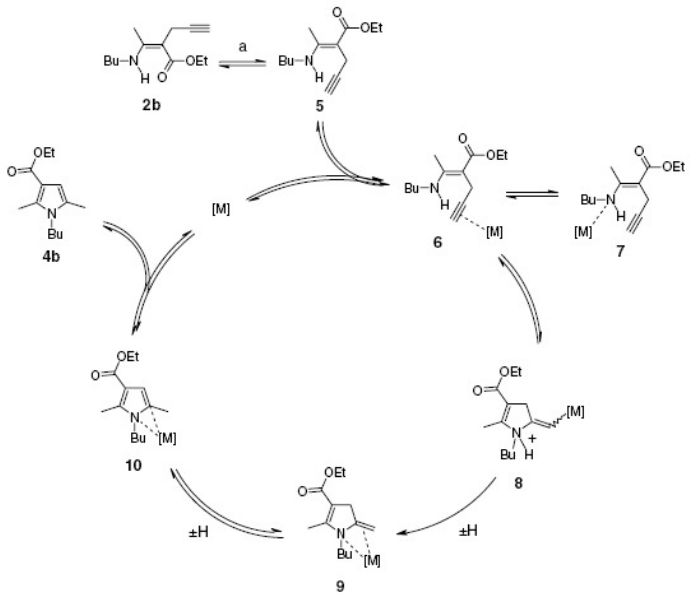

Scheme 3. Metal catalyzed isomerization adapted from Muller et al. Note: Formal [1,3]-hydrogen shifts are depicted by ±H.

an amine activation type mechanism will exist in this case as none of the catalysts employed in this study are basic enough for amino proton extraction.[28]

In conclusion, it can be seen that metals of the late transition series can indeed serve as efficient and regioselective catalysts in facilitating the hydroamination of functionalized *C*-propargyl vinylogous carbamates into pyrroles. Advantages lie in the fact that these metal salts are commonly available, inexpensive and stable to air and moisture. The zinc catalysts with the exception of ZnO gave the highest yields under mild conditions, however, all the group 12 metals afforded excellent yields of product when longer reaction times, higher catalytic loading and increased microwave energy were utilized. The stability of the catalysts in solution, as well as the Lewis acidity of the catalysts, plays an important role in the efficiency of hydroamination reactions. Changing the counterion had a noticeable effect on hydroamination, and it has been suggested that less coordinating anions result in higher rates up to a point at which catalyst stability in solution becomes compromised as a result of anions becoming too non-coordinating.

Acknowledgements

The authors would like to acknowledge The National Research Foundation for providing generous funding, as well as Mr. Craig Grimmer for acquiring ^{1}H NMR data.

References and notes

1. (a) Louie, J.; Hartwig, J. F. *Tetrahedron Lett.* **1995**, *36*, 3609–3612; (b) Ma, D.; Yao, J. *Tetrahedron: Asymmetry* **1996**, *7*, 3075–3078; (c) Driver, M. S.; Hartwig, J. F. *J. Am. Chem. Soc.* **1996**, *118*, 7217–7218; (d) Wolfe, J. P.; Wagaw, S.; Buchwald, S. L. *J. Am. Chem. Soc.* **1996**, *118*, 7215–7216; (e) Robinson, R. S.; Dovey, M. C.; Gravestock, D. *Eur. J. Org. Chem.* **2005**, *3*, 505–511; (f) Wolfe, J. P.; Buchwald, S. L. *J. Org. Chem.* **1997**, *62*, 1264–1267; (g) Louie, J.; Driver, M. S.; Hamann, B. C.; Hartwig, J. F. *J. Org. Chem.* **1997**, *62*, 1268–1273.
2. Nobis, M.; Driebßen-Hölscher, B. *Angew. Chem., Int. Ed.* **2001**, *40*, 3983–3985.
3. Howk, B. W.; Little, E. L.; Scott, S. L.; Whitman, G. M. *J. Am. Chem. Soc.* **1954**, *76*, 1899–1902.
4. Bambirra, S.; Tsurugi, H.; van Leusen, D.; Hessen, B. *Dalton Trans.* **2006**, 1157–1161.
5. Anderson, L. L.; Arnold, J.; Bergman, R. G. *Org Lett.* **2004**, *6*, 2519–2522.
6. Lorber, C.; Choukroun, R.; Vendier, L. *Organometallics* **2004**, *23*, 1845–1850.
7. Müller, T. E.; Pleier, A.-K. *J. Chem. Soc., Dalton Trans.* **1999**, 583–587.
8. Kim, Y. K.; Livinghouse, T.; Bercaw, J. E. *Tetrahedron Lett.* **2001**, *42*, 2933–2935.
9. Severin, R.; Doye, S. *Chem. Soc. Rev.* **2007**, *36*, 1407–1420.
10. Robinson, R. S.; Dovey, M. C.; Gravestock, D. *Tetrahedron Lett.* **2004**, *45*, 6787–6789.
11. Larock, R. C. *Comprehensive Organic Transformations: A Guide to Functional Group Preparations*; VHC, 1989. pp 981–988.
12. Stahly, G. P.; Marlett, E. M.; Nelson, G. E. *J. Org. Chem.* **1983**, *48*, 4423–4426.
13. 2.0 M *n*-BuLi (2.97 mL; 5.94 mmol) was added dropwise to a stirred solution of vinylogous amide (1.00 g; 5.40 mmol) in dry THF (50 mL) at 0 °C. The solution was stirred for 30 min at 0 °C followed by an additional 30 min of stirring at room temperature. The solution was cooled to 0 °C followed by the dropwise addition of propargyl bromide (0.814 g; 6.48 mmol). The solution was stirred at 0 °C for 30 min, allowed to warm to room temperature, and stirred for an additional 14 h. The reaction mixture was quenched with 2 M NH_4Cl (five drops) and concentrated in vacuo to yield the crude *C*-propargyl vinylogous amide as a brown oil, in 80% yield.
14. Transition metal salt (0.0358 mmol, 0.04 equiv) was added to a solution of crude *C*-propargyl vinylogous amide (200 mg, 0.896 mmol) and acetonitrile (2 mL) in a microwave reaction vessel, and subjected to 40 W of microwave irradiation for 20 s whilst being stirred and force cooled. The reaction mixture was purified with a short silica plug (1 cm) and analyzed using ^{1}H NMR spectroscopy. All microwave reactions were performed using a CEM Discover laboratory microwave oven.
15. (a) Baldwin, J. E.; Thomas, R. C.; Kruse, L. I.; Silberman, L. *J. Org. Chem.* **1977**, *42*, 3846–3852; (b) Baldwin, J. E. *J. Chem. Soc., Chem. Commun.* **1976**, 734–736.
16. Refer to Ref. 14 with the exception that 0.2 equiv of catalyst, 100 W of microwave irradiation, and a reaction time of 1 min were utilized.
17. Field, L. D.; Ward, A. J. *J. Organomet. Chem.* **2003**, *681*, 91–97.
18. Bochmann, M. *Organometallics 2: Complexes with Transition Metal–Carbon π-Bonds*; Oxford University Press, 2000; pp 20–21.
19. Hultzsch, K. C. *Org. Biomol. Chem.* **2005**, *3*, 1819–1824.
20. Penzien, J.; Müller, T. E.; Lercher, J. A. *Chem. Commun.* **2000**, 1753–1754.
21. Shanbhag, G. V.; Halligudi, S. B. *J. Mol. Catal. A: Chem.* **2004**, *222*, 223–228.
22. Burling, S.; Field, L. D.; Messerle, B. A.; Turner, P. *Organometallics* **2004**, *23*, 1714–1721.
23. Bodie, D.; McDaniel, D.; Alexander, J. *Concepts and Models of Inorganic Chemistry*, 3rd ed.; John Wiley Sons, 1994; pp 386–387.
24. Pearson, R. G. *J. Chem. Educ.* **1968**, *45*, 581–587.
25. Müller, T. E.; Grosche, M.; Herdtweck, E.; Pleier, A.-K.; Walter, E.; Yan, Y.-K. *Organometallics* **2000**, *19*, 170–183.
26. Martinez, P. H.; Hultzsch, K. I.; Hample, F. *Chem. Commun.* **2006**, 2221–2223.
27. Uchimaru, Y. *Chem. Commun.* **1999**, 1133–1134.
28. Ouh, L. L.; Müller, T. E.; Yan, Y. K. *J. Organomet. Chem.* **2005**, *690*, 3774–3782.

Results from this study illustrated that the group 11 and 12 metals in general served as effective hydroamination catalysts in the conversion of *C*-propargyl vinylogous amides **66** into pyrroles **67**. As the C–C triple bond was deemed *trans* relative to the amine in the starting material 2b, isomerization about the enamine double bond was said to initially take place, allowing for the amine to approach the activated C–C triple bond. This isomerization was attributed to the fact that the metal–olefin complex may exist in equilibrium with a polarized form allowing for rotation about a temporarily polarized double bond to take place as described in the publication inserted above. The hydroamination reactions were completely regioselective with the starting material **66** undergoing 5-*exo*-dig cyclizations (Markovnikov addition) forming the pyrrole **67** in preference to a 6-*endo*-dig cyclizations (anti-Markovnikov addition), albeit both cyclizations being favorable transformations according to the Baldwin rules.[74,75] Increases in catalytic activities were observed upon moving up a periodic group and was attributed to increasing catalytic stabilities in solution, as well as increases in Lewis acidities resulting from increases in charge to radius ratios. The zinc catalyst series namely $ZnCl_2$, $ZnAc_2$ and $Zn(NO_3)_2$ furnished the highest yields of pyrrole **67** with recorded yields of 93%, 96% and 99% respectively under mild reaction conditions. The hydroamination mechanism for these reactions was said to follow a metal catalyzed alkyne activation mechanism as it tapped into the Lewis acidity of the metal centre.[69] This type of mechanism was said to predominate as none of the catalysts were sufficiently basic enough for amino proton extraction therefore ruling out the possibility of a base catalyzed hydroamination mechanism.[69] Additionally, an oxidative addition type mechanism could not be used to rationalize Cu(I) and Zn(II) catalyzed hydroamination reactions as these catalysts do not have further oxidation states available to them for the donation of two more electrons.

Further more, a study is to be done in the near future buy our research group that will assess whether the regioselectivity of this hydroamination reaction can be altered from Markovnikov to anti-Markovnikov by introducing a bulky, chiral hydroamination catalyst to the reaction as demonstrated by Beller and co-workers.[31]

2.3 Model Studies

As mentioned in section 1.4 (page 37), earlier research efforts within our group provided us with a convenient synthetic route to access a bicyclic *N*-bridgehead pyrrole scaffold **61** *via* the intramolecular hydroamination of the corresponding cyclic *cis*-*C*-propargyl secondary enaminone **59** (Scheme 28).[70]

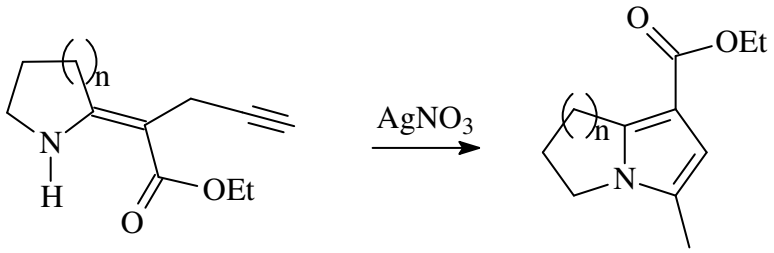

59 **61**

Scheme 28

This presented us with a potentially viable synthetic route accessing molecules with base structures similar to that of pyrrolizidine alkaloids. First off, it was deemed necessary to perform a model study in order to optimize the chemistry behind accessing the *N*-bridgehead pyrrole functionality starting from a common and inexpensive starting material such as 2-pyrrolidine **68** (Scheme 29). The secondary enaminone **58** (Scheme 29) is represented as the *trans*-isomer, as this was the geometrical isomer that was evident in our reactions based on two dimensional NOESY experiments, and is further discussed later in the discussion.

According to our mindset, once the chemistry briefly outlined in Scheme 29 is successfully optimized, it will be implemented in the synthesis of the target alkaloid **223H** (xenovenine) starting from (5*R*)-5-methyltetrahydro-2*H*-pyrrol-2-one **70** as shown briefly in Scheme 30. The following synthetic route if proven successful can provide access to a cyclic *C*-propargyl secondary enaminone **73**, which upon hydroamination can deliver the appropriate *N*-bridgehead pyrrole **74,** a structurally analogous precursor to **223H** (xenovenine).

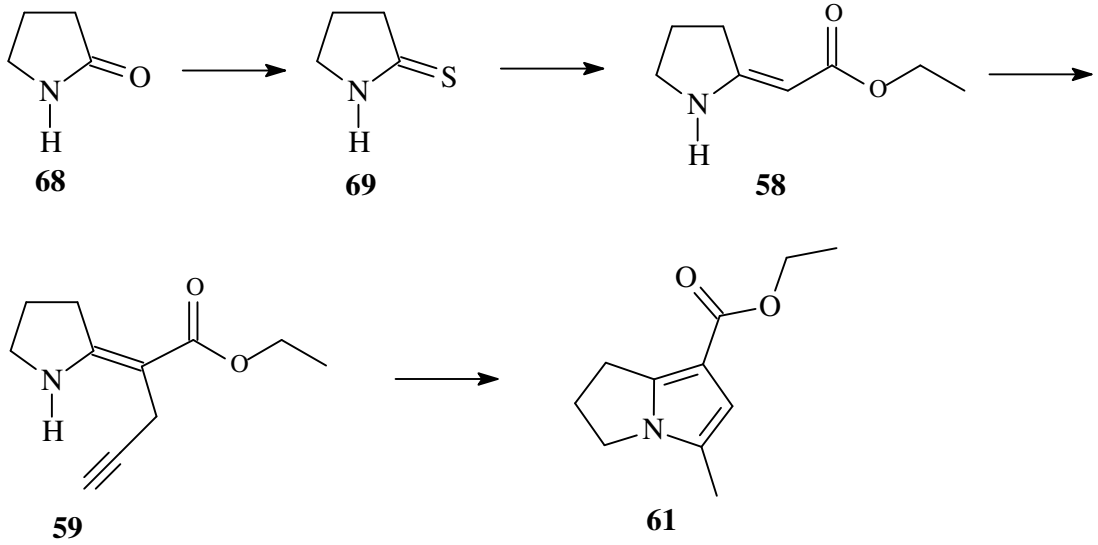

Scheme 29

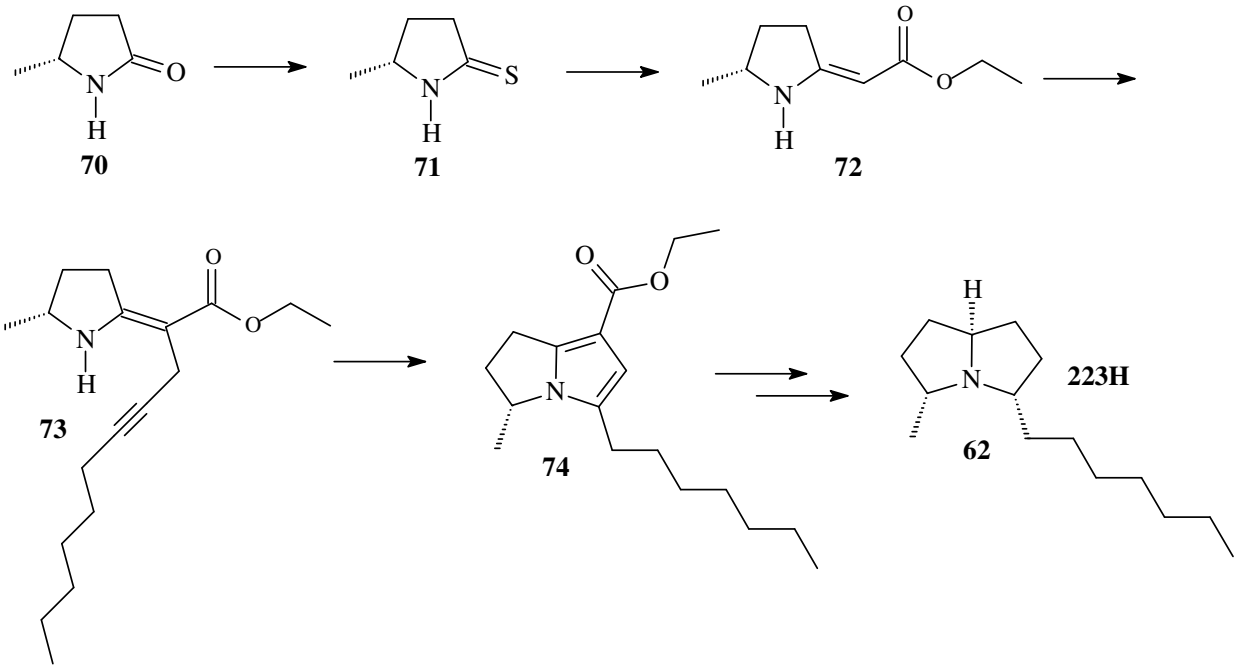

Scheme 30

2.3.1 Preparation of ethyl 2-(2-pyrrolidinylidene)acetate [58]

The preparation of the secondary enaminone **58** was attempted as outlined in Scheme 29. The 2-pyrrolidinone was added dropwise to a mixture of Lawesson's reagent in dry THF and stirred for 17 hours at room temperature. Inspection of the reaction mixture using thin layer chromatography showed the disappearance of the lactam starting material and the appearance of a new spot with an R_f value of 0.22 (ethyl acetate:hexane = 1:1). The reaction solution was concentrated to yield a viscous yellow oil, the purification of which was first attempted by the method of radial chromatography to isolated the product from the unreacted Lawesson's reagent. This method of purification proved unsuccessful as the oil kept solidifying whilst attempting to load the oil onto the chromatotron plate. Alternatively, column chromatography was implemented however the solidification problem was re-encountered and once the oil had solidified it was difficult to re-dissolve it again in any solvent. The purification was later improved upon by warming the oil to *ca*. 50^{o}C using a hair dryer before loading it onto the column. The column was also pre-warmed using the hairdryer. The oil was eluted down the column first using 100% ethyl acetate followed by (ethyl acetate:hexane = 1:1) which resulted in a successful separation and yielded the thiolactam **69** as a white crystalline solid and in a 78% yield. The melting point of 109-110^{o}C for the solid compared favorably to the literature value of 109-110^{o}C.[76] The ^{1}H and ^{13}C NMR spectroscopic data was in close agreement to that reported by Dovey,[68] and the low resolution mass obtained from mass spectrometry was in agreement for that of the desired thiolactam product **69**.

With the thiolactam in hand, it was subject to a reaction with ethyl bromoacetate employing Eschenmoser sulfide contraction conditions in an attempt to synthesize the secondary enaminone **58**. The Eschenmoser sulfide contraction reaction, also known as the Eschenmoser coupling reaction, takes place when a thiolactam derivative is reacted with an α-bromocarbonyl compound in the presence of a base and a thiophile. The result is the formation of a β-enaminocarbonyl compound such as the secondary enaminone **58**

depicted in Scheme 25. The base employed is usually a tertiary amine such as triethylamine and the sulfur scavenger is normally a phosphorus containing thiophile such as triphenylphosphine. Ethyl bromoacetate was thus added to a stirring solution of the thiolactam in dry acetonitrile. The solution was stirred for 12 hours after which triethylamine and triphenylphosphine were added as a solution in dichloromethane. Thin layer chromatography and ^{1}H NMR analysis showed no formation of the desired enaminone product, and the starting material was recovered. The reaction was attempted again using dry dichloromethane as the solvent however no success was achieved.

After reviewing additional literature it was noticed that excellent yields of β-enaminocarbonyl compounds have been achieved when employing tertiary thiolactams in the Eschenmoser coupling reaction.[77-79]

The amine functionality in the thiolactam **69** was subsequently protected using ethyl acrylate in a conjugate addition type reaction catalyzed by sodium hydroxide in THF (Scheme 31).

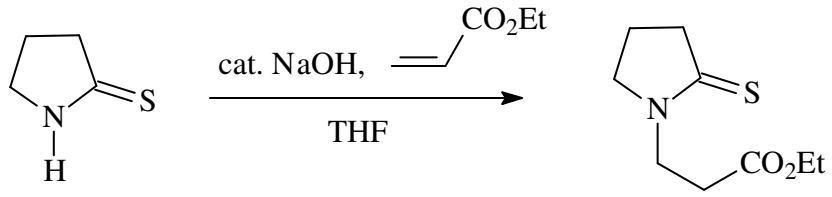

69 **75**

Scheme 31

The tertiary thiolactam **75** was successfully prepared using the above mentioned reaction conditions in an excellent 100% yield after 5 hours as a colourless oil, a 78% overall yield from lactam **68**. The synthesis of the tertiary thiolactam was validated by obtaining ^{1}H and ^{13}C NMR spectroscopic data, which was consistent to that obtained by Dovey.[68] The GC-MS data showed the presence of a single peak in the chromatograph with a parent molecular ion peak (m/z) = 201, which corresponded to the correct product mass.

In an attempt to improve the overall yield of tertiary thiolactam **75**, a slightly different procedure was carried out with the hope of also by-passing the laborious thiolactam purification step. The lactam **68** was first protected with ethyl acrylate using the same reaction conditions as previously described, followed by a thionation step using Lawesson's reagent (Scheme 32).

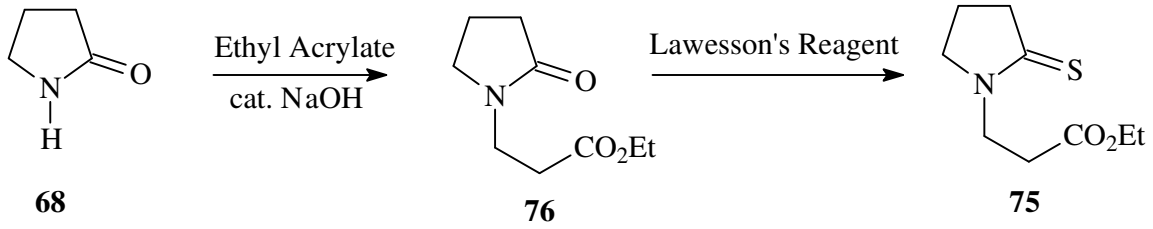

68 **76** **75**

Scheme 32

The protected lactam was **76** was prepared in an excellent 100% yield, and it's structure was confirmed by ^{1}H and ^{13}C NMR spectroscopy as well as Gas Chromatography-Mass Spectrometry. Unfortunately, the thionation of **76** to form **75** was not as fruitful and only a 43% yield of tertiary thiolactam was obtained which only afforded a 43% overall yield of **75** from lactam **68**.

The tertiary thiolactam was then subject to the same Eschenmoser Coupling reaction as previously described using acetonitrile as the reaction solvent (Scheme 33).

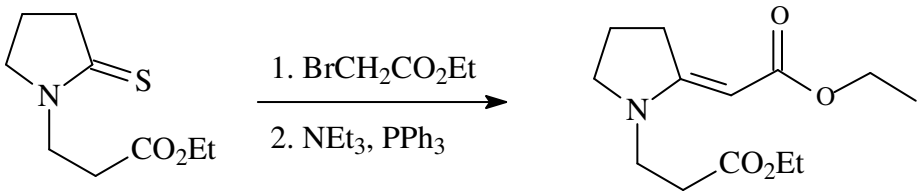

75 **77**

Scheme 33

The results from this approach were very pleasing as the desired tertiary enaminone **77** was synthesized in a 75% isolated yield. The purification however proved to be laborious as two consecutive columns needed to be carried out on the crude material in order to

obtain sufficiently pure product. The reason for this was because unreacted triphenylphosphine was eluting out into all of the fractions from the column. In an attempt to improve the overall reaction efficiency, the Eschenmoser coupling reaction was performed again using the water soluble triethyl phosphite as the thiophile in place of triphenylphosphine. This modified procedure had no effect on the yield of product **77** (75% isolated yield) however work up and purification was less problematic as the water soluble triethyl phosphite and its oxide by-product, could be removed *via* a liquid-liquid extraction prior column chromatography. The ^{1}H and ^{13}C NMR spectroscopic data was in close agreement to that obtained by Dovey[68] and the peaks in the ^{1}H and ^{13}C NMR spectra were assigned accordingly as depicted in Figure 27 and Figure 28.

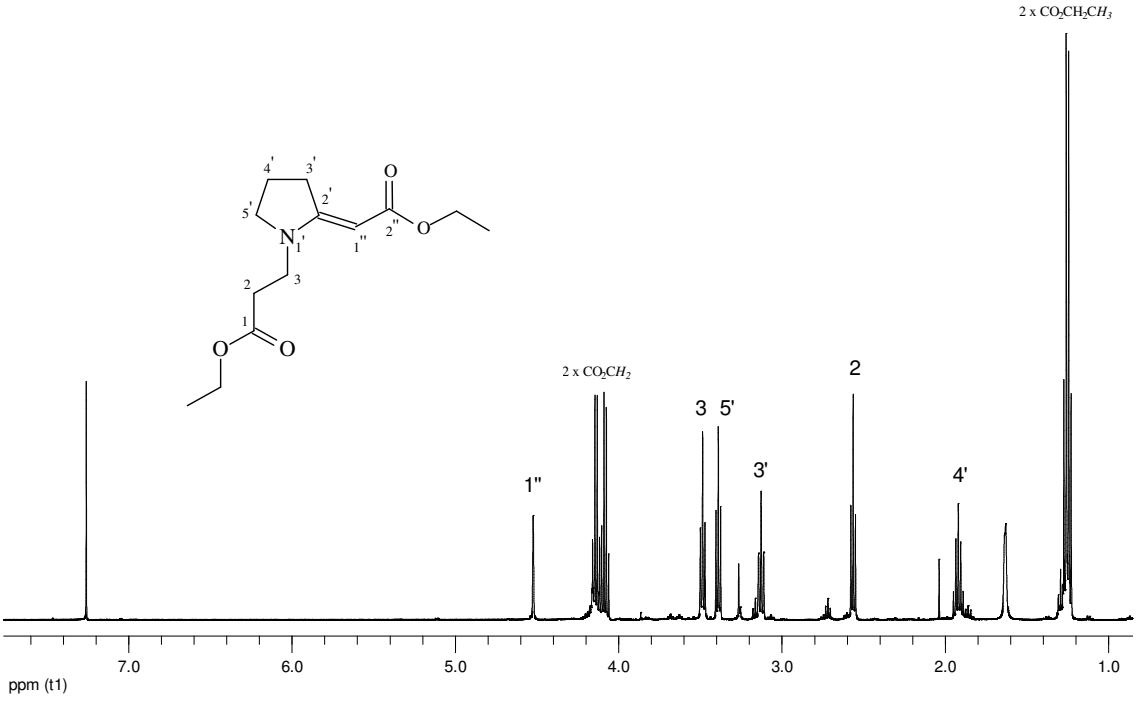

Figure 27: ^{1}H NMR Spectrum for ethyl 3-{2-[(*E*)-2-ethoxy-2-oxoethylidene]-1-pyrrolidinyl}propanoate

The Eschenmoser coupling took place regioselectively forming the *trans* (*E)* geometrical isomer. This deduction could be made by closely examining the ^{1}H NMR spectrum for the enaminone product **77**, and from two-dimensional NOESY experiments.

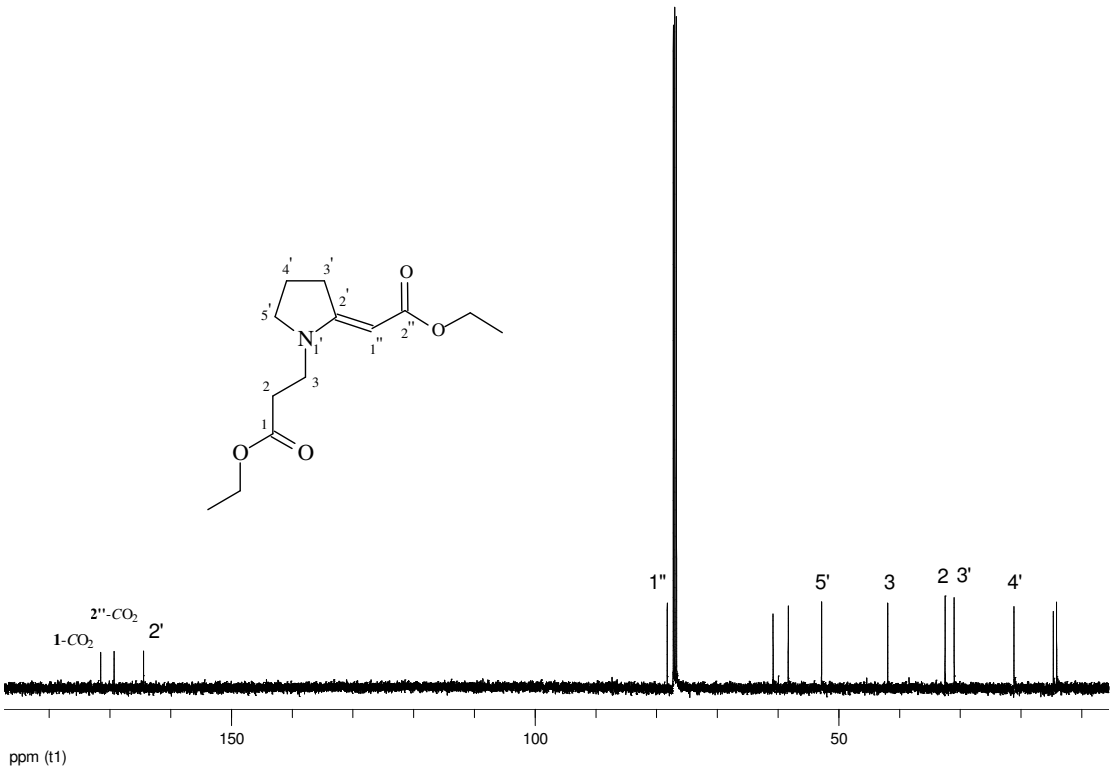

Figure 28: ^{13}C NMR Spectrum for ethyl 3-{2-[(*E*)-2-ethoxy-2-oxoethylidene]-1-pyrrolidinyl}propanoate

Inspection of the chemical shift of the protons 3′-*H* (3.13 ppm) shows that they are experiencing an anisotropic through-space deshielding effect due to the close proximity of the carbonyl group which shifts the signal downfield.[79,80] This chemical shift of 3.13 ppm compares favorably to that of a similar trans-fused derivative reported by Michael,[77] for which the hydrogen atoms at position 3-*H* of the ring were found to resonate at 3.15 ppm. The *cis* analogues exhibit 3-*H* resonance further upfield and possess a chemical shift difference relative to the *trans* analogues of 0.6 ppm.[77]

Further more, the two-dimensional NOESY spectrum (Figure 29) obtained for the enaminone **77** clearly shows the absence of any through-space coupling between the proton atoms at 3′-*H*, and proton atom 1″-*H*, suggesting that they reside *trans* relative to each other across the double bond.

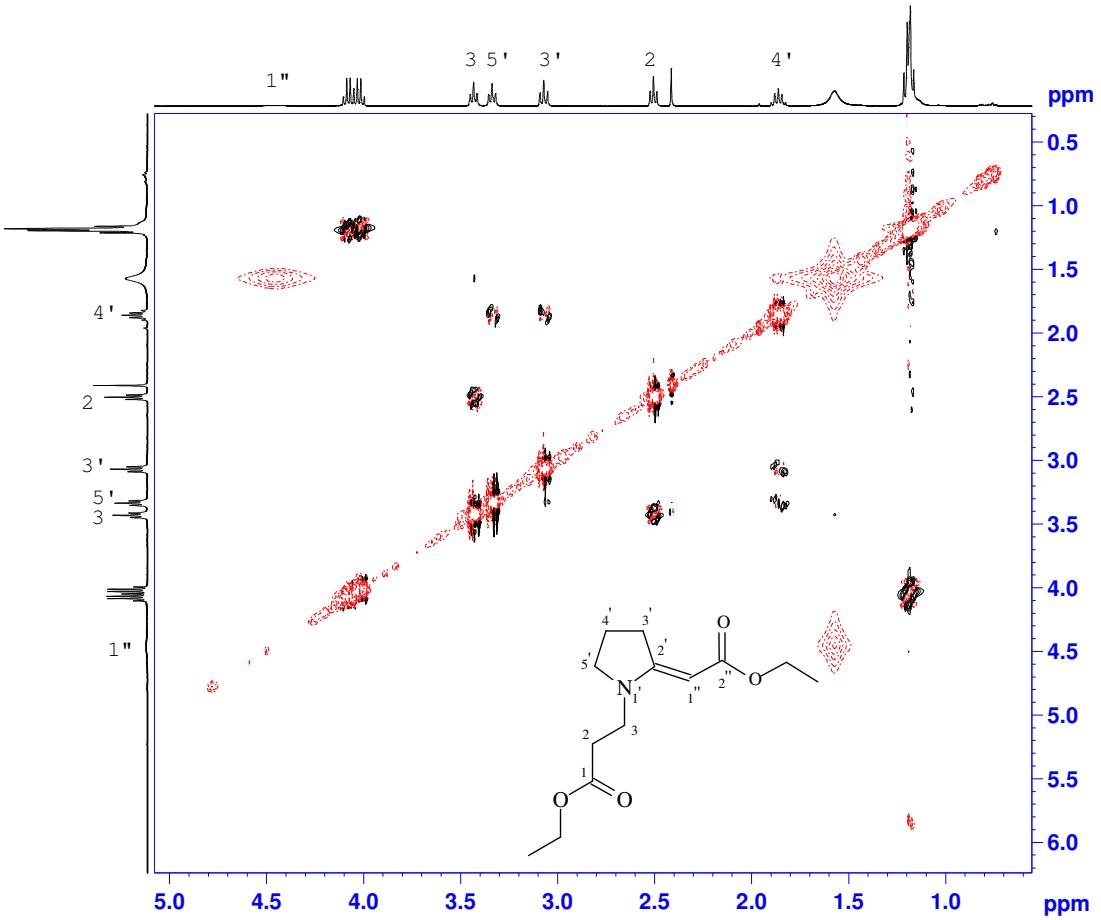

Figure 29: 2D NOESY Spectrum for ethyl 3-{2-[(*E*)-2-ethoxy-2-oxoethylidene]-1-pyrrolidinyl}propanoate

A tentative mechanism for the Eschenmoser coupling reaction is shown in Scheme 34 and is based on that by Eschenmoser.[81] The lone pair of electrons on the nitrogen migrates towards the sp^2 hybridized carbon whilst the sulfur moiety undergoes a S_N2 type nucleophilic substitution with the bromine atom in ethyl bromoacetate to form an α-thio iminium salt **78**. Abstraction of the proton H_a by triethylamine supposedly forms the sulfur bridged intermediate[82] **79**, which is converted into the tertiary enaminone product **77** by reaction with a sulfur scavenging triphenylphosphine molecule.

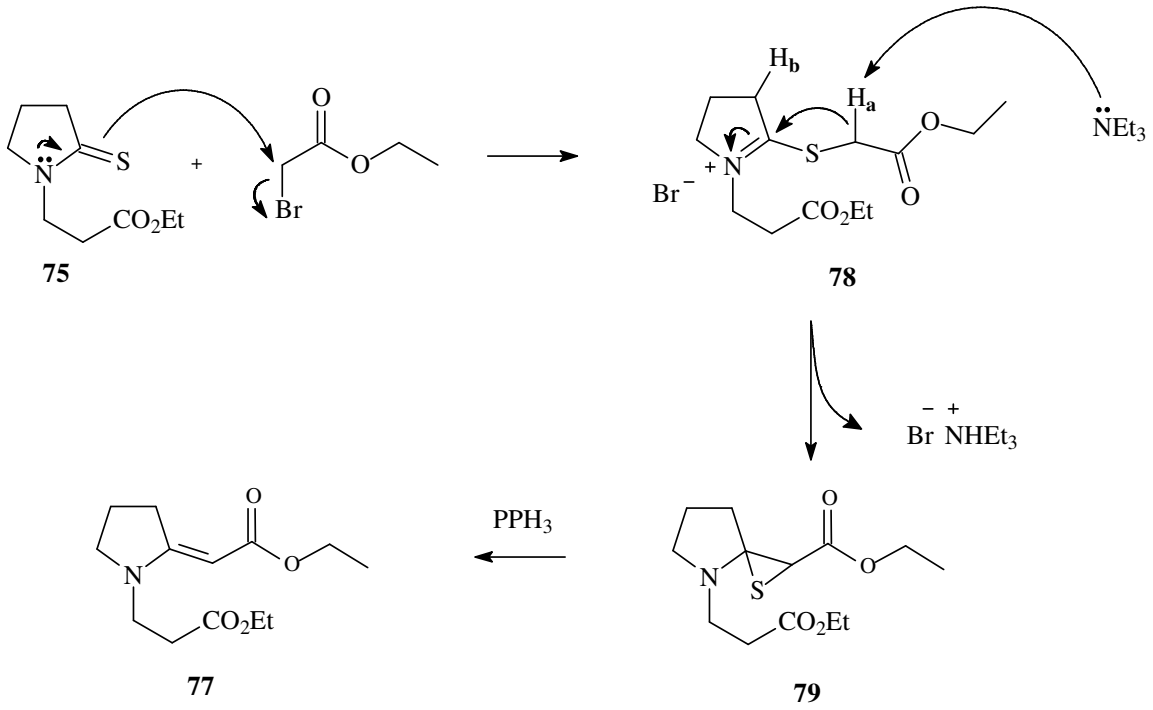

Scheme 34

An alternative reaction pathway has been reported to occur when utilizing similar thiolactam derivatives in Eschenmoser Coupling reactions. This pathway involves the abstraction of proton H_b instead of H_a by triethylamine forming bicyclic thiazolidinone side products.[83] This alternative pathway was not evident however in our reactions.

In order to synthesize the desired secondary enaminone **58**, the ethyl ester moiety on the nitrogen of **77** needed to be removed (Scheme 35).

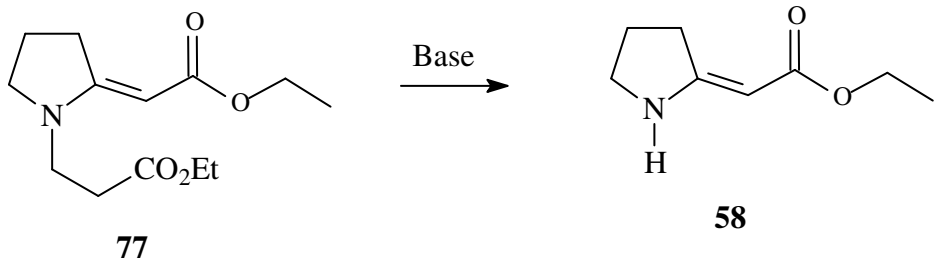

Scheme 35

It had been previously documented that cyanoethyl moieties could be successfully removed from similar enaminone derivatives *via* based-induced elimination of cyanoacrylate in the presence of potassium-*t*-butoxide and in good yields[79] (Scheme 36).

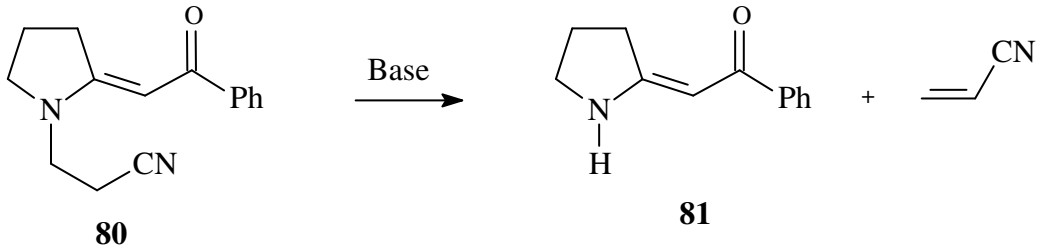

80 **81**

Scheme 36

We were therefore interested in applying this methodology to our system in an attempt to achieve an equivalent result. One molar equivalent of potassium-*t*-butoxide was consequently added to a solution of tertiary enaminone in THF, and the resulting reaction mixture was monitored by intermittent TLC analysis however no observable elimination reaction was apparent. Our attention was immediately focused on implementing alternative, non-nucleophilic bases in the reaction at hand in an attempt to remove the ethyl acrylate from the tertiary enaminone. As a result, lithium hexamethyldisilazane (LiHMDS) was found to remove the *N*-ethyl ester moiety forming the desired secondary enaminone product **58** in a 24% yield. This yield was later improved upon as the reaction conditions were gradually optimized. It was shown that an improved yield of 65% could be obtained when the LiHMDS was rapidly added to the tertiary enaminone as a solution in THF at room temperature, and the resulting mixture allowed to stir for 5 minutes, after which the mixture was immediately quenched with aqueous ammonium chloride. After workup, the crude product was purified *via* radial chromatography to afford the desired product **58** as a white crystalline solid. The melting point for the white crystalline solid was found to be 59-61 ^{o}C and compared favorably to the literature value[84] of 61-62 ^{o}C for the expected secondary enaminone product **58**. Interesting, when potassium hexamethyldisilazane (KHMDS) was used in place of LiHMDS, a further improvement in the yield of **58** (72%) was obtained.

This modified synthesis afforded a 54% overall yield of the secondary enaminone **58** from the thiolactam **69**. The ^{1}H and ^{13}C NMR spectra obtained for the product were found to be consistent with those previously reported.[68] The ^{1}H NMR spectrum (Figure 30) showed the presence of a singlet integrating for one proton at a chemical shift of 7.89 ppm which corresponds to the reformed amine functionality. The Infra-Red spectrum confirmed the presence of the amine functionality as seen by the absorption band at 3347 cm^{-1}.

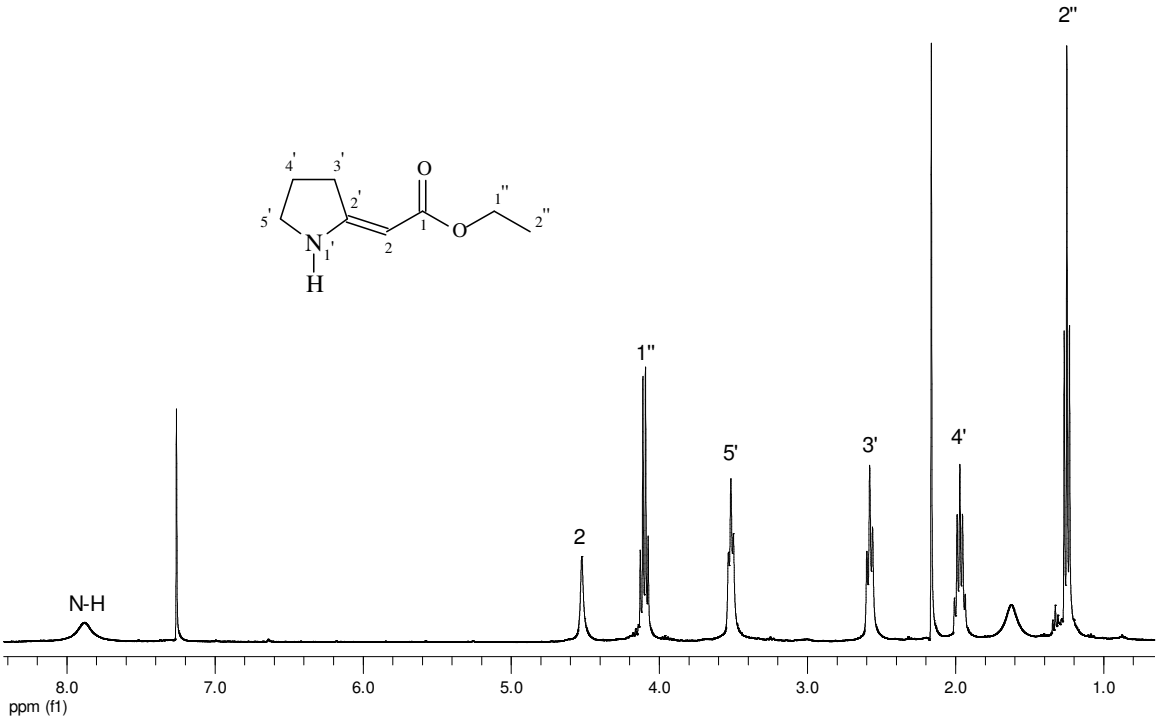

Figure 30: ^{1}H NMR Spectrum for ethyl 2-(2-pyrrolidinylidene)acetate

The two-dimensional NOESY spectrum (Figure 31) showed that the base-induced removal of ethyl acrylate did not affect the geometry about the enamine double bond. Through-space coupling is clearly present between the vinylic proton 2-*H* and the amine proton 1′-*H*, whilst no coupling is apparent between the vinylic proton 2-*H* and the ring protons 3′-*H*. This suggests that the vinylic proton 2-*H* must be positioned on the *cis* side of the double bond relative to the amine proton 1′-*H*.

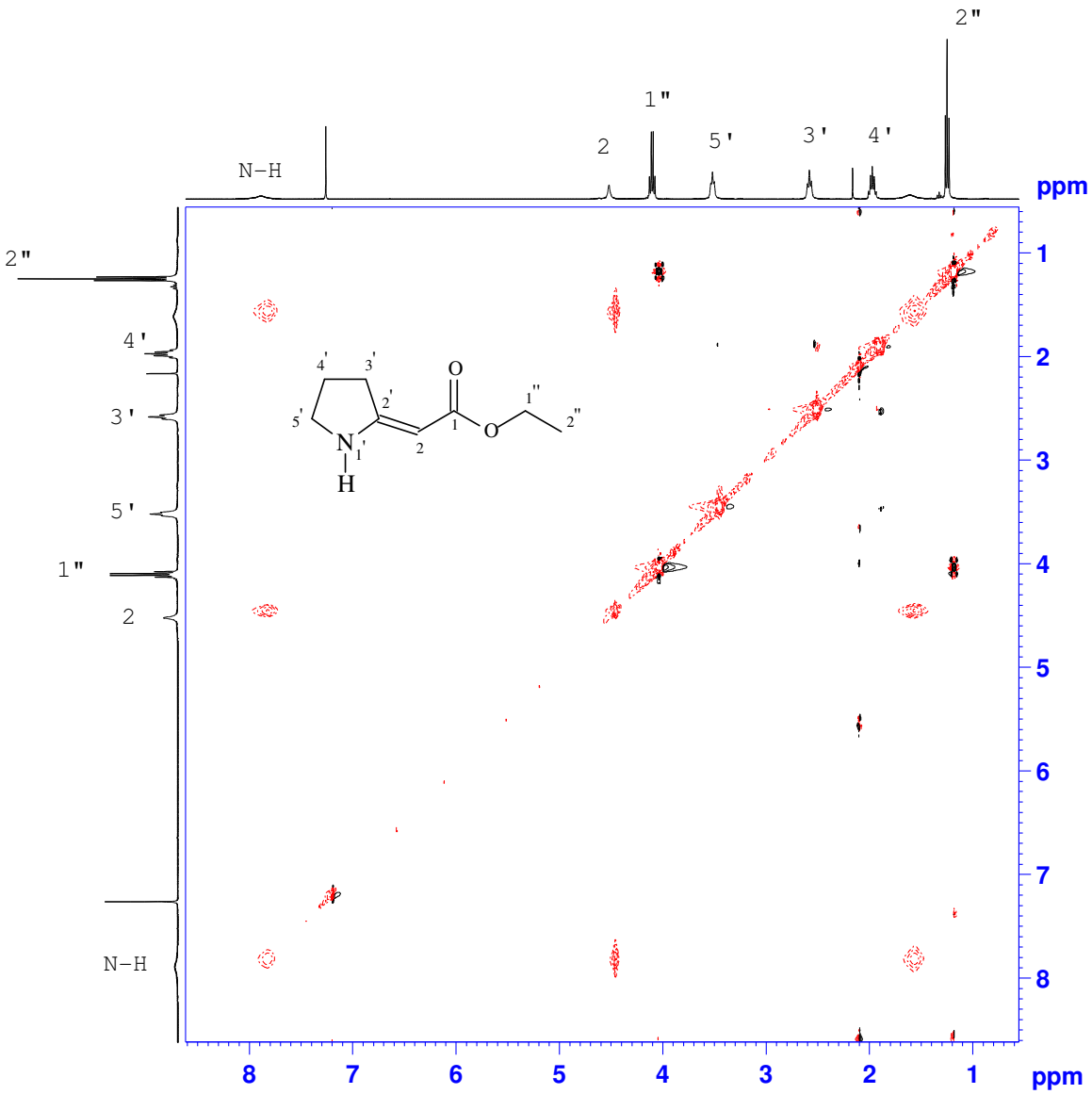

Figure 31: 2D NOESY Spectrum for ethyl 2-(2-pyrrolidinylidene)acetate [58]

A proposed mechanism for the base-induced elimination reaction is presented in Scheme 37. Abstraction of the acidic proton *alpha* to the carbonyl in **77** by the base forms an enolate intermediate **82** which collapses liberating ethyl acrylate and the enaminone salt **83**. Following workup in an acid environment, the amine is protonated thus forming the enaminone product **58**.

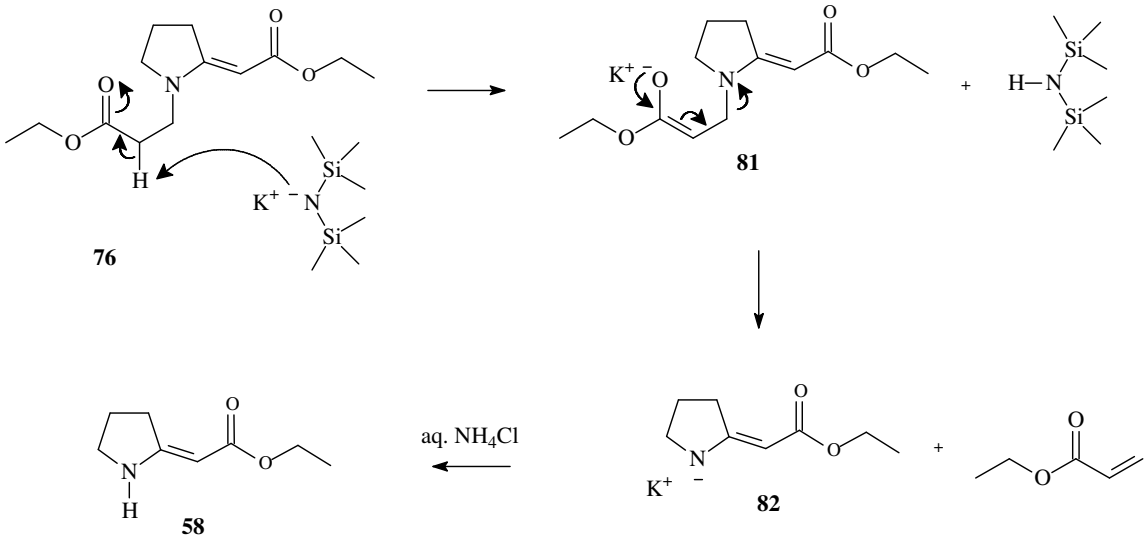

Scheme 37

2.3.2 Preparation of ethyl 2-(2-pyrrolidinylidene)-4-pentynoate [59]

The next challenge in the model study was the optimization of the *C*-propargylation reaction to form the *C*-propargyl secondary enaminone **59** from the secondary enaminone **58** (Scheme 38).

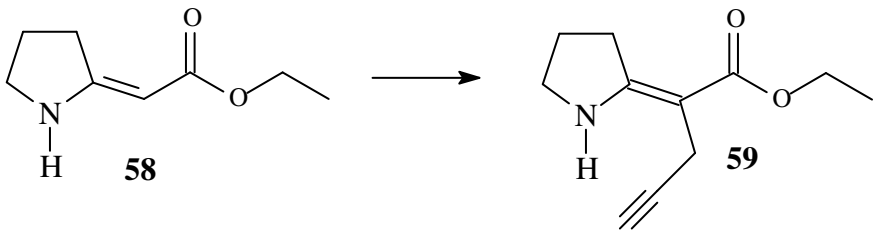

Scheme 38

Due to the similar nature of enaminone **58** to the vinylogous amide **65** encountered earlier in section 2.2.2, our first reaction attempt employed the same reaction conditions that were used to synthesize the *C*-propargyl vinylogous amide **66** from the vinylogous amide **65**. One equivalent of *n*-butyllithium with respect to the enaminone starting material **58**

was added to a solution of **58** in THF at –77 ^{o}C to achieve amino proton extraction. This supposedly resulted in the formation of the two nucleophilic resonance hybrids **A** + **B** (Figure 32) as denoted for the vinylogous amides described earlier in section 2.2.2.

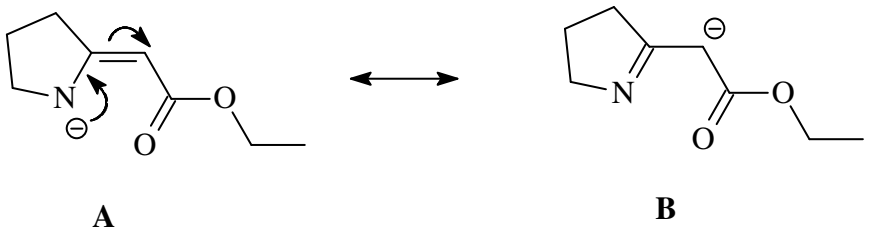

A **B**

Figure 32

One equivalent of propargyl bromide was lastly added to the reaction and the resulting solution was allowed to stir overnight. After work up, the remaining oil was analyzed using ^{1}H NMR spectroscopy. The NMR spectrum (Figure 33) showed the successful formation of product however a significant amount of starting material remained unreacted. The peaks corresponding to the product were assigned in the following spectrum by comparing them to those reported by Dovey.[68]

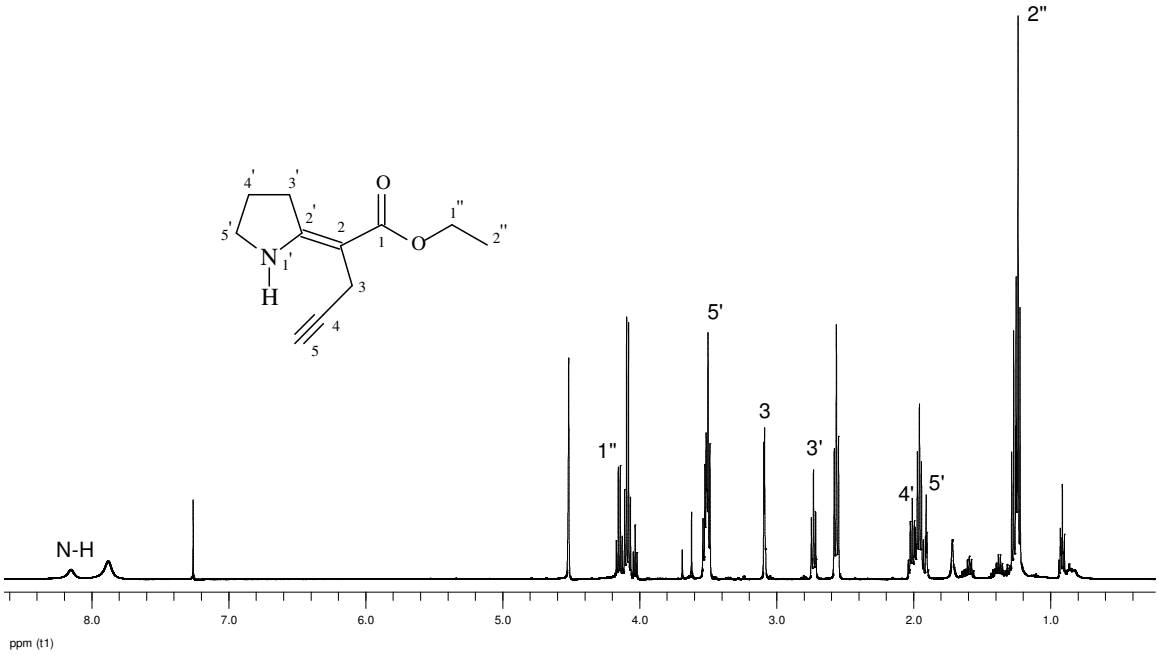

Figure 33: Crude ^{1}H NMR spectrum for ethyl 2-(2-pyrrolidinylidene)-4-pentynoate

Immediately apparent was the presence of the two N-*H* peaks at 8.15 and 7.89 ppm which corresponded to the resonance of the amino protons 1′-*H* of the product and starting material respectively. Integration of these amino proton peaks in the ^{1}H NMR spectrum showed that the product and starting material were present in a 2:3 ratio, and therefore a 40% yield of product was obtained with the remainder being starting material.

In an attempt to drive the following reaction to completion, the reaction was again performed using double the equivalency of propargyl bromide with respect to the starting material **58** but keeping the equivalents of *n*-butyllithium utilized unchanged. The modified procedure had little effect on the reaction outcome and a mixture of starting material and product were again obtained with only a marginal improvement in the yield of product being achieved (45%).

In an effort to further increase the yield of product **59**, higher equivalencies of *n*-butyllithium and propargyl bromide were employed. The new reaction stoichiometry thus involved using 2 equivalents of *n*-butyllithium and 1.1 equivalents of propargyl bromide. Following overnight stirring, the reaction mixture was worked up and analyzed using ^{1}H NMR spectroscopy and GC-MS, the results from which are presented in Figures 34 and 35 respectively.

The ^{1}H NMR spectrum (Figure 34) again showed the presence of both product and unreacted starting material, however a lower proportion of starting was present as compared to the previous two reactions as the ratio of product to starting material based on amino peak integration was found to be 4:1. Newly added peaks in the ^{1}H NMR spectrum inferred that an additional compound/s had been formed as by-product/s in the reaction. The GC chromatograph (Figure 35) confirmed the existence of starting material, product material, and an additional by-product as seen by the incidence of three significant peaks in the GC trace with retention times of 13.56, 15.24 and 16.14 minutes respectively.

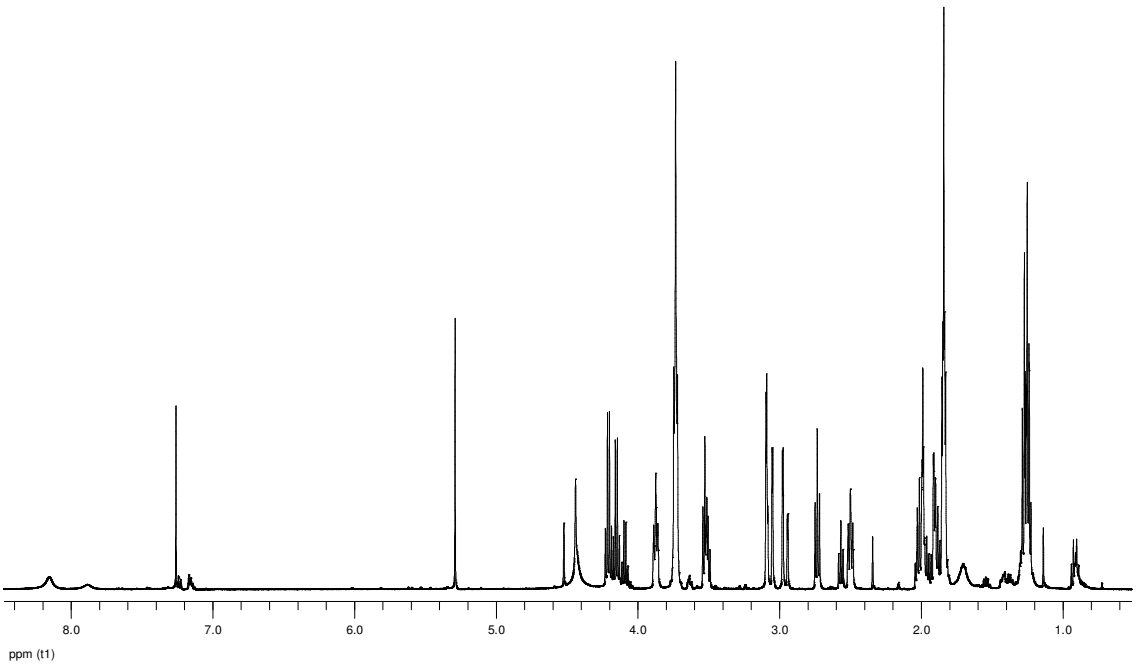

Figure 34

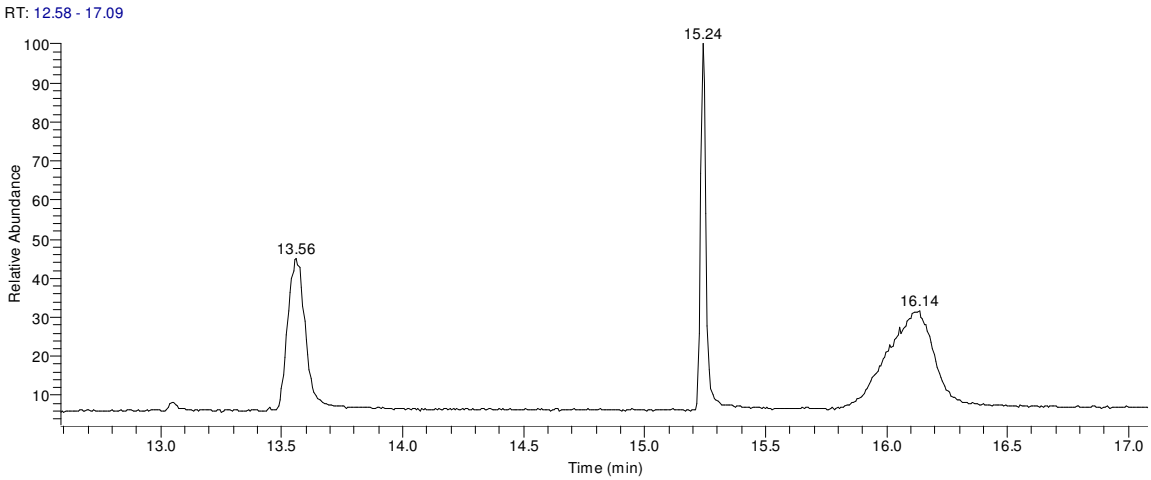

Figure 35

The peak at 13.56 minutes had a parent molecular ion (*m*/*z*) ratio of 155 and corresponded to the enaminone starting material. The peak at 16.14 minutes was found to be that for the desired product as it had a (*m*/*z*) ratio of 193. This product mass was the result of a newly added propargyl group which accounted for the additional mass of 38 $g.mol^{-1}$. The unknown by-product peak at 15.24 minutes had a parent molecular ion mass

of 231 which was greater than the product **59** mass by an additional 38 g.mol^{-1}. Stemming from the fact that the unknown by-product had a mass greater than the desired product by 38 mass units, it was hypothesized that this unknown by-product formed as a result of the addition of a second propargyl to the enaminone backbone. Purification of the crude reaction mixture *via* radial chromatography afforded a pure sample of the unknown by-product, however a pure sample of the *C*-propargylated enaminone product **59** was not successfully obtained as it seemed to have undergone decomposition on silica.

In order to fully elucidate and characterize the structure for the unknown product, both one and two dimensional NMR spectroscopic data was obtained, the results of which confirmed the presence of a di-propargylated product and this structure is shown below in Figure 36.

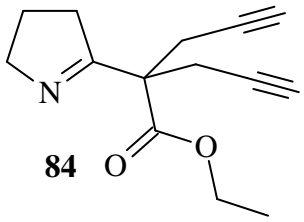

84

Figure 36

The ^{1}H NMR spectrum (Figure 37) shows that the proton peaks typical for the pyrrolidine ring and ethyl ester are present. Additionally, an interesting peak integrating for four protons has appeared in the spectrum (*ca*. 3 ppm) as well as a triplet integrating for two protons (*ca*. 2 ppm). This result was harmonious with the idea that two propargyl groups had added to the starting material which would certainly add six new protons to the molecule and also the ^{1}H NMR spectrum. The new signal at *ca*. 3 ppm was assigned as the methylene protons on the two equivalent propargyl groups (1′-*H* and 3-*H*). These four protons existed as a pair of doublet of doublets, as they are diastereotopic protons attached to a pro-chiral carbon centre, which were further split due to the incidence of long range coupling (J = 2.6 Hz) across the alkyne triple bonds to the terminal acetylenic protons (3′-*H* and 5-*H*).

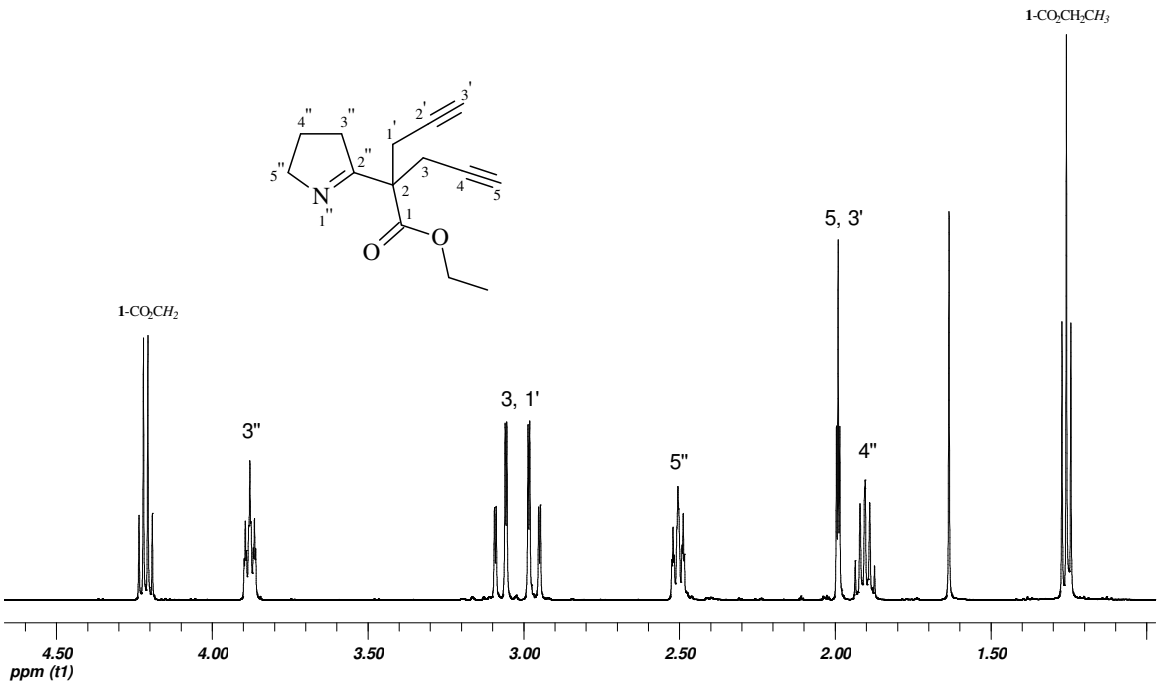

Figure 37: ^{1}H NMR Spectrum for ethyl 2-(3,4-dihydro-2*H*-pyrrol-5-yl)-2-(2-propynyl)-4-pentynoate

The triplet signal integrating for two protons at *ca*. 2 ppm appears as the result of the two equivalent acetylenic protons coupling back to the methylene protons on the propargyl groups (J = 2.6 Hz). This long range coupling was clearly evident in the two dimensional COSY spectrum which shows coupling between the doublet of doublet of doublet peak at *ca*. 3 ppm and the triplet at *ca*. 2 ppm (Figure 38). The two dimensional HSQC NMR spectrum (Figure 39) shows that the methylene proton signals at *ca*. 3 ppm are directly attached to the carbon atom resonating at 23 ppm. At first glance, both sets of methylene protons seem to be attached to the same carbon atom, however it was later determined that the two methylene carbon atoms do exist as one peak in the ^{13}C NMR spectrum as they are equivalent carbons as seen in the ^{13}C NMR spectrum (Figure 40). The ^{13}C NMR spectrum shows a total of eleven carbon peaks despite the di-propargylated product containing thirteen carbon atoms. This is a result of the two propargyl groups being chemically and electronically equivalent to each other due to free rotation about the single bond bonded *alpha* to the nitrogen.

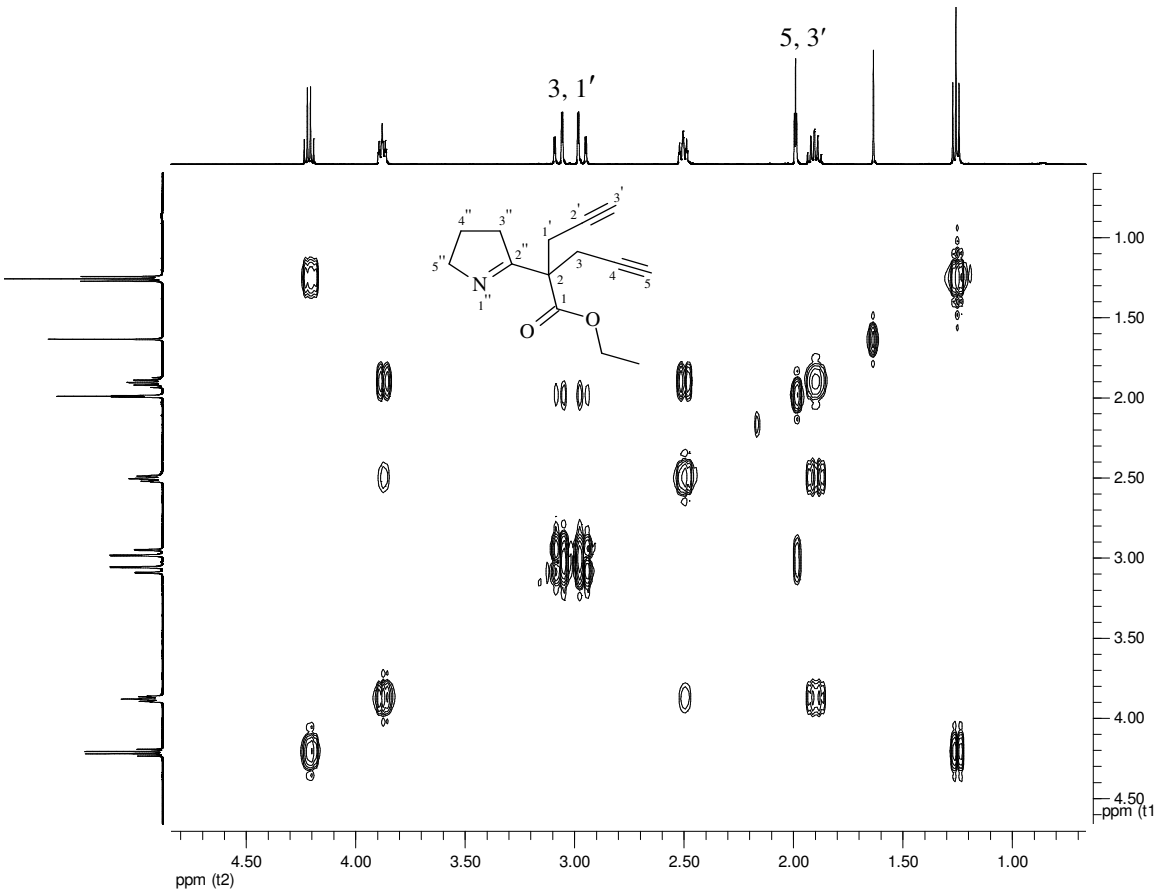

Figure 38: 2D COSY spectrum for ethyl 2-(3,4-dihydro-2*H*-pyrrol-5-yl)-2-(2-propynyl)-4-pentynoate

The corresponding carbon atoms in each propargyl group therefore have the same chemical shifts and therefore the six carbon atoms exist as three single peaks in the ^{13}C NMR spectrum. The four carbon peaks appearing at 174, 171, 80 and 54 ppm were all quaternary carbons as determined by DEPT 135 NMR analysis, and the carbon peak at 71 ppm was a tertiary carbon as determined by DEPT 90 NMR analysis. The peak at 71 ppm was thus assigned as that for the two equivalent acetylenic carbon atoms 3′-*C* and 5-*C*. The quaternary carbon peak at 79 ppm was in the acceptable range to be assigned as the equivalent alkyne carbons 4-*C* and 2′-*C* and was done so accordingly.

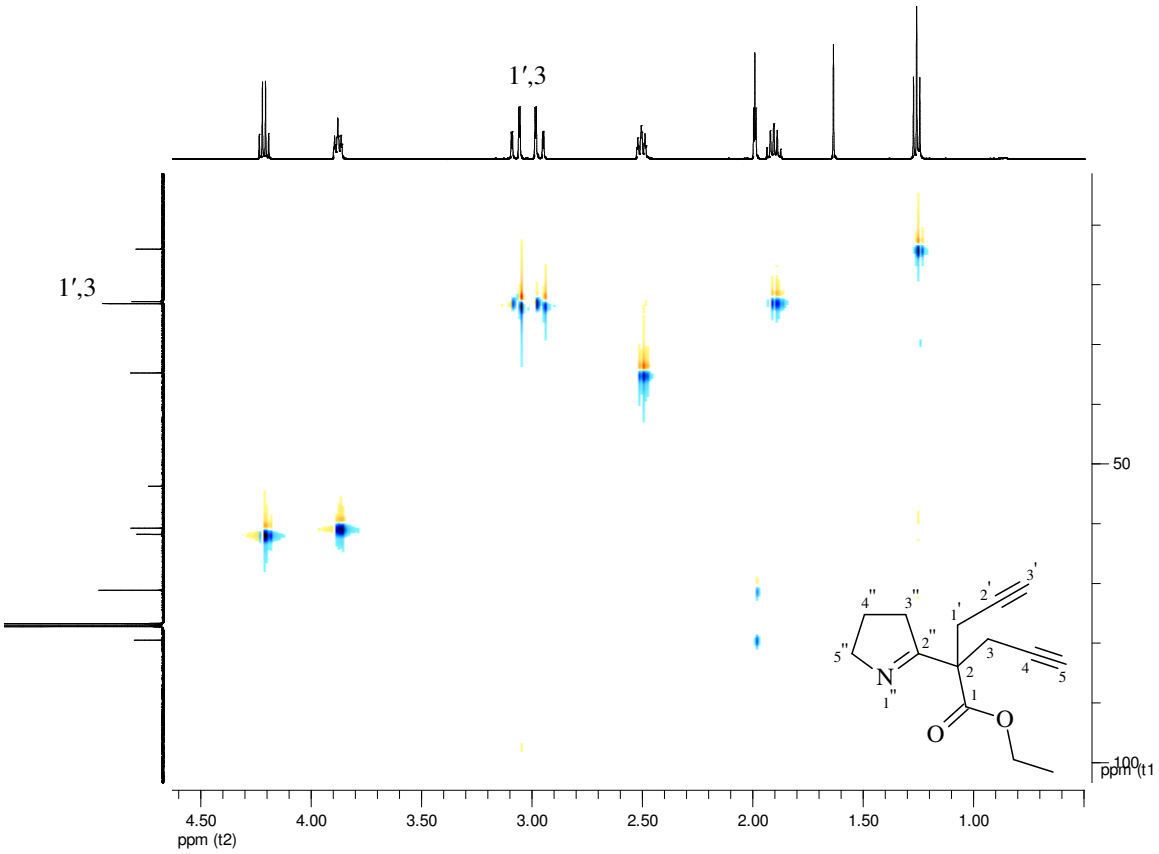

Figure 39: 2D HSQC Spectrum for ethyl 2-(3,4-dihydro-2*H*-pyrrol-5-yl)-2-(2-propynyl)-4-pentynoate

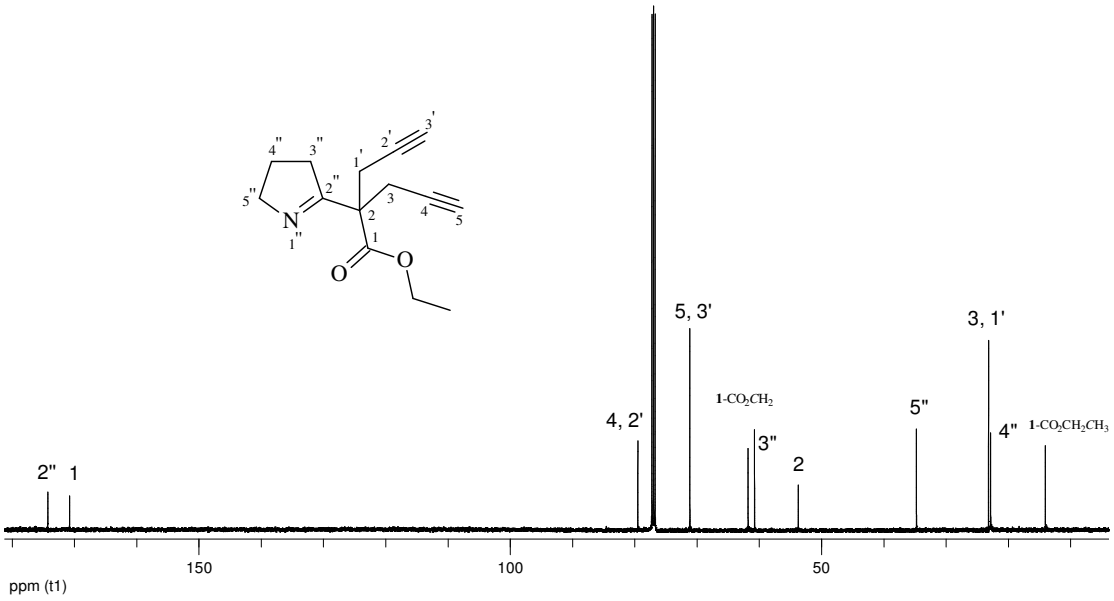

Figure 40: ^{13}C NMR Spectrum for ethyl 2-(3,4-dihydro-2*H*-pyrrol-5-yl)-2-(2-propynyl)-4-pentynoate

The quaternary carbon atom at 171 ppm was assigned as the carbonyl carbon 1-*C* due to the presence of long range coupling to the CO_2CH_2 methylene protons on the ethyl ester moiety as seen in the two dimensional HMBC NMR spectrum (Figure 41). The signal appearing at 174 ppm was assigned as the quaternary carbon 2″ and could be seen coupling with the three sets of ring protons 3″, 4″ and 5″ as well as with the methylene protons 3 and 1′. The remaining quaternary carbon peak at 54 ppm was therefore assigned as the carbon atom *alpha* to the carbonyl carbon 1-*C* and is represented as 2-*C* in the molecule. This carbon atom (2-*C*) was seen to exhibit long range coupling across to the pair of pyrrolidine ring protons at 3.9 ppm in the ^{1}H NMR spectrum. This set of ring protons were thus assigned 3″-*H* as they are situated closest to the carbon 2-*C*.

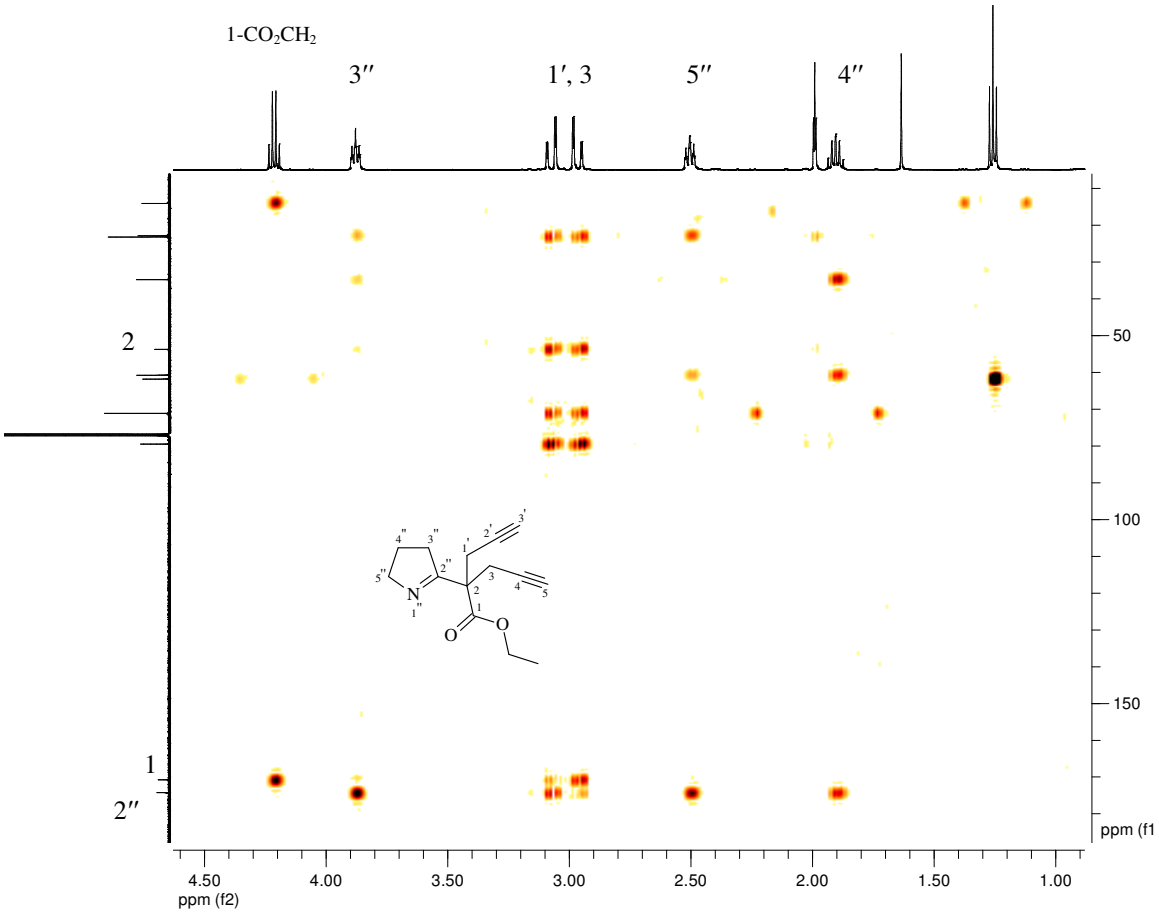

Figure 41: 2D HMBC Spectrum for ethyl 2-(3,4-dihydro-2*H*-pyrrol-5-yl)-2-(2-propynyl)-4-pentynoate

Efforts to minimize the formation of this di-propargylated by-product and maximize the formation of product were unsuccessful however, in the process a method which utilized 2 equivalents of *n*-butyllithium and 2 equivalents of propargyl bromide relative to the secondary enaminone starting material in THF was discovered which exclusively formed the di-propargyl product in a 91% isolated yield. Interestingly when toluene was used in place of THF as the solvent employing the same reaction stoichiometry as described above, a new by-product was formed as shown in the GC trace obtained for the reaction mixture (Figure 42).

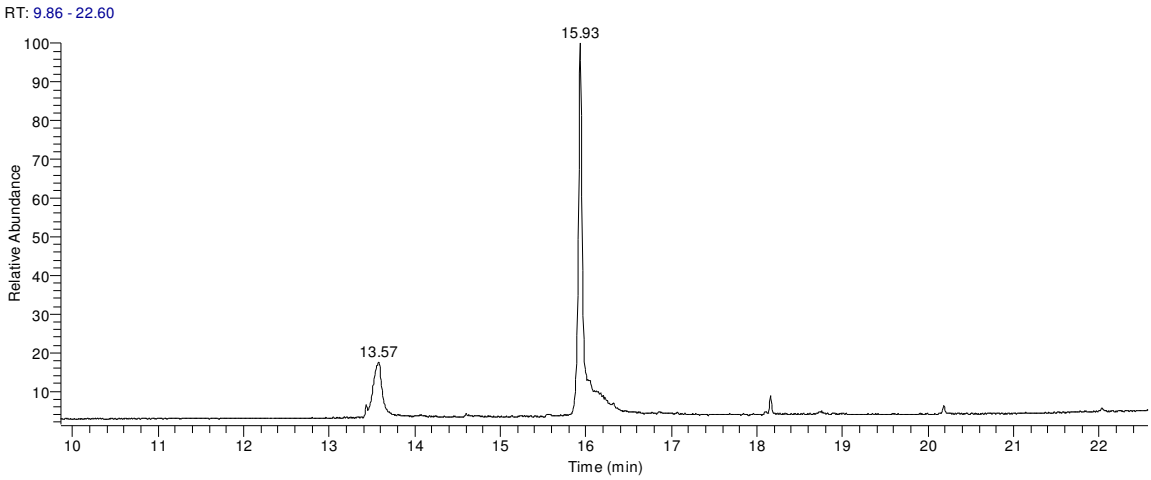

Figure 42

The peak at 13.57 minutes again corresponded to unreacted starting material as seen from the mass spectrum which showed a parent molecular ion mass of 155. The major peak at 15.93 minutes showed similar fragmentation patterns in its mass spectrum to that of the starting material, but instead possessed a parent molecular ion mass of 167 as shown in Figure 43.

This molecular mass obtained from the mass spectrum fitted harmoniously with a plausible molecular structure as shown in Figure 44.

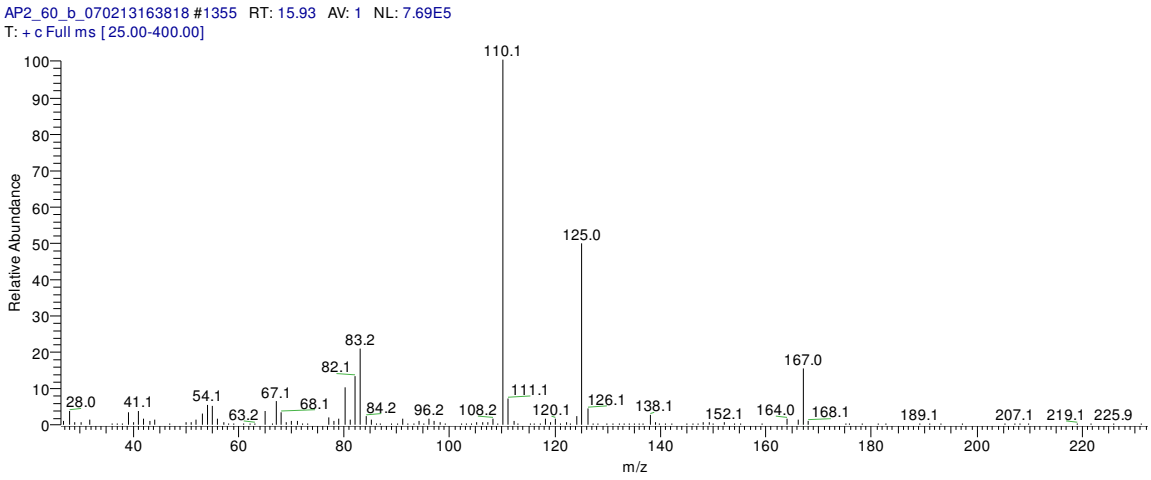

Figure 43

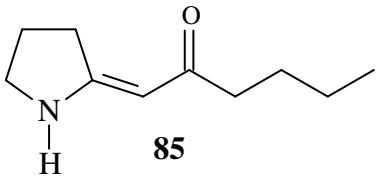

85

$C_{10}H_{17}NO$
167.25

Figure 44

The proposed structure (**85**, Figure 44) has a molecular mass of 167.25 $g.mol^{-1}$ and could have been formed as a result of nucleophilic attack by the *n*-butyllithium on the carbonyl carbon displacing the ethoxide when employing toluene as the reaction solvent (Scheme 39).

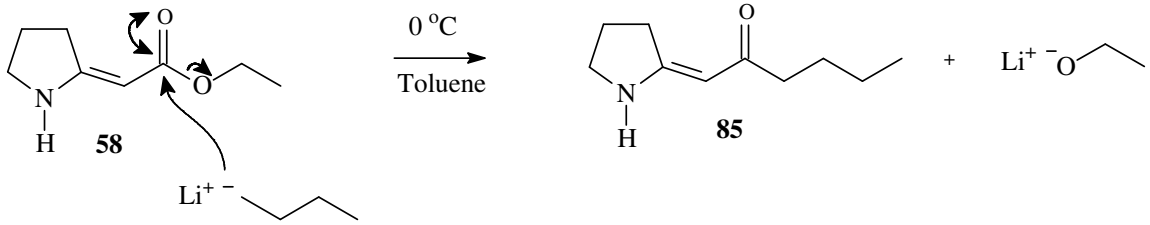

Scheme 39

Unfortunately, NMR spectroscopic data was not obtained as the sample decomposed in the fridge, and as a result, the proposed structure for this by-product could not be unambiguously assigned.*

Despite being unable to fully optimize the *C*-propargylation reaction, or purify the resulting reaction mixture to yield a pure sample of *C*-propargyl secondary enaminone **59**, we decided to carry the crude oil across into the next step without further purification.

2.3.3 Preparation of ethyl 5-methyl-2,3-dihydro-1*H*-pyrrolizine-7-carboxylate [61]

In an attempt to cyclize the *C*-propargyl compound **59** into the corresponding *N*-bridgehead pyrrole **61** (Scheme 40), the crude oil from the previous reaction (*ca*. 1.5 g) consisting of secondary enaminone **58**, *C*-propargyl secondary enaminone **59** and the *C*-di-propargyl secondary enaminone **84** was dissolved up in acetonitrile and transferred into a microwave reaction vessel.

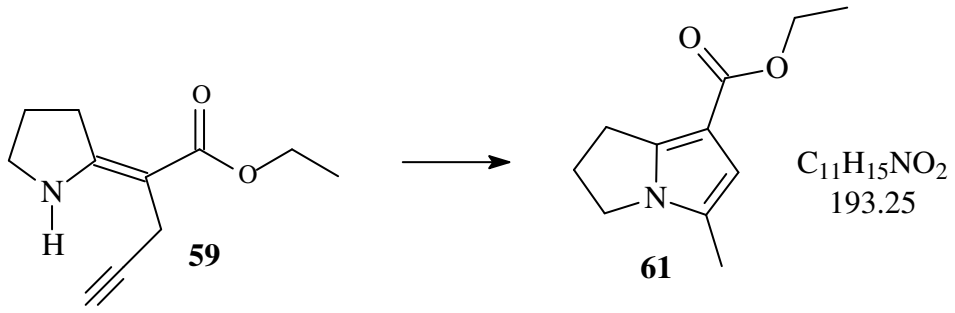

Scheme 40

Zinc chloride (140 mg) was added to the resulting solution and the mixture was irradiated with 100 watts of microwave energy for one minute. Inspection of the resulting reaction mixture using thin layer chromatography showed the presence of a major spot (R_f = 0.66), a minor spot (R_f = 0.59), and a dark black spot on the baseline using (ethyl acetate:

* The sample was not sent immediately for NMR spectroscopic analysis as the instrument was out of order and in the process of being upgraded.

hexane = 1:1) as the solvent system. The reaction mixture was passed through a short silica plug to remove the baseline impurity and concentrated *in vacuo* to yield a brown oil which was sent for GC-MS analysis. The GC trace (Figure 45) showed a minor peak at 13.6 minutes and a major peak at 17.8 minutes. The peak at 13.6 minutes had a molecular mass of 155 and was indicative of unreacted secondary enaminone **58**. The peak at 17.8 minutes was of great interest as its retention time did not correspond to any of the starting material compounds. The mass spectrum showed this new compound to have a molecular mass of 193 as expected for the desired cyclized product. Surprisingly, no such peak corresponding to any di-propargyl compound **84** was evident(!).

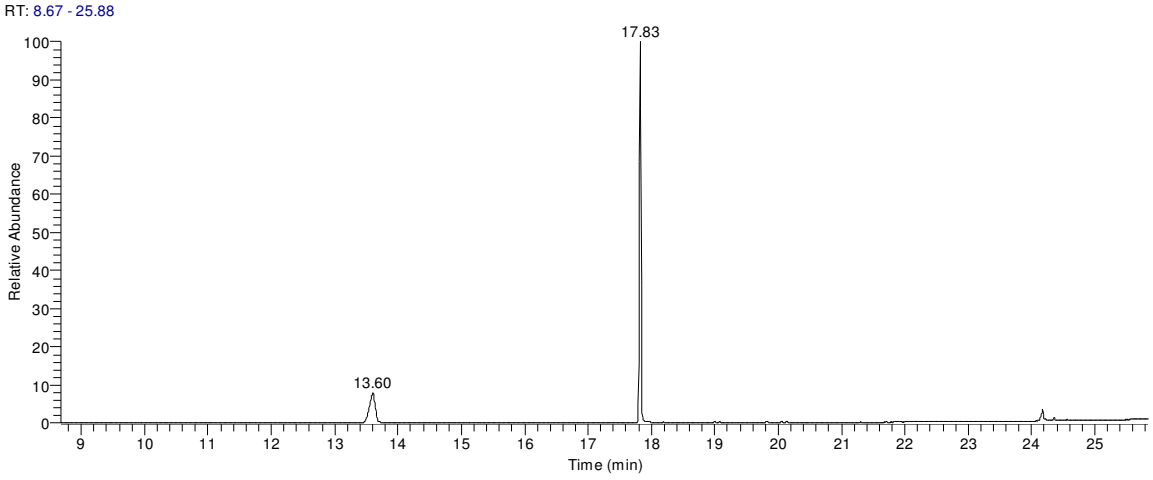

Figure 45

The new compound was successfully isolated using radial chromatography to yield 0.85 g of a pure white solid which was analyzed using both one and two dimensional NMR spectroscopy to elucidate its structure. The spectroscopic data confirmed the formation of the desired *N*-bridgehead pyrrole **61** which was obtained in a 68% overall yield from **58**, and also proved necessary in the assignment of the relevant peaks in the ^{1}H and ^{13}C spectra. A ^{1}H NMR spectrum depicting these assignments is shown below in Figure 46.

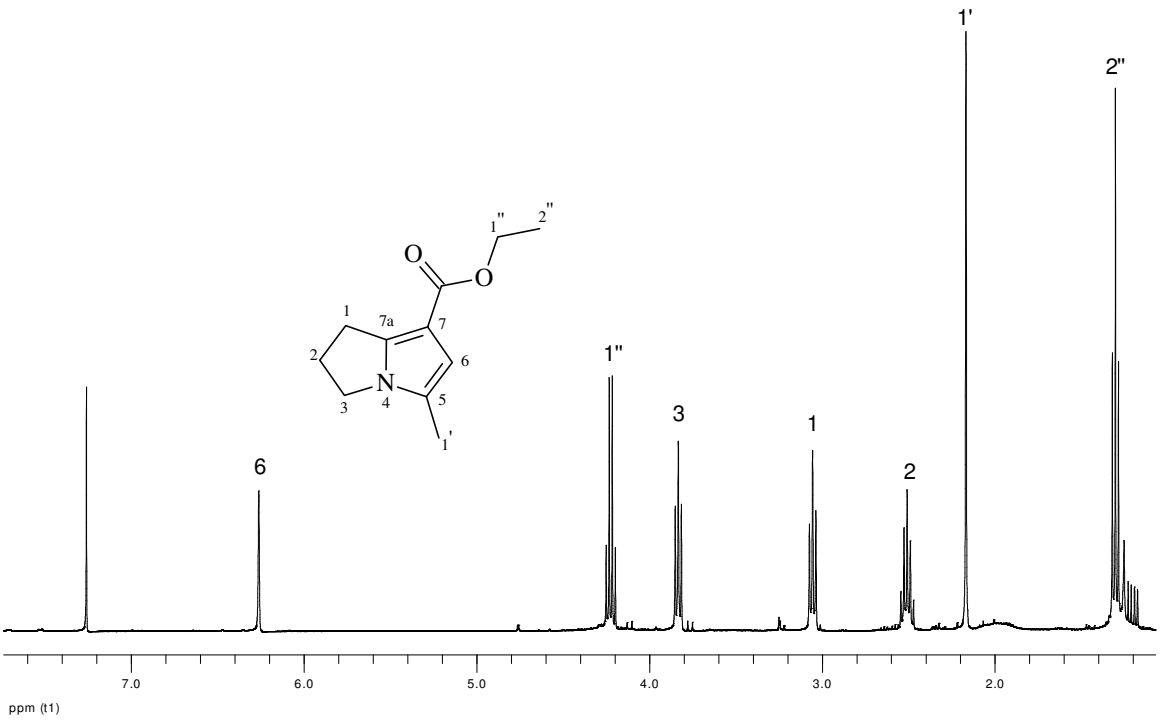

Figure 46: ^{1}H NMR Spectrum for ethyl 5-methyl-2,3-dihydro-1*H*-pyrrolizine-7-carboxylate

The ^{1}H NMR spectrum contained seven peaks which fitted aptly with the product structure which has seven differing sets of protons. The presence of the ethyl ester functionality was evident from the quartet (4.2 ppm) and triplet (1.3 ppm) peaks which corresponded to protons 1″-*H* and 2″-*H* respectively. These two signals were also seen coupling to each other in the two dimensional COSY spectrum (Figure 47). A singlet integrating for three protons was seen resonating at 2.2 ppm due to the methyl group 1′-*H* and a singlet integrating for one proton was present at 6.3 ppm due to the aromatic proton (6-*H*) on the pyrrole ring. Of the three remaining peaks, the multiplet integrating for two protons at 2.5 ppm was assigned to the methylene protons 2-*H* as it is surrounded by four adjacent protons. The last two triplet peaks were assigned accordingly after their coupling was analyzed in the HSQC and HMBC spectra.

The ^{13}C NMR spectrum showed eleven carbon peaks which corresponded to the eleven carbon atoms in the molecular structure, which have also been assigned accordingly (Figure 48).

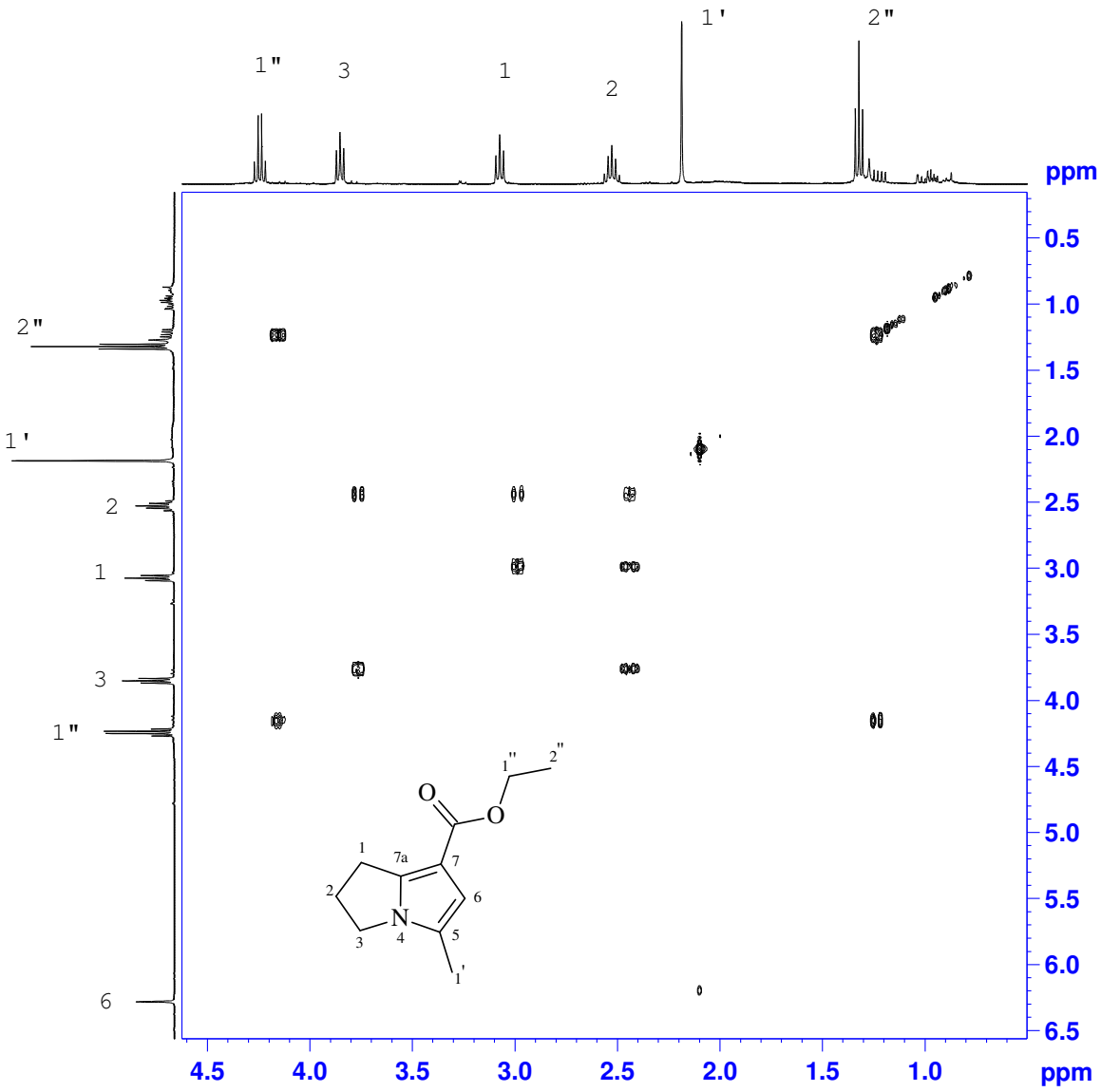

Figure 47: 2D COSY Spectrum for ethyl 5-methyl-2,3-dihydro-1*H*-pyrrolizine-7-carboxylate

The DEPT 135 spectrum (Figure 49) helped differentiate between the CH, CH_2 and CH_3 carbon peaks in the ^{13}C NMR spectrum as the CH and CH_3 peaks point upwards while the CH_2 peaks point downwards. The peak at 110 ppm was assigned as the CH carbon (6-*C*) and was confirmed by inspecting the two dimensional HSQC spectrum (Figure 50). The peaks at 59, 45, 27 and 27 ppm were all CH_2 carbons and the peaks at 15 and 12 ppm were both CH_3 carbons.

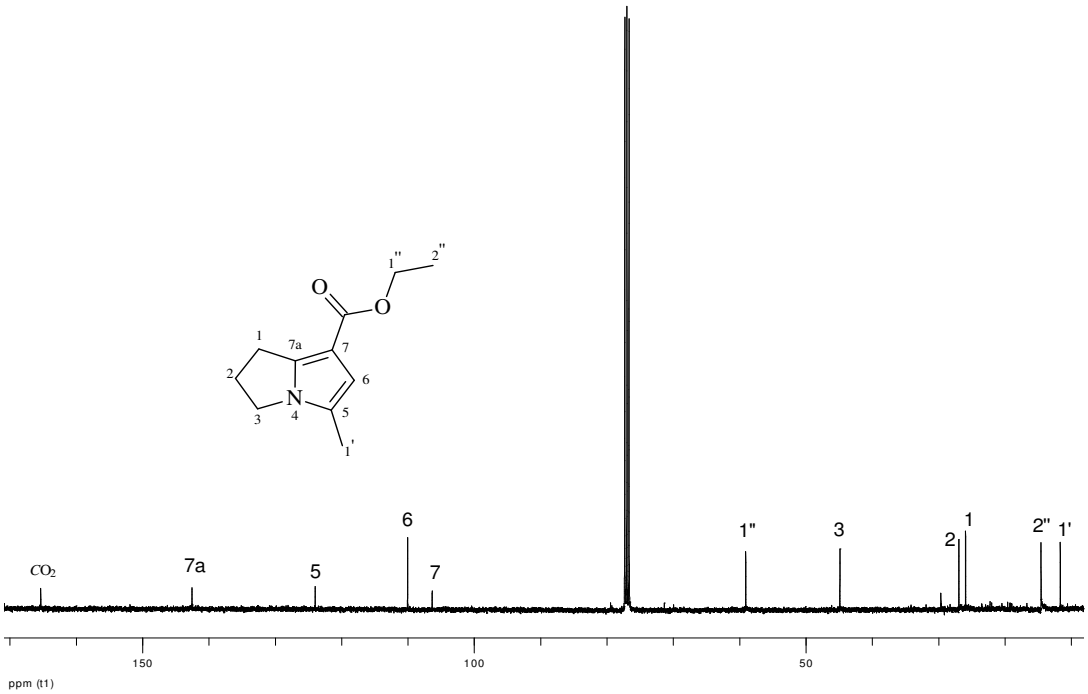

Figure 48: ^{13}C NMR Spectrum for ethyl 5-methyl-2,3-dihydro-1*H*-pyrrolizine-7-carboxylate

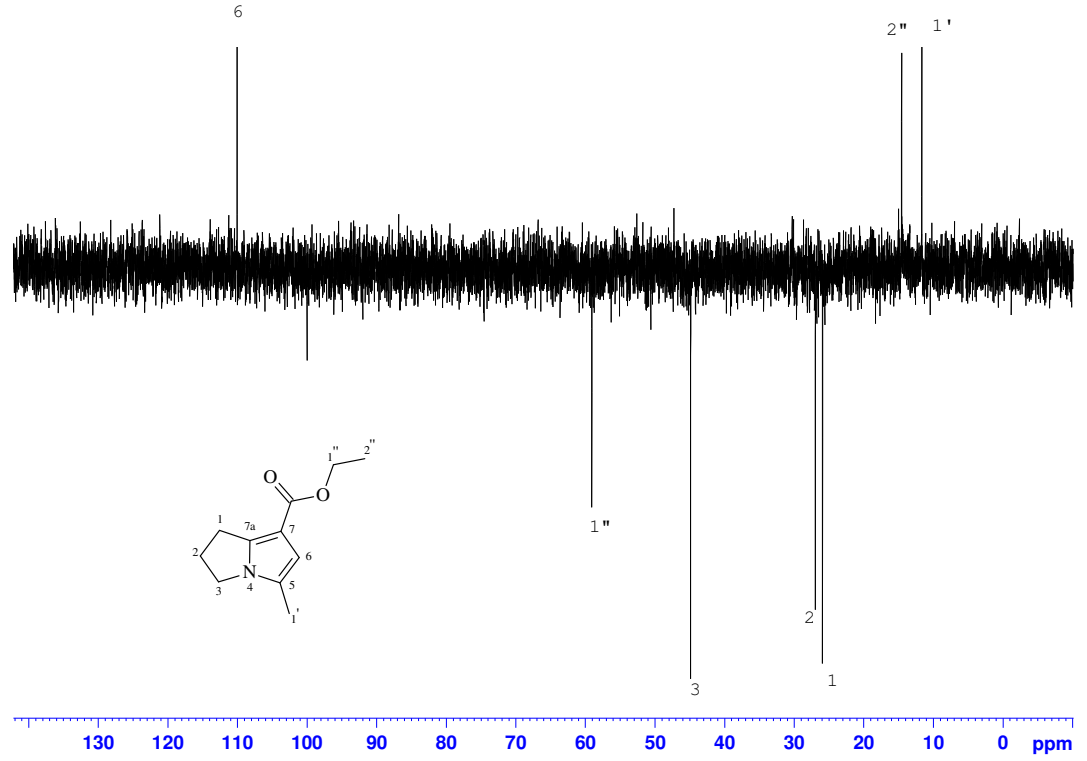

Figure 49: DEPT 135 Spectrum for ethyl 5-methyl-2,3-dihydro-1*H*-pyrrolizine-7-carboxylate

The HSQC NMR spectrum (Figure 50) was useful in assigning the specific peaks in the ^{13}C NMR spectrum, as it showed which carbon atoms were directly attached to which proton peaks in the ^{1}H NMR spectrum.

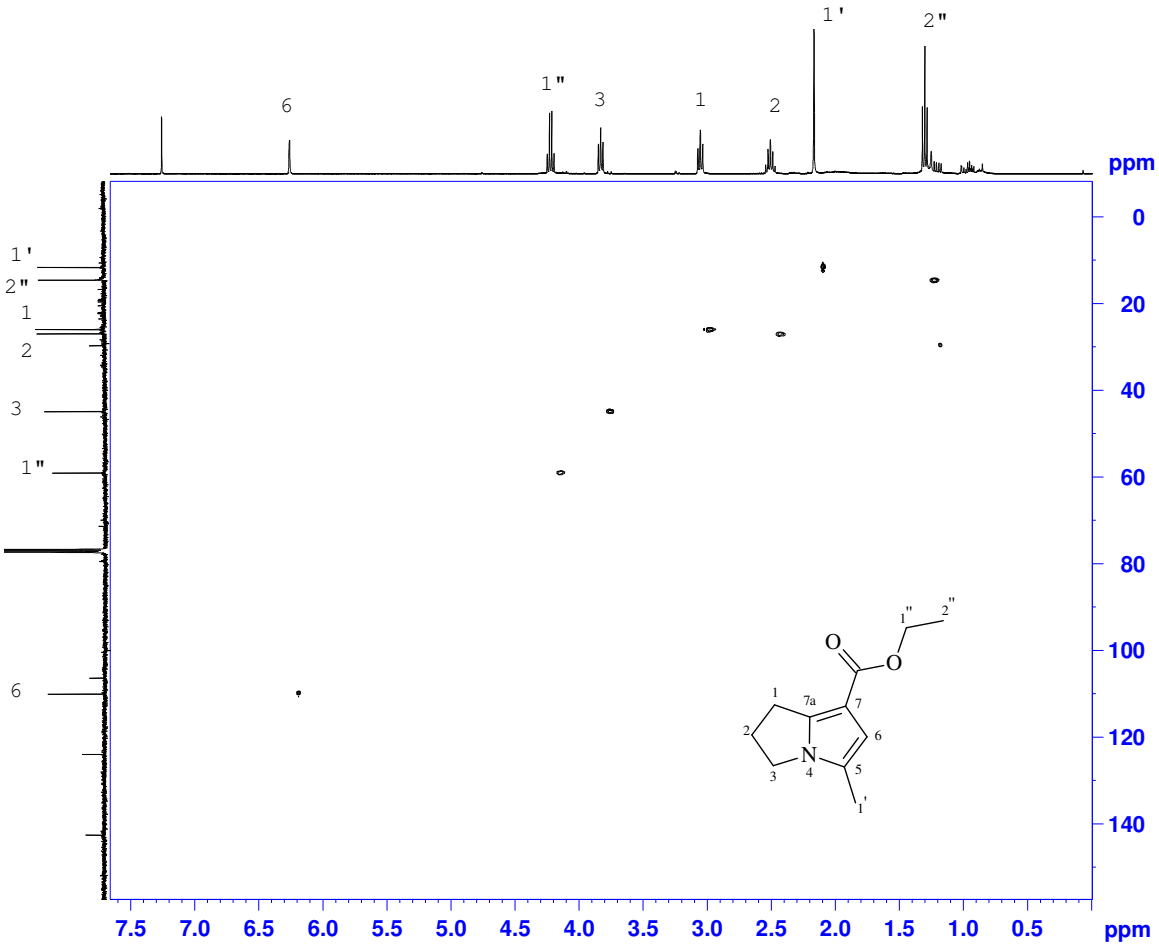

Figure 50: 2D HSQC Spectrum for ethyl 5-methyl-2,3-dihydro-1*H*-pyrrolizine-7-carboxylate

The remaining four carbon peaks at 165, 142, 124 and 107 ppm did not show up in the DEPT 135 experiment and were therefore quaternary in nature. These quaternary carbon peaks were assigned by analyzing their chemical shift in the ^{13}C NMR spectrum as well as from their coupling seen in the HMBC NMR spectrum (Figure 51). The peak at 165 ppm was assigned as the carbonyl carbon as its chemical shift was in the appropriate range for that of an ester carbon. This assignment was confirmed by the presence of strong coupling through to the ester protons 1″-*H* which was indicative of their close proximity. The peak at 142 ppm showed strong coupling to the protons 1-*H* on the ring

and weaker coupling to protons 2-*H* and 3-*H* and was consequentially assigned as the bridgehead carbon 7a-*C*. The quaternary carbon peak resonating at 124 ppm showed strong coupling through to the methyl protons 1′-*H* and was assigned as carbon 5-*C*. The remaining quaternary carbon at 107 ppm showed no observable coupling in the HMBC NMR spectrum and was assigned as carbon 7-*C*.

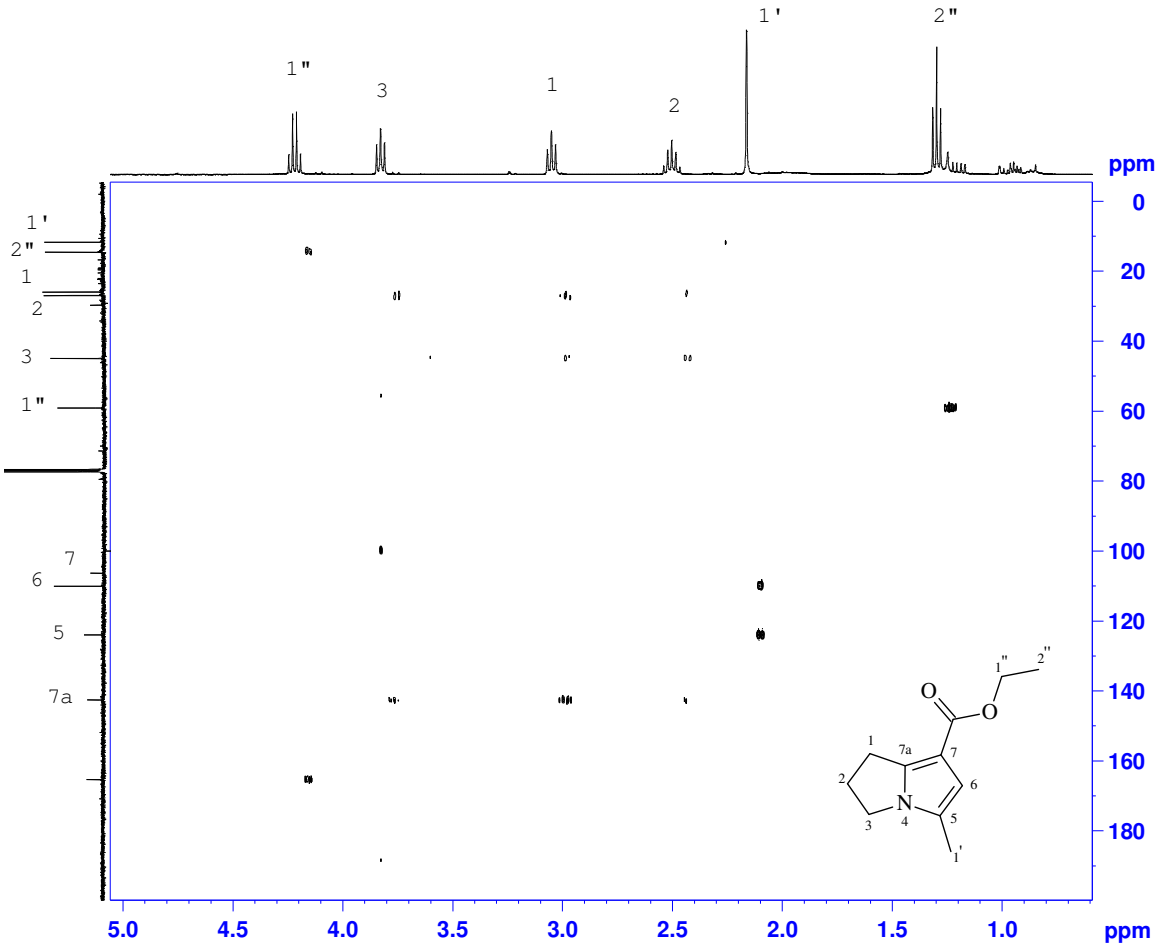

Figure 51: 2D HMBC Spectrum for ethyl 5-methyl-2,3-dihydro-1*H*-pyrrolizine-7-carboxylate

2.3.4 Overview of Model Study

The model study that was incorporated into this project established that the *N*-bridgehead pyrrole scaffold **61** could be successfully synthesized starting from the commercially

available lactam derivative **67**. A scheme depicting this overall synthetic strategy is shown below in Scheme 41.

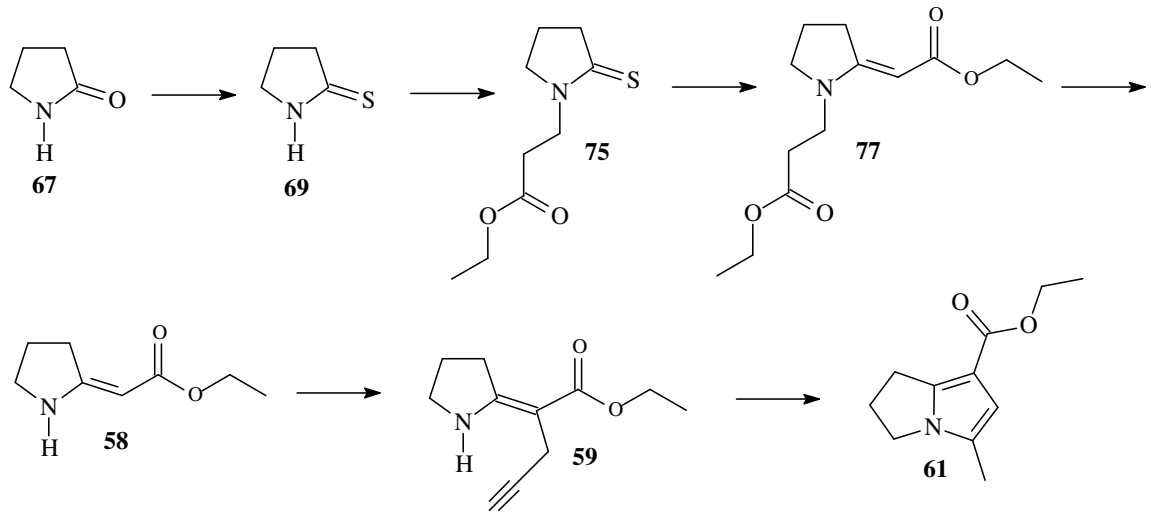

Scheme 41

The thiolactam **69** was prepared by the reaction of lactam **67** with Lawesson's reagent in dry THF, and was obtained in a pleasing 78% yield after column chromatography. Performing an Eschenmoser coupling reaction on the thiolactam directly to yield **58** proved unsuccessful and therefore a protection-deprotection strategy was implemented to the synthesis. The thiolactam **69** was subsequently combined with ethyl acrylate and sodium hydroxide (cat.) in THF to yield the *N*-protected tertiary thiolactam **75** in a 100% isolated yield. The tertiary thiolactam **75** was successfully elaborated upon employing Eschenmoser coupling conditions to yield the *N*-protected tertiary enaminone **77** in an excellent 75% yield after column chromatography. The acrylate protection group was removed from **77** by reaction with a strong, non-nucleophilic base (KHMDS) to yield the enaminone **58** in a 72% isolated yield after radial chromatography. The *C*-propargyl enaminone derivative **59** was successfully obtained, but as a mixture also containing starting material **58** and an interesting di-propargylated side product **84**. Purification of **59** was unsuccessful and it showed signs of decomposition on silica gel. The crude reaction mixture containing 40% *C*-propargyl enaminone **59** was therefore subject to hydroamination conditions in the presence of a $ZnCl_2$ catalyst which afforded the *N*-bridgehead pyrrole **61** in a 68% overall yield from **58**. Overall, the *N*-bridgehead pyrrole **61** was obtained in a 29% yield from the lactam **67** over the six synthetic steps. With this

methodology optimized, it was integrated into the total synthesis of the pyrrolizidine ant alkaloid **223H** (xenovenine).

2.4 Studies Toward Ant Alkaloid 223H (xenovenine)

The results attained from the model study validated that an *N*-bridgehead pyrrole scaffold could be certainly obtained from a lactam starting material. With the objective of accessing the ant alkaloid **223H** (xenovenine) **62** (Scheme 42) this methodology was utilized in the synthesis of **223H** (xenovenine) but with two main differences.

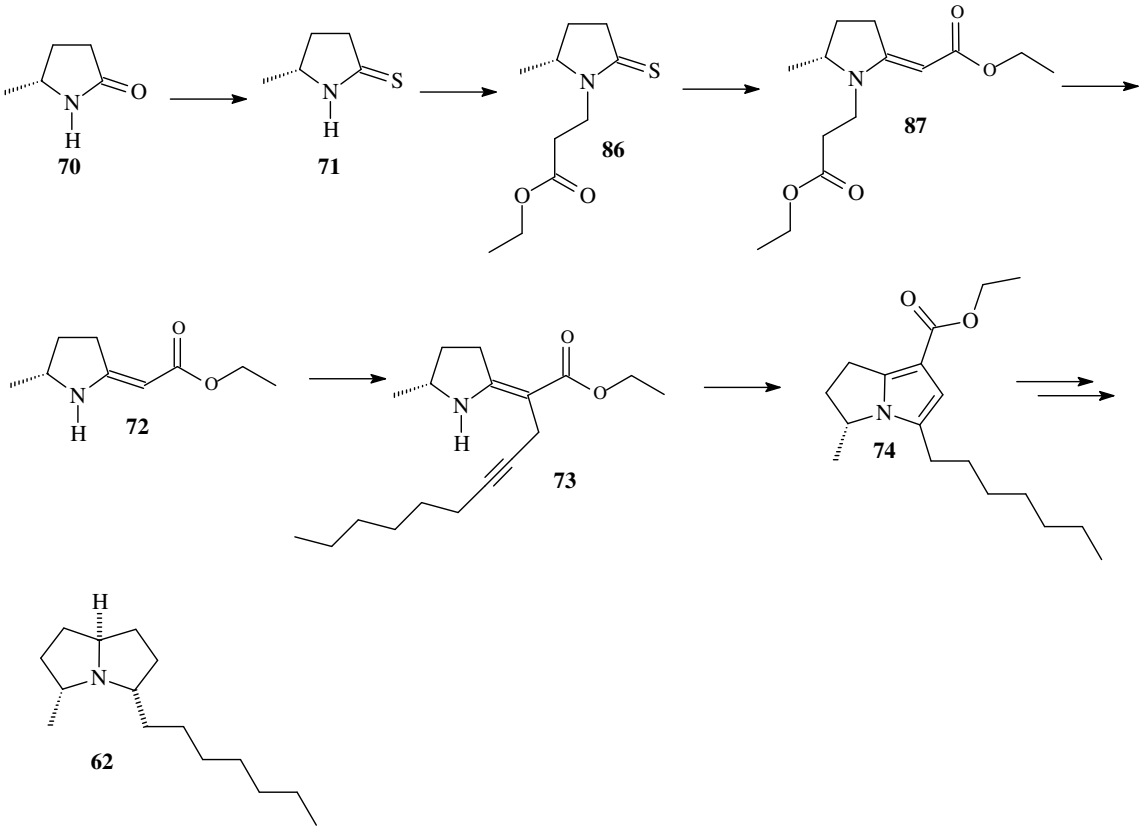

Scheme 42

Firstly, by starting with a methyl lactam derivative **70** (Scheme 42), the methyl functionality at position 5 on the pyrrolizidine alkaloid product **62** could potentially be obtained. Secondly, when carrying out the *C*-propargylation step, 1-bromo-2-nonyne will

be utilized in place of propargyl bromide with the purpose of forming a *C*-propargylated product **73**, which following a successful hydroamination/cyclization reaction could allow access to **74**, a structurally analogous precursor to the target molecule **223H** (xenovenine).

With this synthetic plan in hand, we set about designing a synthetic route which could access the methyl lactam starting material **70**. The following section describes the retrosynthetic analysis and formal synthesis towards its formation.

2.4.1 Preparation of (5*R*)-5-methyltetrahydro-2*H*-pyrrol-2-one [70]

A retrosynthetic strategy was proposed for the synthesis of the lactam **70** and is depicted in Scheme 43.

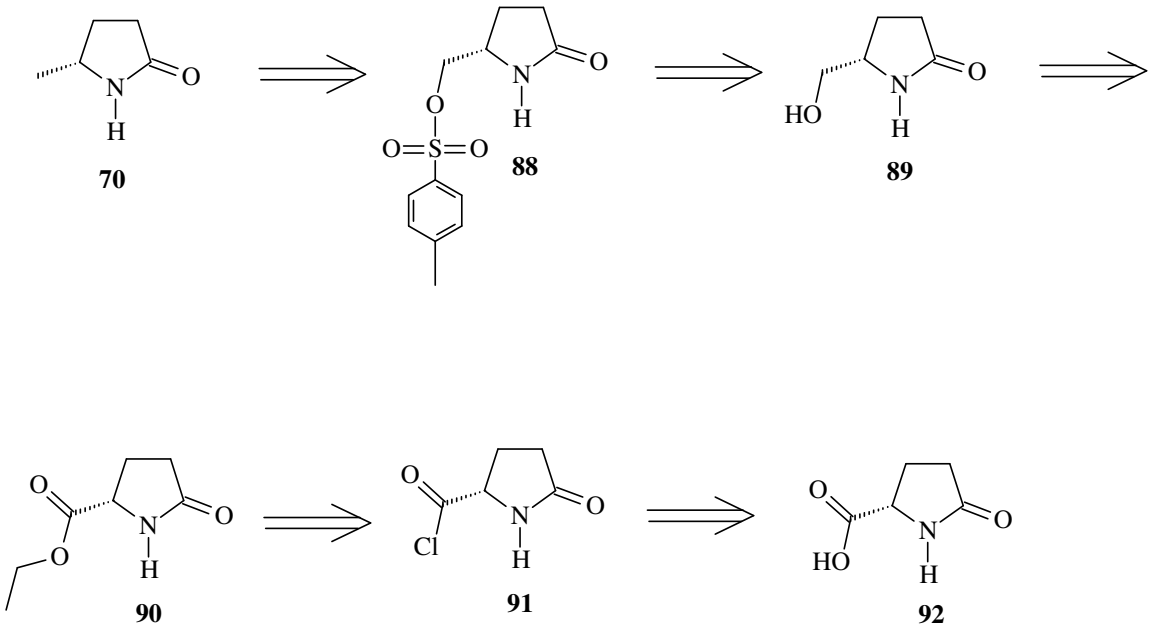

Scheme 43

It has been well documented that methyl functionalities can be obtained by reduction of the corresponding tosylate derivatives using tributyltin hydride in the presence of 2, 2′-azobisisobutyronitrile. It was thus proposed that the methyl lactam **70** could be obtained from a tosylated derivative such as **88**. Due to the vast amount of literature evidence supporting the fact the tosylated compound can be easily prepared from alcohols, the synthesis of the tosylated compound **88** from an alcohol functionality as depicted in **89** seemed a viable assumption. It is well known that the formation of alcohols from acyl chlorides, aldehydes, and certain esters can be readily achieved using sodium borohydride as the reducing agent. The ethyl ester **90** was thus chosen as a synthetic precursor to the alcohol due to the wealth of literature evidence supporting this transformation. The ethyl ester seemed a more practicable precursor over the corresponding acyl chloride or aldehyde derivative due to its higher chemical stability in protic solvents such as water or methanol which are required solvents to be used in conjunction with reduction reactions employing sodium borohydride. It was proposed that the ethyl ester derivative **90** could be synthesized from an optically pure carboxylic acid such as (*S*)-pyroglutamic acid **92** *via* a highly reactive acyl chloride derivative **91**. The use of (*S*)-pyroglutamic acid **92** was advantageous as it was commercially available, non-expensive and of excellent optical purity.

The first step in the proposed synthesis utilized the optically pure (*S*)-pyroglutamic acid **92** with the intent of obtaining the optically pure ethyl ester derivative **90** *via* the reactive acyl chloride intermediate **91** (Scheme 44).

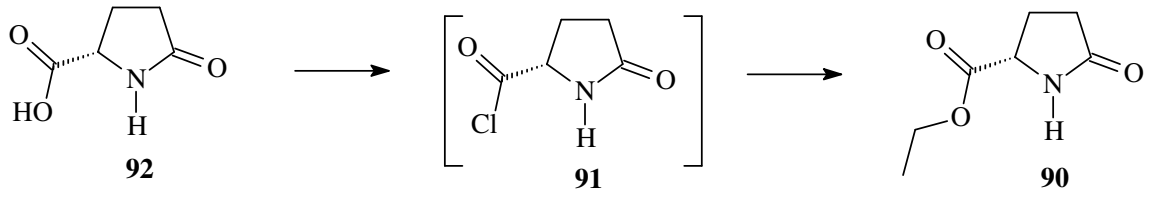

Scheme 44

The thionyl chloride reagent was added to a stirring mixture of (*S*)-pyroglutamic acid in dry ethanol and stirred for 1 hour at room temperature followed by 3 hours at reflux

temperature. The reaction solution was concentrated *in vacuo* to furnish a pale yellow oil which was kept under vacuum for an additional 2 hours to remove excess thionyl chloride and hydrogen chloride. The oil was purified *via* column chromatography to afford the ethyl ester derivative **90** in a 53% isolated yield from the acid **92** as a colourless oil that solidified upon standing, the structure of which was confirmed using both one and two dimensional NMR spectroscopy.

Analysis of the coupling in the NMR spectra allowed us to unambiguously assign the peaks in the ^{1}H and ^{13}C NMR spectrum, the assignments of which are depicted in the spectra that follow. The ^{1}H NMR spectrum (Figure 52) clearly showed the presence of the N-*H* functionality as a broad singlet resonating at 6.6 ppm and integrating for one proton.

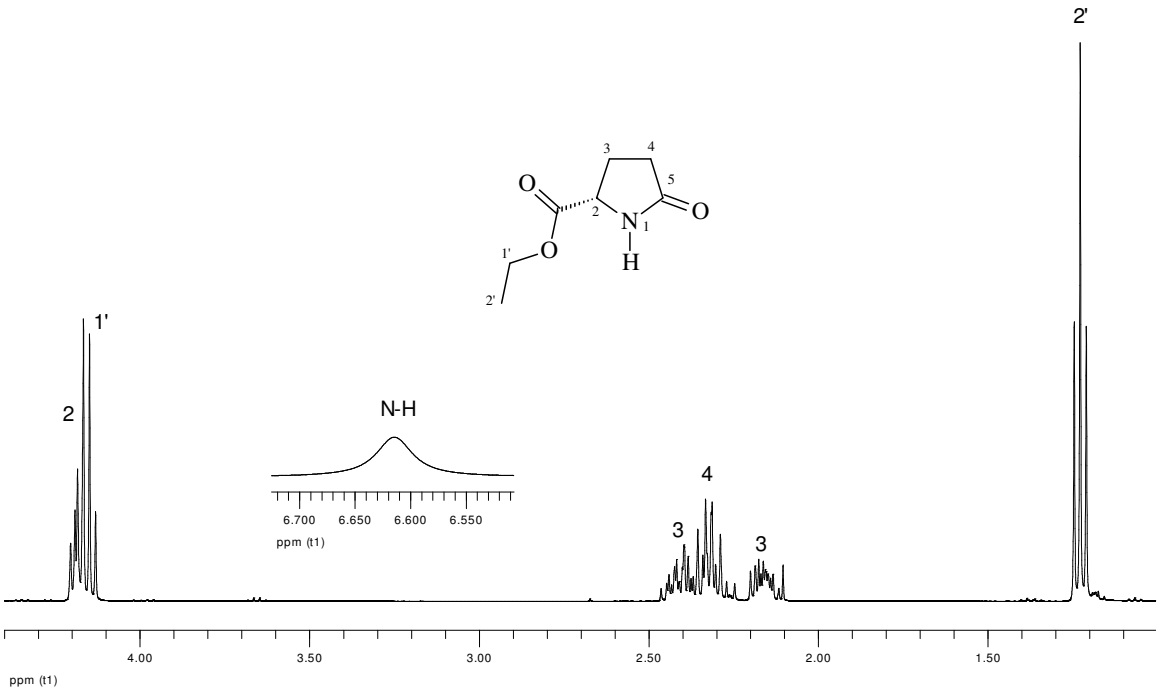

Figure 52: ^{1}H NMR Spectrum for ethyl (2*S*)-5-oxotetrahydro-1*H*-pyrrole-2-carboxylate

The triplet at 1.23 ppm was seen coupling to the quartet at 4.16 ppm in the COSY spectrum (Figure 53) and their respective chemical shifts and integration were indicative of the existence of the ethyl ester functionality. The remaining peaks in the ^{1}H NMR

spectrum resonating at 4.19, 2.40, 2.33 and 2.16 ppm together integrated for a total of five protons and were deemed those of the ring protons.

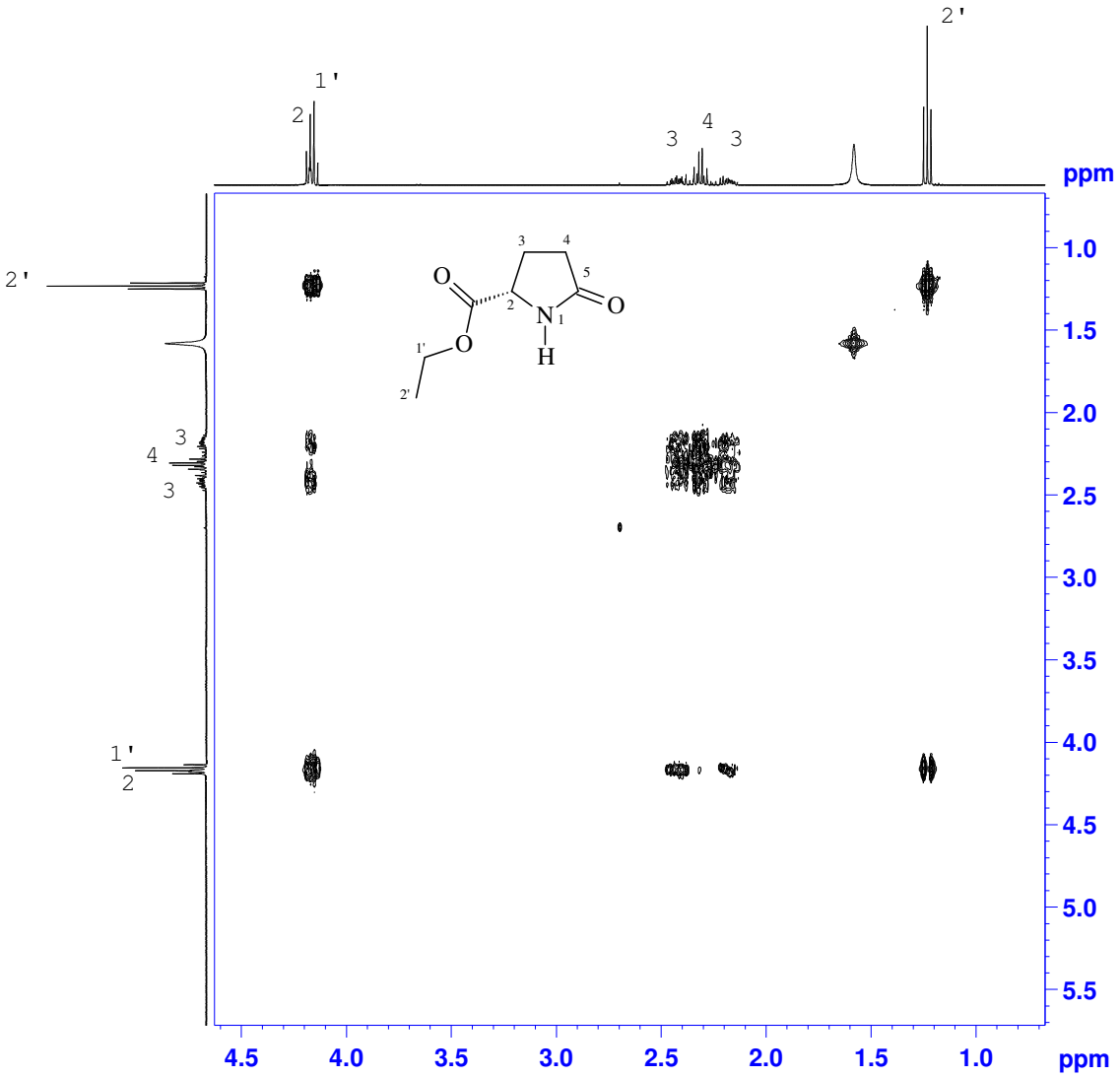

Figure 53: 2D COSY Spectrum for ethyl (2*S*)-5-oxotetrahydro-1*H*-pyrrole-2-carboxylate

The ^{13}C NMR spectrum (Figure 54) showed the presence of seven carbon peaks as expected for the ethyl ester **90**. Analysis of the DEPT 135 NMR (Figure 55) spectrum inferred that the carbon peaks at 61.7, 29.3 and 24.8 ppm were secondary in nature and that the carbon peak at 14.2 ppm was primary in nature. The peak resonating at 55.6 ppm was assigned as being tertiary in nature due to its downfield shift in the DEPT 135 experiment which was confirmed using DEPT 90 NMR spectroscopy. The carbon peaks

resonating at 178.1 and 172.0 ppm did not appear in the DEPT experiments and were considered quaternary in nature.

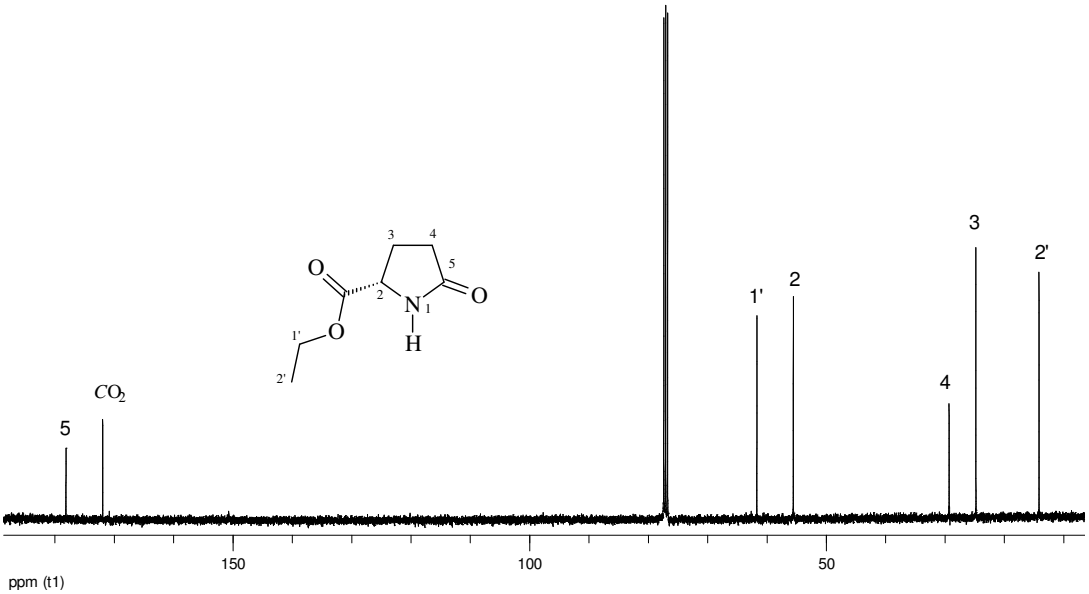

Figure 54: ^{13}C NMR Spectrum for ethyl (2*S*)-5-oxotetrahydro-1*H*-pyrrole-2-carboxylate

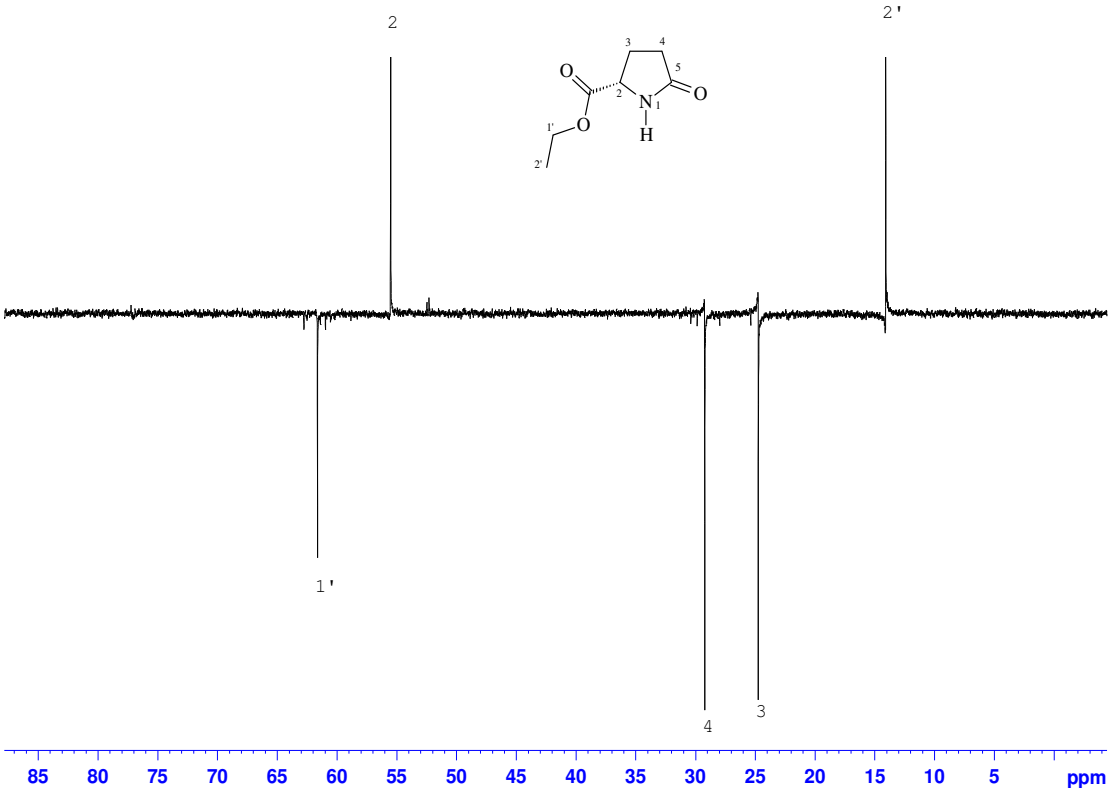

Figure 55: DEPT 135 Spectrum for ethyl (2*S*)-5-oxotetrahydro-1*H*-pyrrole-2-carboxylate

The two dimensional HSQC NMR spectrum shown in Figure 56 was useful in determining which protons in the ^{1}H NMR spectrum were directly attached to which carbon atoms in the ^{13}C NMR spectrum. The tertiary carbon peak at 55.6 ppm in the ^{13}C spectrum was shown to directly couple to the proton peak at 4.19 ppm in the ^{1}H spectrum. As this was the only tertiary carbon in the molecule it could be unambiguously assigned as the carbon at position 2-*C*.

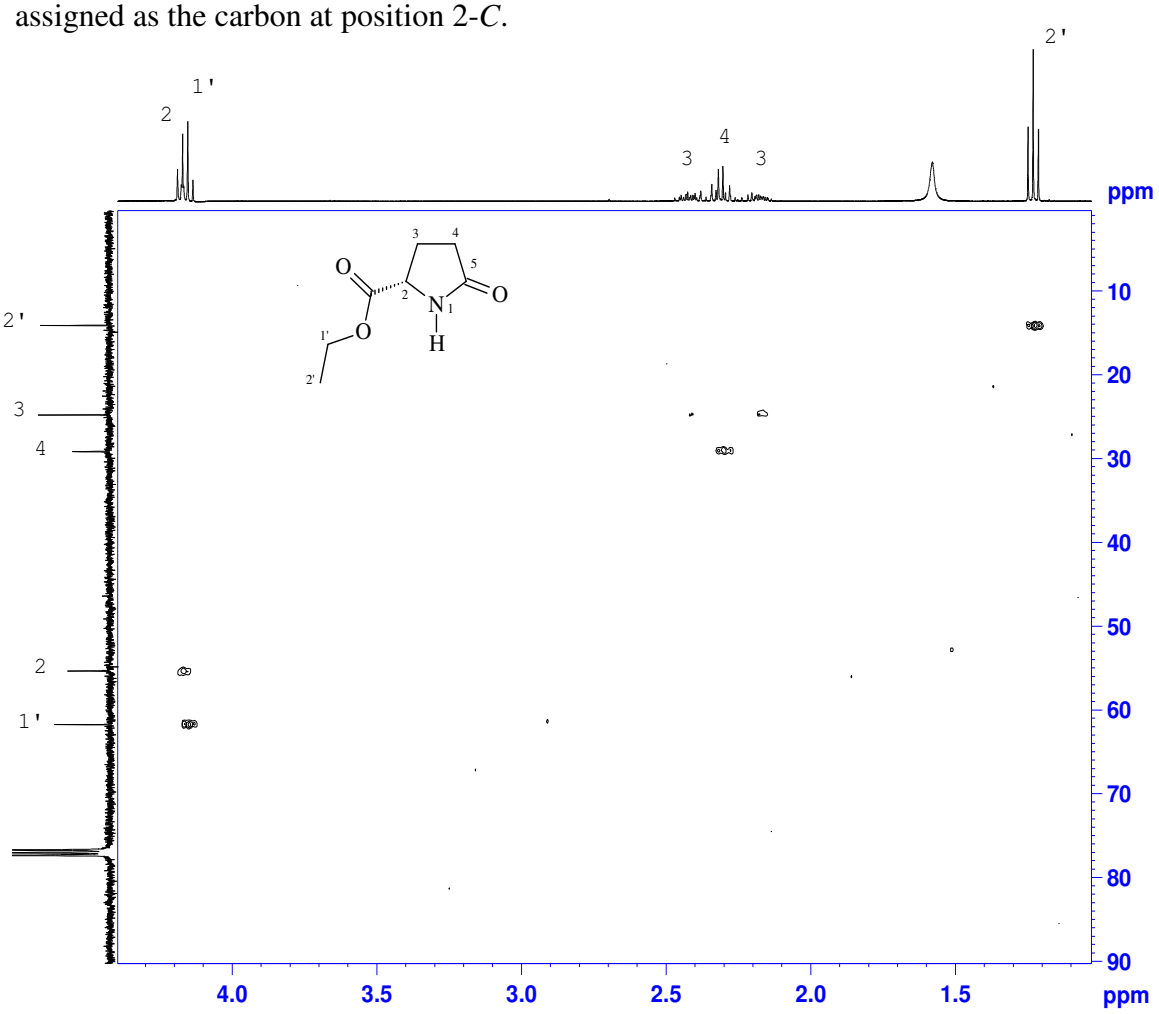

Figure 56: 2D HSQC Spectrum for ethyl (2*S*)-5-oxotetrahydro-1*H*-pyrrole-2-carboxylate

The two peaks resonating at 2.40 and 2.16 ppm in the ^{1}H spectrum were shown to reside on the same CH_2 carbon atom appearing at 24.8 ppm in the ^{13}C spectrum. The fact that these two proton peaks integrated for one proton each as well as the fact that they were seen coupling with the CH proton 2-*H* in the COSY spectrum (Figure 53) lead us to

believe that these peaks were the result of the ring protons at position 3-*H* of the ring. These ring protons were evident as two separate peaks as they existed directly adjacent to a chiral centre which placed each proton in a different electronic environment. The CH_2 proton peak at 2.33 ppm was assigned as 4-*H* and could be seen coupling back to the protons 3-*H* in the two dimensional COSY spectrum which was evident of their close proximity. The two quaternary carbons were assigned accordingly based on their long range coupling exhibited in the two dimensional HMBC spectrum (Figure 57). The quaternary carbon peak at 172 ppm could be seen coupling with adjacent protons 2-*H* and 1′-*H* and was thus assigned as the ester carbonyl carbon 2-CO_2. The remaining quaternary carbon peak at 178.1 ppm was in the appropriate chemical shift to assigned as the amide carbonyl 5-*C*.

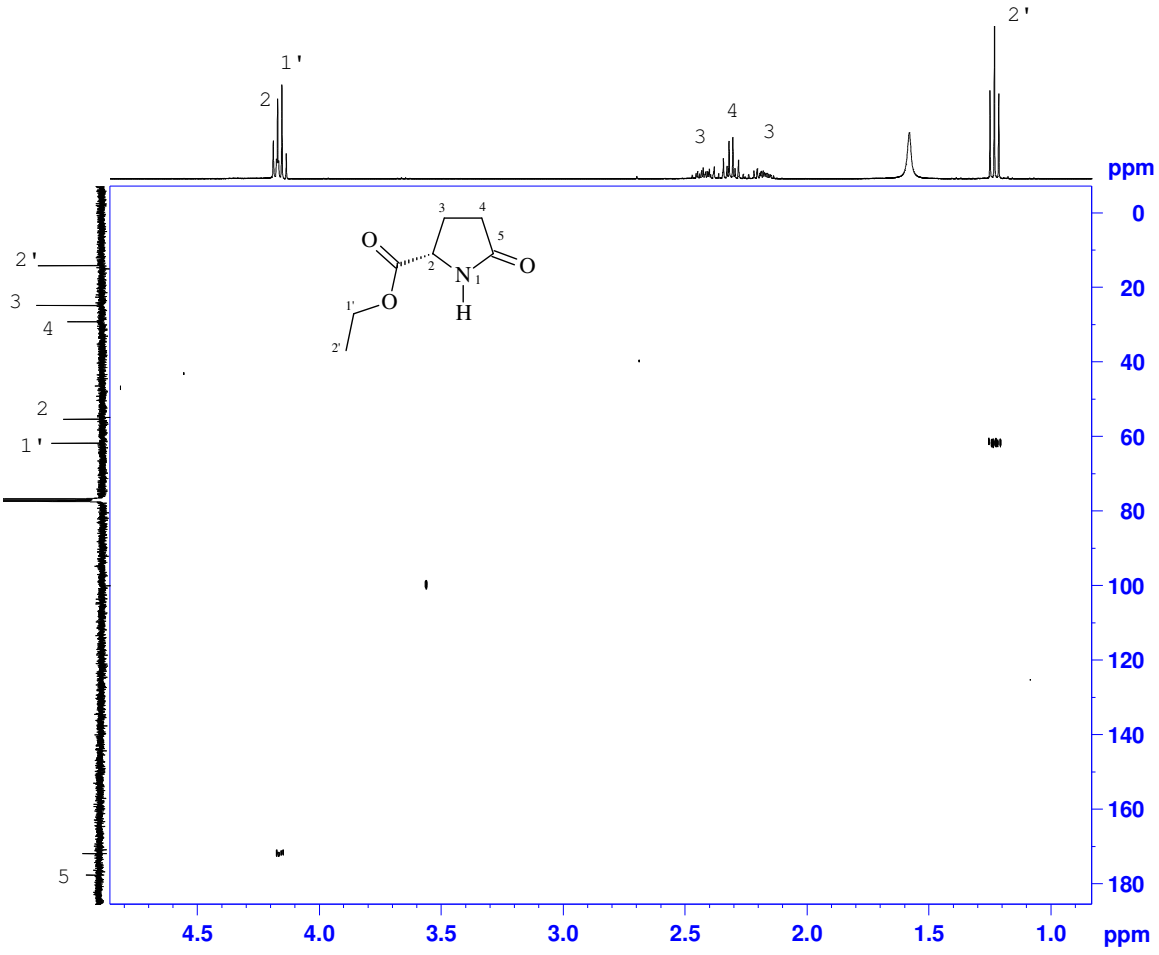

Figure 57: 2D HMBC Spectrum for ethyl (2*S*)-5-oxotetrahydro-1*H*-pyrrole-2-carboxylate

Despite the successful formation of the desired ethyl ester **90** using the above mentioned procedure, the yield was poor (53%) and the method required the use of a corrosive reagent, thionyl chloride. The method of Fischer esterification was subsequently employed in an attempt to increase the overall yield of **90** as well as eliminate the need to utilize thionyl chloride.

It has been well documented that esters can be synthesized by the reaction between carboxylic acids and alcohols in the presence of an acid catalyst. The underlying theory to such a reaction is that one of the reagents must be introduced into the reaction mixture in an excess which drives the forward reaction to near completion according to Lé Chatelier's principle. This method of Fischer esterification was therefore utilized in an attempt to form the ethyl ester **90** as depicted by Scheme 45.

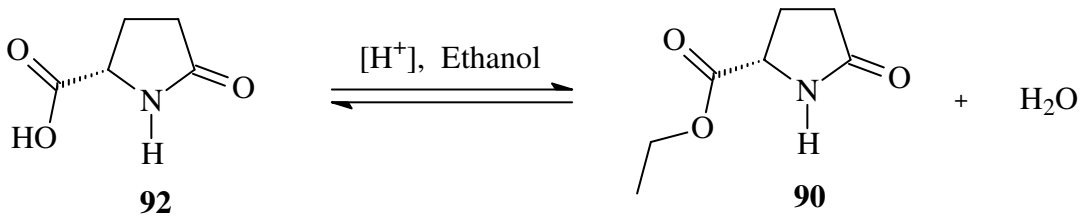

Scheme 45

Pyroglutamic acid **92** was added to a 75% ethanol:toluene solution along with 4 ml of concentrated sulfuric acid. The mixture was refluxed using a Dean and Stark apparatus for 10 hours to remove water after which the reaction mixture was worked up to furnish a colourless oil. Analysis of the oil using GC-MS showed the formation of two compounds with retentions times of 13.95 and 14.44 minutes respectively (Figure 58).

The oil was purified using a short path distillation setup and the two compounds were successfully separated. The first compound distilled off with a temperature range of 125-135^{o}C (6 mmHg) followed by the second component which distilled off at a range of 168-170 ^{o}C at the same pressure.

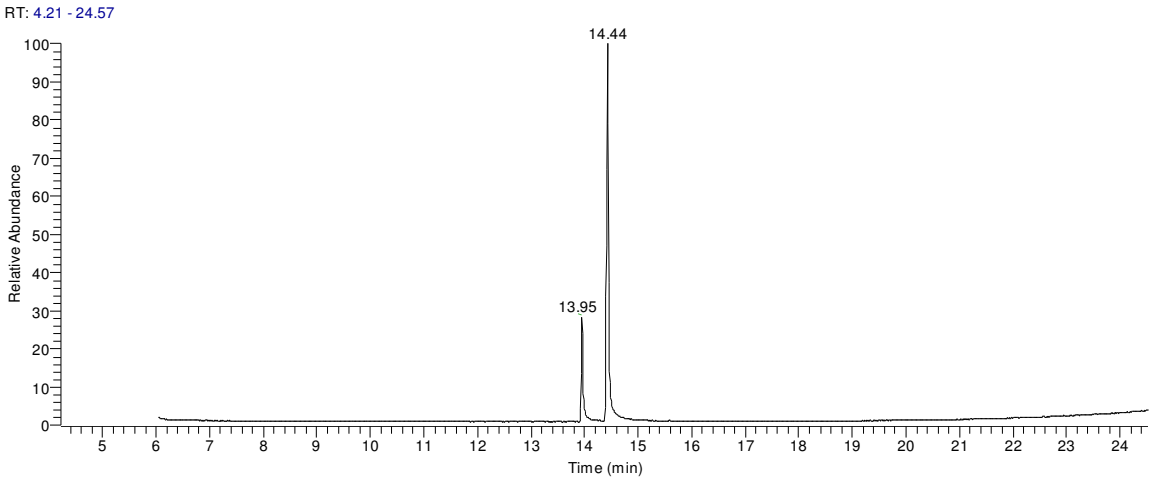

Figure 58

The first fraction was obtained as a colourless oil whilst the second fraction was obtained as a colourless oil that solidified upon standing. The first fraction was sent for GM-MS analysis, the chromatograph from which is shown below in Figure 59.

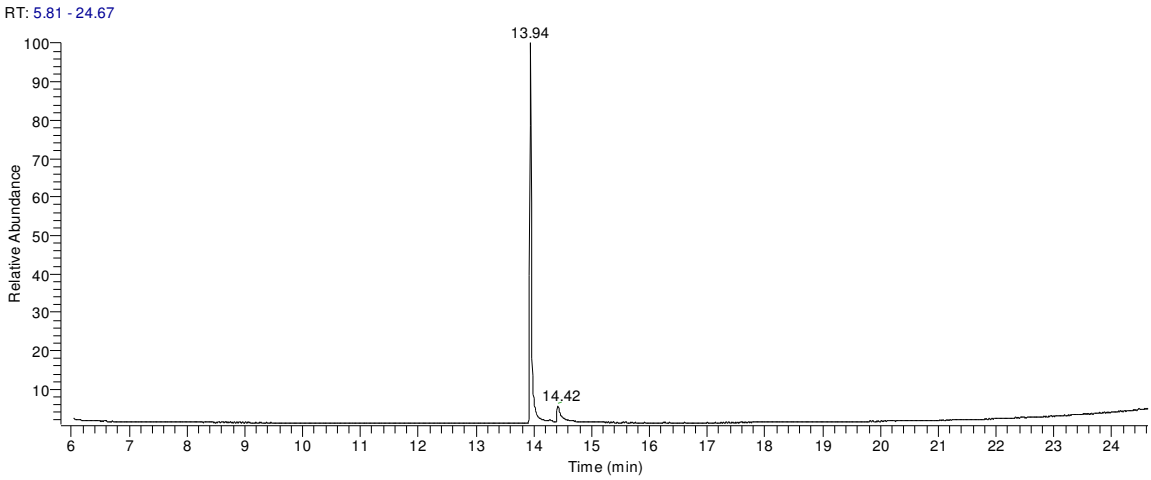

Figure 59

The chromatograph (Figure 59) showed that the lower boiling component corresponded to the peak at 13.9 minutes. The mass spectrum for this compound was referenced against the National Institute of Standards and Technology (NIST) database which predicted the fragmentation pattern to be that from diethyl-2-aminopentanedioate (**93**, Figure 60) with an 89% probability.

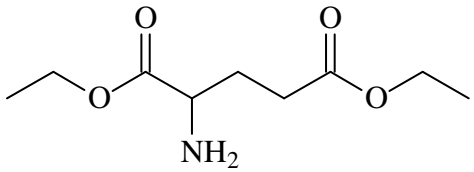

93

Figure 60

The apparent formation of diethyl-2-aminopentanedioate **93** was validated by obtaining both one and two dimensional NMR spectroscopic data for the sample which confirmed the presence of the predicted structure.

The solidified product was analyzed using NMR spectroscopy and GC-MS and was found to be the desired ethyl ester product **90**. The acquired results were consistent with those previously obtained for the ethyl ester **90** using the former thionyl chloride procedure.

Although the ethyl ester **90** was attained in a higher yield (65%) as compared with the thionyl chloride procedure (53%), it was alleged that the isolated yield of **90** could be improved upon by preventing or minimizing the apparent ring opening pathway from taking place which yields the undesired by-product **93**. In this light, the Fischer esterification method was again attempted using benzene in place of toluene as the co-solvent with the mind set that the lower boiling point of benzene would input less energy into the system whilst still encourage the azeotropic removal of water in the Dean and Stark apparatus. The results from this modified procedure were encouraging since analysis of the obtained GC trace (Figure 61) for the reaction mixture showed very little side product **93** to have formed, even after 12 hours of refluxing in the 25% benzene:ethanol solvent mixture.

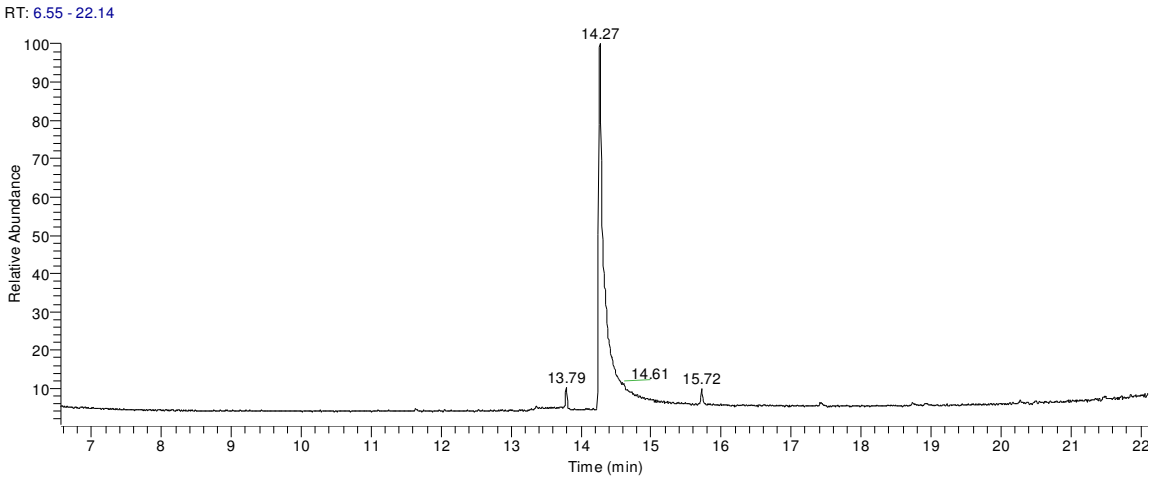

Figure 61

The reaction mixture was concentrated *in vacuo*, worked up and purified *via* short path distillation to yield the ethyl ester **90** in a much improved 84% yield as a colourless oil that solidified upon standing. The product was found to have a specific optical rotation of +3.4° (*c* 4.6, H_2O) which compared favorably to the literature value[85] of +3.5° ± 0.5° (*c* 10, Ethanol) resulting in a 97% enantiomeric excess being achieved.

With the purified ethyl ester **90** in hand, the next synthetic step towards the ultimate synthesis of (5*R*)-5-methyltetrahydro-2*H*-pyrrol-2-one **70** was attempted as depicted in Scheme 46.

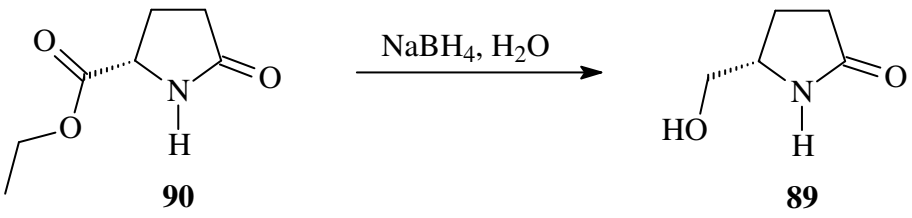

Scheme 46

Although esters and acids usually require stronger reducing agents such as lithium borohydride, to afford the corresponding alcohol functionality, we were interested in first employing a milder reducing reagent such as sodium borohydride in an attempt to

selectively reduce the ester functionality while leaving the amide functionality unchanged.

A solution of sodium borohydride in distilled water was cautiously added to a stirred solution of ethyl ester **90** in distilled water at 0 ^{o}C. The solution was allowed to stir for 3 hours at room temperature after which it was quenched with acetone to remove any unreacted sodium borohydride. The reaction mixture upon TLC analysis was shown to contain two compounds as seen by a base line spot and a spot at R_f = 0.33 (ethyl acetate:methanol = 2:1). The baseline spot was supposedly boronic acid, an expected by-product from sodium borohydride reactions performed in water. The new spot at R_f = 0.33 was the compound of interest and after the reaction mixture was worked up, the resulting milky white oil was purified *via* column chromatography to yield a pure sample of the unknown compound as a colourless oil that solidified upon standing. Analysis of the solid using one and two dimensional NMR spectroscopy confirmed the presence of the desired alcohol product **89** (80% yield) and also proved useful in assigning the relevant peaks in the ^{1}H and ^{13}C spectra. The ^{1}H NMR spectrum for the alcohol **89** showing the relevant peak assignments is depicted below in Figure 62.

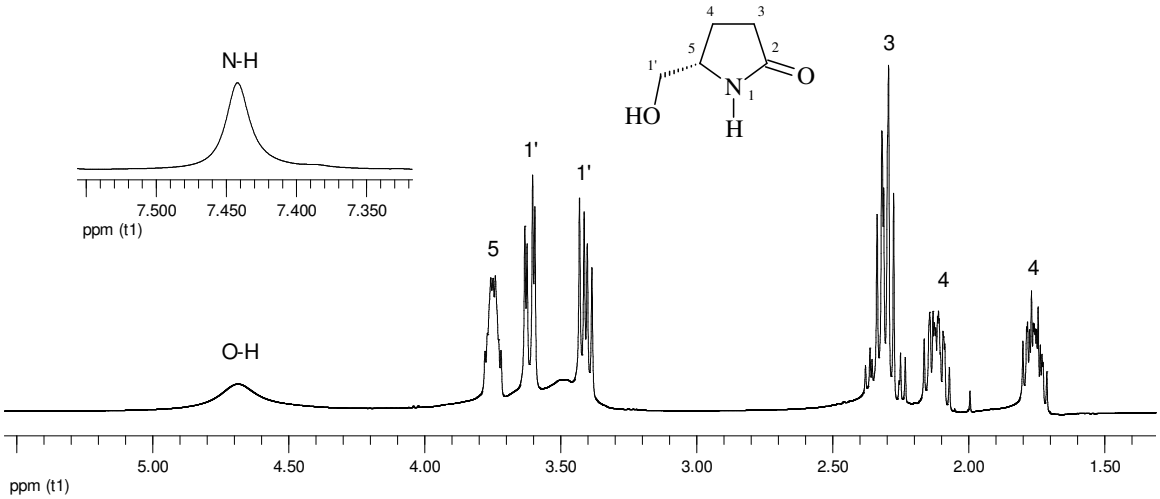

Figure 62: ^{1}H NMR Spectrum for (5*S*)-5-(hydroxymethyl)tetrahydro-2*H*-pyrrol-2-one

The ^{1}H NMR spectrum (Figure 62) contained eight different signals; the signal at 2.30 ppm integrated for two protons while the remaining seven signals integrated for one proton each signifying a total of nine protons, as expected. It thus became immediately apparent that the presence of the chiral centre at position 5 was splitting the degeneracy of the two neighboring proton pairs at positions 4-*H* and 1′-*H* respectively. The peak resonating at 2.3 ppm and integrating for two protons was therefore assigned as the ring protons furthest away from the chiral centre and depicted as 3-*H*. The N-*H* signal had shifted slightly downfield from 6.6 ppm in the starting material (**90**, Figure 52) to 7.4 ppm the in product (**89**, Figure 62). The new singlet at resonating at 4.7 ppm was therefore assigned to the alcohol functionality 1′-O*H*. The ^{13}C NMR spectrum showed the presence of five carbon peaks as expected for the alcohol product **89** and is shown below in Figure 63.

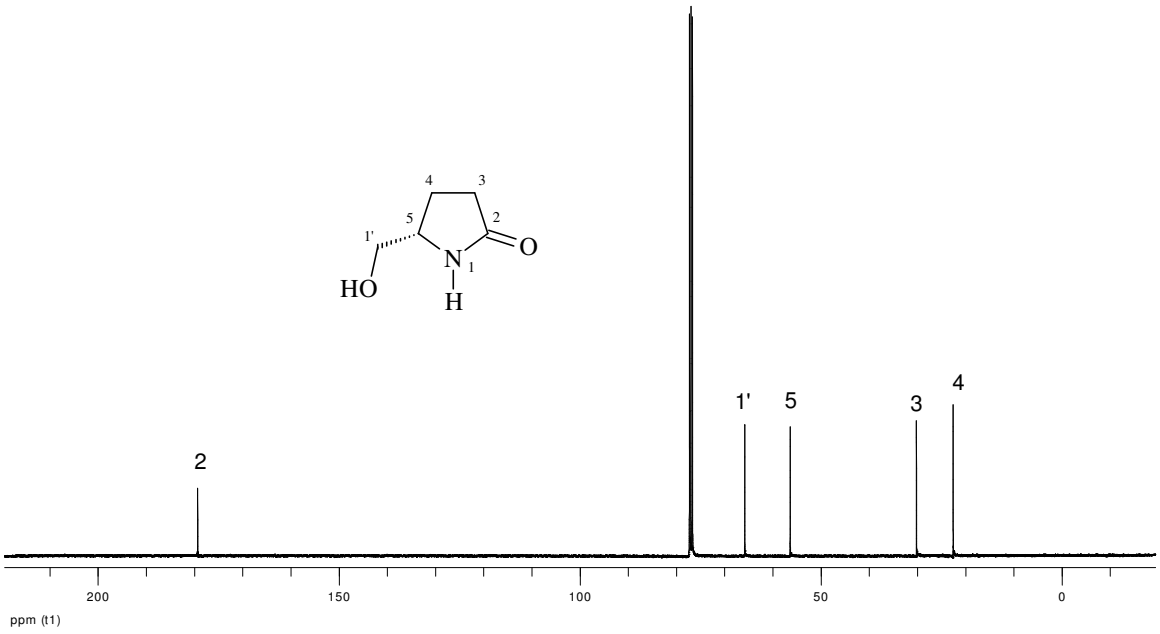

Figure 63: ^{13}C NMR Spectrum for (5*S*)-5-(hydroxymethyl)tetrahydro-2*H*-pyrrol-2-one

The peak at 179 ppm was assigned as the carbonyl carbon 2-*C* due to its downfield chemical shift and absence in the DEPT 135 spectrum (Figure 64) which confirmed it's quaternary nature. The DEPT 135 experiment also confirmed the presence of three CH_2

carbons at 65.8, 30.2 and 22.6 ppm and one CH carbon at 56.4 ppm which was assigned as the carbon atom 5-*C*.

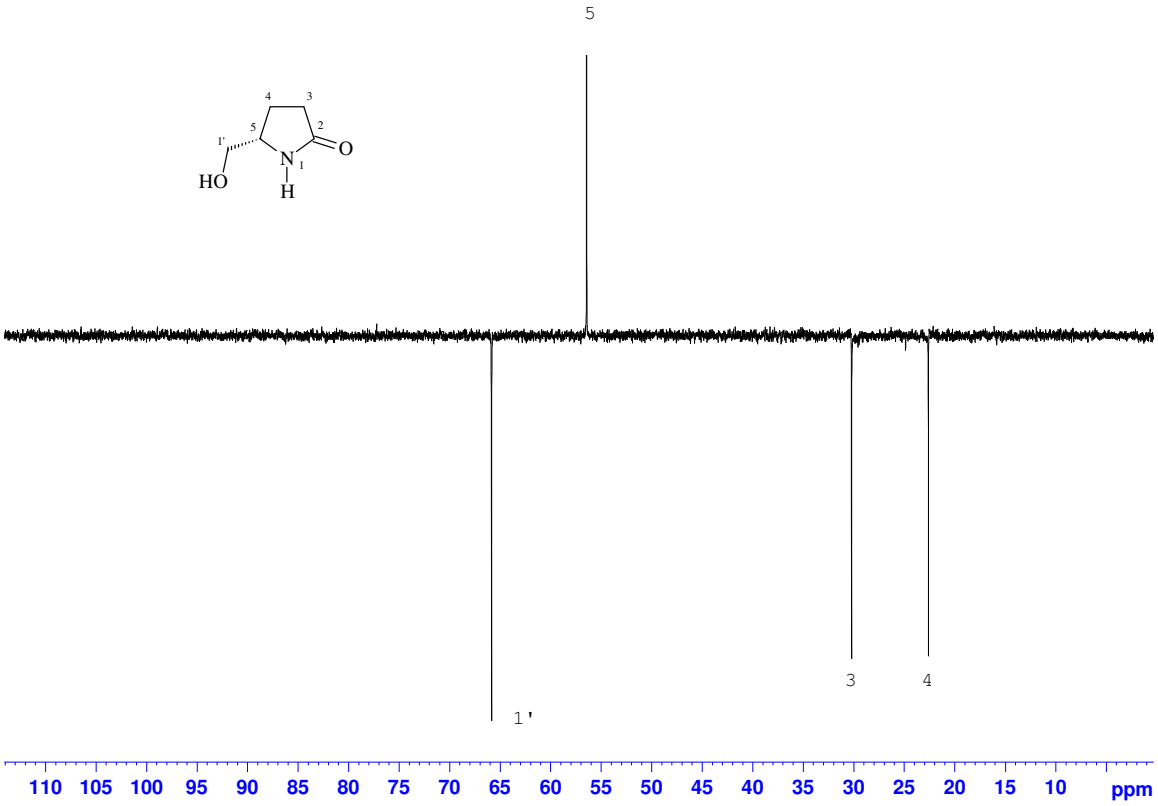

Figure 64: DEPT 135 Spectrum for (5*S*)-5-(hydroxymethyl)tetrahydro-2*H*-pyrrol-2-one

Inspection of the two dimensional HSQC NMR spectrum (Figure 65) showed that the proton signal at 3.76 ppm was directly attached to the tertiary carbon 5-*C* and was therefore assigned as 5-*H*. The HSQC NMR spectrum showed that the two proton peaks resonating at 3.62 and 3.40 ppm were directly attached to the carbon atom resonating at 65.8 ppm and the proton peaks resonating at 2.12 and 1.76 ppm were directly attached to the carbon peak resonating at 22.6 ppm. The carbon peak at 30.2 ppm in the ^{13}C NMR spectrum was coupling directly with the protons 3-*H* and was thus assigned as carbon atom 3-*C*. The pair of peaks resonating at 2.12 and 1.76 pm in the ^{1}H NMR spectrum were assigned as the ring protons 4-*H* adjacent to the chiral centre since the two dimensional COSY spectrum (Figure 66) showed the presence of strong coupling between these proton signals and the ring protons 3-*H*.

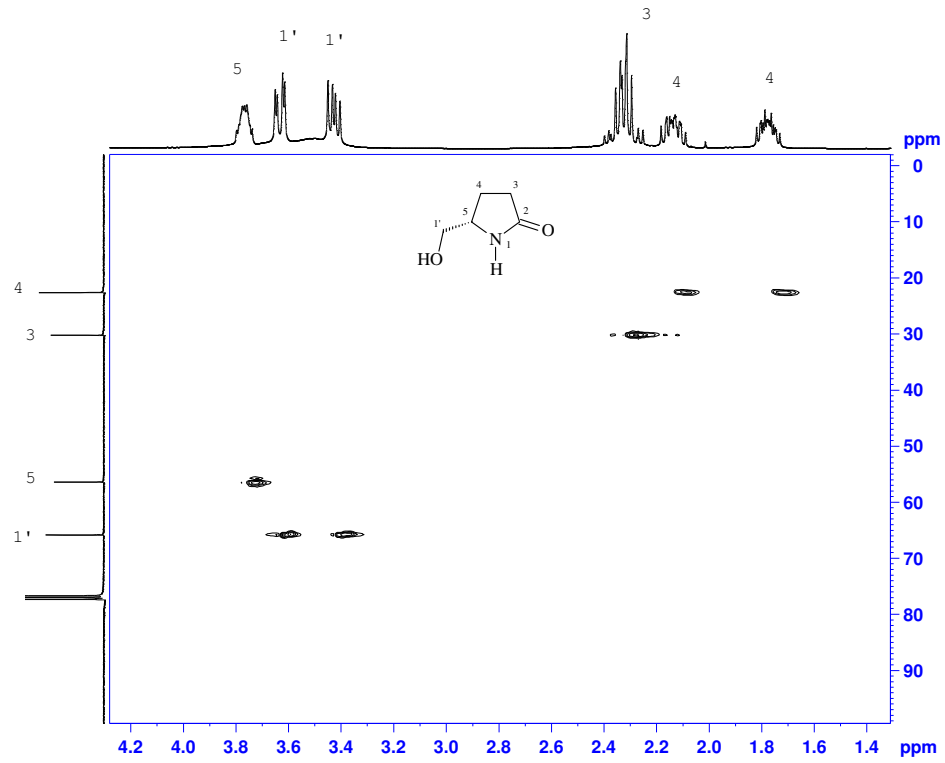

Figure 65: 2D HSQC Spectrum for (5*S*)-5-(hydroxymethyl)tetrahydro-2*H*-pyrrol-2-one

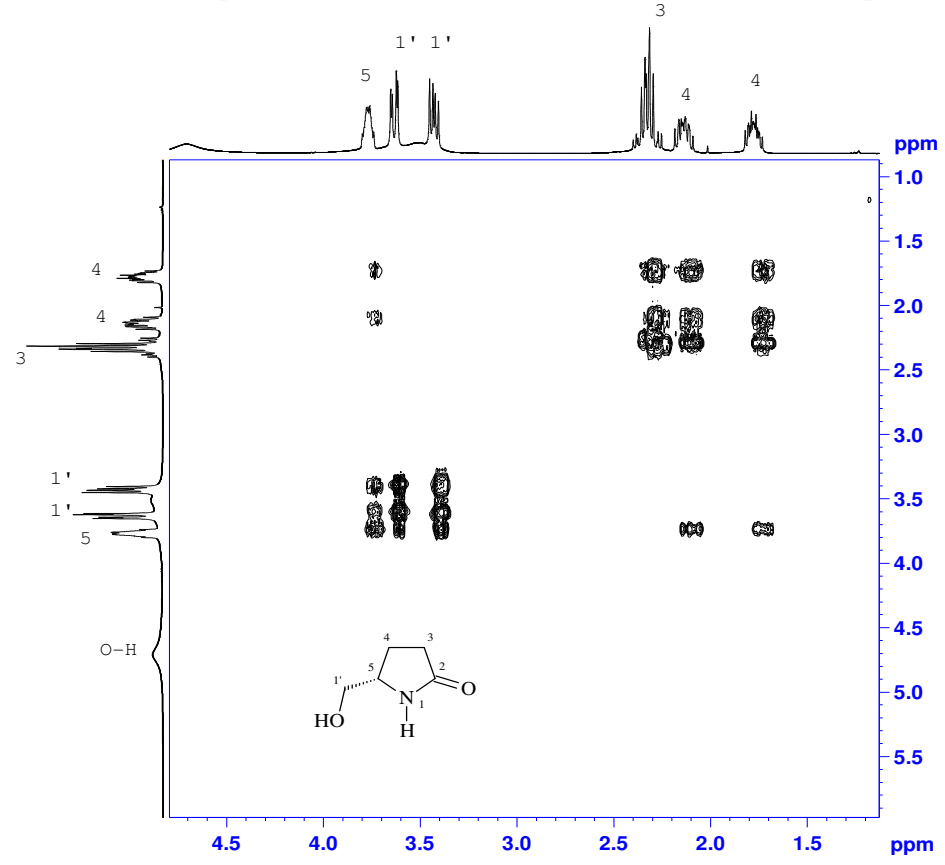

Figure 66: 2D COSY Spectrum for (5*S*)-5-(hydroxymethyl)tetrahydro-2*H*-pyrrol-2-one

On the other hand, the pair of proton peaks at 36.2 and 3.40 ppm could only be seen coupling with the CH proton 5-*H* and were therefore assigned as the proton atoms 1′-*H*.

The next synthetic transformation required for the alcohol functionality of **89** to be converted into a good leaving group so that it could be later removed. Tosylate derivatives of alcohols have long been known for their uncomplicated formation and desirable property as good leaving groups in organic synthesis. Traditional methods for the tosylation of alcohols normally require the use of tosyl chloride and *ca*. 10 equiv. of pyridine base to bring about such reactions.[86] The disadvantages to such methods are that careful conditions are required in order to prevent undesirable side reactions from taking place which involve substitution of the tosyl alcohols (ROTs) to form chlorides (RCl).[86] These methods also require excessive amounts of pyridine, a toxic organic base as well as anhydrous reaction conditions to prevent hydrolysis of the moisture sensitive tosyl chloride reagent. More recently, Morita *et al*.[86] reported an alternative method for the tosylation of alcohols, in which the use of pyridine and dry reaction conditions were not a requirement. This methodology was thus implemented in our laboratory and involved exposing the alcohol **89** to tosyl chloride in the presence of potassium hydroxide and a catalytic amount of a phase transfer catalyst (tetrabutylammonium hydrogen sulfate) and made use of a water-chloroform solvent system (Scheme 47).

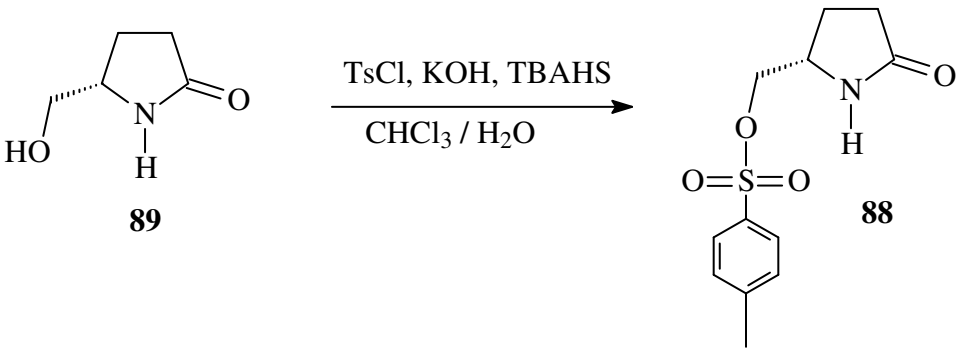

Scheme 47

As mentioned earlier, a major problem associated with the tosylation of alcohols in hydrous reaction conditions is the hydrolysis of tosyl chloride by water. Interestingly, a

study conducted by Morita *et al*. which investigated the stability of tosyl chloride in water as a function of pH at 20-25 ^{o}C determined that at a pH of *ca.* 10, the hydrolysis of tosyl chloride by water was adequately prevented.[86]

The alcohol **59** was thus dissolved in the water-chloroform solvent system followed by the addition of potassium hydroxide to increase the pH to *ca.* 10. A catalytic amount of the tetrabutylammonium hydrogen sulfate phase transfer catalyst was added and the resulting mixture was stirred and sonicated in an ultra-sonic bath. The tosyl chloride was lastly added, and the resulting solution was stirred for 48 hours in the ultra-sonic bath. The reaction mixture was concentrated *in vacuo* to yield a white solid which was recrystallized twice from toluene to yield sufficiently pure product **88** as determined by TLC analysis. The structure of the product was elucidated using NMR spectroscopy which confirmed the formation of the tosylated alcohol **88**. The procedure described above furnished the alcohol **88** in a 76% isolated yield. Analysis of the observed coupling in the two dimensional COSY, HSQC and HMBC NMR spectra aided in the unambiguous assignment of the peaks in the ^{1}H and ^{13}C NMR spectra and are depicted below in Figure 67 and Figure 68 respectively.

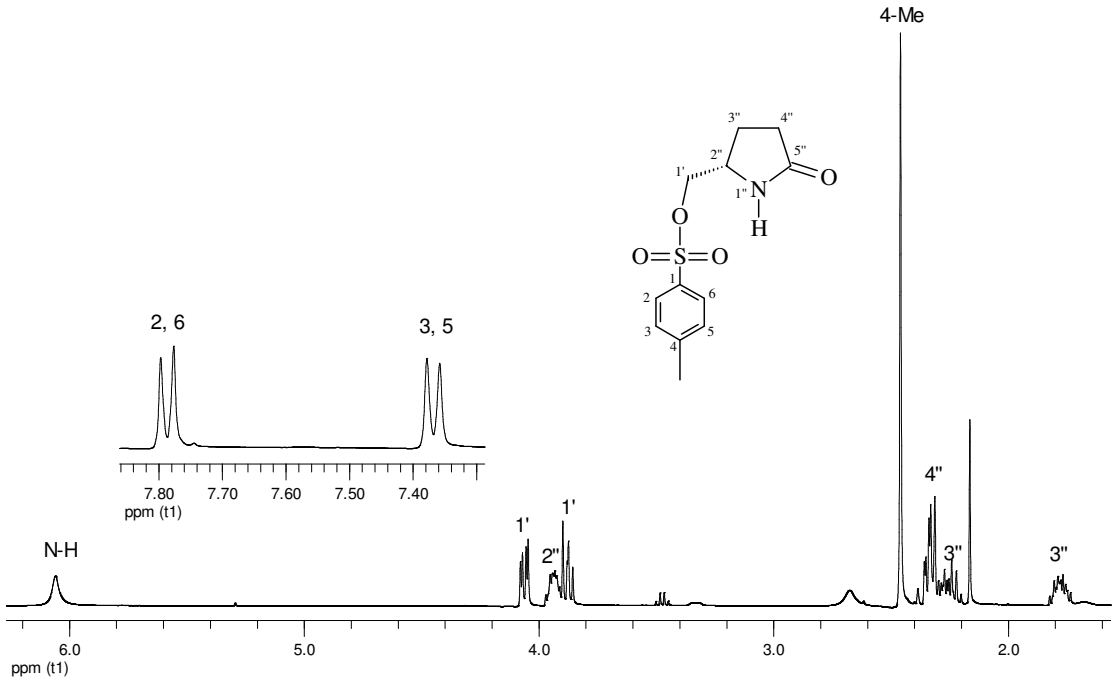

Figure 67: ^{1}H NMR Spectrum for [(2*S*)-5-oxotetrahydro-1*H*-pyrrol-2-yl]methyl 4-methylbenzenesulfonate

The N-*H* signal was observed at 6.08 ppm, the integration of which was assigned for one proton. The four protons on the aryl ring appeared as set doublets integrating for two protons each. The two equivalent protons closest to the sulfonyl group (2-*H* and 6-*H*) appeared at 7.80 ppm and were split into a doublet (J = 8.1 Hz) due to the presence of vicinal ring protons 3-*H* and 5-*H* respectively. The equivalent ring protons 3-*H* and 5-*H* were found to resonate at 7.39 ppm and could be seen coupling back (J = 8.1 Hz) to the protons 2-*H* and 6-*H*. The two diastereotopic protons at position 1′-*H* were shown to exhibit different chemical shifts (4.08 ppm and 3.89 ppm) as they are nonequivalent protons neighboring a chiral centre. The diastereotopic protons (3″-*H*) likewise resonated at different chemical shifts (2.27 ppm and 1.80 ppm), and the proton 2″-*H* resonated at 3.95 ppm. The singlet at 2.48 ppm integrated for three protons and was assigned for that of the methyl group 4-CH_3 and the multiplet integrating for two protons at 2.35 ppm was assigned as 4″-*H*. The ^{13}C NMR spectrum contained ten carbon peaks which were assigned accordingly as depicted in Figure 68 below.

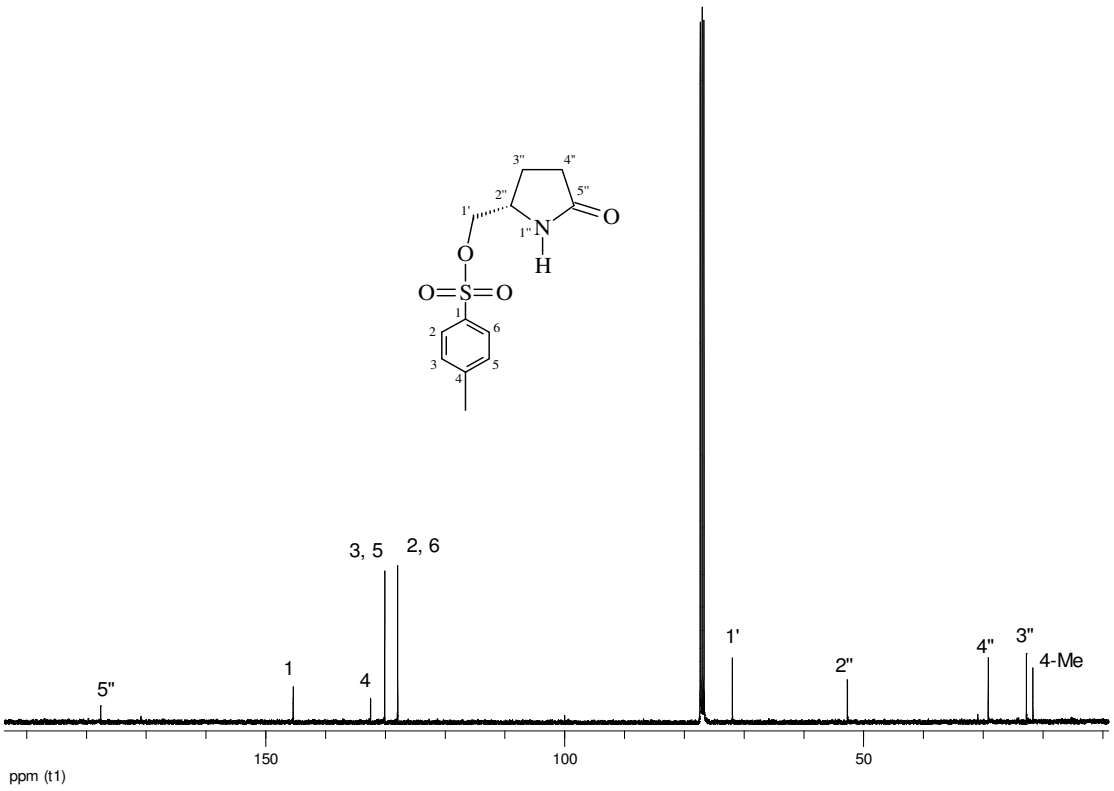

Figure 68: ^{13}C NMR Spectrum for [(2*S*)-5-oxotetrahydro-1*H*-pyrrol-2-yl]methyl 4-methylbenzenesulfonate

The two equivalent carbon atoms 2-*C* and 6-*C* appeared as a single peak and resonated at 127.9 ppm; the other two equivalent carbon atoms (3-*C* and 5-*C*) also appeared as one signal and resonated at 130.2 ppm.

With the tosylated alcohol **88** in hand, it was carried across into the next and last step towards the synthesis of the methyl lactam **70**. After much literature research, it was deemed prudent to first attempt this reaction using a popular free radical reduction method that makes use of tributyltin hydride as the reducing agent in conjunction with an initiator ($In^{\bullet}$). A general reaction mechanism illustrating such a procedure is highlighted in scheme 48.[87-89]

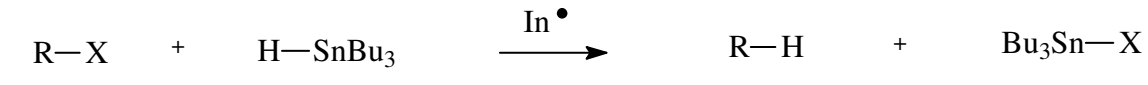

X= halogen, tosyl

Scheme 48

The reduction reaction is initiated by the utilization of 2, 2′-azobisisobutyronitrile (AIBN) which due to its week azide bond can undergo decomposition at a suitable rate at room temperatures. As a result of this decomposition process (Scheme 49), AIBN is a convenient source of highly reactive free radicals which assists in the activation of the tributyltin hydride.

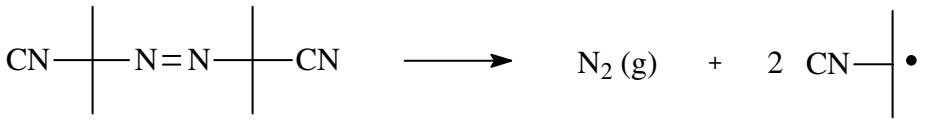

94 **95**

Scheme 49

A general scheme adapted from Perkins[89] outlining the pivotal steps to such a free radical chain reaction; i.e. initiation, propagation and termination is portrayed below in Scheme 50. The external free radical initiator **95** initiates the reaction by reacting with tributyltin hydride to form a tributyltin radical species **96**. The tributyltin radical enters into a propagation state in which a substrate of the type X-R (X = halide, tosylate) is converted

into a free radical species of the type **97**. Combination of **97** with a hydride ion from tributyltin hydride generates the product **98** and regenerates the tributyltin radical **96** which returns to the chain reaction until the substrate X-R has been depleted. Typical termination products are formed by the eventual combination of any remaining free radical species.

Initiation

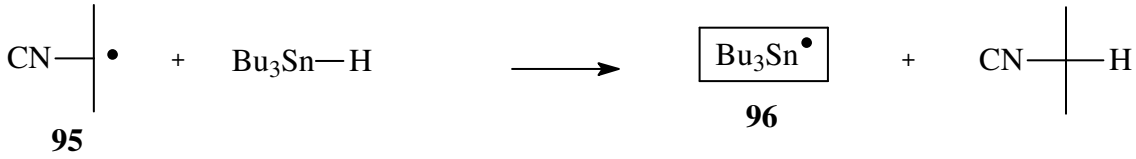

95 **96**

Propagation

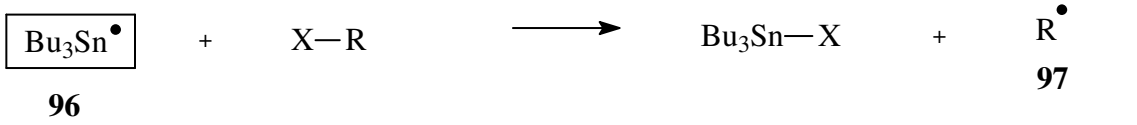

96 **97**

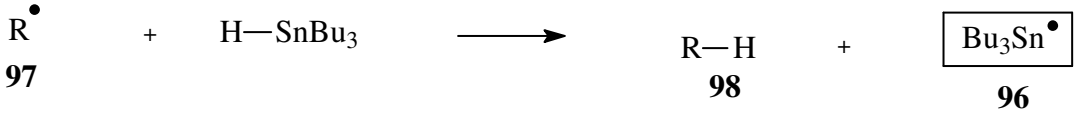

97 **98** **96**

Termination

e.g.

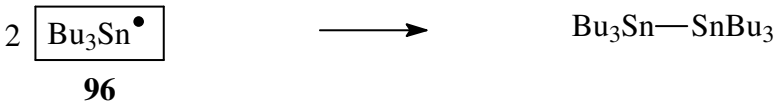

96

Scheme 50

The tosylated alcohol **88** was reacted with tributyltin hydride and AIBN in the hope the above described method would achieve the efficient reduction and formation of the methyl lactam **70** as shown in Scheme 51.

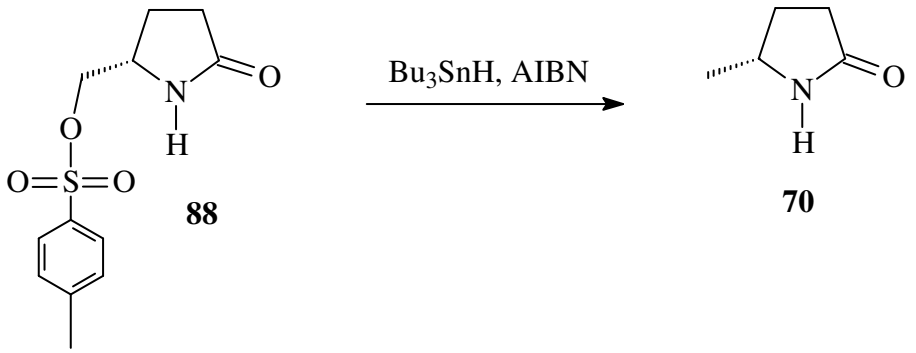

Scheme 51

Tributyltin hydride was slowly added to a stirring solution of tosyl alcohol **88**, 2, 2′-azobisisobutyronitrile and sodium iodide in 1,2-dimethoxyethane and refluxed for 14 hours. The reaction mixture was filtered and concentrated *in vacuo* to furnish a colourless oil that was purified *via* radial chromatography which furnished two isolated compounds. After structural elucidation on each of the compounds using NMR spectroscopy, the presence of tributyltin iodide and methyl lactam **70** was evident. This result was pleasing as the methyl lactam **70** was afforded in a 61% isolated yield. The peaks in the ^{1}H and ^{13}C NMR spectra were assigned accordingly by analysis of the coupling in the two dimensional NMR spectra and by their respective chemical shifts.

The ^{1}H NMR spectrum (Figure 69) showed the presence of six signals and the diastereotopic protons 4-*H* were again found to exist as two separate signals resonating at 2.23 and 1.61 ppm respectively and integrating for one proton each. The N-*H* proton appeared at 6.11 ppm while the CH proton 5-*H* appeared at 3.74 ppm. The methylene protons 3-*H* appeared at 2.30 ppm and the methyl protons 1′-*H* appeared at 1.18 ppm, the integrations of which integrated for two and three protons respectively.

The ^{13}C NMR spectrum (Figure 70) showed five carbon peaks as expected for the lactam molecular structure. The amide carbonyl (2-*C*) appeared at 178.3 ppm and the methyl carbon 1′-*C* appeared at 22.2 ppm. The carbon peak at 50.1 ppm was shown to be tertiary in nature from DEPT experiments and was assigned as 5-*C*. The carbon peaks at 30.6 and 29.2 ppm were later assigned as carbon atoms 3-*C* and 4-*C* respectively.

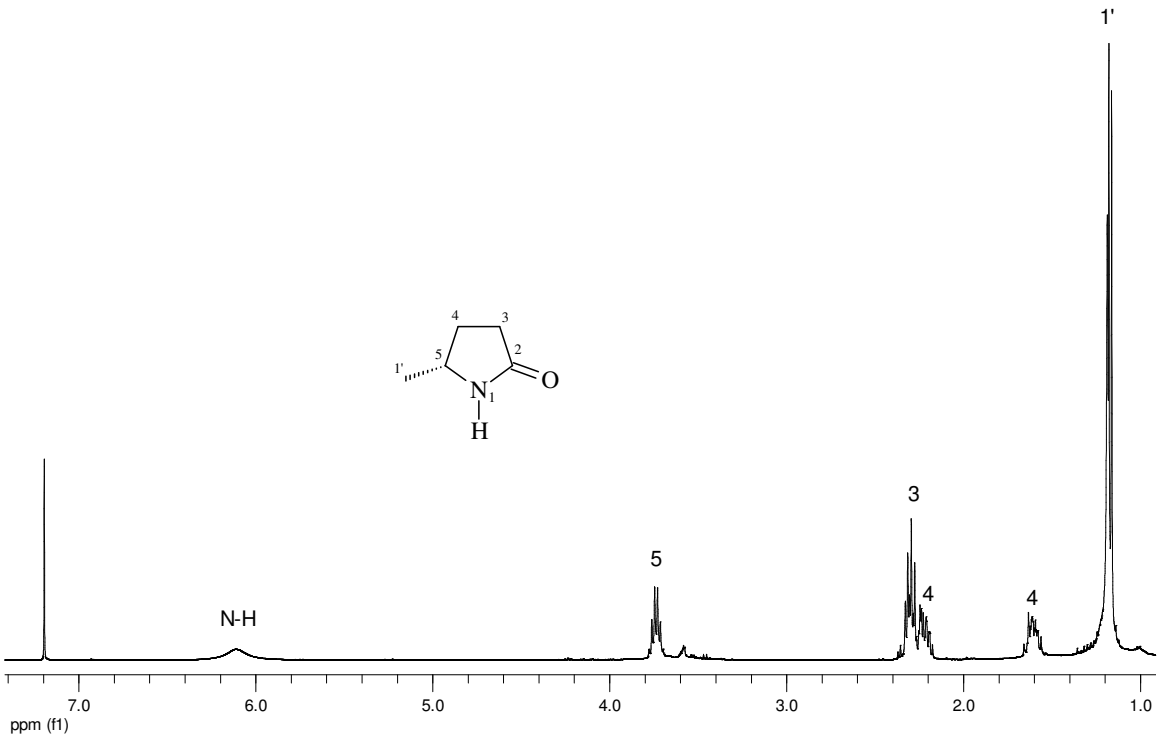

Figure 69: ^{1}H NMR Spectrum for (5*R*)-5-methyltetrahydro-2*H*-pyrrol-2-one

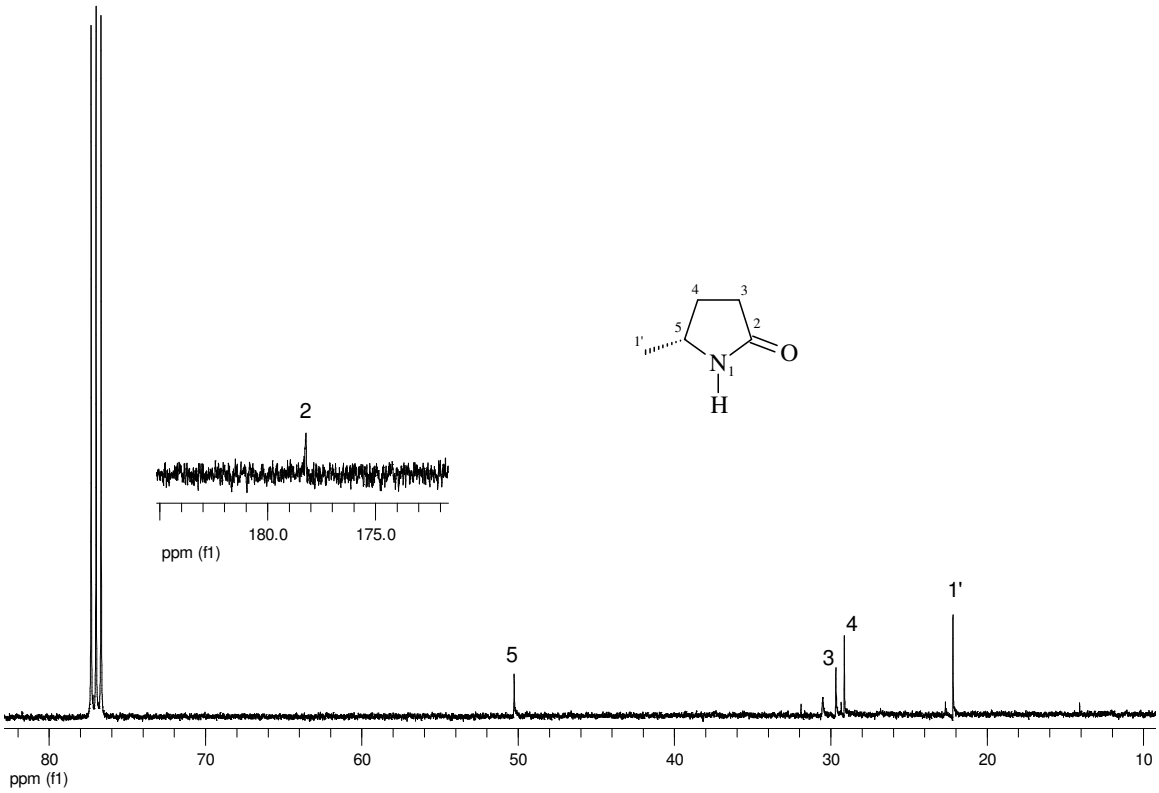

Figure 70: ^{13}C NMR Spectrum for (5*R*)-5-methyltetrahydro-2*H*-pyrrol-2-one

The synthesis described in this section afforded the methyl lactam **70** in a 31% overall yield from (*S*)-pyroglutamic acid **92**. After a pure supply of methyl lactam **70** had been synthesized, it was carried across into the next phase towards the total synthesis of the target ant alkaloid **223H** (xenovenine).

The chemistry associated with a number of the succeeding synthetic transformations had been already optimized due to former model studies performed on structurally analogous compounds as described earlier in section 2.3. The following sections thus describe the incorporation of these previously optimized reaction conditions to the core synthetic route accessing ant alkaloid **223H** (xenovenine), and the methyl lactam **70** was merely substituted in place of the original lactam **68**.

2.4.2 Preparation of (5*R*)-5-methyltetrahydro-2*H*-pyrrole-2-thione [71]

The newly obtained methyl lactam **70** was therefore subjected to the same thionation reaction conditions that were utilized in the former model study as depicted earlier in Scheme 29 (page 55). The presence of the methyl group on the methyl lactam **70** did not influence the reaction outcome and the methyl thiolactam product **71** was successfully obtained in a pleasing 80% isolated yield (Scheme 52) as a white solid. High resolution mass spectrometry on the solid provided a high resolution molecular mass of 116.0529 g.mol^{-1}, which compared favorably to the calculated mass of 116.0534 g.mol^{-1} for $C_5H_{10}NS$.

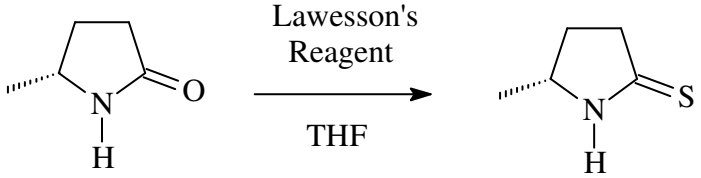

70 **71**

Scheme 52

The methyl thiolactam **71** was characterized using both one and two dimensional NMR spectroscopy and the peak assignments are depicted in the ^{1}H and ^{13}C spectra that follow. The ^{1}H NMR spectrum (Figure 71) clearly showed the resonance of the N-*H* proton as a broad singlet at 8.05 ppm. The signal at 1.3 ppm integrated for three protons and was assigned as the methyl group 1′-*H*. It existed as a doublet due to the presence of the one neighboring methine proton 5-*H* on the ring. The methine proton appeared at 4.05 ppm and was a multiplet signal. The two methylene protons (4-*H*) appeared as two separate signals (2.37 ppm and 1.76 ppm) due to their close proximity to the chiral centre at position 5, a phenomenon that has been repeatedly encountered in similar synthetic precursors. The two methylene protons (3-*H*) also appeared at different chemical shifts to each other but the difference in their chemical shifts were not as significant as that seen for protons 4-*H* as they are situated further away from the stereogenic centre.

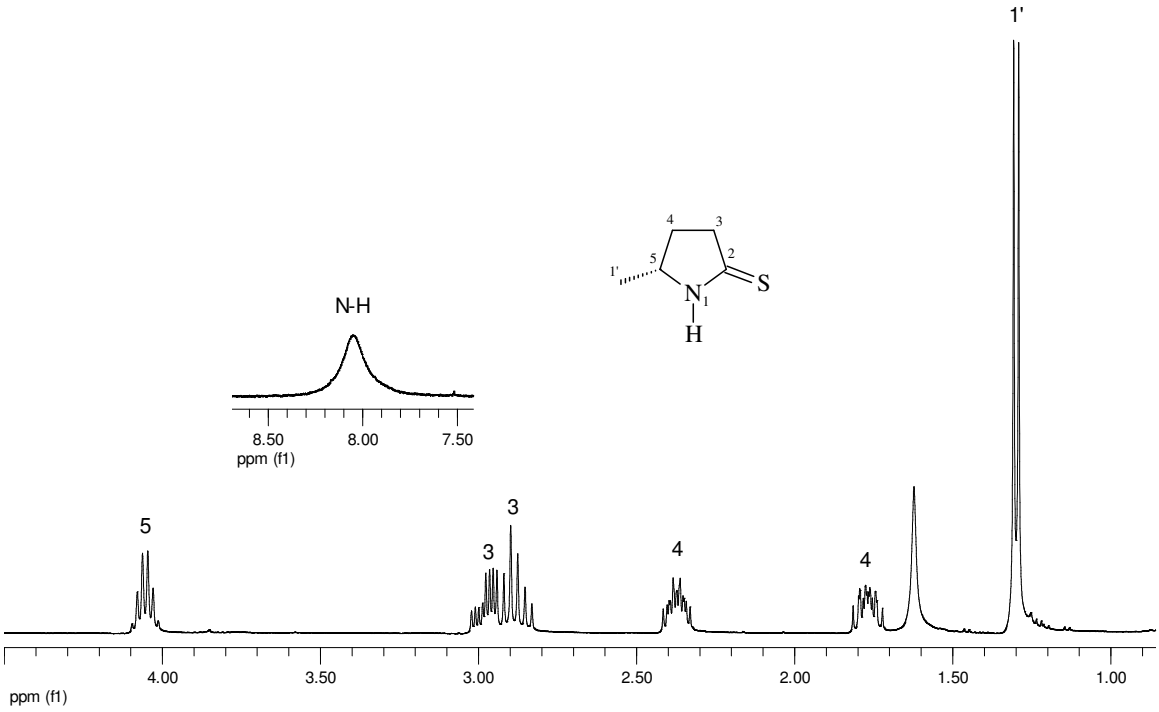

Figure 71: ^{1}H NMR Spectrum for (5*R*)-5-methyltetrahydro-2*H*-pyrrole-2-thione

The ^{13}C NMR spectrum (Figure 72) clearly shows the presence of five carbon signals as expected for the methyl thiolactam product **71**. The respective peaks were assigned after careful analysis of the two dimensional NMR spectra.

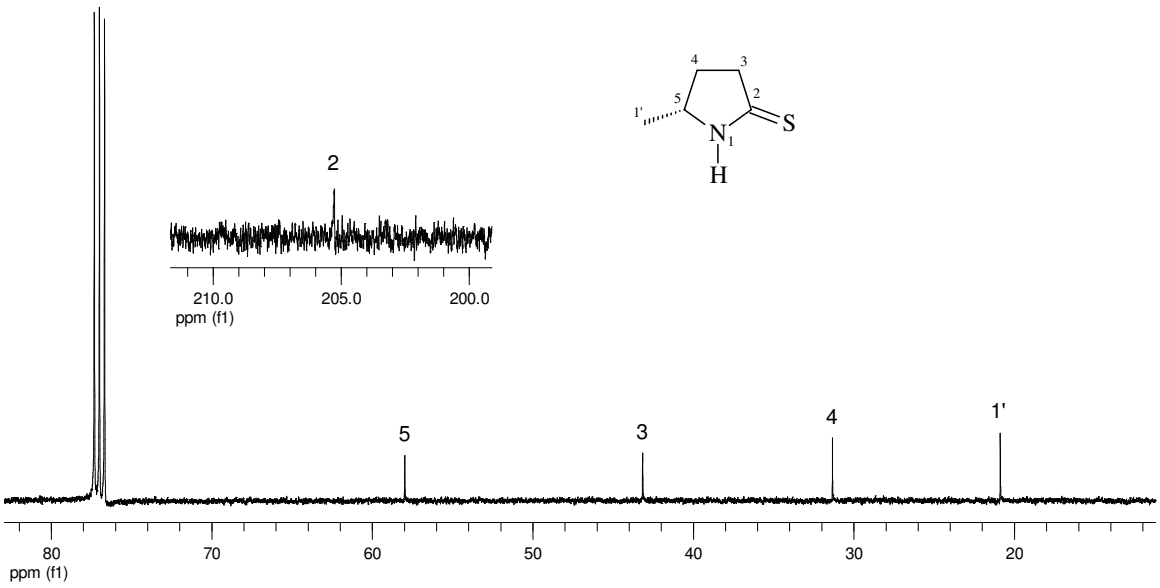

Figure 72: ^{13}C NMR Spectrum for (5*R*)-5-methyltetrahydro-2*H*-pyrrole-2-thione

2.4.3 Preparation of ethyl 3-[(2*R*)-2-methyl-5-thioxotetrahydro-1*H*-pyrrol-1-yl]propanoate [86]

In keeping with the optimized synthetic protocol determined by the model studies, it was necessary to convert the methyl thiolactam **71** into the tertiary thiolactam **86** (Scheme 53) in order to activate the molecule for the succeeding Eschenmoser sulfide contraction reaction.

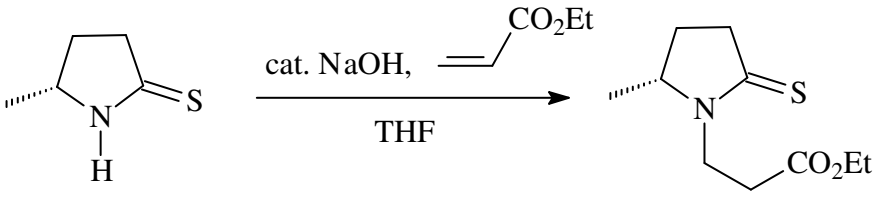

71 **86**

Scheme 53

Ethyl acrylate was therefore added to a stirring solution of methyl thiolactam **71** and sodium hydroxide (cat.) in THF and stirred for 5 hours. The reaction mixture was worked

up accordingly to afford the tertiary methyl thiolactam **86** as a colourless oil and in a quantitative yield from the starting material **71**. High resolution mass spectrometry performed on the oil provided a mass of 216.1067 g.mol^{-1} which compared favorably to the calculated (M+H) mass of 116.1058 g.mol^{-1} for $C_{10}H_{18}NO_2S$. The ^{1}H NMR spectrum (Figure 73) confirmed the presence of the product **86** and the peaks were assigned by analyzing the coupling present in the respective two dimensional NMR spectra. Interestingly, the eight methylene protons at positions 3′-*H*, 4′-*H*, 3-*H* and 2-*H* all existed as eight separate signals integrating for one proton each in the ^{1}H NMR spectrum and are labeled accordingly. The chemical shift for methyl doublet 1″-*H* was not affected with the addition of the *N*-acrylate functionality as its position remained unchanged at 1.3 ppm in the ^{1}H NMR spectrum. The ethyl group of the ester functionality on the newly added acrylate group was clearly evident by the prevalence of the triplet and quartet peaks at 1.25 and 4.12 ppm that integrated for three and two protons respectively. These signals were also seen coupling to each other in the 2D COSY spectrum. The ^{13}C NMR spectrum consisted of ten carbon signals as expected for the tertiary methyl thiolactam product **86**, and is labeled accordingly in Figure 74.

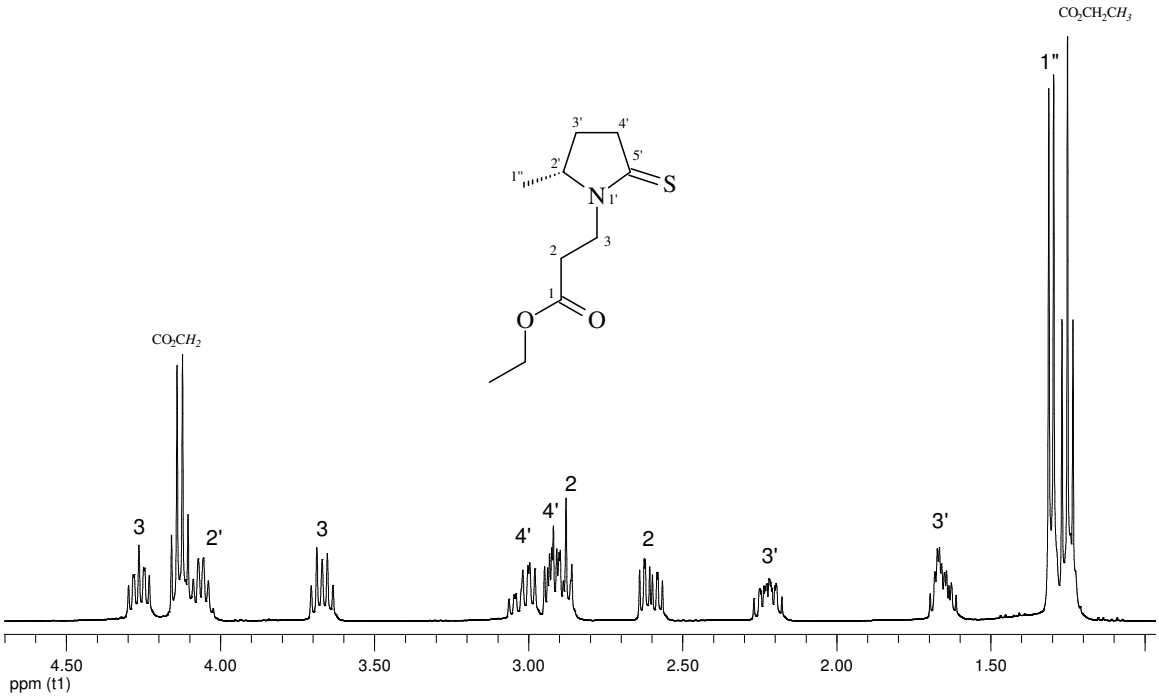

Figure 73: ^{1}H NMR Spectrum for ethyl 3-[(2*R*)-2-methyl-5-thioxotetrahydro-1*H*-pyrrol-1-yl]propanoate

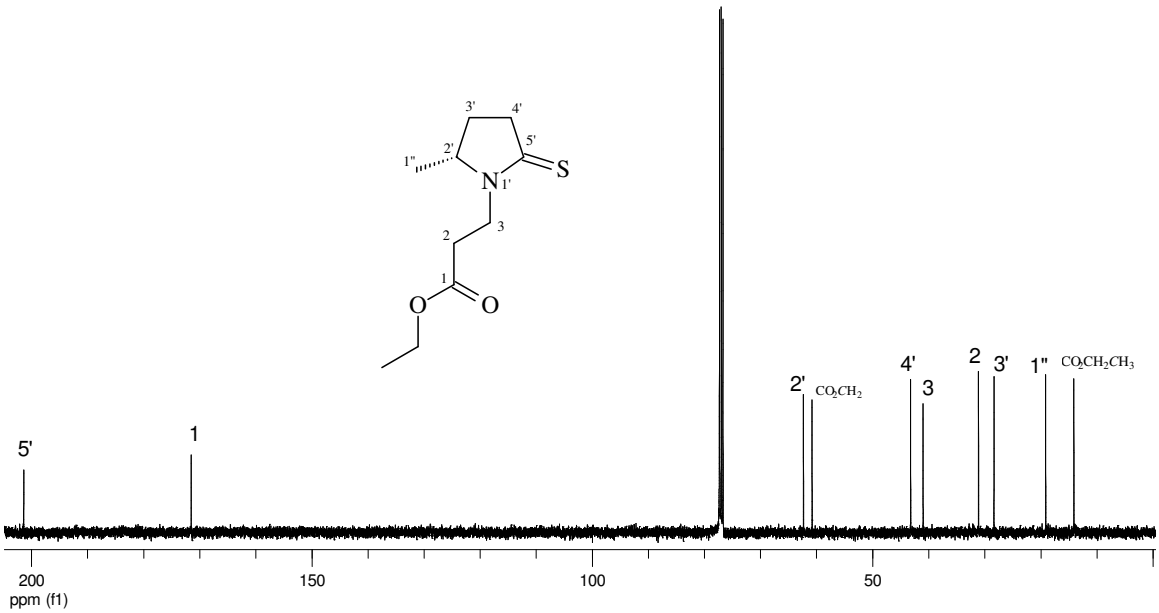

Figure 74: ^{13}C NMR Spectrum for ethyl 3-[(2*R*)-2-methyl-5-thioxotetrahydro-1*H*-pyrrol-1-yl]propanoate

2.4.4 Preparation of ethyl 3-{(5*R*)-2-[(*E*)-2-ethoxy-2-oxoethylidene]-5-methyltetrahydro-1*H*-pyrrol-1-yl}propanoate [87]

With the tertiary thiolactam **86** in hand, it was immediately subjected to the same optimized Eschenmoser coupling reaction conditions that were determined from prior model studies (Scheme 54).

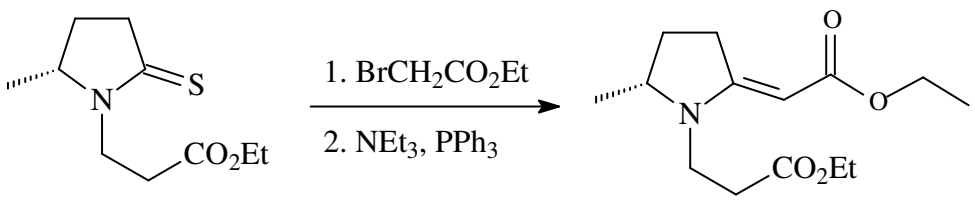

86 **87**

Scheme 54

As expected the methyl group on the pyrrolidine ring did not affect the reaction pathway and the Eschenmoser coupling reaction successfully afforded the methyl tertiary enaminone **87** as a colourless oil in a 70% isolated yield after column chromatography. High resolution mass spectrometry performed on the oil provided a mass of 270.1718 $g.mol^{-1}$ which compared favorably to the calculated (M+H) mass of 270.1705 $g.mol^{-1}$ for $C_{14}H_{24}NO_4$. The ^1H NMR spectrum (Figure 75) showed similar characteristics to that obtained for the starting material **86** (Figure 73) possessing only minor differences. The successful formation of the product **87** was clearly evident from the appearance of a singlet peak integrating for one proton at 4.45 ppm due to the vinylic methine proton 1″-*H*. The spectrum showed the presence of two ethyl groups evident from the two quartets at 4.09 and 4.03 ppm integrating for two protons each, and the large triplet signal at *ca*. 1.2 ppm integrating for a total of six protons (2 x 3 protons). These two sets of signals corresponded to the methylene and methyl protons respectively from the ethyl groups and could be seen coupling to each other in the 2D COSY spectrum.

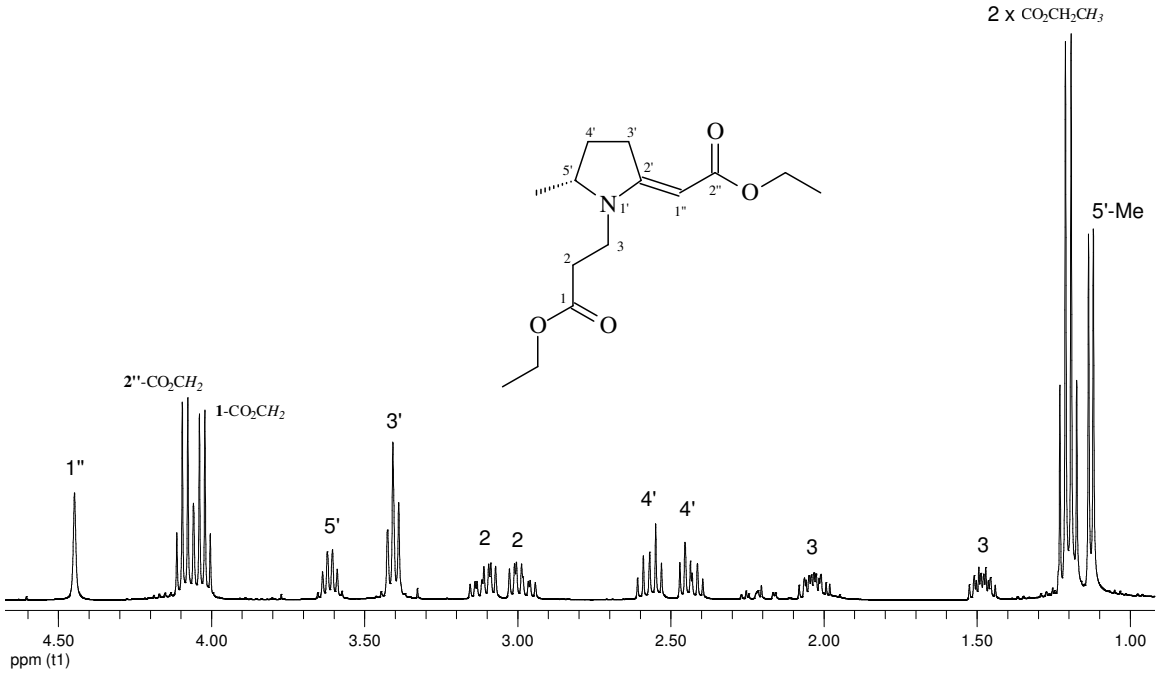

Figure 75: ^1H NMR Spectrum for ethyl 3-{(5*R*)-2-[(*E*)-2-ethoxy-2-oxoethylidene]-5-methyltetrahydro-1*H*-pyrrol-1-yl}propanoate

The ^{13}C NMR spectrum (Figure 76) contained fourteen signals as expected for the product **87** which contained fourteen carbon atoms. The DEPT 135 experiment

established that the three carbon peaks (172-164 ppm) were quaternary in nature as they were absent from the DEPT 135 spectrum (Figure 77).

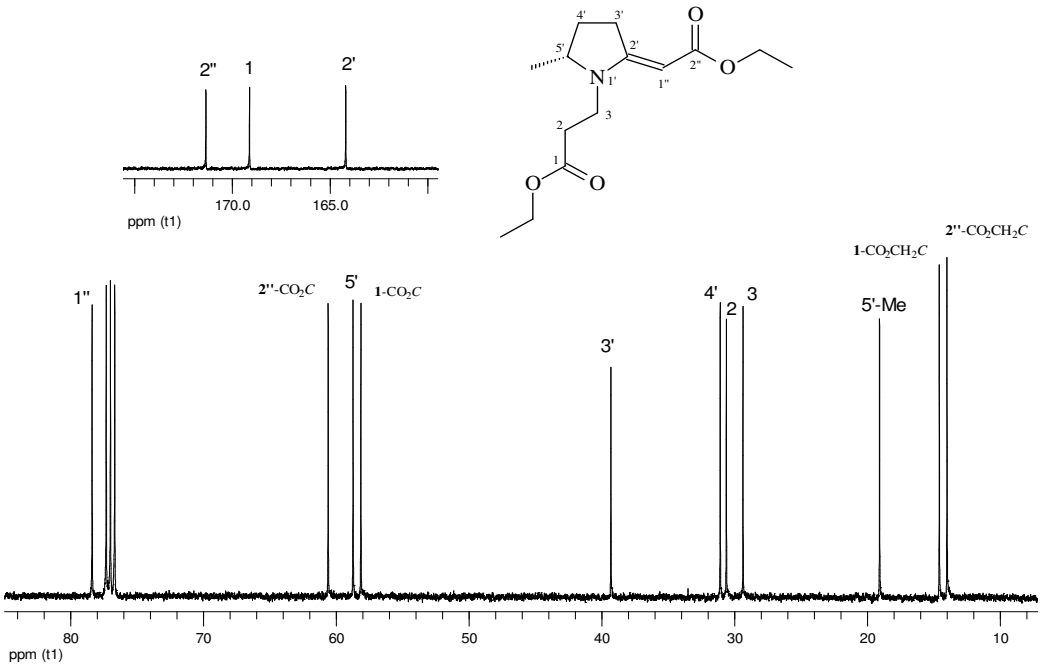

Figure 76: ^{13}C NMR Spectrum for ethyl 3-{(5*R*)-2-[(*E*)-2-ethoxy-2-oxoethylidene]-5-methyltetrahydro-1*H*-pyrrol-1-yl}propanoate

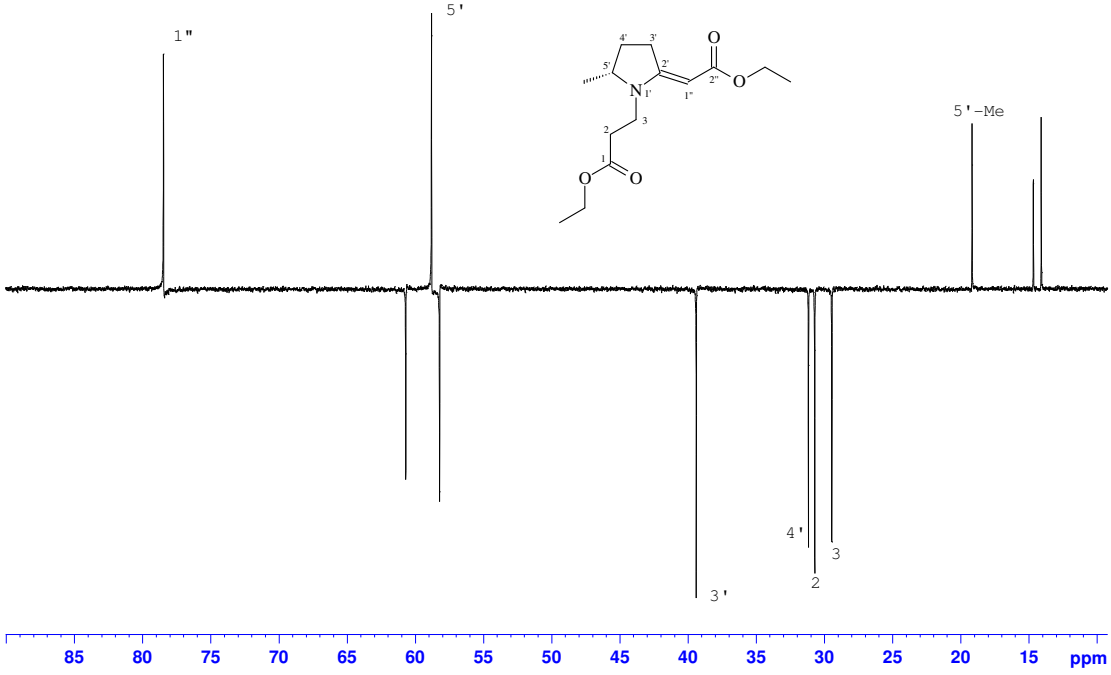

Figure 77: DEPT 135 Spectrum for ethyl 3-{(5*R*)-2-[(*E*)-2-ethoxy-2-oxoethylidene]-5-methyltetrahydro-1*H*-pyrrol-1-yl}propanoate

The three methyl carbons appeared further upfield within the region of 20-14 ppm, and the two tertiary carbons resonated at 78.5 and 58.8 ppm. The remaining six downward pointing signals in the DEPT 135 spectrum fitted accordingly with the six remaining CH_2 carbon atoms in the molecule.

2.4.5 Preparation of ethyl 2-[(5*R*)-5-methyltetrahydro-2*H*-pyrrol-2-ylidene]acetate [72]

The deprotection of **87** to afford the methyl secondary enaminone **72** proceeded smoothly in dry THF when employing lithium hexamethyldisilazane (LiHMDS) as the base and using the previously optimized reaction conditions (Scheme 55).

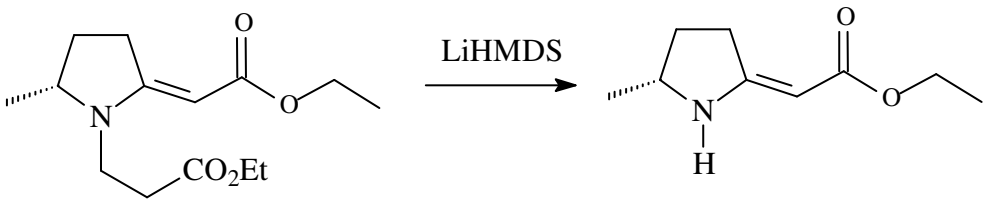

87 **72**

Scheme 55

Although KHMDS afforded the highest yields of secondary enaminone product in the model study reactions, when employed to the current reaction, zero formation of **72** was evident(!). LiHMDS was therefore utilized in place of KHMDS which achieved a 55% conversion of **87** to **72**. High resolution mass spectrometry confirmed the formation of the product **72** as the acquired mass of 170.1178 $g.mol^{-1}$ compared favorably to the calculated (M+H) mass of 170.1181 $g.mol^{-1}$ for $C_9H_{16}NO_2$.

The removal of the acrylate group reformed the amine functionality which was evident from the absorption band at 3360 cm^{-1} in the in the IR spectrum, and the broad singlet at 7.88 ppm in the ^1H NMR spectrum (Figure 78). The ^{13}C NMR spectrum (Figure 79)

contained nine carbon signals, five less than that contained by the starting material **87** and was indicative of the successful removal of ethyl acrylate.

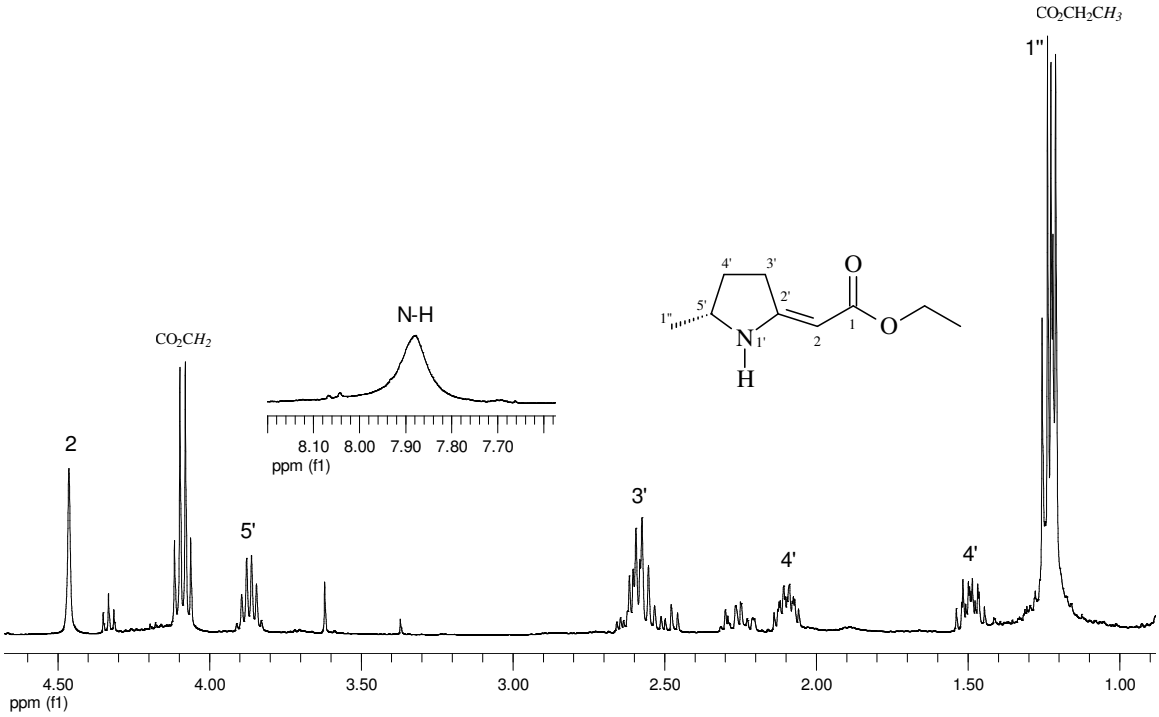

Figure 78: ^{1}H NMR spectrum for ethyl 2-[(5*R*)-5-methyltetrahydro-2*H*-pyrrol-2-ylidene]acetate

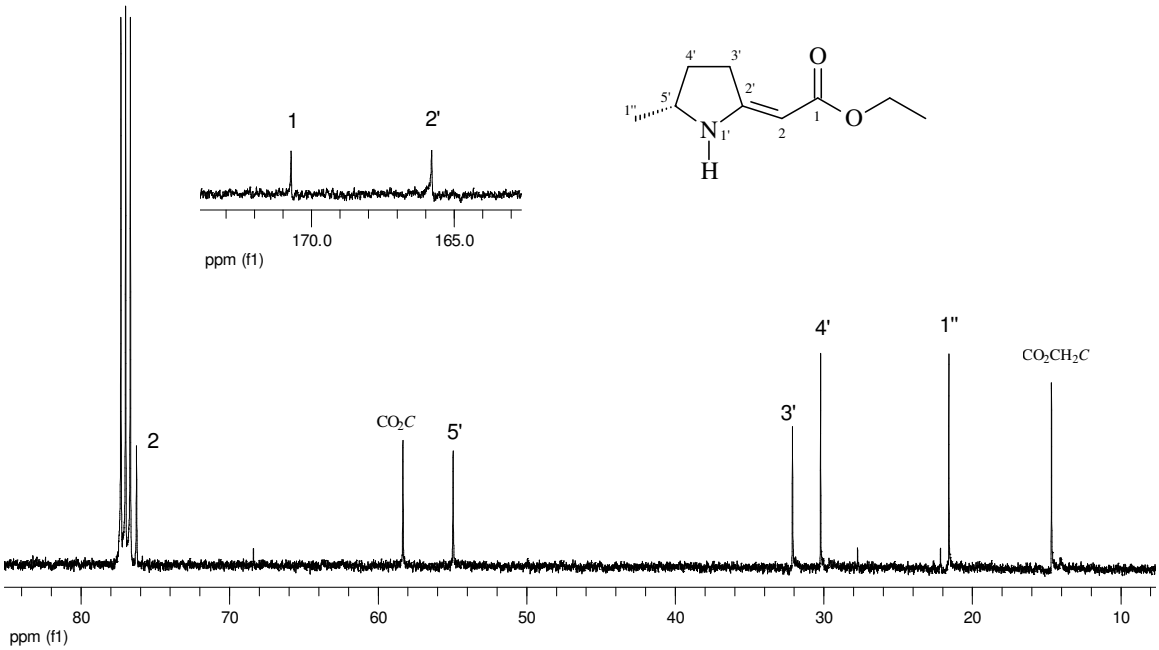

Figure 79: ^{13}C NMR spectrum for ethyl 2-[(5*R*)-5-methyltetrahydro-2*H*-pyrrol-2-ylidene]acetate

In order to perform the subsequent *C*-propargylation reaction on the methyl secondary enaminone **72**, the reagent 1-bromo-2-nonyne was required which was to be utilized in place of the formerly used propargyl bromide reagent. The following section describes the methodology employed in the formal synthesis of 1-bromo-2-nonyne.

2.4.6 Preparation of 1-bromo-2-nonyne [99]

In order to perform the subsequent *C*-propargylation reaction on the methyl vinylogous enaminone **72**, we were in need of the appropriate alkyl propargyl bromide reagent 1-bromo-2-nonyne (**99**, Figure 80).

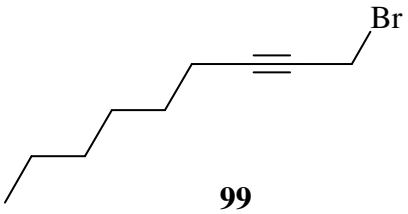

99

Figure 80

The proposed synthetic route towards the formation of 1-bromo-2-nonyne **99** is outlined in Scheme 56 and makes use of propargyl alcohol **100** as the starting material.

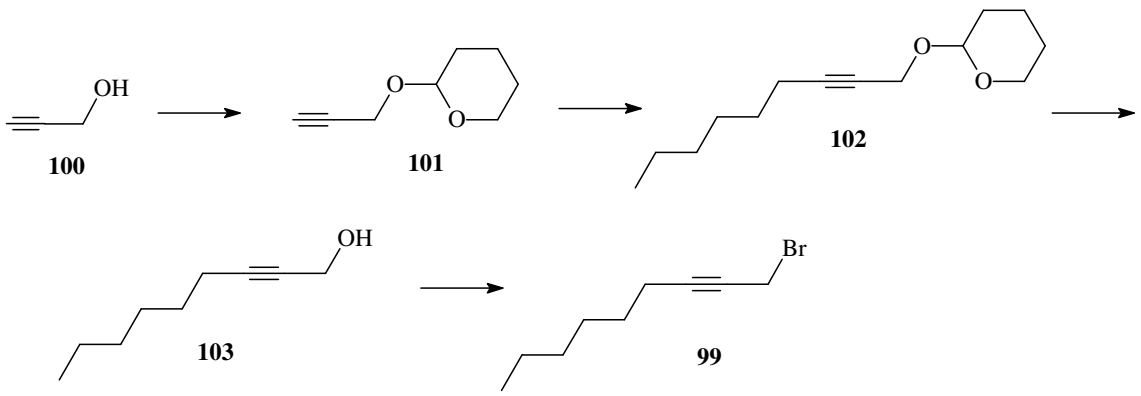

100 **101** **102** **103** **99**

Scheme 56

It was alleged that the alkylated propargyl alcohol species **103** could be obtained *via* the alkylation of an *O*-tetrahydropyranyl (THP) protected derivative **101** employing a base and alkyl halide followed by removal of the THP protecting group on the alcohol. Bromination of the alkylated propargyl alcohol **103** could potentially furnish the desired alkylated propargyl bromide reagent **99**.

The first step in this projected synthesis involved the protection of the alcoholic functionality on the propargyl alcohol (**100**, Scheme 57) which proceeded smoothly in the presence of 3,4-dihydro-2*H*-pyran and a catalytic amount of *p*-toluenesulfonic acid in dichloromethane.

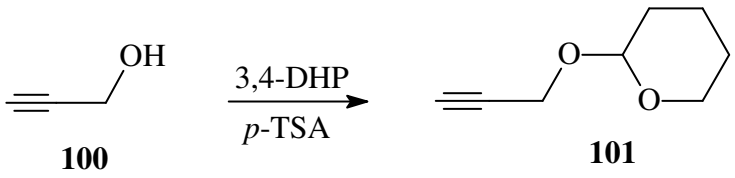

100 **101**

Scheme 57

The THP alcohol **101** was formed in an excellent 98% isolated yield as a yellow oil, and its structure was confirmed using one and two dimensional NMR spectroscopy and gas chromatography-mass spectrometry. The GC-MS trace (Figure 81) showed the oil to be sufficiently pure and free from unreacted starting materials.

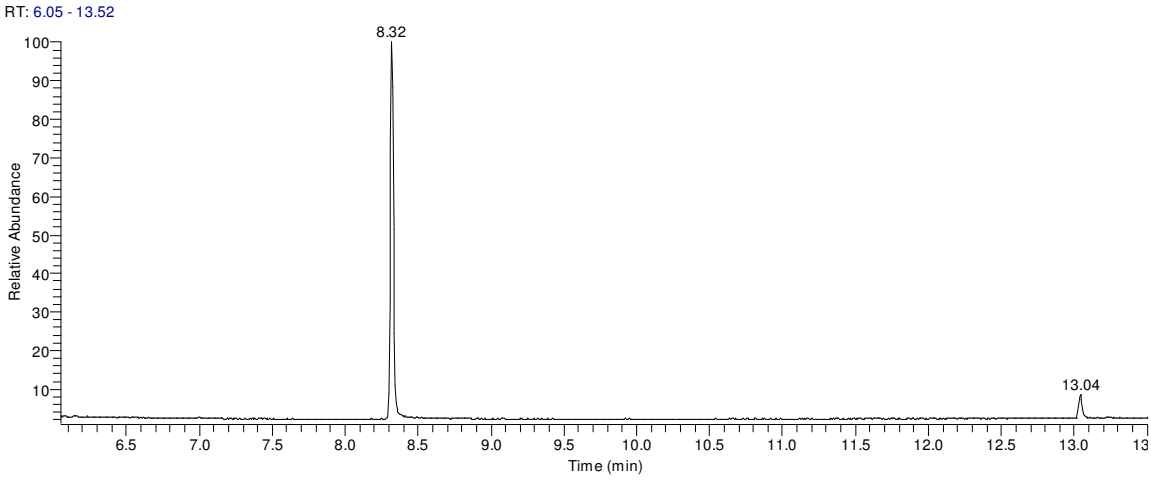

Figure 81

The major component at 8.32 minutes was found to have a mass spectrum consistent to that found in the National Institute of Standards and Technology (NIST) database and possessed a parent molecular ion peak of 140 $g.mol^{-1}$. The THP alcohol **101** was therefore carried across into the next reaction with out further purification.

With the THP alcohol **101** in hand, it was carried across into the subsequent reaction with the hope that a *n*-hexyl functionality could be introduced onto the terminal position of the triple bond as highlighted in Scheme 58.

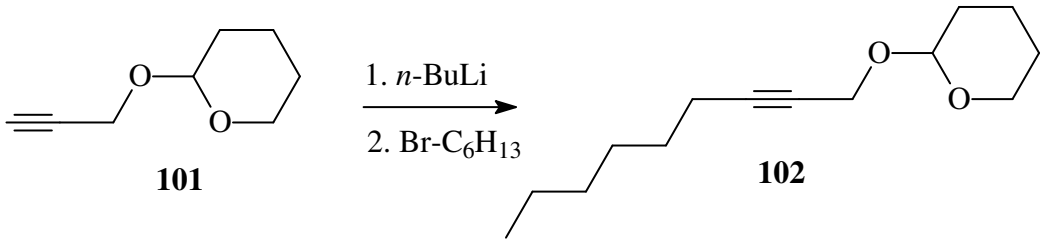

101 **102**

Scheme 58

Our reaction objectives were to abstract the terminal acetylenic proton using *n*-butyllithium to yield a lithium salt with increased nucleophilicity which could undergo an S_N2 type nucleophilic substitution reaction with 1-bromohexane to furnish **102**.

One equivalent of *n*-butyllithium was added dropwise to a solution of THP alcohol in dry THF at 0 ^oC. The solution was stirred for 30 minutes at 0 ^oC after which it was allowed to warm to room temperature and stir for an additional 30 minutes. The solution was again cooled to 0 ^oC and 1-bromohexane was added dropwise over a period of 10 minutes. The solution was allowed to warm to room temperature and stir for an additional 12 hours. The reaction mixture was quenched using aqueous ammonium chloride and was analyzed using thin layer chromatography as well as gas chromatography-mass spectrometry. Unfortunately, these results showed that the reaction was unsuccessful and the starting materials were later recovered.

Hexamethylphosphoramide (HMPA), a highly polar aprotic solvent is well known for its strong complexing affinity for lithium ions.[90] We were therefore interested in utilizing

HMPA in the reaction at hand with the mind set that following base mediated acetylenic proton abstraction on the THP alcohol **101**, the HMPA will complex with the lithium ions *via* its basic oxygen atom thus preventing the potentially stabilized lithium-substrate salt species from forming. The presence of HMPA could therefore furnish an uncomplexed anionic substrate species that should act as a much stronger nucleophile towards the electrophilic 1-bromohexane reagent (Scheme 59).

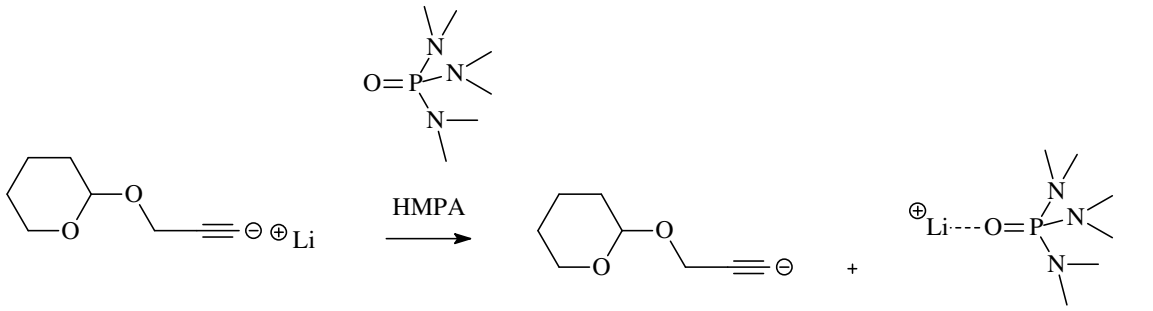

Scheme 59

An alkylation reaction was therefore attempted employing one equivalent of HMPA to the synthetic protocol. The *n*-butyllithium was added to a stirring solution of THP propargyl alcohol in dry THF using the previously described reaction procedure however, the HMPA and 1-bromohexane were added together as a solution in dry THF (5 cm^3). The reaction was allowed to stir for 12 hours after which it was analyzed using thin layer chromatography which showed the presence of a new spot with an R_f of 0.80 (ethyl acetate:hexane = 1:1) as well as starting material spots. The new spot was immediately isolated using column chromatography and sent for NMR and GC-MS analysis which confirmed the presence of the desired alkylated THP propargyl alcohol product **102**.

A ^1H NMR spectrum for the product is shown below in Figure 82, and shows the proton peak assignments which were made possible by analyzing the coupling present in the two dimensional NMR spectra.

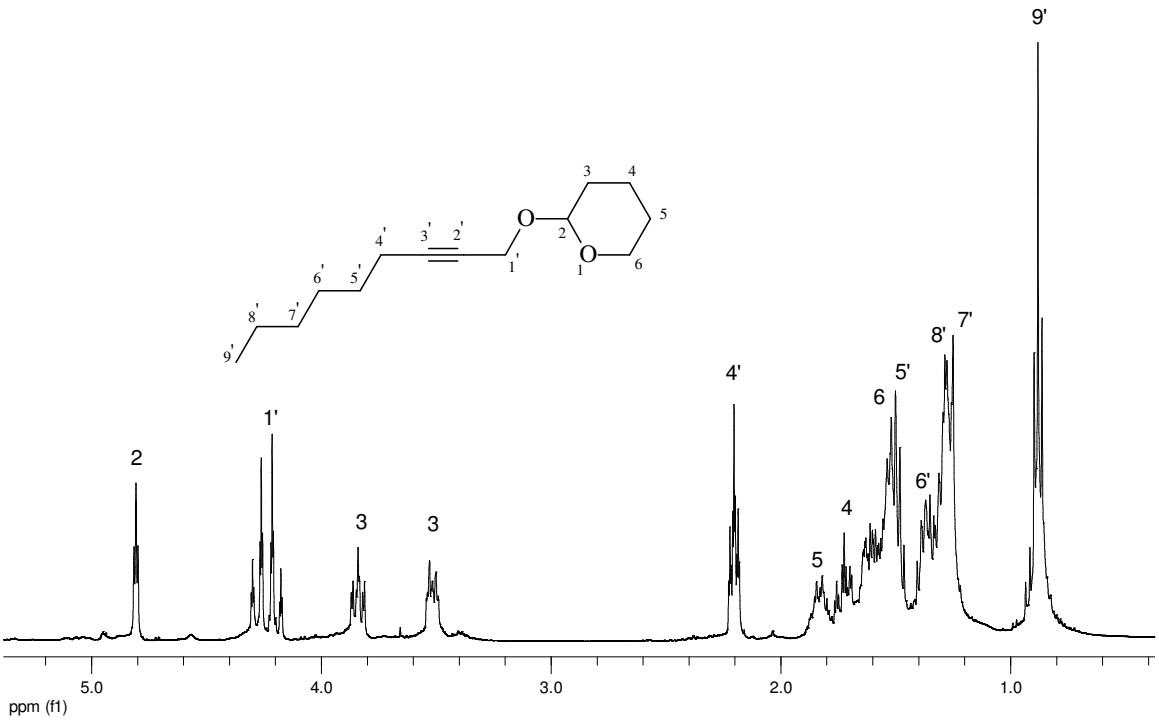

Figure 82: ^{1}H NMR Spectrum for 2-nonynyl tetrahydro-2*H*-pyran-2-yl ether

This reaction, albeit successful, only afforded a 41% isolated yield of the product **102** and also made use of HMPA, a liquid reagent considered to be carcinogenic.[91] It thus seemed necessary to further optimize this reaction whilst eliminating the necessity to utilize HMPA.

Based on a report by Kocieński *et al*.,[92] a successful alkylation reaction can be attained when employing *n*-butyllithium as the base to achieve acetylenic proton extraction whilst utilizing an alkyl iodide as the electrophile followed by prolonged reaction times (*ca*. 20 hours) in refluxing THF. This methodology was subsequently applied to our system in an attempt to facilitate the alkylation of the THP propargyl alcohol **101** with 1-bromohexane to form **102**. *n*-Butyllithium was added to a solution of THP propargyl alcohol in dry THF at 0 ^{o}C and allowed to stir for 30 minutes after which the reaction was allowed to warm to room temperature and stir for an additional 30 minutes. The reaction solution was again cooled to 0 ^{o}C followed by the dropwise addition of 1-bromohexane. After a stirring period of 30 minutes at 0 ^{o}C, the reaction was warmed and allowed to reflux for 20 hours under dry reaction conditions. Inspection of the resulting reaction mixture using

TLC analysis inferred the successful formation of the alkylated THP propargyl alcohol product **102**, as well as complete exhaustion of the starting materials. The reaction mixture was purified *via* column chromatography and the major component was sent for NMR and GC-MS analysis, the results of which confirmed the presence of the desired alkylated product **102** as the results were consisted with those previously obtained. This alternative reaction procedure employing refluxing reaction conditions furnished the alkylated product **102** in a pleasing 88% isolated yield. This successful outcome was in contrast to a failed reaction when no refluxing of the reaction was performed. A plausible reaction mechanism for the above mentioned reaction is depicted below in scheme 60.

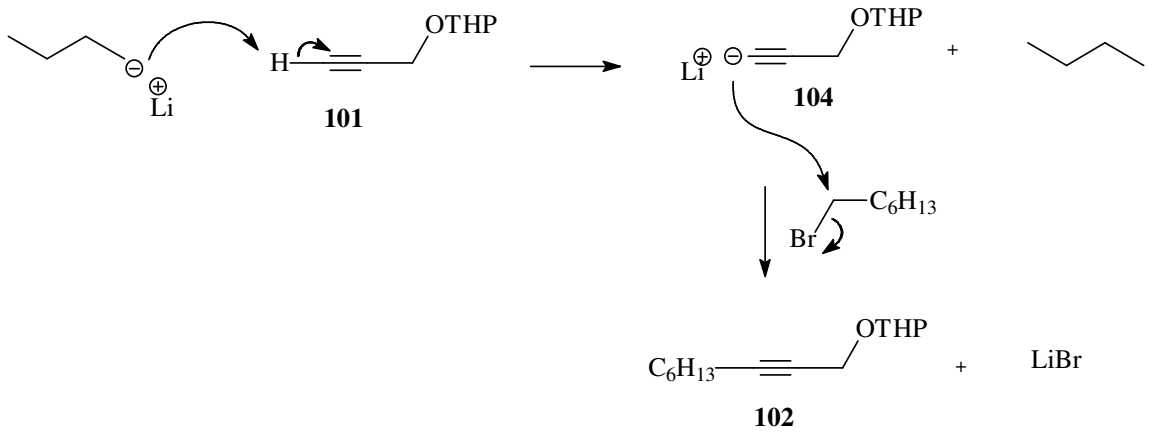

Scheme 60

The *n*-butyllithium abstracts the terminal acetylenic proton on **101** to furnish the lithium salt **104**. The nucleophilic lithium salt **104** undergoes a subsequent S_N2 type nucleophilic substitution reaction with 1-bromohexane to afford the alkylated THP propargyl alcohol product **102** under refluxing reaction conditions.

The next step toward the synthesis of the much needed hexyl propargyl bromide reagent **99** involved the removal of the THP protecting group as depicted in Scheme 61.

Procedures for the removal of THP protecting groups from alcohols are found extensively in the literature, and normally require the use of acidic reaction conditions i.e. HCl,[92] or *p*-TSA[93,94] in methanol.

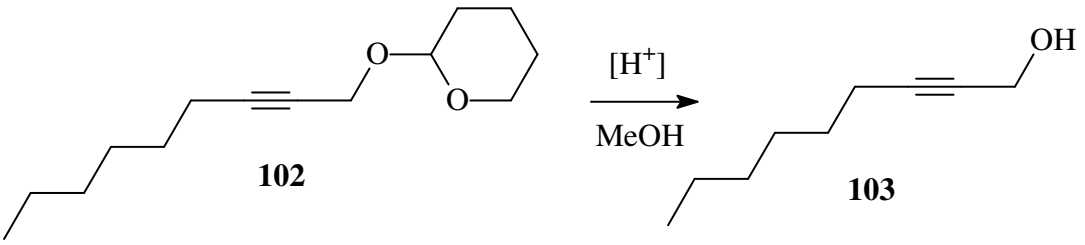

Scheme 61

The hexyl THP propargyl alcohol **102** was dissolved in methanol, acidified with 5 cm^3 of 4 M hydrochloric acid and allowed to stir at room temperature for 1 hour. Analysis of the resulting solution using TLC analysis clearly showed the disappearance of the starting material and the formation of a prominent spot at R_f = 0.60 (ethyl acetate:hexane = 1:1). The reaction mixture was neutralized with potassium carbonate, filtered and concentrated *in vacuo* after which the new spot was isolated *via* column chromatography. The structure for the new compound was determined by acquiring both one and two dimensional NMR spectroscopic data as well as GC-MS data, and was found to be that of the desired alcohol product **103**. The following deprotection reaction was shown to be highly efficient and afforded the alcohol product **103** in a 98% yield. The one dimensional ^1H NMR spectrum for the product showing the relevant peak assignments is depicted below in Figure 83.

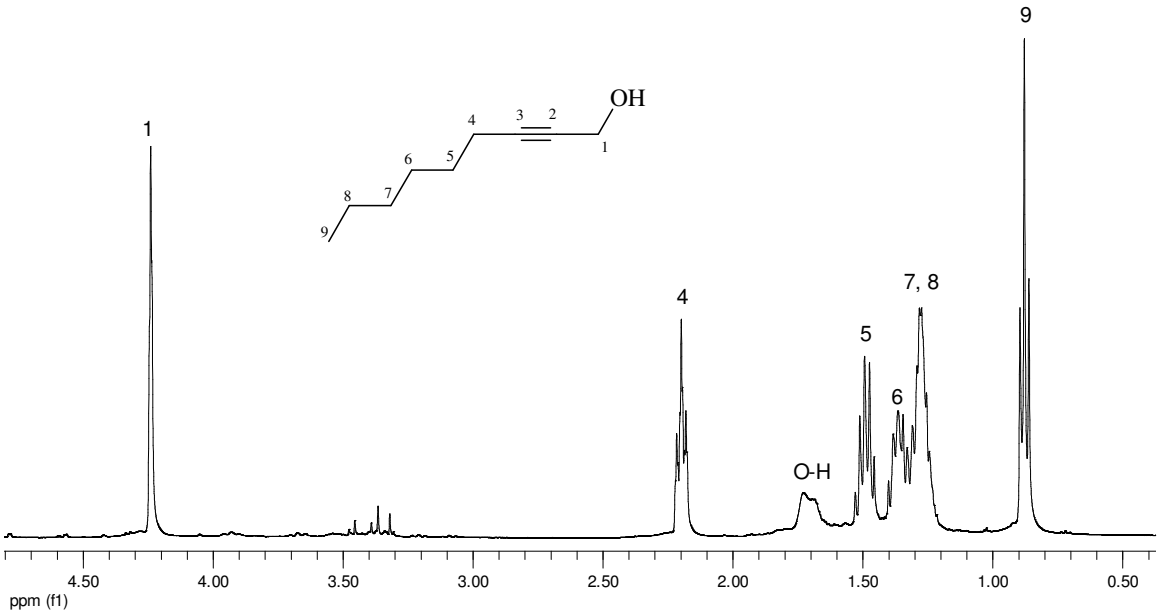

Figure 83: ^1H NMR Spectrum for 2-nonyn-1-ol

Immediately apparent in the ^{1}H NMR spectrum (Figure 83) was the presence of the O*H* singlet peak integrating for one proton at 1.73 ppm, and the adjacent methylene singlet 1-*H* integrating for two protons at 4.24 ppm. The two triplet peaks at 2.20 and 0.88 ppm integrated for two and three protons respectively and were thus assigned as the protons 4-*H* and 9-*H* respectively. The COSY spectrum (Figure 84) showed the existence of coupling between the protons at 4-*H* to the multiplet at 1.49 ppm. This multiplet was found to integrate for two protons and was assigned to alkyl protons 5-*H*. The multiplet at 1.37 ppm was assigned as the protons 6-*H* as they could be seen coupling to the protons 5-*H* in the COSY spectrum. The multiplet integrating for four protons could be seen coupling with protons 6-*H* and 9-*H* in the COSY spectrum and was assigned as the overlapping proton signals 7-*H* and 8-*H*.

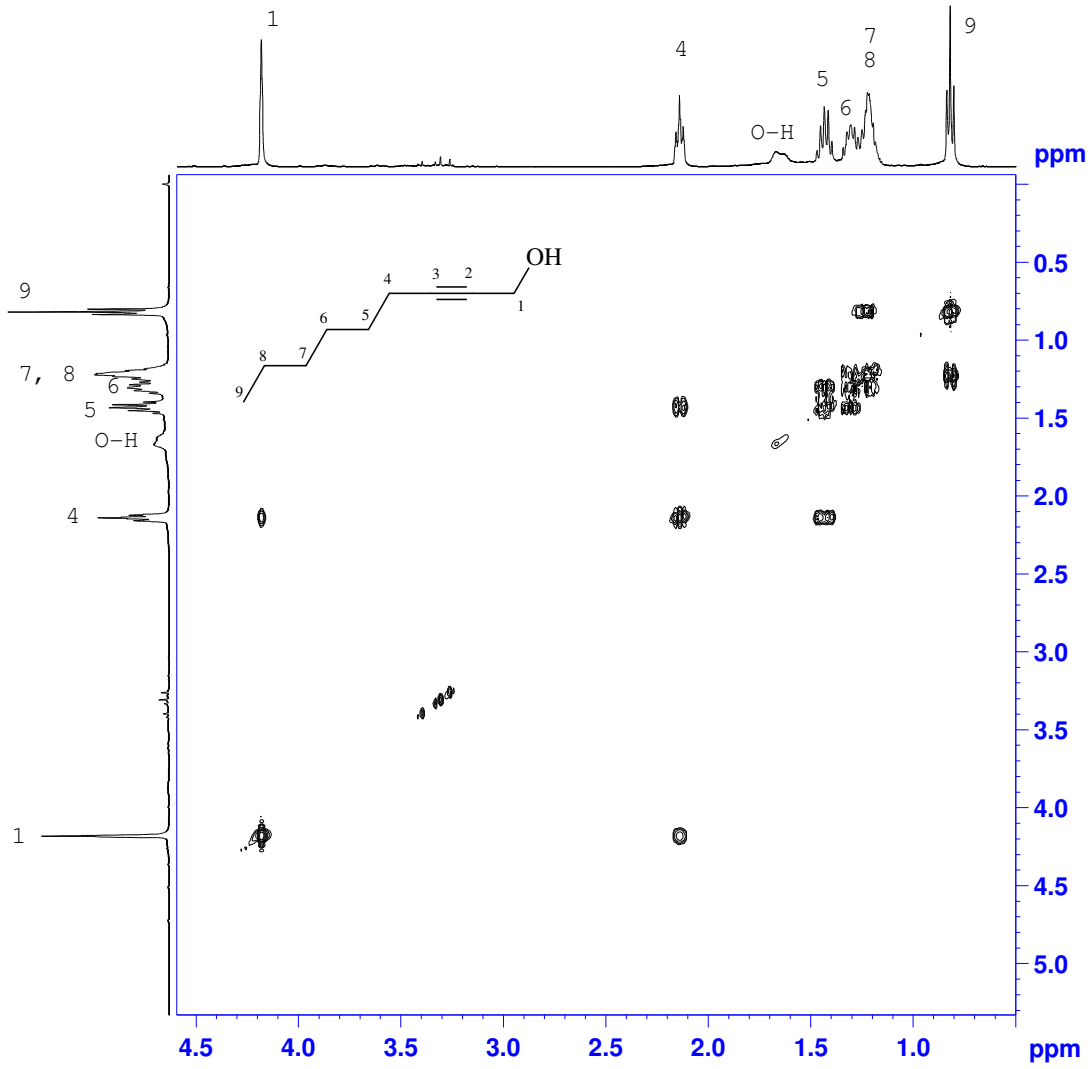

Figure 84: 2D COSY Spectrum for 2-nonyn-1-ol

Upon initial inspection of the ^{13}C NMR spectrum (Figure 85) eight obvious carbon signals were observed however the alcohol product **103** contained nine carbon atoms. This incongruity was resolved after analysis of the two dimensional HSQC spectrum (Figure 86).

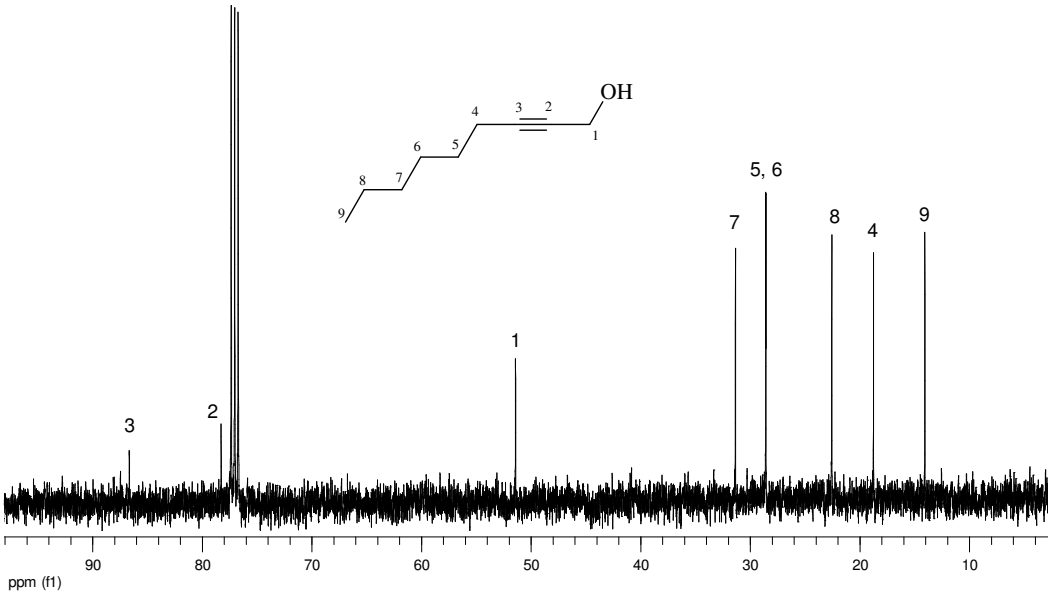

Figure 85: ^{13}C NMR Spectrum for 2-nonyn-1-ol

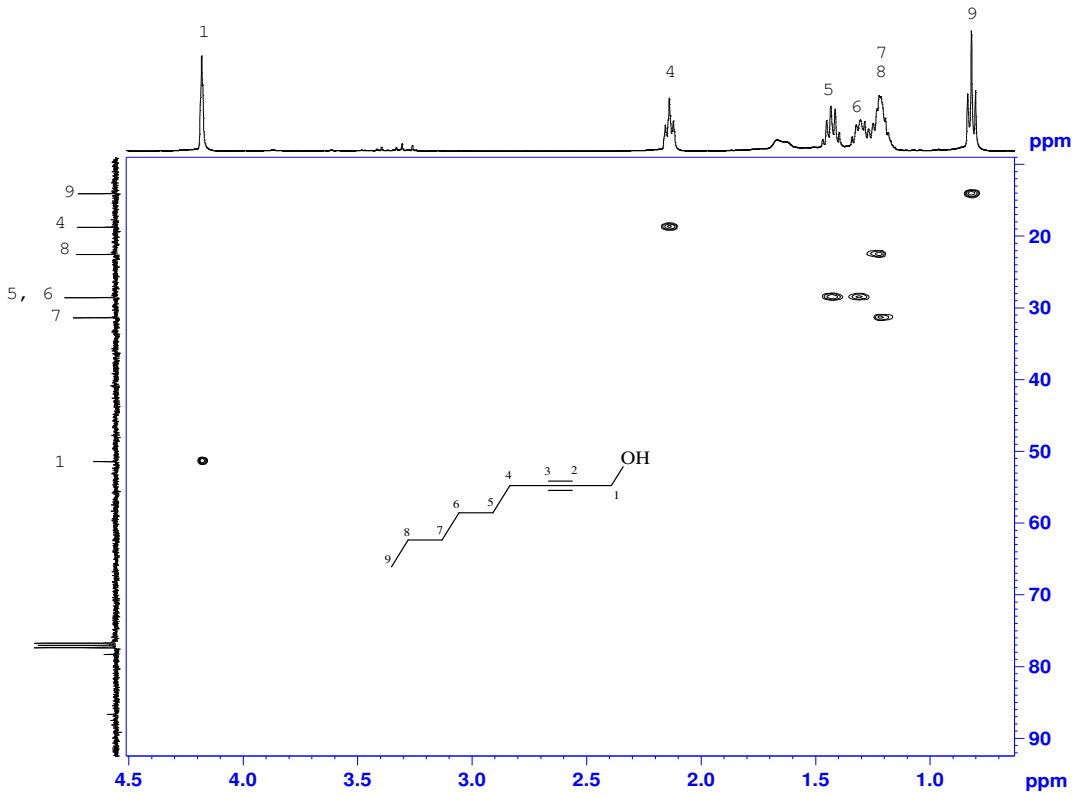

Figure 86: 2D HSQC Spectrum for 2-nonyn-1-ol

Analysis of the two dimensional HSQC spectrum (Figure 86) explained this discrepancy as being attributed to the fact that the carbon atoms giving rise to proton signals 5-*H* and 6-*H* respectively in the ^{1}H spectrum seem to appear at the same chemical shift in the ^{13}C spectrum (*ca*. 28.5 ppm). After closer inspection of the ^{13}C NMR spectrum under higher magnification, it could be seen that these carbon peaks at *ca*. 28.5 ppm were indeed present as two separate signals, however with an extremely small chemical shift difference of 0.02 ppm.

In order to furnish the desired hexyl propargyl bromide **99**, the alcohol **103** was brominated employing a commonly encountered halogenation technique developed by Rolf Appel[95,96] and made use of carbon tetrabromide and triphenylphosphine in toluene.

The alcohol **103** was added to a mixture of carbon tetrabromide and triphenylphosphine in dry toluene and stirred for 4 hours at room temperature as highlighted in Scheme 62.

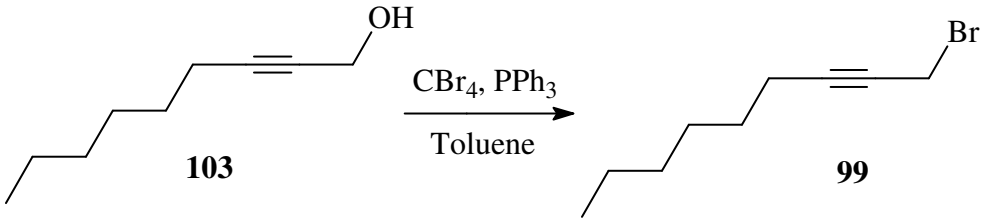

Scheme 62

The resulting reaction mixture was extracted three times with hexane after which the organic fractions were combined and concentrated *in vacuo* to furnish a brown oil. The major component based on TLC analysis was isolated from the crude material using column chromatography and sent for NMR and GC-MS analysis. The results from these techniques confirmed the successful formation of the hexyl propargyl bromide **99**, which was obtained in a pleasing 81% isolated yield.

The ^{1}H NMR spectrum (Figure 87) for the product **99** has been included below and was shown to be comparable to the ^{1}H NMR spectrum for the alcohol precursor **103**, possessing only minor differences. Immediately apparent was the disappearance of the

O*H* signal from the alcohol functionality and an upfield shift of the methylene protons 1-*H* from 4.12 ppm in the starting material (Figure 83) to 3.93 ppm in the brominated product (Figure 87). The remaining peaks in the ^{1}H NMR spectrum for the product **99** did not exhibit any significant change in their chemical shifts as compared to the corresponding peaks in the ^{1}H spectrum for the starting material **103** probably due to their further distance away from the altered functional group.

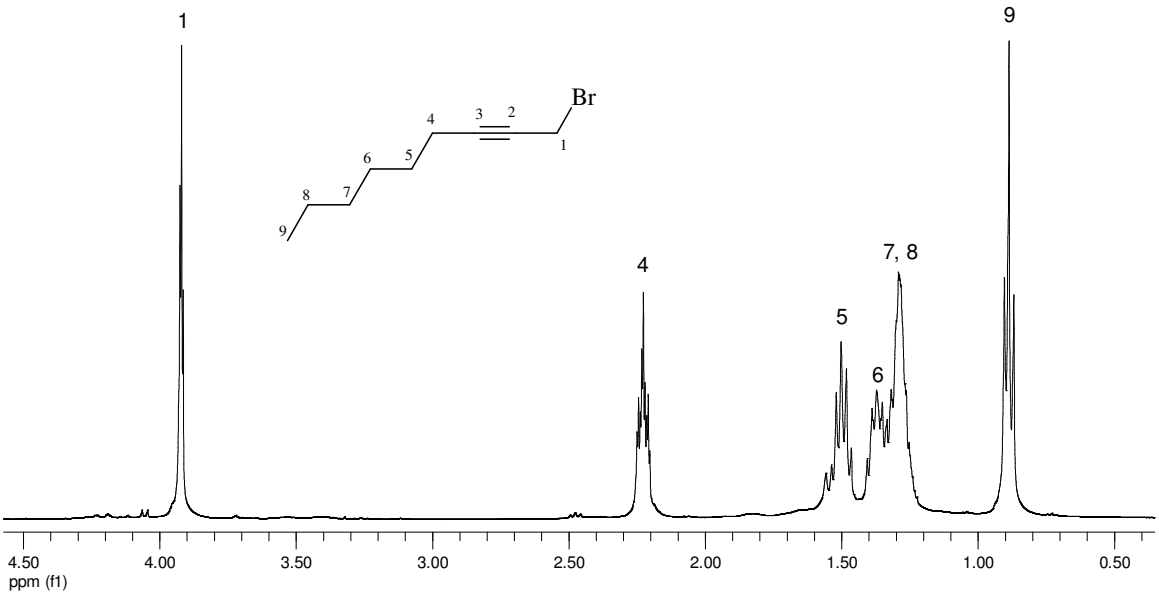

Figure 87: ^{1}H NMR Spectrum for 1-bromo-2-nonyne

The ^{13}C NMR spectrum (Figure 88) contained nine carbon signals as expected for the brominated product **99**. The peaks in the spectrum could be unambiguously assigned after careful analysis of the observed coupling present in the two dimensional NMR spectra. The ^{13}C NMR spectrum obtained for the product **99** was comparable to that obtained for the alcohol starting material **103** (Figure 85). A major difference worthy of mention was the significant upfield shift of the methylene carbon signal 1-*C* from 51.4 ppm in the starting material to 15.7 ppm in the brominated product. Additionally, the two carbon peaks 5-*C* and 6-*C* resonated at chemical shifts of *ca*. 28.3 and 28.5 ppm respectively, which resulted in them being slightly separated from each other in the spectrum and allowed them to be easily identified as two separate peaks in the full ^{13}C NMR spectrum.

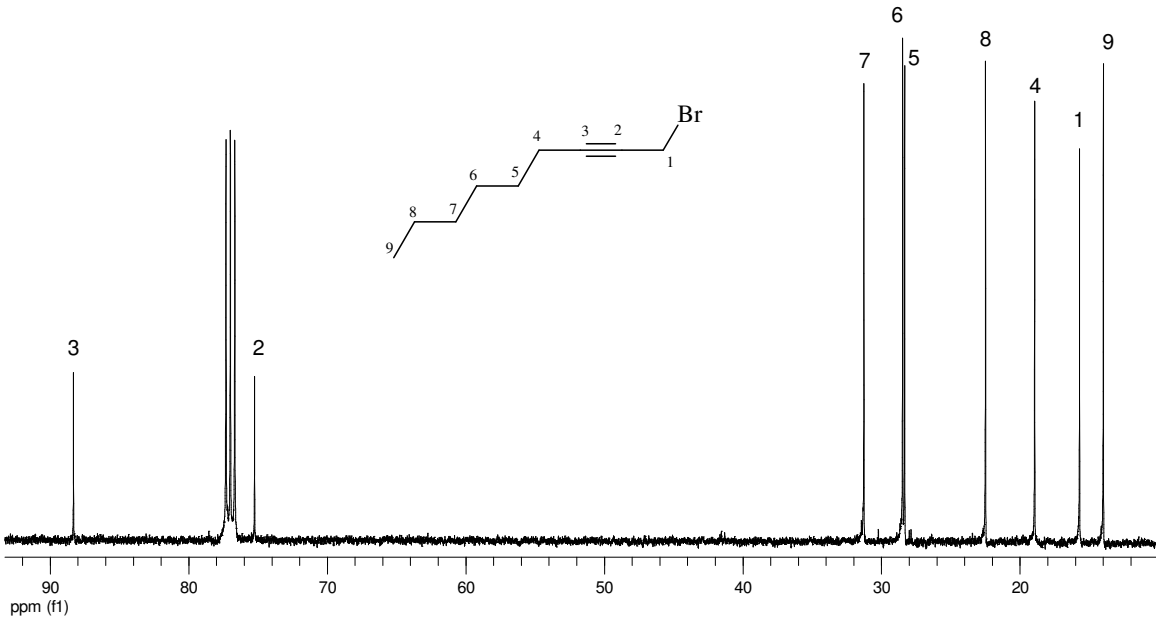

Figure 88: ^{13}C NMR Spectrum for 1-bromo-2-nonyne

A generally accepted reaction mechanism for the Appel halogenation reaction[95-97] is depicted below in Scheme 63. The triphenylphosphine **105** initially becomes activated by reaction with carbon tetrabromide to form the phosphonium salt pair **106**.

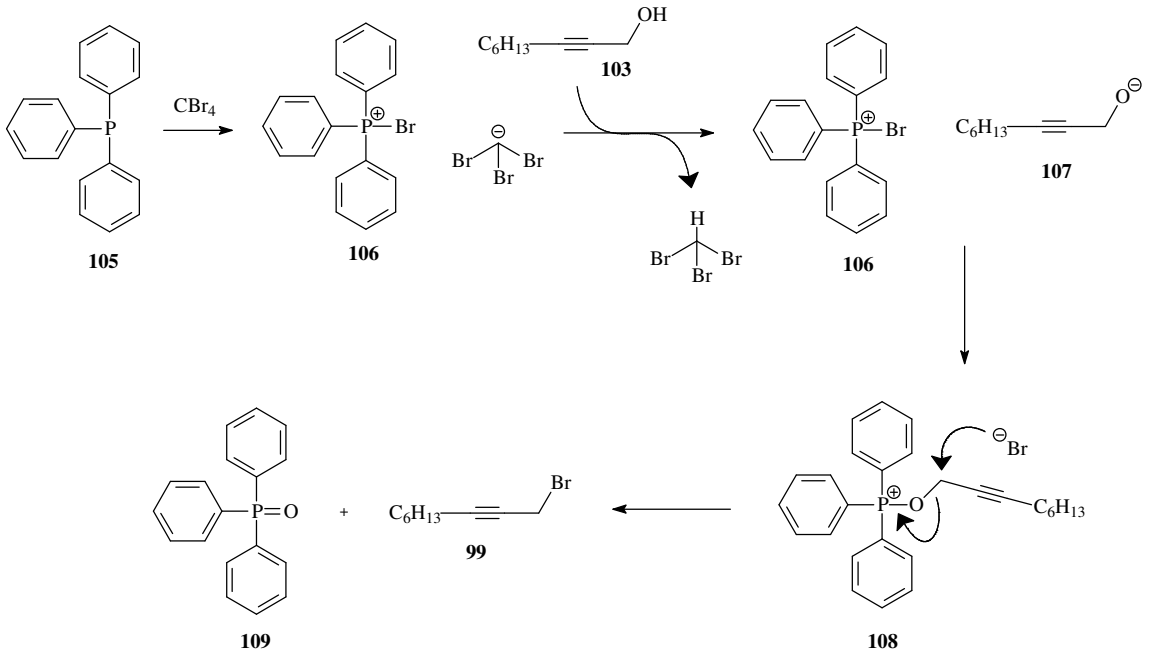

Scheme 63

Deprotonation of the alcohol **103** to form tribromomethane generates the alkoxide **107** which reacts with the phosphonium species **106** in a nucleophilic displacement reaction to form the oxyphosphonium intermediate **108**. Attack by the bromide ion on the oxyphosphonium complex **108** *via* an S_N2 type mechanism forms the brominated product **99** and triphenylphosphine oxide **109**.

The desired hexyl propargyl bromide **99** was therefore successfully obtained in a 68% overall yield from propargyl alcohol **100** over the 4 synthetic steps as originally proposed in Scheme 56 (page 117). With a pure stock of the hexyl propargyl bromide **99** in hand, it was implemented in the subsequent *C*-propargylation reaction towards the total synthesis of the pyrrolizidine ant alkaloid **223H** (xenovenine).

2.4.7 Preparation of ethyl (3*R*)-5-heptyl-3-methyl-2,3-dihydro-1*H*-pyrrolizine-7-carboxylate [74]

The former model studies determined that a *N*-bridgehead pyrrole functionality could be obtained from a secondary enaminone *via* *C*-propargylation followed by a hydroamination/cyclization reaction without isolating the seemingly unstable *C*-propargyl intermediate. This reaction protocol was thus implemented in the attempt to synthesize the *N*-bridgehead pyrrole **74** from the methyl secondary enaminone **72** *via* the *C*-propargyl intermediate **73** (Scheme 64).

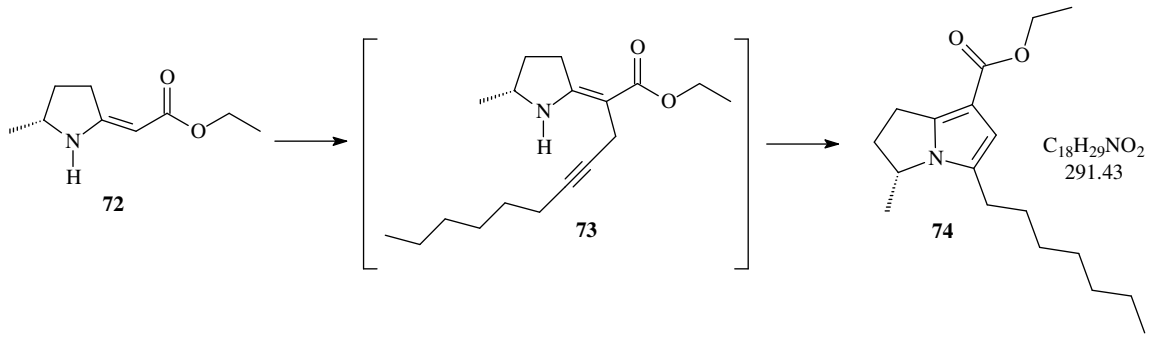

Scheme 64

n-Butyllithium was added cautiously to a stirring solution of methyl secondary enaminone **72** in dry THF at –77 ^{o}C and stirred for 30 minutes. The solution was allowed to warm to room temperature and stirred for an additional 30 min. The solution was again cooled to –77 ^{o}C followed by the addition of 1-bromo-2-nonyne **99** and a stirring period of 30 minutes. The reaction mixture was allowed to warm to room temperature and stir for 14 hours. The resulting reaction mixture was quenched using aqueous ammonium chloride and concentrated *in vacuo* to yield a yellow oil which was subject to hydroamination conditions employing $ZnCl_2$ as the hydroamination catalyst. Analysis of the resulting reaction mixture using TLC analysis showed the disappearance of the starting material **72** and the formation of a prominent spot at R_f = 0.78 (ethyl acetate:hexane = 1:1). A GC-MS trace obtained for the oil inferred the presence one major component whose mass spectrum possessed a parent molecular ion mass of 291 g.mol^{-1} as depicted in Figure 89. This result was exceptionally promising as the desired *N*-bridgehead pyrrole **74** was calculated to possess a molecular mass of 291.43 g.mol^{-1}.

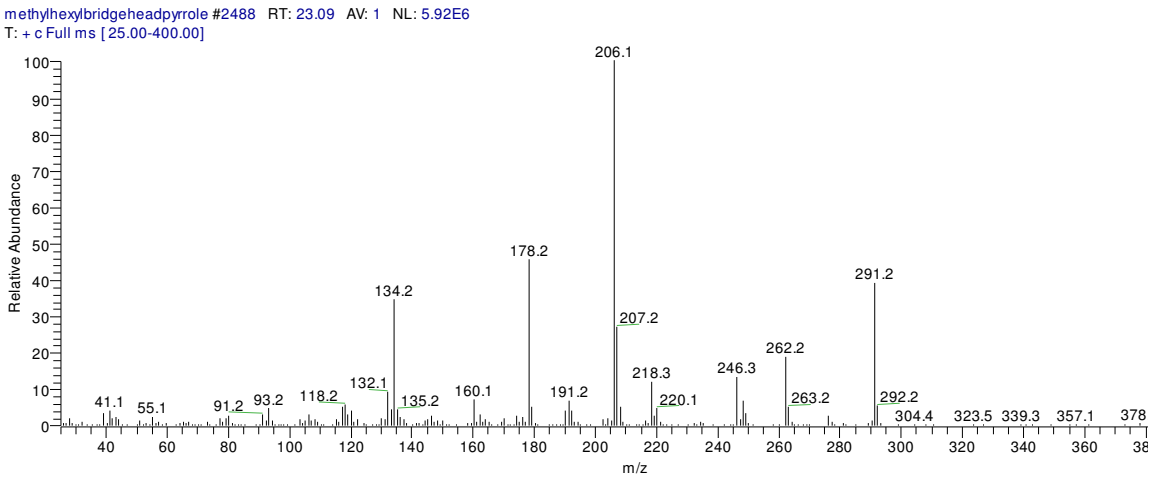

Figure 89

This compound was immediately isolated from the crude material using the method of radial chromatography to furnish an oil that was sent for HRMS and NMR analysis. High resolution mass spectrometry found the compound to possess a molecular mass of 292.2286 g.mol^{-1} which compared favorably to the calculated (M+H) mass of 292.2277 g.mol^{-1} for $C_{18}H_{30}NO_2$. Analysis of the one and two dimensional NMR spectra confirmed

the successful formation of the *N*-bridgehead pyrrole **74** and the ^{1}H and ^{13}C NMR spectra have been included below in Figures 90 and 91 respectively.

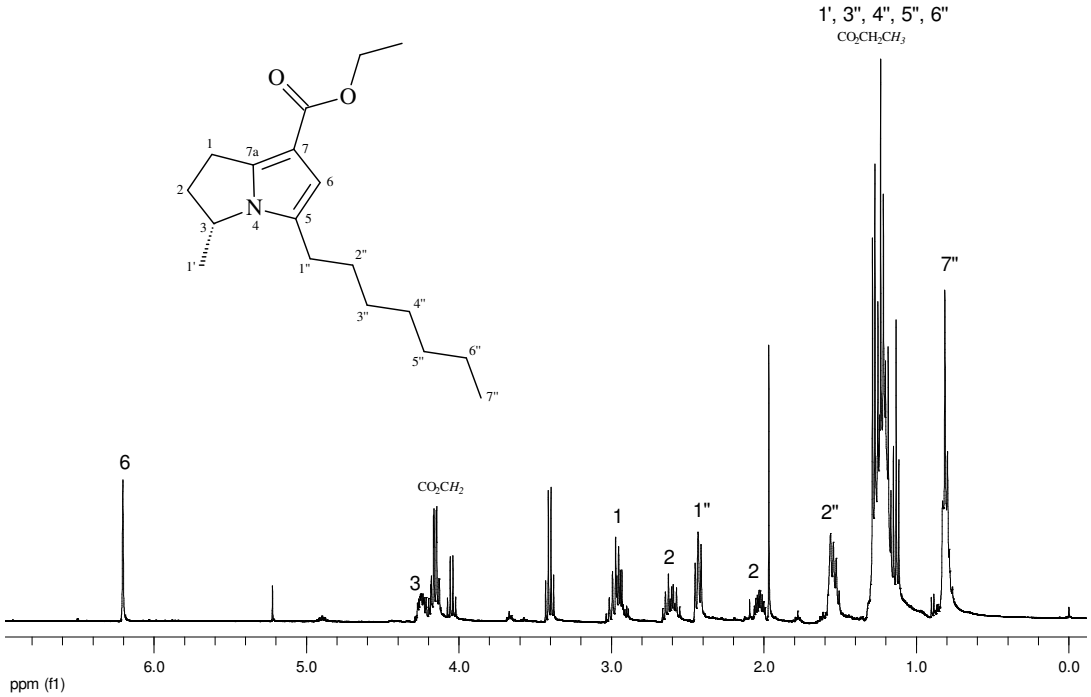

Figure 90: ^{1}H NMR Spectrum for ethyl (3*R*)-5-heptyl-3-methyl-2,3-dihydro-1*H*-pyrrolizine-7-carboxylate

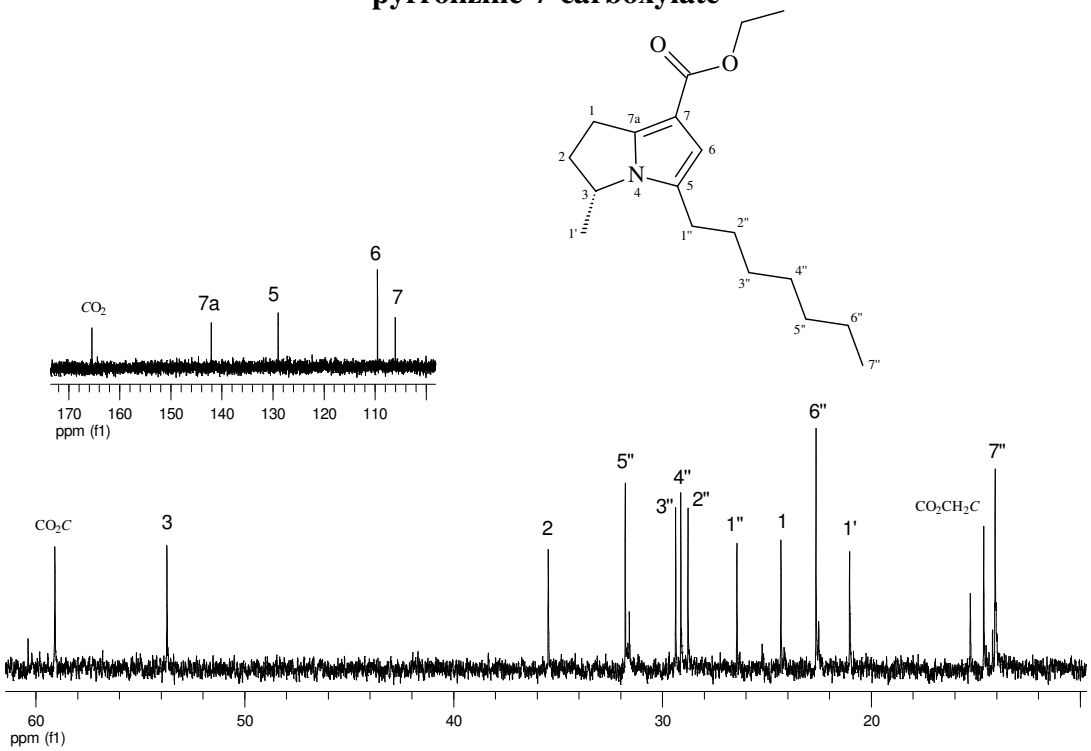

Figure 91: ^{13}C NMR Spectrum for ethyl (3*R*)-5-heptyl-3-methyl-2,3-dihydro-1*H*-pyrrolizine-7-carboxylate

The key signal in the ^{1}H NMR spectrum (Figure 90) that corroborated a successful hydroamination/cyclization reaction was the new singlet peak at 6.27 ppm which corresponded to the methine proton 6-*H* on the unsaturated ring. The signals typical for the pyrrolidine ring were present in the ^{1}H spectrum with the methylene protons 2-*H* being splint into two separate signals due to the presence neighboring chiral centre. The methyl signals 1′-*H* and $CO_2CH_2CH_3$ could not be individually assigned as they resonated in the same region as the 8 methylene protons 3″-*H* to 6″-*H* on the alkyl chain at *ca*. 1.3 ppm. Analysis of the two dimensional NMR spectra assisted in the assignment of the signals in the ^{13}C NMR spectrum and are shown in Figure 91. The above mentioned synthesis afforded the *N*-bridgehead pyrrole **74** in a 43% yield from **72** and in a 4.1% overall yield from (*S*)-pyroglutamic acid **92** over 10 synthetic steps.

The remaining two steps toward the total synthesis of ant alkaloid **223H** (xenovenine) could not be attempted due to time constraints, but are presented below in the section titled future work.

2.4.8 Future work

In order to ultimately furnish the ant alkaloid **223H** (xenovenine) (**62**, Scheme 65), two synthetic steps remained which were the removal of the ester moiety in **74** *via* decarboxylation followed by the stereoselective reduction of the double bonds in **110** to afford **223H** (xenovenine).

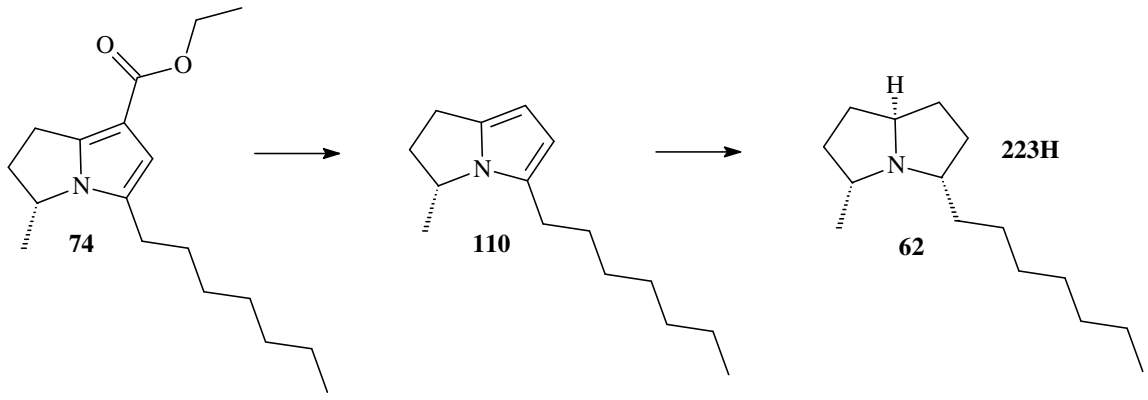

Scheme 65

Although the decarboxylation of **74** to afford **110** was supposed to be a problematic step, the successful decarboxylation of a monocyclic derivative (**67**, Scheme 66) to yield the pyrrole product **112** *via* the acid **111** that was achieved in our hands corroborated the proposed methodology behind accessing **110** from **74**. The decarboxylated monocyclic product **112** was obtained by employing a reverse Fischer esterification technique to afford a carboxylic acid intermediate **111** which was subsequently decarboxylated in refluxing ethanolamine. This procedure successfully afforded the decarboxylated product **112**, however in a low yield (31%), and will therefore be the focus of further optimization studies in future.

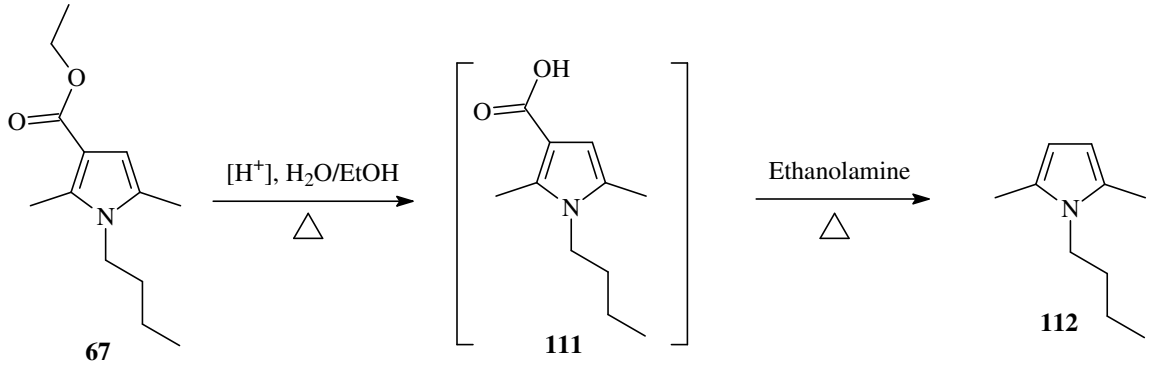

Scheme 66

The final reduction of the *N*-bridgehead pyrrole **111** to afford **223H** (xenovenine) **62** also remains the focus of future studies. It is predicted that the reduction of **110** to yield **62** (Scheme 65) must take place in a controlled fashion so as to achieve a stereoselective reduction.

Our first attempt at reduction will involve employing H_2 (g) and a $Pd/CaCO_3$ hydrogenation catalyst at low temperatures in the hope that the methyl group at position 3-*C* of the *N*-bridgehead structure in **110** will, due to steric effects, direct the addition of hydrogen to the opposite face of the ring allowing for the alkyl chain at position 5-*C* to take on a *cis* orientation relative to the methyl group 3-*C*. It must be mentioned at this time that the following synthetic strategy, if successful, will most probably furnish a stereo analogue of **223H** (xenovenine) such as that shown in Figure 92 due to the fact that

the hydrogen atoms will be added to the same side of the molecule. The newly added protons 7a-*H* and 3-*H* would thus most probably reside *cis* relative to the proton 5-*H*.

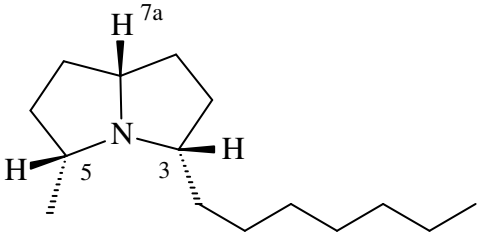

Figure 92

2.4.8.1 An Alternative Synthetic Approach

An alternative synthetic strategy was later developed in order to synthesize the opposite stereoisomer to **223H** (xenovenine). The proposed synthesis will be considered for future studies and is presented below in Scheme 67.

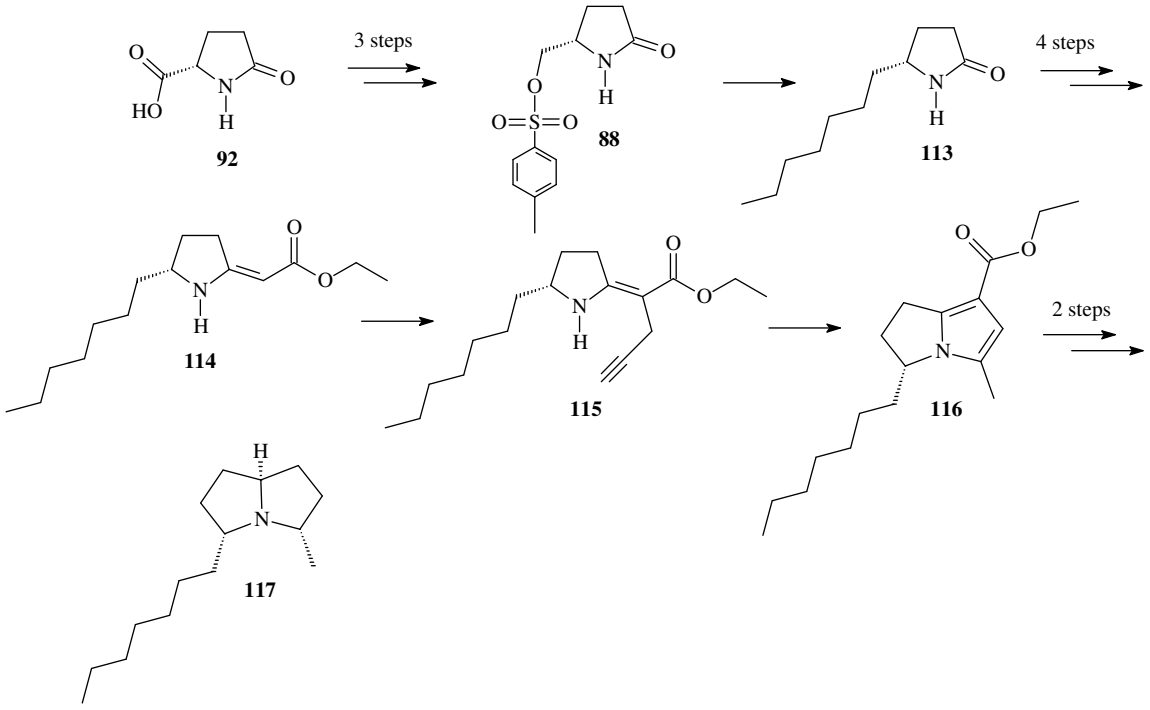

Scheme 67

This alternative synthetic route adapted from the former total synthesis of **223H** (xenovenine) contains one major difference, as seen in the reduction step of the tosylated compound **88**. It had been pre-established that the tosylated compound **88** could be obtained from (*S*)-pyroglutamic acid **92** over 3 synthetic steps in a 51% yield. In place of the original (Bu_3SnH, AIBN) reaction to yield the methyl lactam (**70**, Scheme 51), the reduction of **88** using an organocopper reagent, or Gilman Reagent[98,99] could be employed potentially accessing the heptyl lactam **113**. This alkylated derivative **113** could later be converted into the heptyl secondary enaminone **114** *via* the pre-established synthetic techniques developed in the former synthesis. *C*-Propargylation of **114** utilizing propargyl bromide to yield **115** could undergo hydroamination to yield the appropriate *N*-bridgehead pyrrole **116**, a structurally analogous precursor to the pyrrolizidine alkaloid **117**.

In an effort to substantiate whether the alkylation of **88** using the above described technique was possible, a Gilman reagent was synthesized by the *in situ* combination of a monovalent alkylcopper compound (R′-Cu) with an organolithium compound (R-Li) to form the Gilman reagent (R_2CuLi). Being a convenient source of organolithium reagent, *n*-butyllithium was employed in a model reaction in order verify whether the alkylated compound **118** could be obtained from the tosylated compound **88** (Scheme 68).

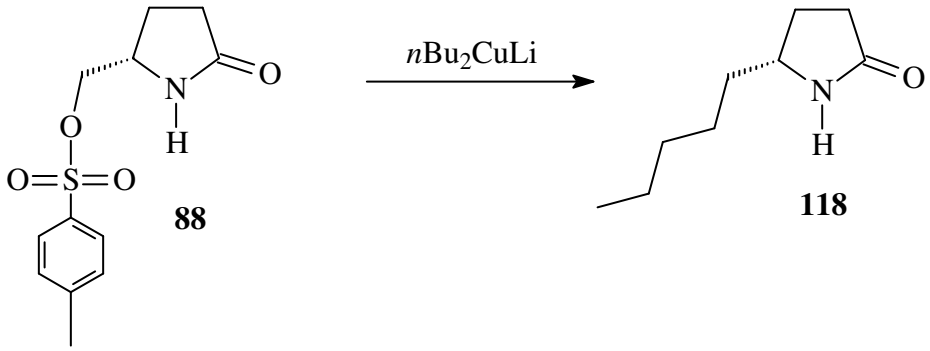

Scheme 68

The Gilman reagent (nBu_2CuLi) was therefore synthesized *in situ* by adding *n*-butyllithium to a stirred suspension of copper cyanide in dry THF at –40 °C over a period of 1 hour. A solution of **88** in dry THF was cannulated into the resulting cuprate at –40

^{o}C and the mixture was stirred at –40 ^{o}C for 3 hours followed by overnight stirring at room temperature. The reaction was quenched using saturated ammonium chloride and the resulting two layers were separated. The organic layer was washed with saturated ammonium chloride and the aqueous layer was extracted with dichloromethane. The organic portions were combined and concentrated *in vacuo* to yield a yellow oil which was purified by radial chromatography. The major component was analyzed using HRMS and NMR spectroscopy and was found to be that of the desired pentyl lactam **118**, which formed in an excellent 96% yield. These pleasing results demonstrated the validity of employing Gilman reagents in the alkylation of tosylated compounds and it was therefore concluded that by employing *n*-hexyl lithium as the organolithium reagent (R-Li) in the following reaction, the heptyl lactam **113** could feasibly be obtained.

2.4.9 Overview of Total Synthesis

An overall synthetic scheme depicting the attempted route employed to access the pyrrolizidine ant alkaloid **223H** (xenovenine) is presented below in Scheme 69. (*S*)-Pyroglutamic acid **92** was converted into the corresponding ethyl ester **90** in an 84% yield and with 97% ee when employing Fischer esterification. The ethyl ester **90** was subsequently reduced into its corresponding alcohol **89** using Sodium borohydride in water in an 80% yield and with an 87% ee. Efficient tosylation of the alcohol **89** utilizing tosyl chloride, potassium hydroxide and tetrabutylammonium hydrogen sulfate in aqueous chloroform furnished **88** in a 76% yield. The tosylated derivative **88** was reduced to the methyl lactam **70** using tributyltin hydride and AIBN in a 61% yield, and was subsequently thionated employing Lawesson's reagent in THF to furnish the methyl thiolactam **71** in an 80% yield. In order to promote the Eschenmoser sulfide contraction reaction, the methyl thiolactam **71** was first converted into the tertiary methyl thiolactam **86** in a quantitative yield, and subsequently employed in the Eschenmoser sulfide contraction reaction which formed the tertiary methyl enaminone **87** in a 70% yield.

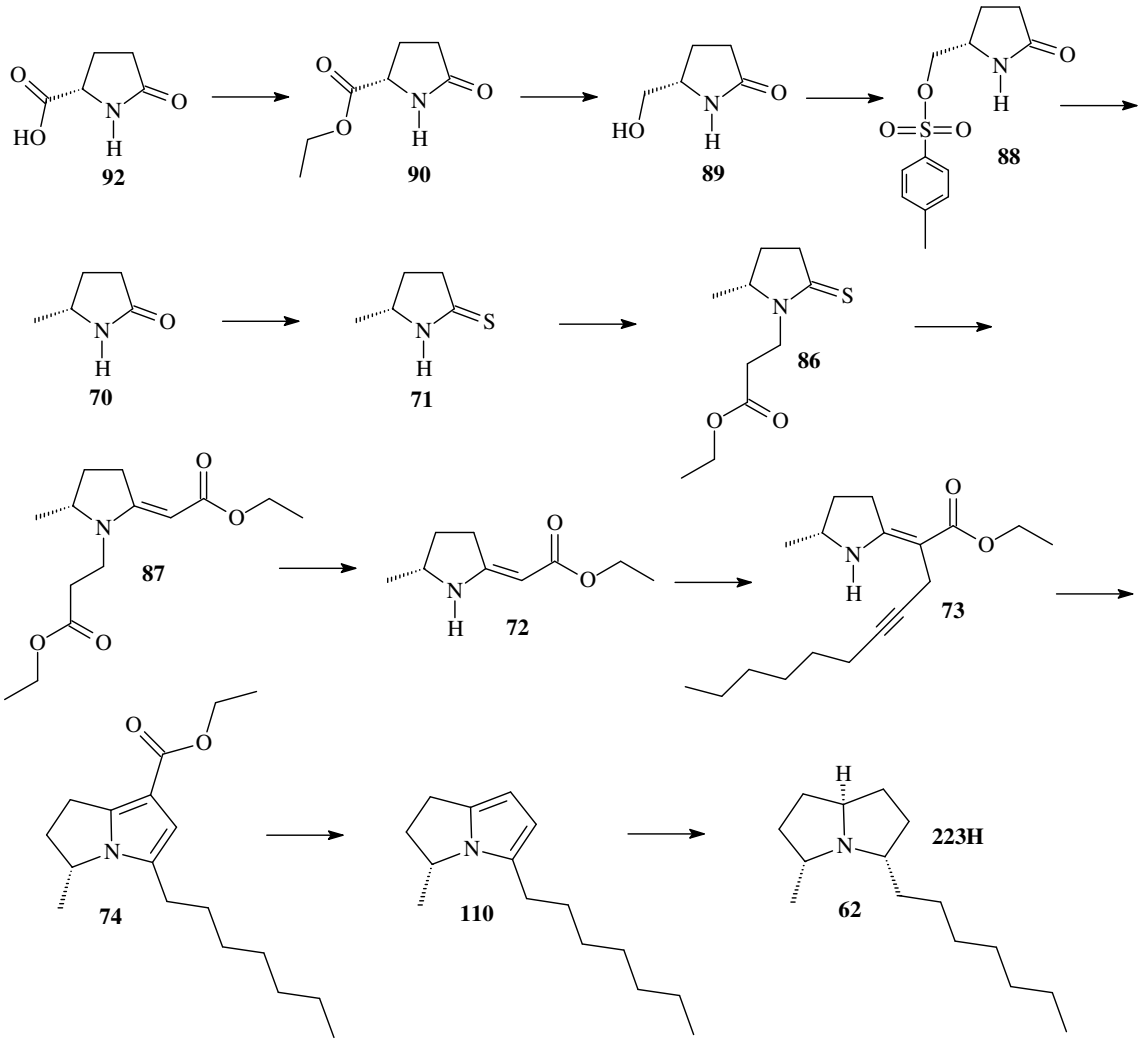

Scheme 69

The acrylate group was successfully removed utilizing LiHMDS in THF to afford the secondary methyl enaminone **72** in a 55% yield. Following the successful synthesis of 1-bromo-2-nonyne, it was used in the *C*-propargylation of **72** to form the *C*-propargyl intermediate **73** which was cyclized in the pivotal hydroamination reaction to afford the *N*-bridgehead pyrrole **74** in a 43% yield from the secondary methyl enaminone **72** and 4.1% overall yield from (*S*)-pyroglutamic acid (**92**). The last two synthetic transformations remain the focus of future studies and involve the decarboxylation of **74** to form **110** followed by subsequent stereoselective reduction of the double bonds to furnish the pyrrolizidine alkaloid **223H** (xenovenine) **62**.

2.5 Summary

These studies towards the total synthesis of the pyrrolizidine ant alkaloid **223H** (xenovenine) **62** furnished some interesting results and incorporated the efficient hydroamination methodology as the key ring forming step. It also resulted in the synthesis of three novel compounds namely ethyl 3-[(2*R*)-2-methyl-5-thioxotetrahydro-1*H*-pyrrol-1-yl]propanoate **86**, ethyl 3-{(5*R*)-2-[(*E*)-2-ethoxy-2-oxoethylidene]-5-methyltetrahydro-1*H*-pyrrol-1-yl}propanoate **87** and (3*R*)-5-heptyl-3-methyl-2,3-dihydro-1*H*-pyrrolizine-7-carboxylate **74**.

The results from a catalytic hydroamination study were accepted by Tetrahedron Letters[69] for publication and illustrated that the group 11 and 12 metals in general served as effective hydroamination catalysts in the conversion of *C*-propargyl vinylogous amides **66** into pyrroles **67**. The hydroamination reactions were completely regioselective with the starting material **66** undergoing 5-*exo*-dig cyclizations (Markovnikov addition) forming the pyrrole **67** in preference to a 6-*endo*-dig cyclizations (anti-Markovnikov addition), albeit both cyclizations being favorable transformations according to the Baldwin rules.[74,75] Increases in catalytic activities were observed upon moving up a periodic group and was attributed to increasing catalytic stabilities in solution, as well as increases in Lewis acidities resulting from increases in charge to radius ratios. The zinc catalyst series namely $ZnCl_2$, $ZnAc_2$ and $Zn(NO_3)_2$ furnished the highest yields of pyrrole **67** with recorded yields of 93%, 96% and 99% respectively under mild reaction conditions.

Model studies performed in this project established that an *N*-bridgehead pyrrole scaffold **61** could be successfully synthesized from a commercially available lactam starting material **67** in a 29% overall yield. Subsequently, once the desired methyl lactam **70** had been synthesized, it was integrated into the total synthesis of the pyrrolizidine ant alkaloid **223H** (xenovenine) utilizing the previously optimized reaction conditions stemming from the model studies. The *N*-bridgehead pyrrole **74** was successfully furnished when employing this methodology in a 13.2% yield from the methyl lactam **70**

resulting in a 4.1% overall yield from (*S*)-pyroglutamic acid **92** being achieved. The last two synthetic transformations remain the focus of future studies and involve the decarboxylation of **74** to form **110** followed by subsequent stereoselective reduction of the double bonds to furnish the pyrrolizidine alkaloid **223H** (xenovenine) **62**.

3 Experimental

3.1 Materials and Methods

The NMR spectra were obtained using a Bruker Avance 400 MHz spectrometer. ^{1}H spectra were obtained at 400 MHz and referenced against the $CDCl_3$ singlet at 7.26 ppm. ^{13}C spectra were obtained at 100 MHz and were referenced against the central line of the $CDCl_3$ triplet at 77.0 ppm. Abbreviations used: s – singlet; d – doublet; t – triplet; q – quartet; m – multiplet. High resolution mass spectra were obtained using a Waters Acquity (LCT premier) ultra performance liquid chromatography-mass spectrometry instrument. Low resolution mass spectra (electron impact) were obtained using a Thermofinnigan trace GC coupled with a Polaris Q mass spectrometer. The trace GC column used was a 30 m BPX5 - 5% phenyl (equivalent) / 95% methylpolysilphenylene / siloxane phase column with a 0.25 µm ID. Infrared spectra were obtained as thin films (neat) / thin films (chloroform) or as a nugul mixes using a Perkin-Elmer Spectrum One Spectrometer with a scan window of 4000 - 400 cm^{-1}. The spectral resolution was 1.0 cm^{-1} and the average from 3 scans was taken. Optical rotations were obtained using a Perkin-Elmer 241 polarimeter using a sodium lamp with a D line at 589 nm. A path length of 10 cm was used and all concentrations are quoted in g/100 cm^3. Melting points were measured using a Kofler Hotstage melting point apparatus. All microwave reactions were performed using CEM Discovers Microwave System™. The X-Ray data was obtained using an Oxford Diffraction Xcalibur 2 CCD diffractometer.

All column chromatography was performed using Merck silica gel 60 PF_{254} and all thin layer chromatography (TLC) was performed using Merck silica gel 60 F_{254} supported on an aluminum backing. Visualization of compounds on TLC plates was achieved by inspection under UV-light (254/365 nm) and/or by exposure to iodine vapour or by staining with a potassium permanganate or anisaldehyde staining solution.

All reaction solvents were purified by distillation prior to use. Tetrahydrofuran and diethyl ether were distilled over sodium metal/benzophenone, and toluene from sodium metal. Dichloromethane and acetonitrile were distilled over calcium hydride, and methanol from magnesium turnings. Hexane and ethyl acetate were distilled under 1 atmosphere for use in chromatography.

The following research resulted in the synthesis of three novel compounds namely ethyl 3-[(2*R*)-2-methyl-5-thioxotetrahydro-1*H*-pyrrol-1-yl]propanoate **86**, ethyl 3-{(5*R*)-2-[(*E*)-2-ethoxy-2-oxoethylidene]-5-methyltetrahydro-1*H*-pyrrol-1-yl}propanoate **87** and (3*R*)-5-heptyl-3-methyl-2,3-dihydro-1*H*-pyrrolizine-7-carboxylate **74**.

3.2 Procedures and Spectrometric Data

Ethyl (*Z*)-3-(butylamino)-2-butenoate [65]

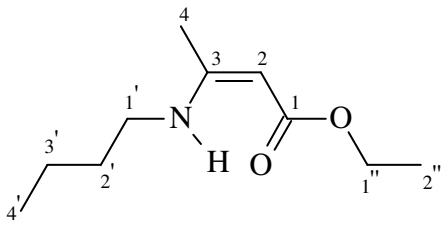

n-Butylamine (7.1 g, 97 mmol) was added to a stirring solution of ethylacetoacetate (6.3 g, 49 mmol) and toluene (200 cm^3), and refluxed using a Dean and Stark apparatus for 5 hours. The solution was concentrated *in vacuo* to yield ethyl (*Z*)-3-(butylamino)-2-butenoate **65** (8.7 g, 47 mmol, 96%) as a yellow oil; R_f 0.65 (EtOAc/Hex 1:1); (Found: M^+, 186.1499. Calc. for $C_{10}H_{20}NO_2$, *M:* 186.1494); ν_{max}(film)/cm^{-1} 3285, 2960, 2932, 2873, 1651, 1607, 1272, 1172, 1148, 1059 and 783; δ_H(400 MHz; $CDCl_3$) 8.51 (1 H, s, N-*H*), 4.38 (1 H, s, 2-*H*), 4.04 (2 H, q, *J* = 7.1 Hz, 1′′-*H*), 3.16 (2 H, q, *J* = 6.9 Hz, 1′-*H*), 1.87 (3 H, s, 4-*H*), 1.51 (2 H, m, 2′-*H*), 1.36 (2 H, m, 3′-*H*), 1.20 (3 H, t, *J* = 7.1 Hz, 2′′-*H*), 0.89 (3 H, t, *J* = 7.3 Hz, 4′-*H*); δ_C(100 MHz; $CDCl_3$) 170.5 (s, 1-*C*), 161.8 (s, 3-*C*),

81.7 (d, 2-*C*), 58.0 (t, 1″-*C*), 42.6 (t, 1′-*C*), 32.4 (t, 2′-*C*), 19.9 (t, 3′-*C*), 19.2 (q, 4-*C*), 14.5 (q, 2″-*C*) 13.6 (q, 4′-*C*); *m/z* (EI) 185 (M^+, 53%), 170 (34), 140 (44), 122 (36), 110 (31), 98 (93), 96 (100) and 71 (65).

Ethyl 2-[(*Z*)-1-(butylamino)ethylidene]-4-pentynoate [66]

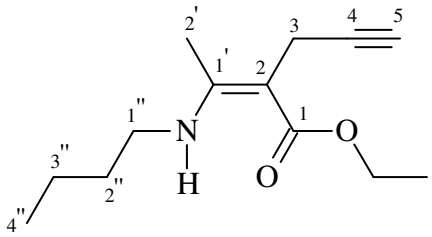

2.5 M *n*-BuLi (7.2 cm^3, 18 mmol) was added dropwise over a period of 10 minutes to a stirred solution of ethyl (*Z*)-3-(butylamino)-2-butenoate (3 g; 16 mmol) in dry THF (150 cm^3) at –77 ^oC, and stirred for 30 minutes whilst maintaining temperature at –77 ^oC. The solution was allowed to slowly warm to room temperature and stir for an additional 30 minutes whilst at room temperature. The solution was again cooled to –77 ^oC followed by the dropwise addition of propargyl bromide (2.5 cm^3, 22 mmol), and the resulting solution stirred for 30 minutes whilst maintaining temperature at –77 ^oC. The solution was allowed to slowly warm to room temperature, and stir for 14 hours. The reaction mixture was quenched with 2 M ammonium chloride (5 drops) and concentrated *in vacuo* to yield the crude ethyl 2-[(*Z*)-1-(butylamino)ethylidene]-4-pentynoate **66** (2.4 g, 78% determined by ^1H NMR spectroscopy) as a brown oil and utilized without further purification; R_f 0.73 (EtOAc/Hex 1:1); δ_H(400 MHz; $CDCl_3$) 9.37 (1 H, s, N-*H*), 4.13 (2 H, q, *J* = 7.1 Hz, 1-CO_2CH_2), 3.21 (2 H, m, 1″-*H*), 3.17 (2 H, d, *J* = 2.6 Hz, 3-*H*), 2.06 (3 H, s, 2′-*H*), 1.90 (1 H, s, 5-*H*), 1.55 (2 H, m, 2″-*H*), 1.40 (2 H, m, 3″-*H*), 1.27 (3 H, t, *J* = 7.1 Hz, 1-$CO_2CH_2CH_3$), 0.92 (3 H, t, *J* = 7.3 Hz, 4″-*H*); δ_C(100 MHz; $CDCl_3$) 169.8 (s, 1-*C*), 161.2 (s, 1′-*C*), 84.9 (s, 2-*C*), 66.4 (s, 4-*C*), 58.9 (t, 1-CO_2CH_2), 43.1 (t, 1″-*C*), 32.3 (t, 2″-*C*), 20.0 (t, 3″-*C*), 19.3 (d, 5-*C*), 16.8 (t, 3-*C*), 15.1 (q, 2′-*C*), 14.6 (q, 1-$CO_2CH_2CH_3$), 13.7 (q, 4″-*C*); *m/z* (EI) 223 (M^+, 45%), 194 (53), 150 (43), 138 (37), 120 (25),108 (52), 94 (31) and 28 (100).

Ethyl 1-butyl-2,5-dimethyl-1*H*-pyrrole-3-carboxylate [67]

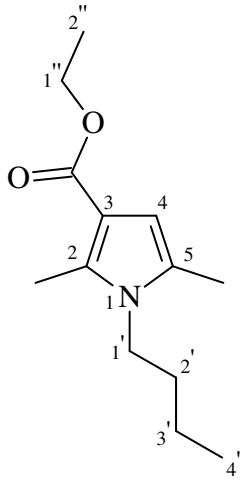

Zinc chloride (0.61 g, 4.5 mmol) was added to a solution of crude ethyl 2-[(*Z*)-1-(butylamino)ethylidene]-4-pentynoate (5 g, 22 mmol) and acetonitrile (100 cm^3) in a microwave reaction vessel fitted with a reflux condenser. The resulting mixture was subjected to 100 watts of microwave irradiation for 5 minutes whilst being stirred and force cooled. The reaction mixture was passed through a short silica plug (3 cm), after which the filtrate was concentrated *in vacuo* to yield a brown oil which was purified by radial chromatography (EtOAc:Hex = 1:4) to give ethyl 1-butyl-2,5-dimethyl-1*H*-pyrrole-3-carboxylate **67** (4.8 g, 21.5 mmol, 98%) as a yellow oil; R_f 0.77 (EtOAc/Hex 1:1); (Found: M^+, 224.1643. Calc. for $C_{13}H_{22}NO_2$, *M:* 224.1651); ν_{max}(film)/cm^{-1} 2960, 2933, 2873, 1696, 1229, 1216, 1188, 1065 and 773; δ_H(400 MHz; $CDCl_3$) 6.24 (1 H, s, 4-*H*), 4.23 (2 H, q, *J* = 7.1 Hz, 1′′-*H*), 3.74 (2 H, t, *J* = 7.7 Hz, 1′-*H*), 2.51 (3 H, s, 2-C*H*$_3$), 2.19 (3 H, s, 5- C*H*$_3$), 1.59 (2 H, m, 2′-*H*), 1.35 (2 H, m, 3′-*H*), 1.31 (3 H, t, *J* = 7.1 Hz, 2′′-*H*), 0.95 (3 H, t, *J* = 7.3 Hz, 4′-*H*); δ_C(100 MHz; $CDCl_3$) 165.7 (s, 3-C*C*O_2), 134.8 (s, 2-*C*), 127.2 (s, 5-*C*), 110.9 (s, 3-*C*), 107.7 (d, 4-*C*), 59.1 (t, 1′′-*C*), 43.8 (t, 1′-*C*), 32.9 (t, 2′-*C*), 20.2 (t, 3′-*C*), 14.8 (q, 2′′-*C*), 13.9 (q, 4′-*C*), 12.5 (q, 5-C*C*H_3), 11.4 (q, 2- C*C*H_3); *m/z* (EI) 223 (M^+, 100%), 194 (51), 152 (55), 108 (91) and 28 (89).

2-pyrrolidinethione [69]

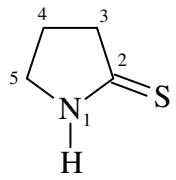

2-pyrrolidinone (10 g, 0.12 mol) was added to a stirring mixture of lawessons reagent (24 g, 0.06 mol) in dry THF (200 cm^3) and stirred for 17 hours at room temperature. The solution was concentrated *in vacuo* to yield a yellow viscous oil which was purified immediately by column chromatography on silica (100% EtOAc) followed by (EtOAc:Hex = 1:1) to give the 2-pyrrolidinethione **69** (9.5 g, 0.094 mol, 78%) as a white crystalline solid; R_f 0.22 (EtOAc/Hex 1:1); mp 109-110 ^oC (lit.,[76] 109-110 ^oC); ν_{max}(KBr)/cm^{-1} 2882, 2735, 2652, 2354, 1539, 1290, 1111, 781 and 480; δ_H(400 MHz; $CDCl_3$) 8.51 (1 H, s, 1-*H*), 3.65 (2 H, t, *J* = 7.3 Hz, 5-*H*), 2.90 (2 H, t, *J* = 8.0 Hz, 3-*H*), 2.21 (2 H, m, 4-*H*); δ_C(100 MHz; $CDCl_3$) 206.2 (s, 2-*C*), 49.9 (t, 5-*C*), 43.5 (t, 3-*C*), 23.2 (m, 4-*C*); *m/z* (EI) 101 (M^+, 100%), 100 (36), 71 (17), 45 (14) and 41 (37).

Ethyl 3-(2-thioxo-1-pyrrolidinyl)propanoate [75]

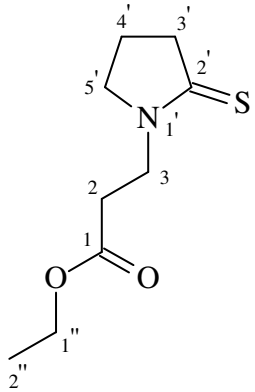

Ethyl acrylate (31 cm^3, 0.30 mol) was added to a mixture of 2-pyrrolidinethione (15 g, 0.15 mol) and NaOH (90 mg) in THF (150 cm^3) and stirred at room temperature for 5 hours. Distilled water (150 cm^3) was added and the aqueous phase was extracted with

dichloromethane (3 x 70 cm^3) after which the organic portions were combined and concentrated *in vacuo* to yield ethyl 3-(2-thioxo-1-pyrrolidinyl)propanoate **75** (30 g, 0.15 mol, 100%) as a colourless oil; R_f 0.40 (EtOAc/Hex 1:1); ν_{max}(film)/cm^{-1} 2979, 1730, 1514, 1121, 1026 and 917; δ_H(400 MHz; $CDCl_3$) 4.15 (2 H, q, *J* = 7.2 Hz, 1′′-*H*), 4.00 (2 H, t, *J* = 6.7 Hz, 3-*H*), 3.79 (2 H, t, *J* = 7.3 Hz, 5′-*H*), 3.01 (2 H, t, *J* = 7.9 Hz, 3′-*H*), 2.76 (2 H, t, *J* = 6.7 Hz, 2-*H*), 2.05 (2 H, m, 4′-*H*), 1.26 (3 H, t, *J* = 7.2 Hz, 2′′-*H*); δ_C(100 MHz; $CDCl_3$) 202.0 (s, 2′-*C*), 171.8 (s, 1-*C*), 61.1 (t, 1′′-*C*), 56.2 (t, 5′-*C*), 45.2 (t, 3′-*C*), 44.1 (t, 3-*C*), 31.4 (t, 2-*C*), 20.2 (t, 4′-*C*), 14.4 (q, 2′′-*C*); *m/z* (EI) 201 (M^+, 100%), 172 (30), 156 (18), 128 (81), 114 (15) and 85 (25).

Ethyl 3-(2-oxo-1-pyrrolidinyl)propanoate [76]

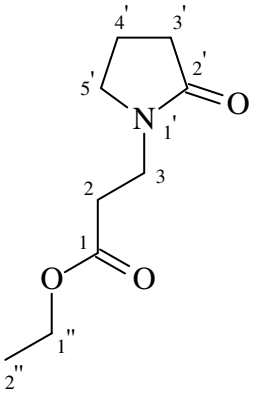

Ethyl acrylate (31 cm^3, 0.30 mol) was added to a mixture of 2-Pyrrolidinone (12.8 g, 0.15 mol) and NaOH (90 mg) in THF (150 cm^3) and stirred at room temperature for 5 hours. Distilled water (150 cm^3) was added and the aqueous phase was extracted with dichloromethane (3 x 70 cm^3) after which the organic portions were combined and concentrated *in vacuo* yielding ethyl 3-(2-oxo-1-pyrrolidinyl)propanoate **76** (27.8 g, 0.15 mol, 100%) as a colourless oil; R_f 0.39 (EtOAc/Hex 1:1); ν_{max}(film)/cm^{-1} 2982, 1731, 1677, 1290 and 1192; δ_H(400 MHz; $CDCl_3$) 4.12 (2 H, q, *J* = 7.1 Hz, 1′′-*H*), 3.55 (2 H, t, *J* = 6.9 Hz, 3-*H*), 3.40 (2 H, t, *J* = 7.1 Hz, 5′-*H*), 2.53 (2 H, t, *J* = 6.9 Hz, 2-*H*), 2.34 (2 H, t, *J* = 8.1 Hz, 3′-*H*), 1.99 (2 H, m, 4′-*H*), 1.24 (3 H, t, *J* = 7.1 Hz, 2′′-*H*); δ_C(100 MHz; $CDCl_3$) 175.0 (s, 2′-*C*), 171.6 (s, 1-*C*), 60.6 (t, 1′′-*C*), 47.6 (t, 5′-*C*), 38.5 (t, 3′-*C*), 32.6 (t,

3-*C*), 30.8 (t, 2-*C*), 18.0 (t, 4′-*C*), 14.1 (q, 2″-*C*); *m/z* (EI) 185 (M^+, 39%), 139 (36), 111 (49), 98 (100) and 70 (87).

Ethyl 3-{2-[(*E*)-2-ethoxy-2-oxoethylidene]-1-pyrrolidinyl}propanoate [77]

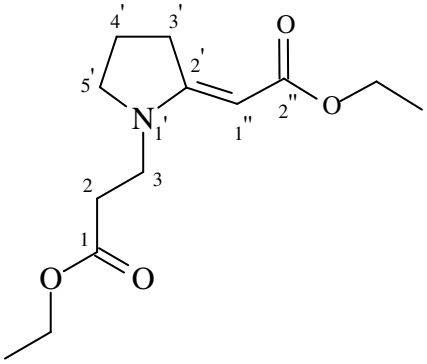

Ethylbromoacetate (4.6 cm^3, 42 mmol) was added to a solution of Ethyl 3-(2-thioxo-1-pyrrolidinyl)propanoate (7g, 35 mmol) in dry acetonitrile (200 cm^3), and allowed to stir for 12 hours at room temperature. Triethylamine (5.3 cm^3, 38 mmol) and triethylphosphite (6.6 cm^3, 38 mmol) as a solution in dry acetonotrile (40 cm^3) was then added dropwise over a period of 10 minutes, and the resulting solution stirred for 6 hours at room temperature. Distilled water (100 cm^3) was added and the aqueous layer extracted with dichloromethane (3 x 90 cm^3) after which the organic portions were combined and concentrated *in vacuo* to yield a yellow oil which was purified by radial chromatography (EtOAc:Hex = 1:4) to give ethyl 3-{2-[(*E*)-2-ethoxy-2-oxoethylidene]-1-pyrrolidinyl}propanoate **77** (6.7 g, 26 mmol, 75%) as a yellow oil; R_f 0.52 (EtOAc/Hex 1:1); ν_{max}(film)/cm^{-1} 2979, 2942, 2903, 1732, 1682, 1593, 1134, 1051 and 785; δ_H(400 MHz; $CDCl_3$) 4.52 (1 H, s, 1″-*H*), 4.14 (2 H, q, *J* = 7.1 Hz, 2″-O_2CH_2), 4.08 (2 H, q, *J* = 7.1 Hz, 1-O_2CH_2), 3.49 (2 H, t, *J* = 7.0 Hz, 3-*H*), 3.39 (2 H, t, *J* = 7.1 Hz, 5′-*H*), 3.13 (2 H, t, *J* = 7.7 Hz, 3′-*H*), 2.56 (2 H, t, *J* = 7.0 Hz, 2-*H*), 1.92 (2 H, m, 4′-*H*), 1.25 (6 H, m, 1-$O_2CH_2CH_3$, 2″-$O_2CH_2CH_3$); δ_C(100 MHz; $CDCl_3$) 171.5 (s, 1-*C*), 169.3 (s, 2″-*C*), 164.4 (s, 2′-*C*), 78.2 (d, 1″-*C*), 60.8 (t, 1-O_2CH_2), 58.3 (t, 2″- O_2CH_2), 52.8 (t, 5′-*C*), 41.9 (t, 3-*C*), 32.5 (t, 2-*C*), 31.0 (t, 3′-*C*), 21.2 (t, 4′-*C*), 14.7 (q, 1-$O_2CH_2CH_3$), 14.1 (q, 2″-

$O_2CH_2CH_3$); *m/z* (EI) 255 (M^+, 56%), 210 (77), 183 (67), 182 (100), 154 (39), 136 (53), 111 (82) and 110 (74).

Ethyl 2-(2-pyrrolidinylidene)acetate [58]

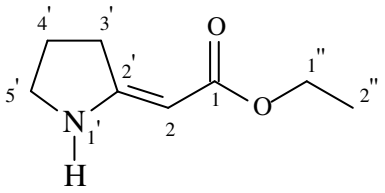

Potassium hexamethyldisilazane (2.5 g, 12.7 mmol) as a solution in dry THF (20 cm^3), was added rapidly to a stirring solution of ethyl 3-{2-[(*E*)-2-ethoxy-2-oxoethylidene]-1-pyrrolidinyl}propanoate (1.6 g, 6.3 mmol) in dry THF (150 cm^3), and stirred for 5 minutes at room temperature. The reaction mixture was quenched by the dropwise addition of methanol (1 cm^3) followed by concentration *in vacuo* to yield a yellow oil which was purified by radial chromatography (EtOAc:Hex = 1:4) to give ethyl 2-(2-pyrrolidinylidene)acetate **58** (0.7 g, 4.5 mmol, 72%) as a white crystalline solid; R_f 0.58 (EtOAc/Hex 1:1); mp 59-61 °C (lit.,[84] 61-62 °C); ν_{max}(KBr)/cm^{-1} 3347, 2978, 2872, 1736, 1661, 1603, 1238, 1056, and 780; δ_H(400 MHz; $CDCl_3$) 7.89 (1 H, s, 1′-*H*), 4.53 (1 H, s, 2-*H*), 4.10 (2 H, q, *J* = 7.1 Hz, 1″-*H*), 3.51 (2 H, t, *J* = 6.9 Hz, 5′-*H*), 2.58 (2 H, t, *J* = 7.8 Hz, 3′-*H*), 1.97 (2 H, m, 4′-*H*), 1.25 (3 H, t, *J* = 7.1 Hz, 2″-*H*); δ_C(100 MHz; $CDCl_3$) 170.8 (s, 1-*C*), 166.3 (s, 2′-*C*), 76.5 (d, 2-*C*), 58.4 (t, 1″-*C*), 47.0 (t, 5′-*C*), 32.2 (t, 3′-*C*), 22.0 (t, 4′-*C*), 14.7 (q, 2″-*C*); *m/z* (EI) 155 (M^+, 46%), 110 (80), 83 (100), 82 (55), 80 (31), 54 (22), 39 (29), and 28 (44).

1-(2-pyrrolidinylidene)-2-hexanone [85]

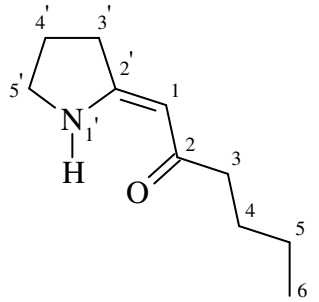

2.0 M *n*-BuLi (4.1 cm^3, 8 mmol) was added dropwise over a period of 10 minutes to a stirred solution of ethyl 2-(2-pyrrolidinylidene)acetate (1.00 g; 6.5 mmol) in dry toluene (150 cm^3) at 0 ^oC, and stirred for 30 minutes whilst maintaining temperature at 0 ^oC. The solution was allowed to slowly warm to room temperature and stir for an additional 30 minutes whilst at room temperature. The solution was again cooled to 0 ^oC followed by the dropwise addition of propargyl bromide (0.64 cm^3, 7.2 mmol), and the resulting solution stirred for 30 minutes whilst maintaining temperature of 0 ^oC. The solution was allowed to slowly warm to room temperature, and stir for 14 hours. The reaction mixture was quenched with 2 M ammonium chloride (5 drops) and concentrated *in vacuo* to yield a brown oil. *m/z* (EI) 167 (M^+, 10%), 125 (43), 110 (100) and 83 (19).

Ethyl 2-(2-pyrrolidinylidene)-4-pentynoate [59]

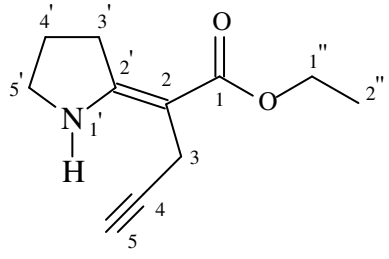

2.0 M *n*-BuLi (6.6 cm^3, 13 mmol) was added dropwise over a period of 10 minutes to a stirred solution of ethyl 2-(2-pyrrolidinylidene)acetate (1.00 g; 6.5 mmol) in dry THF (150 cm^3) at –77 ^oC, and stirred for 30 minutes whilst maintaining temperature at –77 ^oC.

The solution was allowed to slowly warm to room temperature and stir for an additional 30 minutes whilst at room temperature. The solution was again cooled to –77 ^{o}C followed by the dropwise addition of propargyl bromide (0.64 cm^3, 7.2 mmol), and the resulting solution stirred for 30 minutes whilst maintaining temperature of –77 ^{o}C. The solution was allowed to slowly warm to room temperature, and stir for 14 hours. The reaction mixture was quenched with 2 M ammonium chloride (5 drops) and concentrated *in vacuo* to yield a crude mixture of ethyl 2-(2-pyrrolidinylidene)acetate, ethyl 2-(2-pyrrolidinylidene)-4-pentynoate and ethyl 2-(3,4-dihydro-2*H*-pyrrol-5-yl)-2-(2-propynyl)-4-pentynoate (1.2 g) as a brown oil and utilized without further purification as decomposition of **59** in a silica column was evident. Ethyl 2-(2-pyrrolidinylidene)-4-pentynoate **59** (40% determined by ^{1}H NMR spectroscopy); R_f 0.60 (EtOAc/Hex 1:1); δ_H(400 MHz; $CDCl_3$) 8.15 (1 H, s, 1′-*H*), 4.15 (2 H, q, *J* = 7.2 Hz, 1″-*H*), 3.52 (2 H, t, *J* = 7.0 Hz, 5′-*H*), 3.09 (2 H, d, *J* = 2.6 Hz, 3-*H*), 2.73 (2 H, t, *J* = 7.8 Hz, 3′-*H*), 2.01 (2 H, m, 4′-*H*), 1.91 (1 H, t, *J* = 2.6 Hz, 5-*H*), 1.27 (3 H, t, *J* = 7.2 Hz, 2″-*H*); *m/z* (EI) 193 (M^+, 39%), 164 (100), 120 (56), 118 (34) and 91 (21).

Ethyl 2-(3,4-dihydro-2*H*-pyrrol-5-yl)-2-(2-propynyl)-4-pentynoate [84]

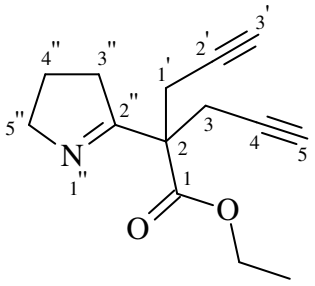

2.0 M *n*-BuLi (6.6 cm^3, 13 mmol) was added dropwise over a period of 10 minutes to a stirred solution of ethyl 2-(2-pyrrolidinylidene)acetate (1.00 g; 6.5 mmol) in dry THF (150 cm^3) at 0 ^{o}C, and stirred for 30 minutes whilst maintaining temperature at 0 ^{o}C. The solution was allowed to slowly warm to room temperature and stir for an additional 30 minutes whilst at room temperature. The solution was again cooled to 0 ^{o}C followed by the dropwise addition of propargyl bromide (1.2 cm^3, 13 mmol), and the resulting solution stirred for 30 minutes whilst maintaining temperature at 0 ^{o}C. The solution was

allowed to slowly warm to room temperature, and stir for 14 hours. The reaction mixture was quenched with 2 M ammonium chloride (5 drops) and concentrated *in vacuo* to yield a brown oil that was purified by radial chromatography (EtOAc:Hex = 1:4) to give the ethyl 2-(3,4-dihydro-2*H*-pyrrol-5-yl)-2-(2-propynyl)-4-pentynoate **84** (1.36 g, 5.9 mmol, 91%) as a dark yellow oil; R_f 0.58 (EtOAc/Hex 1:1); ν_{max}(film)/cm^{-1} 3292, 2961, 2932, 2869, 1732, 1637, 1200 and 644; δ_H(400 MHz; $CDCl_3$) 4.21 (2 H, q, *J* = 7.1 Hz, 1-$O_2CH_2CH_3$), 3.88 (2 H, tt, *J* = 1.9 Hz, *J* = 7.7 Hz, 3″-*H*), 3.02 (4 H, ddd, *J* = 2.6 Hz, *J* = 17.1 Hz, *J* = 53.7 Hz, 1′-*H*, 3-*H*), 2.50 (2 H, tt, *J* = 1.9 Hz, *J* = 9.2 Hz, 5″-*H*), 1.99 (2 H, t, *J* = 2.6 Hz, 3′-*H*, 5-*H*), 1.90 (2 H, m, 4″-*H*), 1.26 (3 H, t, *J* = 7.1 Hz, 1-$O_2CH_2CH_3$); δ_C(100 MHz; $CDCl_3$) 174.2 (s, 2″-*C*), 170.8 (s, 1-*C*), 79.5 (s, 2′-*C*, 4-*C*), 71.1 (d, 3′-*C*, 5-*C*), 61.8 (t, 1-$O_2CH_2CH_3$), 60.8 (t, 3″-*C*), 53.8 (s, 2-*C*), 34.8 (t, 5″-*C*), 23.2 (t, 1′-*C*, 3-*C*), 22.0 (t, 4″-*C*), 14.1 (q, 1-$O_2CH_2CH_3$); *m/z* (EI) 231 (M^+, 5%), 202 (29), 192 (100), 164 (51), 158 (74), 148 (92), 130 (35) and 118 (46).

Ethyl 5-methyl-2,3-dihydro-1*H*-pyrrolizine-7-carboxylate [61]

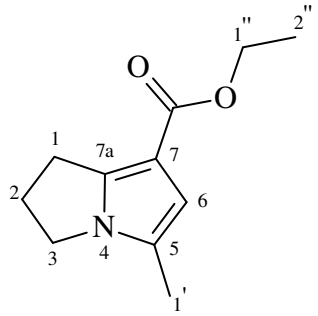

Zinc chloride (0.14 g, 1 mmol) was added to a solution of crude ethyl 2-(2-pyrrolidinylidene)-4-pentynoate (*ca*. 1.5 g,) and acetonitrile (20 cm^3) in a microwave reaction vessel. The resulting mixture was subjected to 100 watts of microwave irradiation for 1 minute whilst being stirred and force cooled. The reaction mixture was passed through a short silica plug (1 cm), after which the filtrate was concentrated *in vacuo* to yield a yellow oil which was purified by radial chromatography (EtOAc:Hex = 1:4) to give ethyl 5-methyl-2,3-dihydro-1*H*-pyrrolizine-7-carboxylate **61** (0.85 g, 4.4 mmol, 68% over two steps from **58**) as colourless crystalline solid; R_f 0.65 (EtOAc/Hex

1:1); mp 57 °C (lit.,[100] 58 °C); δ_H(400 MHz; $CDCl_3$) 6.26 (1 H, s, 6-*H*), 4.22 (2 H, q, *J* = 7.1 Hz, 1″-*H*), 3.83 (2 H, t, *J* = 7.2 Hz, 3-*H*), 3.06 (2 H, t, *J* = 7.5 Hz, 1-*H*), 2.51 (2 H, m, 2-*H*), 2.17 (3 H, s, 1′-*H*), 1.30 (3 H, t, *J* = 7.1 Hz, 2″-*H*); δ_C(100 MHz; $CDCl_3$) 165.4 (s, 7-C*C*O_2), 142.5 (s, 7a-*C*), 124.0 (s, 5-*C*), 110.1 (d, 6-*C*), 106.5 (s, 7-*C*), 59.1 (t, 1″-*C*), 44.9 (t, 3-*C*), 27.0 (t, 2-*C*), 26.0 (t, 1-*C*), 14.6 (q, 2″-*C*), 11.7 (q, 1′-*C*); *m/z* (EI) 193 (M^+, 55%), 164 (100), 148 (48) and 120 (37).

2-propynyl tetrahydro-2*H*-pyran-2-yl ether [101]

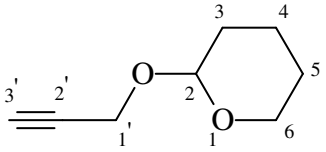

p-Toluenesulfonic acid (70 mg) was added to a stirring solution of 3,4-dihydro-2*H*-pyran (3.7 cm^3, 41 mmol), propargyl alcohol (2.0 cm^3, 34 mmol) and dichloromethane (100 cm^3), and stirred for 6 hours. Distilled water (150 cm^3) was added and the aqueous phase extracted with dichloromethane (3 x 80 cm^3). The organic portions were combined and concentrated *in vacuo* to give 2-propynyl tetrahydro-2*H*-pyran-2-yl ether **101** (4.2 g, 33 mmol, 98%) as a yellow oil; R_f 0.69 (EtOAc/Hex 1:1); ν_{max}(film)/cm^{-1} 2947, 2867, 1687, 1121, 1077, 1031 and 463; δ_H(400 MHz; $CDCl_3$) 4.76 (1 H, t, 2-*H*), 4.20 (2 H, m, 1′-*H*), 3.78 (1 H, m, 3-*H*), 3.49 (1 H, m, 3-*H*), 2.37 (1 H, t, *J* = 2.4 Hz, 3′-*H*), 1.76 (2 H, m, 5-*H*), 1.58 (2 H, m, 4-*H*), 1.49 (2 H, m, 6-*H*); δ_C(100 MHz; $CDCl_3$) 96.8 (d, 2-*C*), 79.7 (s, 2′-*C*), 73.9 (d, 3′-*C*), 61.9 (t, 3-*C*), 53.9 (t, 1′-*C*), 29.8 (t, 4-*C*), 25.3 (t, 6-*C*), 18.9 (t, 5-*C*); *m/z* (EI) 140 (M^+, 2%), 139 (19), 85 (100), 67 (52), 55 (40), 41 (66) and 39 (96).

2-nonynyl tetrahydro-2*H*-pyran-2-yl ether [102]

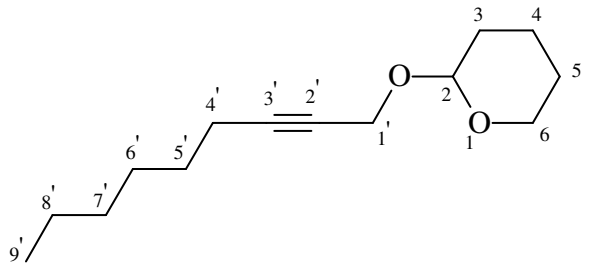

2.5 M *n*-BuLi (30 cm^3, 75.1 mmol) was added dropwise over a period of 10 minutes to a stirring solution of 2-propynyl tetrahydro-2*H*-pyran-2-yl ether (10.5 g, 75.1 mmol) and dry THF (150 cm^3) at 0 ^oC, and stirred for 5 minutes. The solution was allowed to slowly warm to room temperature followed by an additional 1 hour of stirring. The stirring solution was cooled to 0 ^oC followed by the dropwise addition of 1-bromohexane (11.5 cm3, 82 mmol) over a period of 10 minutes after which the solution was refluxed for 12 hours. The reaction mixture was quenched with methanol (1 cm^3) followed by the addition of distilled water (100 cm^3). The aqueous layer was extracted with dichloromethane (3 x 80 cm^3) and the organic portions combined and concentrated *in vacuo* to yield a brown oil. The oil was purified by column chromatography (EtOAc:Hex = 1:1) to give 2-nonynyl tetrahydro-2*H*-pyran-2-yl ether **102** (13.8 g, 66 mmol, 88%) as a yellow oil; R_f 0.80 (EtOAc/Hex 1:1); (Found: M^+, 247.1662. Calc. for $C_{14}H_{24}O_2Na$, *M:* 247.1674); ν_{max}(film)/cm^{-1} 2933, 2858, 2223, 1455, 1345, 1264, 1201, 1118, and 1023; δ_H(400 MHz; $CDCl_3$) 4.81 (1 H, t, *J* = 3.4 Hz, 2-*H*), 4.24 (2 H, m, 1′-*H*), 3.84 (1 H, m, 3-*H*), 3.51 (1 H, m, 3-*H*), 2.20 (2 H, m, 4′-*H*), 1.84 (2 H, m, 5-*H*), 1.72 (2 H, m, 4-*H*), 1.52 (4 H, m, 6-*H*, 5′-*H*), 1.37 (2 H, m, 6′-*H*), 1.28 (2 H, m, 8′-*H*), 1.25 (2 H, m, 7′-*H*), 0.88 (3 H, t, *J* = 6.9 Hz, 9′-*H*); δ_C(100 MHz; $CDCl_3$) 96.6 (d, 2-*C*), 86.7 (s, 3′-*C*), 75.7 (s, 2′-*C*), 61.9 (t, 3-*C*), 54.6 (t, 1′-*C*), 31.3 (t, 7′-*C*), 30.3 (t, 4-*C*), 28.6 (t, 5′-*C*), 28.5 (t, 6′-*C*), 25.4 (t, 6-*C*), 22.5 (t, 8′-*C*), 19.1 (t, 5-*C*), 18.8 (t, 4′-*C*), 14.0 (q, 9′-*C*); *m/z* (EI) 224 (M^+, 0.3%), 153 (8), 101 (27), 93 (28), 85 (55), 81 (70), 79 (100), 67 (82), 55 (39) and 41 (50).

2-nonyn-1-ol [103]

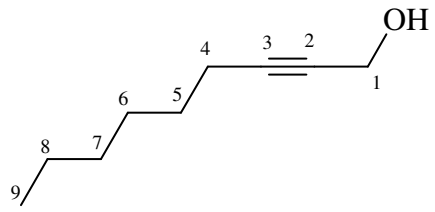

4 M HCl (5 cm^3) was added to a stirring solution of 2-nonynyl tetrahydro-2*H*-pyran-2-yl ether (13.8 g, 66 mmol) and methanol (100 cm^3), and stirred for 1 hour. The reaction solution was neutralized with potassium carbonate and concentrated *in vacuo* to yield a yellow oil which was purified by column chromatography (EtOAc:Hex = 1:1) to give 2-nonyn-1-ol **103** (9.1 g, 65 mmol, 98%) as a yellow oil; R_f 0.60 (EtOAc/Hex 1:1); (Found: M^+, 139.1128. Calc. for $C_9H_{15}O$, *M:* 139.1123); ν_{max}(film)/cm^{-1} 3362, 2932, 2859, 2288, 2225, 1458, 1137, and 1015; δ_H(400 MHz; $CDCl_3$) 4.24 (2 H, s, 1-*H*), 2.20 (2 H, m, 4-*H*), 1.73 (1 H, s, 1-O*H*), 1.49 (2 H, m, 5-*H*), 1.37 (2 H, m, 6-*H*), 1.28 (4 H, m, 7-*H*, 8-*H*), 0.88 (3 H, t, *J* = 6.8 Hz, 9-*H*); δ_C(100 MHz; $CDCl_3$) 86.6 (s, 3-*C*), 78.2 (s, 2-*C*), 51.4 (t, 1-*C*), 31.3 (t, 7-*C*), 28.59 (t, 5-*C*), 28.57 (t, 6-*C*), 22.5 (t, 8-*C*), 18.7 (t, 4-*C*), 14.1 (q, 9-*C*); *m/z* (EI) 139 (0.09), 109 (19), 107 (17), 93 (50), 79 (63), 77 (30), 67 (100), 55 (46), 41 (71) and 39 (66).

1-bromo-2-nonyne [99]

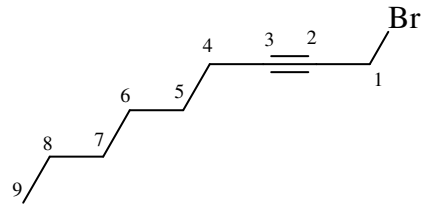

2-nonyn-1-ol (5 g, 36 mmol) was added to a stirring solution of carbon tetrabromide (11.9 g, 36 mmol) and triphenylphosphine (9.4 g, 36 mmol) in dry toluene (150 cm^3), and stirred for 4 hours. Distilled water (100 cm^3) was added and the aqueous layer was extracted with hexane (3 x 60 cm^3). The organic portions were combined and

concentrated *in vacuo* to yield a brown oil which was purified by column chromatography (EtOAc:Hex = 1:1) to give 1-bromo-2-nonyne **99** (5.9 g, 29 mmol, 81%) as a yellow oil; R_f 0.67 (EtOAc/Hex 1:1); (Found: M^+, 203.0443. Calc. for $C_9H_{16}Br$, *M:* 203.0435); ν_{max}(film)/cm^{-1} 2955, 2930, 2857, 2233, 1465, 1208, 670 and 609; δ_H(400 MHz; $CDCl_3$) 3.92 (2 H, t, *J* = 2.3 Hz, 1-*H*), 2.23 (2 H, m, 4-*H*), 1.50 (2 H, m, 5-*H*), 1.37 (2 H, m, 6-*H*), 1.28 (4 H, m, 7-*H*, 8-*H*), 0.89 (3 H, t, *J* = 6.9 Hz, 9-*H*); δ_C(100 MHz; $CDCl_3$) 88.3 (s, 3-*C*), 75.3 (s, 2-*C*), 31.3 (t, 7-*C*), 28.5 (t, 6-*C*), 28.3 (t, 5-*C*), 22.5 (t, 8-*C*), 19.0 (t, 4-*C*), 15.7 (t, 1-*C*), 14.0 (q, 9-*C*); *m/z* (EI) 203 (M^+, 0.001%), 93 (30), 81 (100), 79 (60), 77 (17), 67 (44), 53 (14), 41 (20) and 39 (24).

Ethyl (2*S*)-5-oxotetrahydro-1*H*-pyrrole-2-carboxylate [90]

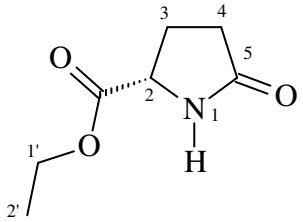

(2*S*)-5-oxotetrahydro-1*H*-pyrrole-2-carboxylic acid (40 g, 0.31 mol) was added to a stirred solution of absolute ethanol (300 cm^3), benzene (100 cm^3) and conc. sulfuric acid (5 cm^3) at 25 ^{o}C. The mixture was heated under reflux using a Dean and Stark apparatus for 12 hours, after which it was cooled, concentrated *in vacuo*, and dissolved up the chloroform (200 cm^3). Potassium carbonate (7 g) was added to the solution, and the resulting mixture was stirred for 30 minutes. The mixture was filtered under gravity to remove the potassium carbonate after which the filtrate was concentrated *in vacuo* to yield a colourless oil which was purified by distillation under reduced pressure to yield the pyrrole-2-carboxylate **90** (41 g, 0.26 mol, 84%) as a colourless oil that solidified upon standing; R_f 0.65 (100% ethanol); bp 168-170 ^{o}C (6 mmHg) [lit.,[101] bp 152-153 ^{o}C (3 mmHg)]; mp 49-51 ^{o}C (lit.,[102] 50-51 ^{o}C); $[\alpha]_D^{20}$ +3.4^o (*c* 4.6, H_2O) [lit.,[85] $[\alpha]_D$ +3.5^o ± 0.5^o (*c* 10, EtOH)]; (Found: M^+, 158.0820. $C_7H_{12}NO_3$ requires *M,* 158.0817); ν_{max}(film)/cm^{-1} 2984, 1737, 1697 and 1205; δ_H(400 MHz; $CDCl_3$) 6.61 (1 H, s, 1-*H*), 4.19 (1 H, dd, *J* = 6.1 Hz, *J* = 9.1 Hz, 2-*H*), 4.16 (2 H, q, *J* = 7.1 Hz, 1′-*H*), 2.40 (1 H, m,

3-*H*), 2.33 (2 H, m, 4-*H*), 2.16 (1 H, m, 3-*H*), 1.23 (3 H, t, *J* = 7.1 Hz, 2′-*H*); δ_C(100 MHz; $CDCl_3$) 178.1 (s, 5-*C*), 172.0 (s, 2-C*C*O_2), 61.7 (t, 1′-*C*), 55.6 (d, 2-*C*), 29.3 (t, 4-*C*), 24.8 (t, 3-*C*), 14.2 (q, 2′-*C*); *m/z* (EI) 84 (100%), 56 (7) and 41 (25).

Diethyl (2*S*)-2-aminopentanedioate [93]

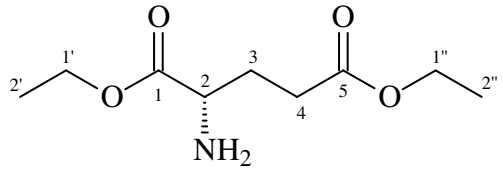

(2*S*)-5-oxotetrahydro-1*H*-pyrrole-2-carboxylic acid (40 g, 0.31 mol) was added to a stirred solution of absolute ethanol (300 cm^3), toluene (100 cm^3) and conc. sulfuric acid (5 cm^3) at 25 ^oC. The mixture was heated under reflux using a Dean and Stark apparatus for 24 hours, after which it was cooled, concentrated *in vacuo*, and dissolved up in chloroform (200 cm^3). Potassium carbonate (7 g) was added to the solution, and the resulting mixture was stirred for 30 minutes. The mixture was filtered under gravity to remove the potassium carbonate after which the filtrate was concentrated *in vacuo* to yield a colourless oil which was purified by distillation under reduced pressure to yield diethyl (2*S*)-2-aminopentanedioate **93** (38 g, 0.19 mol, 61%) as a colourless oil; R_f 0.53 (100% ethanol); bp 125-135^oC (6 mmHg); $[\alpha]_D^{29}$ +0.83^o (*c* 4.8, EtOH); (Found: M^+, 204.1245. Calc. for $C_9H_{18}NO_4$, *M:* 204.1236); ν_{max}(film)/cm^{-1} 2982, 1732, 1692, 1200 and 1027; δ_H(400 MHz; $CDCl_3$) 4.20 (5 H, m, 2-*H*, 1′-*H*, 1″-*H*), 2.73 (2 H, s, 2-NH_2), 2.48 (1 H, m, 3-*H*), 2.37 (2 H, m, 4-*H*), 2.23 (1 H, m, 3-*H*), 1.27 (6 H, m, 2′-*H*, 2″-*H*); δ_C(100 MHz; $CDCl_3$) 177.8 (s, 5-*C*), 172.0 (s, 1-*C*), 61.7 (t, 1′-*C*, 1″-*C*), 55.4 (d, 2-*C*), 29.2 (t, 4-*C*), 24.8 (t, 3-*C*), 14.2 (q, 2′-*C*, 2″-*C*); *m/z* (EI) 158 (7%), 130 (54), 100 (8), 84 (100), 56 (23) and 41 (10).

(5*S*)-5-(hydroxymethyl)tetrahydro-2*H*-pyrrol-2-one [89]

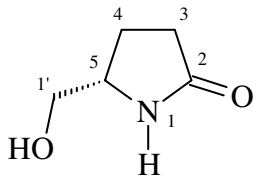

A solution of sodiumborohydride (15 g, 0.39 mol) in distilled water (80 cm^3) was added cautiously to a stirred solution of ethyl (2*S*)-5-oxotetrahydro-1*H*-pyrrole-2-carboxylate (62 g, 0.39 mol) in distilled water (200 cm^3) at 0 ^oC. The solution was stirred for 10 minutes at 0 ^oC after which it was allowed to warm to room temperature, and stir for 3 hours. The solution was cooled to 0 ^oC followed by the dropwise addition of acetone (40 cm^3) over a period of 15 minutes. The solution was stirred for 30 minutes at 0 ^oC after which being allowed to warm to room temperature, and stir for 2 hours. The reaction mixture was concentrated *in vacuo* yielding a milky white oil which was purified by column chromatography on silica (EtOAc:MeOH = 2:1) to furnish hydroxymethyl)tetrahydro-2*H*-pyrrol-2-one **89** (36 g, 0.31 mol, 80%) as a colourless oil that solidified upon standing; R_f 0.33 (EtOAc/MeOH 2:1); mp 85-86 ^oC (lit.,[85] 84-86 ^oC); $[\alpha]_D^{28}$ +27.7^o (*c* 0.97, H_2O) [lit.,[85] $[\alpha]_D$ +31.7^o (*c* 5, EtOH)]; (Found: M^+, 116.0711. Calc. for $C_5H_{10}NO_2$, *M:* 116.0712); ν_{max}(film)/cm^{-1} 3279, 2936, 1676, 1422, 1283, 1098 and 1056; δ_H(400 MHz; $CDCl_3$) 7.44 (1 H, s, 1-*H*), 4.70 (1 H, s, 1′-O*H*), 3.76 (1 H, m, 5-*H*), 3.62 (1 H, m, 1′-*H*), 3.40 (1 H, m, 1′-*H*), 2.30 (2 H, m, 3-*H*), 2.12 (1 H, m, 4-*H*), 1.76 (1 H, m, 4-*H*); δ_C(100 MHz; $CDCl_3$) 179.3 (s, 2-*C)*, 65.8 (t, 1′-*C*), 56.4 (d, 5-*C*), 30.2 (t, 3-*C*), 22.6 (t, 4-*C*).

[(2*S*)-5-oxotetrahydro-1*H*-pyrrol-2-yl]methyl 4-methylbenzenesulfonate [88]

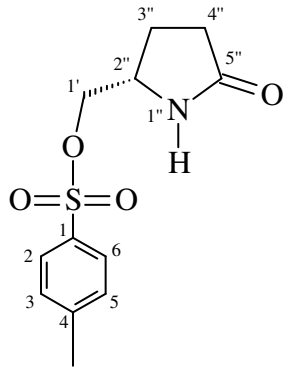

4-methylbenzenesulfonyl chloride (40 g, 0.21 mol) was added to a solution of (5*S*)-5-(Hydroxymethyl) tetrahydro-2*H*-pyrrol-2-one (20 g, 0.17 mol), potassium hydroxide (19 g, 0.34 mol), tetrabutylamonium hydrogen sulfate (1.7 g, 5.1 mmol) and distilled water (100 cm^3) in chloroform (350 cm^3), and stirred vigorously whist submerged in an ultrasonic bath for 48 hours. The resulting solution was concentrated in vacuo to yield a white solid which was recrystallized twice from toluene to give the 5-oxotetrahydro-1*H*-pyrrol-2-yl]methyl 4-methylbenzenesulfonate **88** (35 g, 0.13 mol, 76%) as a white crystalline solid; R_f 0.63 (EtOH/Ether 1:1); mp 110-113 ^oC; $[\alpha]_D^{30}$ +12.1^o (*c* 1.65, EtOH); (Found: M^+, 270.0802. Calc. for $C_{12}H_{16}NO_4S$, *M:* 270.0800); ν_{max}(KBr)/cm^{-1} 3033, 2970, 2928, 1927, 1702, 1657, 1355, 1167, 946, 880, 818, 669 and 554; δ_H(400 MHz; $CDCl_3$) 7.80 (2 H, d, *J* = 8.1 Hz, 2-*H,* 6-*H*), 7.39 (2 H, d, *J* = 8.1 Hz, 3-*H,* 5-*H*), 6.08 (1 H, s, 1″-*H*), 4.08 (1 H, dd, *J* = 3.4 Hz, *J* = 9.6 Hz, 1′-*H*), 3.95 (1 H, m, 2″-*H*), 3.89 (1 H, dd, *J* = 7.3 Hz, *J* = 9.6 Hz,1′-*H*), 2.48 (3 H, s, 4-*CH₃*), 2.35 (2 H, m, 4″-*H*), 2.27 (1 H, m, 3″-*H*), 1.80 (1 H, m, 3″-*H*); δ_C(100 MHz; $CDCl_3$) 177.7 (s, 5″-*C*), 145.4 (s, 1-*C*), 132.5 (s, 4-C*CH₃*), 130.2 (d, 3-*C,* 5-*C*), 127.9 (d, 2-*C,* 6-*C*), 72.0 (t, 1′-*C*), 52.7 (d, 2″-*C*), 29.0 (t, 4″-*C*), 22.8 (t, 3″-*C*), 21.6 (q, 4-C*C*H_3).

(5*R*)-5-methyltetrahydro-2*H*-pyrrol-2-one [70]

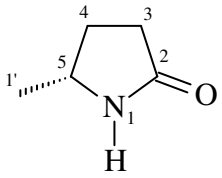

Tributyltin hydride (10.8 cm^3, 41 mmol) was slowly added to a stirring solution of (2*S*)-5-Oxotetrahydro-1*H*-pyrrol-2-yl]methyl 4-methylbenzenesulfonate (10 g, 37 mmol), sodium iodide (11 g, 74 mmol) and 2, 2′-azobisisobutyronitrile (0.24 g, 1.5 mmol) in 1,2 dimethoxyethane (200 cm^3) and refluxed for 14 hours. The precipitate was removed *via* filtration after which the filtrate was concentrated *in vacuo* to yield a colourless oil. The oil was purified by radial chromatography (diethyl ether) to remove the tributyl tin iodide, followed by (diethyl ether:2-propanol = 8:1) to give 5-methyltetrahydro-2*H*-pyrrol-2-one **70** (2.2 g, 23 mmol, 61%) as a colourless oil; R_f 0.17 (diethyl ether); $[\alpha]_D^{30}$ +7.3° (*c* 5.6, EtOH); (Found: M^+, 100.0757. Calc. for $C_5H_{10}NO$, *M:* 100.0762); ν_{max}(film)/cm^{-1} 3265, 2964, 2927, 2871 and 1673; δ_H(400 MHz; $CDCl_3$) 6.11 (1 H, s, 1-*H*), 3.74 (1 H, dd, *J* = 6.4 Hz, *J* = 12.9 Hz, 5-*H*), 2.30 (2 H, m, 3-*H*), 2.23 (1 H, m, 4-*H*), 1.61 (1 H, m, 4-*H*), 1.18 (3 H, t, 1′-*H*); δ_C(100 MHz; $CDCl_3$) 178.3 (s, 2-*C*), 50.1 (d, 5-*C*), 30.6 (t, 3-*C*), 29.2 (t, 4-*C*), 22.2 (q, 1′-*C*); *m/z* (EI) 99 (M^+, 13%), 84 (100), 56 (9), 44 (14), 41 (36), 39 (20) and 28 (23).

(5*R*)-5-methyltetrahydro-2*H*-pyrrole-2-thione [71]

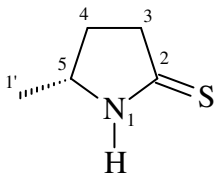

(5*R*)-5-methyltetrahydro-2*H*-pyrrol-2-one (2.0 g, 20.2 mmol) was added to a stirring mixture of Lawesson's reagent (4.1 g, 10.1 mmol) in dry THF (100 cm^3) and stirred for 17 hours at room temperature. The solution was concentrated *in vacuo* to yield a yellow

viscous oil which was purified immediately by column chromatography on silica (EtOAc:Hex = 1:1) to give (5*R*)-5-Methyltetrahydro-2*H*-pyrrole-2-thione **71** (1.86 g, 16.2 mmol, 80%) as a white crystalline solid; R_f 0.40 (EtOAc/Hex 1:1); $[\alpha]_D^{30}$ +13.8° (*c* 4.8, EtOH); (Found: M^+, 116.0529. Calc. for $C_5H_{10}NS$, *M:* 116.0534); ν_{max}(KBr)/cm^{-1} 3164, 2965, 1505, 1377, 1279, 1146, 1086, 1045 and 772; δ_H(400 MHz; $CDCl_3$) 8.05 (1 H, s, 1-*H*), 4.05 (1 H, m, 5-*H*), 2.95 (1 H, m, 3-*H*), 2.90 (1 H, m, 3-*H*), 2.37 (1 H, m, 4-*H*), 1.76 (1 H, m, 4-*H*), 1.30 (3 H, d, *J* = 6.4 Hz, 1′-*H*); δ_C(100 MHz; $CDCl_3$) 205.5 (s, 2-*C*), 58.0 (d, 5-*C*), 43.2 (t, 3-*C*), 31.3 (t, 4-*C*), 20.9 (q, 1′-*C*); *m/z* (EI) 115 (M^+, 100%), 100 (48), 71 (9), 67 (21) and 41 (13).

Ethyl 3-[(2*R*)-2-methyl-5-thioxotetrahydro-1*H*-pyrrol-1-yl]propanoate [86]

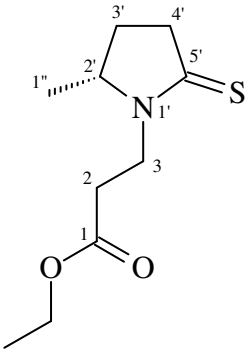

Ethyl acrylate (5.7 cm^3, 52 mmol) was added to a mixture of (5*R*)-5-methyltetrahydro-2*H*-pyrrole-2-thione(3 g, 26 mmol) and NaOH (50 mg) in THF (100 cm^3) and stirred at room temperature for 5 hours. Distilled water (100 cm^3) was added and the aqueous phase was extracted with dichloromethane (3 x 50 cm^3) after which the organic portions were combined and concentrated *in vacuo* to yield ethyl 3-[(2*R*)-2-methyl-5-thioxotetrahydro-1*H*-pyrrol-1-yl]propanoate **86** (5.59 g, 26 mmol, 100%) as a colourless oil; R_f 0.45 (EtOAc/Hex 1:1); $[\alpha]_D^{30}$ +64.9° (*c* 6.2, EtOH); (Found: M^+, 216.1067. Calc. for $C_{10}H_{18}NO_2S$, *M:* 116.1058); ν_{max}(film)/cm^{-1} 2976, 2934, 1732, 1492, 1419, 1379, 1314, 1278, and 1187; δ_H(400 MHz; $CDCl_3$) 4.27 (1 H, m, 3-*H*), 4.12 (2 H, q, *J* = 7.2 Hz, 1-$O_2CH_2CH_3$), 4.06 (1 H, m, 2′-*H*), 3.67 (1 H, m, 3-*H*), 3.00 (2 H, m, 4′-*H*), 2.91 (1 H, m, 2-*H*), 2.60 (1 H, m, 2-*H*), 2.21 (1 H, m, 3′-*H*), 1.67 (1 H, m, 3′-*H*) 1.30 (3 H, d, *J* = 6.4

Hz, 1″-*H*), 1.25 (3 H, t, *J* = 7.1 Hz, 1-$O_2CH_2CH_3$); δ_C(100 MHz; $CDCl_3$) 201.4 (s, 5′-*C*), 171.6 (s, 1-*C*), 62.4 (d, 2′-*C*), 60.8 (t, 1-$O_2CH_2CH_3$), 43.3 (t, 4′-*C*), 41.0 (t, 3-*C*), 31.1 (t, 2-*C*), 28.4 (t, 3′-*C*), 19.2 (q, 1″-*C*), 14.1 (q, 1-$O_2CH_2CH_3$); *m/z* (EI) 215 (M^+, 100%), 186 (32), 182 (25), 170 (17), 142 (44), 116 (11) and 99 (16).

Ethyl 3-{(5*R*)-2-[(*E*)-2-ethoxy-2-oxoethylidene]-5-methyltetrahydro-1*H*-pyrrol-1-yl}propanoate [87]

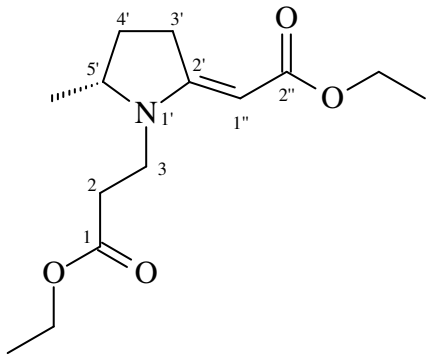

Ethylbromoacetate (1.55 cm^3, 13.9 mmol) was added to a solution of ethyl 3-[(2*R*)-2-methyl-5-thioxotetrahydro-1*H*-pyrrol-1-yl]propanoate (2.0g, 9.29 mmol) in dry acetonitrile (150 cm^3), and allowed to stir for 12 hours at room temperature. Triethylamine (1.42 cm^3, 10.2 mmol) and triethylphosphite (1.75 cm^3, 10.2 mmol) as a solution in dry acetonotrile (20 cm^3) was then added dropwise over a period of 10 minutes, and the resulting solution stirred for 6 hours at room temperature. Distilled water (80 cm^3) was added and the aqueous layer extracted with dichloromethane (3 x 70 cm^3) after which the organic portions were combined and concentrated *in vacuo* to yield a yellow oil which was purified by radial chromatography (EtOAc:Hex = 1:4) to give ethyl 3-{(5*R*)-2-[(*E*)-2-ethoxy-2-oxoethylidene]-5-methyltetrahydro-1*H*-pyrrol-1-yl}propanoate **87** (1.75 g, 6.51 mmol, 70%) as a yellow oil; R_f 0.51 (EtOAc/Hex 1:1); $[\alpha]_D^{31}$ +81.4° (*c* 2.1, EtOH); (Found: M^+, 270.1718. Calc. for $C_{14}H_{24}NO_4$, *M:* 270.1705); ν_{max}(film)/cm^{-1} 2977, 2936, 1732, 1685, 1591, 1378, 1132, 1050 and 786; δ_H(400 MHz; $CDCl_3$) 4.45 (1 H, s, 1″-*H*), 4.09 (2 H, q, 2″-$O_2CH_2CH_3$), 4.03 (2 H, q, 1-$O_2CH_2CH_3$), 3.61 (1 H, m, 5′-*H*), 3.41 (2 H, t, *J* = 7.2 Hz, 3′-*H*), 3.10 (1 H, m, 2-*H*), 3.01 (1 H, m, 2-

H), 2.56 (1 H, m, 4′-*H*), 2.44 (1 H, m, 4′-*H*), 2.03 (1 H, m, 3-*H*), 1.49 (1 H, m, 3-*H*), 1.21 (3 H, t, 2″-$O_2CH_2CH_3$), 1.19 (3 H, q, 1-$O_2CH_2CH_3$), 1.13(3 H, d, *J* = 6.3 Hz, 5′-CH_3); δ_C(100 MHz; $CDCl_3$) 171.5 (s, 2″-*C*), 169.2 (s, 1-*C*), 164.3 (s, 2′-*C*), 78.5 (d, 1″-*C*), 60.7 (t, 2″-$O_2CH_2CH_3$), 58.8 (d, 5′-*C*), 58.2 (t, 1-$O_2CH_2CH_3$), 39.4 (t, 3′-*C*), 31.2 (t, 4′-*C*), 30.7 (t, 2-*C*), 29.5 (t, 3-*C*), 19.2 (q, 5′-CH_3), 14.7 (q, 1-$O_2CH_2CH_3$), 14.1 (q, 2″-$O_2CH_2CH_3$); *m/z* (EI) 269 (M^+, 37%), 224 (55), 197 (47), 196 (100), 150 (44), 125 (73), 124 (91) and 108 (42).

Ethyl 2-[(5*R*)-5-methyltetrahydro-2*H*-pyrrol-2-ylidene]acetate [72]

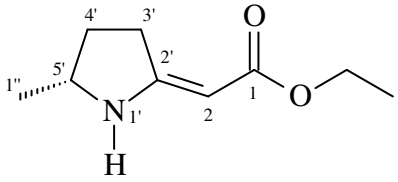

Lithiumhexamethyldisilazane (962 mg, 5.74 mmol) as a solution in dry THF (8 cm^3), was added rapidly to a stirring solution of ethyl 3-{(5*R*)-2-[(*E*)-2-ethoxy-2-oxoethylidene]-5-methyltetrahydro-1*H*-pyrrol-1-yl}propanoate (387 mg, 1.43 mmol) in dry THF (90 cm^3), and stirred for 5 minutes at room temperature. The reaction mixture was quenched by the dropwise addition of methanol (1 cm^3) followed by concentration *in vacuo* to yield a yellow oil which was purified by radial chromatography (EtOAc:Hex = 1:4) to give ethyl 2-[(5*R*)-5-methyltetrahydro-2*H*-pyrrol-2-ylidene]acetate **72** (133 mg, 0.79 mmol, 55%) as a yellow oil; R_f 0.69 (EtOAc/Hex 1:1); $[\alpha]_D^{28}$ –44.9° (*c* 2.3, EtOH); (Found: M^+, 170.1178. Calc. for $C_9H_{16}NO_2$, *M:* 170.1181); ν_{max}(film)/cm^{-1} 3340, 2971, 1731, 1660, 1600, 1237, 1145, 1048 and 780; δ_H(400 MHz; $CDCl_3$) 7.88 (1 H, s, 1′-*H*), 4.46 (1 H, s, 2-*H*), 4.09 (2 H, q, *J* = 7.1 Hz, 1-$O_2CH_2CH_3$), 3.86 (1 H, m, 5′-*H*), 2.58 (2 H, m, 3′-*H*), 2.01 (1 H, m, 4′-*H*), 1.49 (1 H, m, 4′-*H*), 1.24 (3 H, t, *J* = 7.1 Hz, 1-$O_2CH_2CH_3$), 1.22 (3 H, d, *J* = 6.3 Hz, 1″-*H*); δ_C(100 MHz; $CDCl_3$) 170.7 (s, 1-*C*), 165.8 (s, 2′-*C*), 76.5 (d, 2-*C*), 58.4 (t, 1-$O_2CH_2CH_3$), 55.0 (d, 5′-*C*), 32.1 (t, 3′-*C*), 30.2 (t, 4′-*C*), 21.6 (q, 1″-*C*), 14.7 (q, 1-$O_2CH_2CH_3$); *m/z* (EI) 169 (M^+, 49%), 124 (100), 108 (92), 97 (75) and 82 (83).

Ethyl (3*R*)-5-heptyl-3-methyl-2,3-dihydro-1*H*-pyrrolizine-7-carboxylate [74]

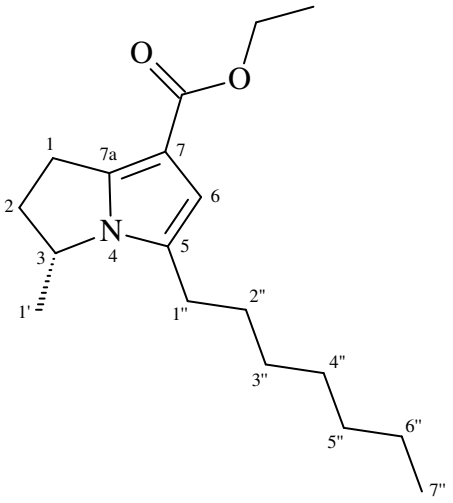

1.6 M *n*-BuLi (4.75 cm^3, 7.6 mmol) was added dropwise over a period of 10 minutes to a stirred solution of ethyl 2-[(5*R*)-5-methyltetrahydro-2*H*-pyrrol-2-ylidene]acetate (0.64 g; 3.8 mmol) in dry THF (100 cm^3) at –77 ^oC, and stirred for 30 minutes whilst maintaining temperature at –77 ^oC. The solution was allowed to slowly warm to room temperature and stir for an additional 30 minutes whilst at room temperature. The solution was again cooled to -77 ^oC followed by the dropwise addition of a solution of 1-bromo-2-nonyne (0.85 g, 4.17 mmol) in dry THF (5 cm^3), and the resulting solution stirred for 30 minutes whilst maintaining temperature of –77 ^oC. The solution was allowed to slowly warm to room temperature, and stir for 14 hours. The reaction mixture was quenched with 2 M ammonium chloride (5 drops) and concentrated *in vacuo* to yield a brown oil. Zinc chloride (90 mg, 0.90 mmol) and acetonitrile (20 cm^3) was added to the oil and the mixture was refluxed for 5 hours. The reaction mixture was passed through a short silica plug (1 cm), after which the filtrate was concentrated *in vacuo* to yield a yellow oil which was purified by radial chromatography (EtOAc:Hex = 1:4) to give ethyl (3*R*)-5-heptyl-3-methyl-2,3-dihydro-1*H*-pyrrolizine-7-carboxylate **74** (475 mg, 1.6 mmol, 43%) as a yellow oil; R_f 0.78 (EtOAc/Hex 1:1); $[\alpha]_D^{31}$ –21.4^o (*c* 0.15, EtOH); (Found: M^+, 292.2286. Calc. for $C_{18}H_{30}NO_2$, *M:* 292.2277); ν_{max}(film)/cm^{-1} 2956, 2928, 2857, 1702, 1577, 1526, 1455, 1434, 1377, 1226, 1077 and 772; δ_H(400 MHz; $CDCl_3$) 6.27 (1 H, s, 6-

H), 4.31 (1 H, m, 3-*H*), 4.23 (2 H, g, *J* = 7.1 Hz, 7-$CO_2C\mathit{H}_2CH_3$), 3.02 (2 H, m, 1-*H*), 2.67 (1 H, m, 2-*H*), 2.50 (2 H, m, 1″-*H*), 2.10 (1 H, m, 2-*H*), 1.61 (2 H, m, 2″-*H*), 1.36-1.25 (14 H, m, 7-$CO_2CH_2C\mathit{H}_3$, 1′-*H*, 3″-*H*, 4″-*H*, 5″-*H*, 6″-*H*), 0.88 (3 H, t, *J* = 6.5 Hz, 7″-*H)*; δ_C(100 MHz; $CDCl_3$) 165.4 (s, 7-$\mathit{C}O_2$), 142.1 (s, 7a-*C*), 129.0 (s, 5-*C*), 109.5 (d, 6-*C*), 106.0 (s, 7-*C*), 59.1 (t, 7-$CO_2\mathit{C}H_2CH_3$), 53.7 (d, 3-*C*), 35.5 (t, 2-*C*), 31.8 (t, 5″-*C*), 29.4 (t, 3″-*C*), 29.1 (t, 4″-*C*), 28.8 (t, 2″-*C*), 26.4 (t, 1″-*C*), 24.3 (t, 1-*C*), 22.6 (t, 6″-*C*), 21.0 (q, 1′-*C*), 14.6 (q, 7-$CO_2CH_2\mathit{C}H_3$), 14.0 (q, 7″-*C*); *m/z* (EI) 291 (M^+, 31%), 207 (28), 206 (100), 178 (55) and 134 (44).

1-butyl-2,5-dimethyl-1*H*-pyrrole [112]

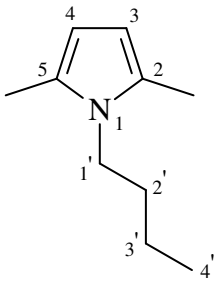

Distilled water (100 cm^3) was added to a stirring solution of ethyl 1-butyl-2,5-dimethyl-1*H*-pyrrole-3-carboxylate (3.0 g, 13.4 mmol) in ethanol (10 cm^3), followed by the addition of concentrated sulfuric acid (2 cm^3). After allowing the solution to boil under reflux for 18 hours, the solvent was removed *in vacuo* to yield a brown oil. Ethanolamine (90 cm^3) was added to the oil and the resulting solution was refluxed for 20 hours. Distilled water (100 cm^3) was added and the remaining solution was extracted with dichloromethane (3 x 90 cm^3), after which the organic portions were combined and concentrated *in vacuo* to yield a brown oil which was purified by radial chromatography (EtOAc:Hex = 1:4) to furnish 1-Butyl-2,5-dimethyl-1*H*-pyrrole **112** (0.63 g, 4.2 mmol, 31%) as a yellow oil; R_f 0.79 (EtOAc/Hex 1:1); (Found: M^+, 152.1436. Calc. for $C_{10}H_{18}N$, *M:* 152.1439); δ_H(400 MHz; $CDCl_3$) 5.76 (2 H, s, 3-*H*, 4-*H*), 3.72 (2 H, t, 1′-*H*), 2.22 (6 H, s, 2-CH_3, 5-CH_3), 1.60 (2 H, m, 2′-*H*), 1.37 (2 H, m, 3′-*H*), 0.96 (3 H, t, *J* = 7.3 Hz, 4′-*H*); δ_C(100 MHz; $CDCl_3$) 127.1 (s, 2-*C*, 5-*C*), 104.9 (d, 3-*C*, 4-*C*), 43.4 (t, 1′-*C*),

33.1 (t, 2′-*C*), 20.2 (t, 3′-*C*), 13.8 (q, 4′-*C*), 12.5 (q, 2-*C*H_3, 5-*C*H_3); *m/z* (EI) 151 (M^+, 68%), 136 (17), 109 (24), 108 (100), 94 (38), 32 (25) and 28 (53).

(5*R*)-5-pentyltetrahydro-2*H*-pyrrol-2-one [118]

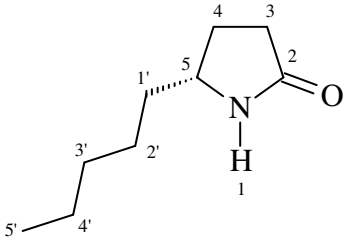

1.6 M *n*-BuLi (51.1 cm^3, 81.7 mmol) was added dropwise over 1 h to a stirred suspension of copper cyanide (3.8 g, 42 mmol) in dry THF (50 cm^3) at –40 °C. A solution of [(2*S*)-5-oxotetrahydro-1*H*-pyrrol-2-yl]methyl 4-methylbenzenesulfonate (2 g, 7.4 mmol) in dry THF (5 cm^3) was cannulated to the cuprate at –40 °C and the resulting mixture was stirred at –40 °C for 3 hours followed by overnight stirring at room temperature. Saturated ammonium chloride (30 cm^3) was added to the reaction mixture and the two layers were separated. The organic layer was washed with saturated ammonium chloride (10 cm^3) and the aqueous layer was extracted with dichloromethane (3 x 20 cm^3). The organic portions were combined and concentrated *in vacuo* to yield a yellow oil which was purified by radial chromatography (diethyl ether : 2-propanol = 9:1) to yield (5*R*)-5-pentyltetrahydro-2*H*-pyrrol-2-one **118** (1.1 g, 7.1 mmol, 96%) as a yellow oil; R_f 0.19 (diethyl ether); $[\alpha]_D^{30}$ +13.6° (*c* 1.25, MeOH); (Found: M^+, 156.1383. Calc. for $C_9H_{18}NO$, *M:* 156.1388); ν_{max}(film)/cm^{-1} 3222, 2955, 2929, 2859 and 1697; δ_H(400 MHz; $CDCl_3$) 6.69 (1 H, s, 1-*H*), 3.61 (1 H, m, 5-*H*), 2.30 (2 H, m, 3-*H*), 2.21 (1 H, m, 4-*H*), 1.68 (1 H, m, 4-*H*), 1.53-1.41 (2 H, m, 1′-*H*), 1.28 (6 H, m, 2′-*H*, 3′-*H*, 4′-*H*), 0.87 (3 H, t, *J* = 6.7 Hz, 5′-*H*); δ_C(100 MHz; $CDCl_3$) 178.4 (s, 2-*C*), 54.7 (d, 5-*C*), 36.7 (t, 1′-*C*), 31.7 (t, 3′-*C*), 30.3 (t, 3-*C*), 27.3 (t, 4-*C*), 25.5 (t, 2′-*C*), 22.5 (t, 4′-*C*), 13.9 (q, 5′-*C*).

4 References

1. Lorber, C.; Choukroun, R.; Vendier, L. *Organometallics* **2004,** *23*, 1845-1850.
2. Louie, J.; Hartwig, J. F. *Tetrahedron Lett.* **1995,** *36*, 3609-3612.
3. Ma, D.; Yao, J. *Tetrahedron* **1996,** *7*, 3075-3078.
4. Nobis, M.; Driebβen-Hölscher, B. *Angew. Chem. Int. Ed.* **2001,** *40*, 3983-3985.
5. Ouh, L. L.; Muller, T. E.; Yan, Y. K. *J. Organomet. Chem.* **2005,** *690*, 3774-3782.
6. Robinson, R. S.; Dovey, M. C.; Gravestock, D. *Tetrahedron Lett.* **2004,** *45*, 6787-6789.
7. Straub, T.; Haskel, A.; Neyroud, T. G.; Kapon, M.; Botoshansky, M.; Eisen, M. S. *Organometallics* **2001,** *20*, 5017-5035.
8. Hultzsch, K. C. *Org. Biomol. Chem* **2005,** *3*, 1819-1824.
9. Howk, B. W.; Little, E. L.; Scott, S. L.; Whitman, G. M. *J. Am. Chem. Soc.* **1954,** *76*, 1899-1902.
10. Bambirra, S.; Tsurugi, H.; van Leusen, D.; Hessen, B. *Dalton Trans.* **2006**, 1157-1161.
11. Anderson, L. L.; Arnold, J.; Bergman, R. G. *Org. lett.* **2004,** *6*, 2519-2522.
12. Müller, T. E.; Pleier, A.-K. *J. Chem. Soc., Dalton Trans* **1999**, 583-587.
13. Kim, Y. K.; Livinghouse, T.; Bercaw, J. E. *Tetrahedron Lett.* **2001,** *42*, 2933-2935.
14. Severin, R.; Doye, S. *Chem. Soc. Rev.* **2007,** *36*, 1407-1420.
15. Cornils, B.; Herrmann, W. A. *Applied Homogeneous Catalysis with Organometallic Compounds*; Wiley-VCH, 2002.
16. Pohlki, F.; Doye, S. *Chem. Soc. Rev.* **2003,** *32*, 104-114.
17. Kruse, C. W.; Kleinschmidt, R. F. *J. Am. Chem. Soc.* **1961,** *83*, 216-220.
18. Roundhill, D. M. *Chem. Rev.* **1992,** *92*, 1-27.
19. Uchimaru, Y. *Chem. Comm.* **1999**, 1133-1134.
20. Hillhouse, G. L.; Bulls, A. R.; Santarsiero, B. D.; Bercaw, J. E. *Organometallics* **1988,** *7*, 1309-1312.

21. Schaad, D. R.; Landis, C. R. *J. Am. Chem. Soc.* **1990,** *112*, 1629-1630.
22. Casalnuovo, A. L.; Calabrese, J. C.; Milstein, D. *Inorg. Chem.* **1987,** *26*, 971-973.
23. Gagne, M. R.; Marks, T. J. *J. Am. Chem. Soc.* **1989,** *111*, 4109-4110.
24. Gagne, M. R.; Nolan, S. P.; Marks, T. J. *Organometallics* **1990,** *9*, 1716-1718.
25. Müller, T. E.; Grosche, M.; Herdtweck, E.; Pleier, A.-K.; Walter, E.; Yan, Y.-K. *Organometallics* **2000,** *19*, 170-183.
26. Barluenga, J.; Perez-Prieto, J.; Asensio, G. *Tetrahedron* **1990,** *46*, 2453-2460.
27. Takaki, K.; Koizumi, S.; Yamamoto, Y.; Komeyama, K. *Tetrahedron Lett.* **2006,** *47*, 7335–7337.
28. Ward, B. D.; Maisse-François, A.; Mountford, P.; Gade, L. H. *Chem. Comm.* **2004**, 704-705.
29. Zhang, Z.; Schafer, L. L. *Org. Lett.* **2003,** *5*, 4733-4736.
30. Gasc, M. B.; Lattes, A.; Perie, J. J. *Tetrahedron* **1983,** *39*, 703-731.
31. Tillack, A.; Khedkar, V.; Beller, M. *Tetrahedron Lett.* **2004,** *45*, 8875-8878.
32. Ryu, J.-S.; Li, G. Y.; Marks, T. J. *J. Am. Chem. Soc.* **2003,** *125*, 12584-12605.
33. Muller, T. E.; Beller, M. *Chem. Rev.* **1998,** *98*, 675-703.
34. Ogata, T.; Ujihara, A.; Tsuchida, S.; Shimizu, T.; Kaneshige, A.; Tomioka, K. *Tetrahedron Lett.* **2007,** *48*, 6648-6650.
35. LaLonde, R. L.; Sherry, B. D.; Kang, E. J.; Toste, F. D. *J. Am. Chem. Soc.* **2007,** *129*, 2452-2453.
36. Riant, O.; Hannedouche, J. *Org. Biomol. Chem* **2007,** *5*, 873-888.
37. Knight, P. D.; Munslow, I.; O'Shaughnessy, P. N.; Scott, P. *Chem. Comm.* **2004**, 894-895.
38. Hong, S.; Kawaoka, A. M.; Marks, T. J. *J. Am. Chem. Soc.* **2003,** *125*, 15878-15892.
39. Giardello, M. A.; Conticello, V. P.; Brard, L.; Sabat, M.; Rheingold, A. L.; Stern, A. L.; Marks, T. J. *J. Am. Chem. Soc.* **1994,** *116*, 10212-10240.
40. Aillaud, I.; Collin, J.; Hannedouche, J.; Schulz, E. *Dalton Trans.* **2007**, 5105–5118.
41. Douglass, M. R.; Ogasawara, M.; Hong, S.; V.Metz, M.; Marks, T. J. *Organometallics* **2002,** *21*, 283-292.

42. O'Shaughnessy, P. N.; Gillespie, K. M.; Knight, P. D.; Munslow, I. J.; Scott, P. *Dalton Trans.* **2004**, 2251-2256.
43. O'Shaughnessy, P. N.; Knight, P. D.; Morton, C.; Gillespie, K. M.; Scott, P. *Chem. Commun.* **2003**, 1770-1771.
44. O'Shaughnessy, P. N.; Scott, P. *Tetrahedron: Asymmetry* **2003,** *14*, 1979-1983.
45. Gribkov, D. V.; Hultzsch, K. C.; F.Hampel. *J. Am. Chem. Soc.* **2006,** *128*, 3748-3759.
46. Thomson, R. K.; Bexrud, J. A.; Schafer, L. L. *Organometallics* **2006,** *25*, 4069-4071.
47. Wood, M. C.; Leitch, D. C.; Yeung, C. S.; Kozak, J. A.; Schafer, L. L. *Angew. Chem. Int. Ed.* **2007,** *46*, 354-358.
48. Patil, N. T.; Pahadi, N. K.; Yamamoto, Y. *Tetrahedron Lett.* **2005,** *46*, 2101–2103.
49. Arredondo, V. M.; Tian, S.; McDonald, F. E.; Marks, T. J. *J. Am. Chem. Soc.* **1999,** *121*, 3633-3639.
50. Daly, J. W. *J. Nat. Prod.* **1998,** *61*, 162-172.
51. Harris, J. B. *Natural Toxins: Animal, Plant and Microbial*; Oxford Science Publications: Oxford, 1986.
52. Mattocks, A. R. *Chemistry and Toxicology of Pyrrolizidine Alkaloids*; Academic Press, 1986.
53. Pelletier, S. W. *Alkaloids: Chemical and Biological Perspectives*; John Wiley and Sons: New York, 1982; Vol. One.
54. Clark, V. C.; Raxworthy, C. J.; Rakotomalala, V.; Sierwald, P.; Fisher, B. L. *PNAS* **2005,** *102*, 11617-11622.
55. Crab, T. A.; Newton, R. F.; Jackson, D. *Chem. Rev.* **1971,** *71*, 109-126.
56. Scarpi, D.; Occhiato, E. G.; Guarna, A. *J. Org. Chem.* **1999,** *64*, 1727-1732.
57. *Toxicants Occurring Naturally in Foods*, Second ed.; National Academy of Sciences: Washington, D.C., 1973.
58. Daly, J. W.; Spande, T. F.; Garraffo, H. M. *J. Nat. Prod.* **2005,** *68*, 1556-1575.
59. Takahata, H.; Takahashi, S.; Azer, N.; Eldefrawi, A. T.; Eldefrawi, M. E. *Bioorg. & Med. Chem. Lett.* **2000,** *10*, 1293-1295.

60. Jones, T. H.; Highet, R. J.; Don, A. W.; Blum, M. S. *J. Org. Chem.* **1986,** *51*, 2712-2716.
61. Jones, T. H.; Blum, M. S. *J. Org. Chem.* **1980,** *45*, 4778-4780.
62. Skvortsov, I. M.; Elvidge, J. A. *J. Chem. Soc. B* **1968**, 1589-1595.
63. Gebauer, J.; Dewi, P.; Blechert, S. *Tetrahedron Lett.* **2005,** *46*, 43-46.
64. Janowitz, A.; Vavrecka, M.; Hesse, M. *Helv. Chem. Act.* **1991,** *74*, 1352-1361.
65. Occhiato, E. G.; Scarpi, D.; Menchi, G.; Guarna, A. *Tetrahedron: Asymmetry* **1996,** *7*, 1929-1942.
66. Ciganek, E. *J. Org. Chem.* **1995,** *60*, 5803-5807.
67. Takano, S.; Otaki, S.; Ogasawara, K. *J. Chem. Soc., Chem. Commun.* **1983**, 1172-1174.
68. Dovey, M. C. PhD Thesis, University of KwaZulu-Natal, 2005.
69. Prior, A. M.; Robinson, R. S. *Tetrahedron Lett.* **2008,** *49*, 411-414.
70. Robinson, R. S.; Dovey, M. C.; Gravestock, D. *Eur. J. Org. Chem.* **2005,** *3*, 505-511.
71. Robinson, R. S.; Dovey, M. C.; Gravestock, D. *Tetrahedron Lett.* **2004,** *45*, 6787-6789.
72. Rechsteiner, B.; Texier-Boullet, F.; Hamelin, J. *Tetrahedron Lett.* **1993,** *34*, 5071-5074.
73. March, J. *Advanced Organic Chemistry*, 4th ed.; Wiley-Interscience: New York.
74. Baldwin, J. E. *J. Chem. Soc., Chem. Commun.* **1976**, 734-736.
75. Baldwin, J. E.; Thomas, R. C.; Kruse, L. I.; Silberman, L. *J. Org. Chem.* **1977,** *42*, 3846-3852.
76. Brillon, D. *Synth. Comm.* **1990,** *20*, 3085-3095.
77. Michael, J. P.; Gravestock, D. *J. Chem. Soc., Perkin Trans. 1* **2000**, 1919-1928.
78. Howard, A. S.; Gerrans, G. C.; Meerholz, C. A. *Tetrahedron Lett.* **1980,** *21*, 1373-1374.
79. Michael, J. P.; Parsons, A. S. *Tetrahedron* **1996,** *52*, 2199-2216.
80. Gravestock, D.; Peirson, I. G. *Tetrahedron Lett.* **2000,** *41*, 3497-3500.
81. Roth, M.; Dubs, P.; Gotschi, E.; Eschenmoser, A. *Helv. Chem. Act.* **1971,** *54*, 710-734.

82. Ghirlando, R.; Howard, A. S.; Katz, R. B.; Michael, J. P. *Tetrahedron* **1984,** *40*, 2879-2884.
83. Russowsky, D.; da Silveira Neto, B. A. *Tetrahedron Lett.* **2003,** *44*, 2923-2926.
84. Bartoli, G.; Cimarelli, C.; Dalpozzo, R.; Palmieri, G. *Tetrahedron* **1995,** *51*, 8613-8622.
85. Thottathil, J. K.; Moniot, J. L.; Mueller, R. H.; Wong, M. K. Y.; Kissick, T. P. *J. Org. Chem.* **1986,** *51*, 3140-3143.
86. Morita, J.-i.; Nakatsuji, H.; Misaki, T.; Tanabe, Y. *Green Chem.* **2005,** *7*, 711-715.
87. Zard, S. Z. *Radical Reactions in Organic Synthesis*; OUP, 2003.
88. Parsons, A. F. *An Introduction to Free Radical Chemistry*; Blackwell: Oxford, 2000.
89. Perkins, M. J. *Radical Chemistry: The Fundamentals*; OUP (Primer No. 91), 2000.
90. Reich, H. J.; Sikorski, W. H. *J. Org. Chem.* **1999,** *64*, 14-15.
91. Lo, C.-C.; Chao, P.-M. *J. Chem. Ecol.* **1990,** *16*, 3245-3253.
92. kocienski, P. J.; Love, C. J.; Whitby, R. J.; Costello, G.; Roberts, D. A. *Tetrahedron* **1989,** *45*, 3839-3848.
93. Suzuki, H.; Mori, M.; Shibakami, M. *Synlett* **2003,** *14*, 2163-2166.
94. Davies, S. G.; Ichihara, O. *Tetrahedron Lett.* **1999,** *10*, 9313-9316.
95. Appel, R. *Angew. Chem. Int. Ed.* **1975,** *14*, 801-811.
96. Appel, R. *Chem. Ber.* **1976**, 58-70.
97. Lakhrissi, Y.; Taillefumier, C.; Chretien, F.; Chapleur, Y. *Tetrahedron Lett.* **2001,** *42*, 7265–7268.
98. Dhimane, H.; Vanucci-Bacque, C.; Hamon, L.; Lhommet, G. *Eur. J. Org. Chem.* **1998**, 1955-1963.
99. Bertz, S. H.; Human, J.; Ogle, C. A.; Seagleb, P. *Org. Biomol. Chem.* **2005,** *3*, 392-394.
100. Calvo, L.; Gonzalez-Ortega, A.; Sanudo, M. C. *Synthesis* **2002**, 2450-2456.
101. Adkins, H.; Billica, H. R. *J. Am. Chem. Soc.* **1948,** *70*, 3121-3125.
102. Smith, M. B.; Dembofsky, B. T.; Son, Y. C. *J. Org. Chem.* **1994,** *59*, 1719-1725.